U.S. DEPARTMENT OF THE INTERIOR

U.S. GEOLOGICAL SURVEY

PROCEEDINGS OF THE

FIRST JOINT MEETING of the U.S.-JAPAN CONFERENCE

ON NATURAL RESOURCES (UJNR)

PANEL ON EARTHQUAKE RESEARCH

Pasadena, California

NOVEMBER 12 - 14, 1996

OPEN-FILE NO 97-467

MENLO PARK, CALIFORNIA

1997

Proceedings of the

First Joint Meeting of the U.S.-Japan Conference on Natural Resources (UJNR) Panel on Earthquake Research

Pasadena, California

November 12 - 14, 1996

Panel Chairmen:

James H. Dieterich
U.S. Geological Survey
Menlo Park, California 94025
U.S.A.

Kunio Nonomura
Geographical Survey Institute
Ibaraki-Ken 305
Japan

Table of Contents

INTRODUCTION

The 1st Joint Meeting of the U.S.-Japan Natural Resources Panel on Earthquake Research was held in Pasadena, California on November 12-14, 1996. The UJNR program fosters the exchange of scientists, information, equipment and knowledge between government agencies in Japan and the United States concerned with problems involving natural resources.

This new panel is the successor to the UJNR Panel on Earthquake Prediction Technology, and was created in recognition of fundamental changes taking place in the earthquake research agenda in both countries as a consequence of the 1994 Northridge, California and 1995 Kobe, Japan earthquakes. Over the past 18 years, the former UJNR panel served as an important bridge between our two countries, providing numerous opportunities for joint technical meetings and scientist-to-scientist exchanges that have done much to improve our common understanding of earthquakes, and to advance the technology we use to study them.

Earlier this year, our two countries agreed to deepen our cooperation through the creation of an Earthquake Disaster Mitigation Partnership, under the umbrella of our broad program of cooperation, the Common Agenda for Cooperation in Global Perspective. As a consequence, our UJNR panel not only has a new name, but also a new mission: to carry out this partnership through the creation of joint projects directed toward the key themes of 1) quantifying the earthquake threat, 2) reducing earthquake damage, and 3) improving technologies for emergency response.

This UJNR panel meeting was hosted by the Southern California Earthquake Center (SCEC) and the U.S. Geological Survey (USGS). Founded in 1991, the Southern California Earthquake Center is a Science and Technology Center of the National Science Foundation and is also funded by the USGS. SCEC brings scientists from universities, government and private industry together for joint research and problem solving to study the earthquake hazard in southern California. The formal mission of the Center is to promote earthquake hazard reduction by estimating when and where future damaging earthquakes will occur, calcuating the expected ground motion, and disseminating that information to the public.

Technical sessions were held on November 12-13, 1996 at the Doubletree hotel in Pasadena, California. A field trip was led by Professor James Dolan of the University of Southern California on November 14 to visit two of his paleoseismic sites in Hollywood and along the Cucamonga fault. Professor Sally McGill of California State University, San Bernardino led the group into her open trench on the San Andreas fault.

The UJNR panel on Earthquake Research wishes to express its gratitude to the local organizing committee, Tom Henyey, Dave Jackson, John McRaney and Jim Mori for their superb arrangements for this meeting.

U.S.-Side Members of the UJNR Panel on Natural Resources on Earthquake Research

Dr. James H. Dieterich, Chairperson
Chief Scientist
Earthquake Hazards Team
U.S. Geological Survey
345 Middlefield Road
Menlo Park, California 94025

Dr. William L. Ellsworth
Earthquake Hazards Team
U.S. Geological Survey
345 Middlefield Road
Menlo Park, California 94025

Dr. David P. Hill
Volcanic Hazards Team
U.S. Geological Survey
345 Middlefield Road
Menlo Park, California 94025

Mr. Robert Volland
Division Director
Development Coordination Division
Federal Emergency Management Agency
Washington, D.C. 20472

Dr. Thomas Henyey
Director
Southern California Earthquake Center
University of Southern California
Los Angeles, California 90089-0740

Dr. James J. Mori
Field Office Scientist in Charge
U.S. Geological Survey
525 S. Wilson Street
Pasadena, California 91106

Captain Melvyn Grunthal
Chief, National Geodetic Survey Division
Office of Charting and Geodetic Services
National Ocean Service
11400 Rockville Pike
Rockville, Maryland 20852

Dr. Wayne Thatcher
Earthquake Hazards Team
U.S. Geological Survey
345 Middlefield Road
Menlo Park, California 94025

Dr. Shelby Tilford
Director
Earth Science and Applications Division
National Aeronautics and Space Administration
Washington, D.C. 20550

Dr. Richard Wright
Director
Building and Fire Research Laboratory
National Institute of Standards and Technology
Gaithersburg, Maryland 20899

Dr. Andy Murphy
Earth Science Branch, MS 007NL
U.S. Nuclear Regulatory Commission
Washington, D.C. 20555

Dr. James Whitcomb
National Science Foundation
1800 G Street, N.W.
Washington, D.C. 20550

Japan-Side Members of the UJNR Panel on Natural Resources on Earthquake Research

Mr. Kunio Nonomura, Chairperson
Director General
Geographical Survey Institute
Kitasato-1, Tsukuba-Shi, Ibaraki-Ken 305

Dr. Yoshimitsu Okada
Director, Earthquake Research Center
National Research Institute for
Earth Science and Disaster Prevention
Tennodai 3-1, Tsukuba-Shi
Ibaraki-Ken 305

Dr. Hirokazu Matsumoto
Chief of Optical Measurement Section
National Research Laboratory of Metrology
Umezono 1-1-4, Tsukuba-Shi
Ibaraki-Ken 305

Dr. Yoshihiro Kinugasa
Chief Senior Researcher
Geological Survey of Japan
Higashi 1-1-3, Tsukuba-Shi
Ibaraki-Ken 305

Dr. Nobuo Hurukawa
Head, Earthquake Information Division
International Institute of Seismology and
Earthquake Engineering
Building Research Institute
Tatehara-1, Tsukuba-Shi
Ibaraki-Ken 305

Mr. Koji Yamamoto
Director-General of Seismological
and Volcanological Department
Japan Meteorological Agency
Ote-Machi 1-3-4, Chiyoda-Ku
Tokyo 100

Dr. Fujinobu Takahashi
Director, Kashima Space Research Center
Communications Research Laboratory
Hirai 893-1 Kashima-Shi
Ibaraki-Ken 314

Dr. Koichi Yokoyama
Director, Earthquake Disaster Prevention
Research Center
Public Works Research Institute
Asahi-1, Tsukuba-Shi, Ibaraki-Ken 305

Dr. Yasuhiro Ganeko
Director of Planning Division
Hydrographic Department
Maritime Safety Agency
Tsukiji 5-3-1, Chuo-Ku
Tokyo 104

Mr. Yoshimitsu Yoshimura
Director, Crustal Dynamics Department
Geographical Survey Institute
Kitasato-1, Tsukuba-Shi
Ibaraki-Ken 305

Participants in the First Joint Meeting of the U.S.-Japan Conference on Natural Resources (UJNR) Panel on Earthquake Research

U.S. Members:

William L. Ellsworth, Chairman
U.S. Geological Survey, MS-977
345 Middlefield Road
Menlo Park, California 94025

Thomas Henyey
Southern California Earthquake Center
University of Southern California
Los Angeles, California 90089

Jim Mori
U.S. Geological Survey
525 South Wilson Boulevard
Pasadena, California 91106

Wayne Thatcher
U.S. Geological Survey, MS-977
345 Middlefield Road
Menlo Park, California 94025

James Whitcomb
Division of Earth Sciences, Room 785
National Science Foundation
4201 Wilson Boulevard
Arlington, Virginia 22230

U.S. Observers:

Ralph Archuleta
Institute for Crustal Studies
University of California
Santa Barbara, California 93106

Brian Atwater
U.S. Geological Survey
University of Washington
Seattle, Washington 98195

Yehuda Ben-Zion
Southern California Earthquake Center
University of Southern California
Los Angeles, California 90089

Yehuda Bock
Scripps Orbit and Permanent Array Center, A-008
University of California
La Jolla, California 90293

James Davis, California State Geologist
Division of Mines and Geology
801 K Street, MS 12-30
Sacramento, California 95814

Paul Davis
Department of Earth and Space Sciences
University of California
Los Angeles, California 90095

James Dolan
Southern California Earthquake Center
University of Southern California
Los Angeles, California 90089

John Hall
Division of Engineering
Department of Civil Engineering
California Institute of Technology
Pasadena, California 91125

Egill Hauksson
Seismological Laboratory
California Institute of Technology
Pasadena, California 91125

Stephen Hickman
U.S. Geological Survey, MS-977
345 Middlefield Road
Menlo Park, California 94025

Susan Hough
U.S. Geological Survey
525 South Wilson Boulevard
Pasadena, California 91106

Kenneth Hudnut
U.S. Geological Survey
525 South Wilson Boulevard
Pasadena, California 91106

David Jackson, Science Director
Southern California Earthquake Center
Department of Earth and Space Sciences
University of California
Los Angeles, California 90095

Lucy Jones
U.S. Geological Survey
525 South Wilson Boulevard
Pasadena, California 91106

Hiroo Kanamori
Seismological Laboratory
California Institute of Technology
Pasadena, California 91125

Yong-Gang Li
Southern California Earthquake Center
University of Southern California
Los Angeles, California 90089

Greg Lyzenga
Jet Propulsion Laboratory
4800 Oak Knoll Drive, MS 238-600
Pasadena, California 91109-8099

Sally McGill
Department of Geological Science
California State University
5500 San Bernardino Parkway
San Bernardino, California 92407

Arben Pitarka
Woodward-Clyde Federal Services
566 El Dorado Street, Suite 100
Pasadena, California 91101

Noel Raufaste
National Institute of Standards and Technology
Building 226, Room B250
Gaithersburg, Maryland 20899

Thomas Rockwell
Department of Geological Sciences
San Diego State University
San Diego, California 92182

David Schwartz
U.S. Geological Survey, MS-977
345 Middlefield Road
Menlo Park, California 94025

David Wald
U.S. Geological Survey
525 South Wilson Boulevard
Pasadena, California 91106

Frank Webb
Jet Propulsion Laboratory
4800 Oak Knoll Drive, MS 238-625
Pasadena, California 91109-8099

Max Wyss
Geophysical Institute
University of Alaska
Fairbanks, Alaska 99775-0800

Participants in the First Joint Meeting of the U.S.-Japan Conference on Natural Resources (UJNR) Panel on Earthquake Research

Japanese Members:

Kunio Nonomura, Chairperson
Director General
Geographical Survey Institute (GSI)
Kitasato 1, Tsukuba-Shi
Ibaraki-Ken 305

Nobuo Hurukawa
Head
Earthquake Information Division
International Institute of Seismology and Earthquake Engineering
Building Research Institute (BRI)
Tatehara 1, Tsukuba-Shi
Ibaraki-Ken 305

Yoshihiro Kinugasa
Chief Senior Researcher
Geological Survey of Japan (GSJ)
Higashi 1-1-3, Tsukuba-Shi
Ibaraki-Ken 305

Shigeru Kasuga (for Dr. Ganeko)
Deputy Director of Planning Division
Hydrographic Department
Maritime Safety Agency (MSA)
Tsukiji 5-3-1, Chuo-Ku
Tokyo 104

Yoshimitsu Okada
Director
Earthquake Research Center
National Research Institute for Earth Science and Disaster Prevention (NIED)
Tennodai 3-1, Tsukuba-Shi
Ibaraki-Ken 305

Fujinobu Takahashi
Director
Kashima Space Research Center
Communications Research Laboratory (CRL)
Hirai 893-1, Kashima-Shi
Ibaraki-Ken 314

Akio Yoshida (for Mr. Yamamoto)
Director of Earthquake Prediction Information Division
Japan Meteorological Agency (JMA)
Ote-machi 1-3-4, Chiyoda-Ku
Tokyo 100

Yoshimitsu Yoshimura
Director of Crustal Dynamics Department
Geographical Survey Institute (GSI)
Kitasato 1, Tsukuba-Shi
Ibaraki-Ken 305

Japanese Observers:

Kazuo Hamada
Data Analysis Division Senior Researcher
Earthquake Research Center (ERC)
Sarugaku-Chou 1-5-18, Chiyoda-Ku
Tokyo 101

Manabu Hashimoto
Chief of Observation and Analysis Division
Geographical Survey Institute (GSI)
Kitasato 1, Tsukuba-Shi
Ibaraki-Ken 305

Hisao Ito
Senior Researcher
Geothermal Research Department
Geological Survey of Japan
Higashi 1-1-3, Tsukuba-Shi
Ibaraki-Ken 305

Masanori Koide
Director for Earthquake Research Planning
Earthquake Research Division
Research and Development Bureau
Science and Technology Agency (STA)
Kasumigaseki 2-2-1, Chiyoda-Ku
Tokyo 100

Toru Matsuzawa
Observation Center for Prediction of Earthquakes and Volcanic Eruptions
Faculty of Science
Tohoku University, Aoba-Ku
Sendai 980-77

Japanese Observers:

Kiyoo Mogi
Nihon University
Chairperson of the Coordinating Committee
for Earthquake Prediction (CCEP)
Izumi-Chou 1-2-1, Narashino-Shi
Chiba-Ken 275

Kenji Satake
Senior Researcher
Seismotectonics Section
Geological Survey of Japan
Higashi 1-1-3, Tsukuba-Shi
Ibaraki-Ken 305

Kunihiko Shimazaki
Earthquake Research Institute (ERI)
University of Tokyo
Yayoi 1-1-1, Bunkyo-Ku
Tokyo 113

Shunroku Yamamoto
Waseda University
Japan

Mamoru Yoshida
Policy Planning Division Senior Staff
Earthquake Research Center (ERC)
Sarugaku-Chou 1-5-18, Chiyoda-Ku
Tokyo 101

Resolution of the First Joint Meeting
of the U.S.-Japan Panel on Earthquake Research
following the Ninth Joint Meeting of the
U.S.-Japan Panel on Earthquake Prediction Technology

U.J.N.R
November 1996

New Panel

The renaming of the UJNR panel on Earthquake Prediction Technology marks the beginning of a new phase of cooperation between the earthquake programs in the U.S. and Japan. The newly named panel on Earthquake Research continues the work of the previous panel, which has provided much of the basis for the current earthquake research programs in the two countries. Recently the focus of much earthquake research has shifted from earthquake prediction toward a more fundamental understanding of the earthquake process and hazard estimation. So, it is appropriate that a new panel be formed to address the challenges of the new set of problems.

Common Agenda

The new UJNR panel recognizes the potential benefits of working together to achieve the goals set forth in the Common Agenda. This agreement seeks cooperative work between our two countries that will accelerate the efforts in earthquake hazard reduction. Among the stated priorities of this agreement, the Earthquake Research Panel will take a lead role in implementing bilateral programs to,

- Quantify the potential for future earthquakes
- Test basic theories about the sources of earthquakes
- Understand the near-source ground motions
- Develop and improve real-time seismic systems
- Improve the modeling of ground motions

Areas of Cooperation

Some specific areas of earthquake research where cooperative research between the U.S. and Japan may lead to significant advancements include, but are not limited to,

- Space technologies for measuring crustal deformations
- Realtime seismic systems
- Fault-zone physics
- Paleoseismology
- Seismic hazard estimation

The panel strongly urges that the appropriate agencies in the U.S. and Japan, that are represented on this panel, work together to support and coordinate the scientific work in these areas of cooperation.

The new panel recognizes the success of the previous panel in promoting exchange of scientific personnel, exchange of data, and fundamental studies that may lead to earthquake prediction. The panel endorses continuation of these activities.

Next Meeting

The next meeting will be held in Japan in the autumn of 1998.

Paper Presented at the First UJNR Meeting

Kunio Nonomura, Masaru Kaidzu and Takashi Saito, *The crustal deformation monitoring system of Geographical Survey Institute*

Kenneth W. Hudnut, *The Southern California Integrated GPS Network (SCIGN)*

F. Takahashi, N. Kurihara, H. Kunimori, Y. Koyama, H. Kiuchi, T. Yoshino, T. Ootsubo, Y. Takahashi, M. Imae, S. Hama, T. Kondo, T. Takaba, T. Iwata, Y. Hanado, M. Sekido, J. Nakajima, T. Gotou, R. Ichikawa, E. Kawai, A. Kaneko, C. Miki, J. Amagai, H. Nojiri, M. Hosokawa and K. Uchida, *The Crustal Deformation Monitoring System in the Tokyo Metropolitan Area*

Andrea Donnellan and Gregory A. Lyzenga, *Modeling Crustal Deformation - Application to the Northridge Earthquake*

Manabu Hashimoto and Yoshimitsu Yoshimura, *Integrated Analysis of Crustal Activity*

Wayne Thatcher, Didier Massonnet and HélèneVadon, *Detection of postseismic deformation following the 1992 M7.3 Landers California earthquake using satellite radar interferometry*

Yoshimitsu Okada, *Recent seismic activity around Tokyo area*

Egill Hauksson and L. M. Jones, *Earthquakes, Faults, and Stress in Los Angeles: Seismotectonic review*

Akio Yoshida, Kohji Hosono and Hidemi Ito, *CHASE: A method for quantitative evaluation of seismic quiescence before large earthquakes*

Y. Bock, S. Wdowinski, P. Fang, J. Zhang, J. Behr, J. Genrich, S. Williams, D. Agnew, F. Wyatt, H. Johnson, et al., K. Hudnut and W. Young, *Southern California Permanent GPS Geodetic Array: Continuous Measurements of Regional Crustal Deformation between the 1992 Landers and 1994 Northridge Earthquakes*

N. Hurukawa and B. Shibazaki, *Foreshock Activities Associated with the Nucleation of the 1995 Off Etorofu Earthquake*

Kiyoo Mogi, *Some features of seismic activities before the recent large earthquakes in and near Japan - the 1995 Kobe earthquake and the 1955 Iturup-oki earthquake -*

David J. Wald, Vince Quitoriano and Rob Graves, *The Los Angeles Basin Response in Simulated and Recorded Ground Motions*

Ralph J. Archuleta and Kim B. Olsen, *Three-Dimensional Wave Propagation in the Los Angeles Basin*

Paul M. Davis, *Evidence of Focusing Effects in Aftershock Seismograms of the Northridge*

John Hall, *Response of US and Japanese Buildings to Strong-Ground Motions*

Yoshihiro Kinugasa, *Studies of active faults in Japan since the Kobe earthquake*

David K. Yamaguchi, Gordon C. Jacoby, Brian F. Atwater, Daniel E. Bunker, Boyd E. Benson, Marion Reid and Connie Woodhouse, *Tree-ring Dating of an Earthquake at the Cascadia Subduction Zone To Within Several Months of January 1700*

Paper Presented at the First UJNR Meeting

Kenji Satake, *Seismotectonic Background for Tsunami Risk Assessments*

Shigeru Kasuga and Yo Iwabuchi, *Survey of Active Faults in the Coastal Areas*

Tom Rockwell, *Blind Thrusting in the Los Angeles Region*

Kunihiko Shimazaki, *Investigation of earthquake potential - status quo -*

David D. Jackson, *Integrated Approach to Seismic Hazard Estimation*

Masanori Koide, *Promotion of Earthquake Research in Japan*

Noel Raufaste, *US-Japan Joint Collaborations in Natural Disaster Reduction*

Stephen Hickman, Mark Zoback and William Ellsworth, *Testing Fundamental Theories of Earthquake Mechanics Through Fault Zone Drilling*

Hisao Ito, *Structure and Physical Properties of the Nojima Fault*

Jim Mori, *Real-Time Seismic Systems in the United States*

Akio Yoshida, *Real-Time Provision of Earthquake Information and Tsunami Forecast*

James F. Davis and Anthony F. Shakal, *Trinet Ground Motion Recording Opportunities: A Joint Effort of Caltech, the Division of Mines and Geology and the USGS*

The crustal deformation monitoring system of Geographical Survey Institute

Kunio Nonomura, Masaru Kaidzu and Takashi Saito
Geographical Survey Institute, Ministry of Construction
Kitasato 1, Tsukuba, 305 Japan

Abstract

Geographical Survey Institute has been carrying out monitoring of crustal deformation using geodetic technology. Recently, advancement of space geodetic technology made us possible to monitor crustal deformation continuously with sufficient precision. Comprehensive Crustal Deformation Monitoring System of GSI presently in operation consists of GPS regional array with 610 on line receiver stations and 2 VLBI permanent stations. By the end of March 1997 (FY 1996 in Japan). It will become 885 on line GPS stations and 4 VLBI permanent stations.

Such dense network arrows us detecting relative motion among plates around Japan. co-seismic deformation fields, regional inter seismic deformation which clearly shows block like behavior. These results helps scientists understanding tectonic setting of Japan. While operating this system. we detected slow deformation which can be interpreted as so-called slow earthquake.

We are expecting this system reveals process of accumulate elastic strain and release of elastic energy as either earthquakes or slow non-seismic deformations.

1. Introduction

Just after the former Joint meeting of Panel for Earthquake Prediction at Kyoto in 1994. a disastrous earthquake hit city of Kobe and surrounding area on 17th January 1995 by which over 5000 people were killed. The tragedic event caused changes in both administrative and observational system related to earthquake research including prediction efforts. In administrative view, enactment of new law started up new system to adjust and enhance earthquake research activities of government agencies and prefectural governments. Enhancement of observational efforts made by agencies, institutes and universities are accelerated. In these two years. we have revealed quite a lot of academic achievement related to earthquake

research especially in research of tectonics. In this paper, we will introduce Crustal Deformation Monitoring System of Geographical Survey Institute and some of its achievements.

2. Enactment of Special Measure Law on Earthquake Disaster Prevention

The occurrence of Hyogoken nanbu (Kobe) Earthquake draw wide attention of Japanese nation and a new law namely Special Measure Law on Earthquake Disaster Prevention was enacted. By the law, The Headquarters of Earthquake Research Promotion was established. The headquarters comprises Policy Comitte and Earthquake Research Comittee. The task of Earthquake Research Comittee is comprehensive evaluation of results of survey, observation and research by institutes, agencies and universities. As the result, system of earthquake prediction research changed. The scheme of the present system of earthquake research is shown in Fig.1.

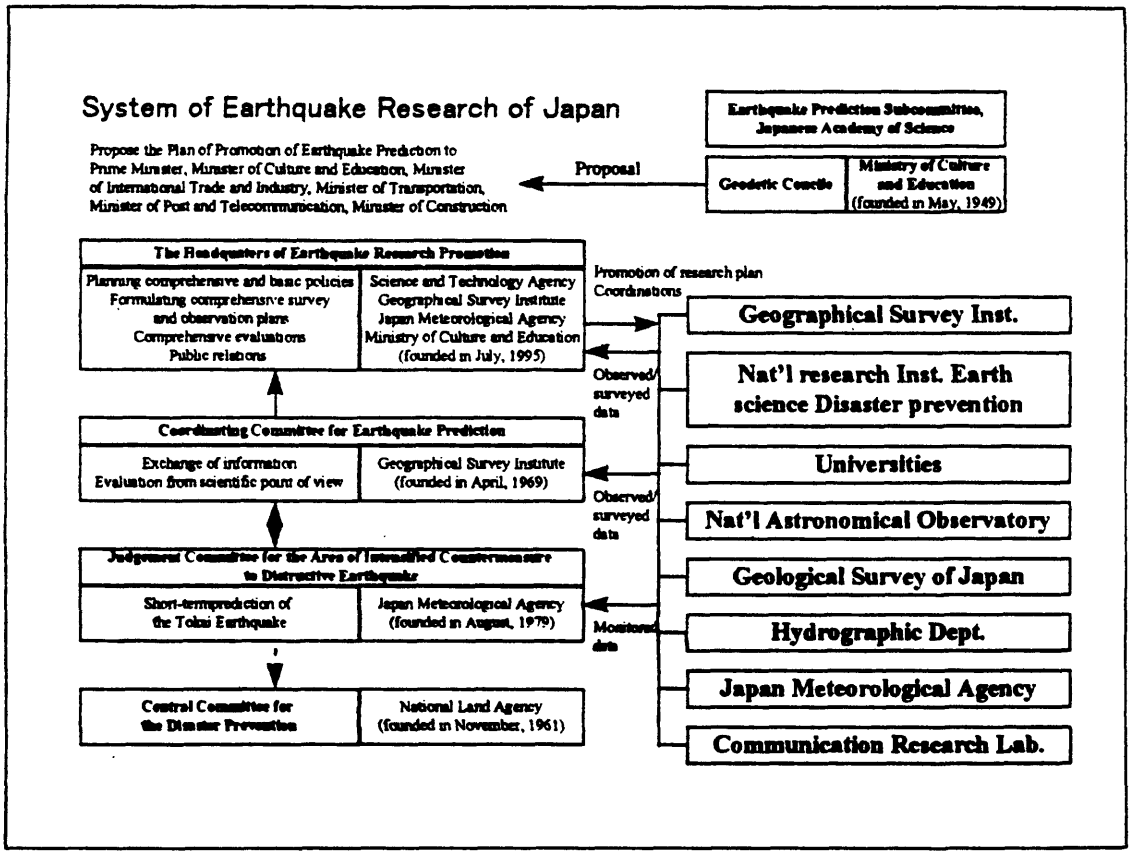

Fig.1 System of Earthquake Research of Japan

Main change from previous sytem of coordination and information exchange is that the promotion of earthquake research and the publicity of the information especially for hazard mitigation bodies are clearly stated as a task of headquarters

which consists of vice ministers of each ministries. Although the new system was established. Coordinating Committee for Earthquake Prediction(CCEP) and other existing bodies are given important role of information source for Earthquake Research Committee.

The Policy committee encourages each responsible organization to establish so called basic observational networks such as GPS array and seismograph array. The information of crustal activities obtained through such observations are to be open to public. This is the key to promote earthquake research and preparedness of hazard mitigation bodies.

3. Comprehensive Crustal Deformation Monitoring System of GSI

Among those activities, we will explain Comprehensive Crustal Deformation Monitoring System using space geodetic technology operated by GSI. Comprehensive Crustal Deformation Monitoring System of GSI presently in operation consists of GPS regional array with 610 on line receiver stations and 2 VLBI permanent stations. By the end of March 1997 (FY 1996 in Japan). it will become 885 on line GPS stations and 4 VLBI permanent stations. The configuration of the network is shown in Fig.2.

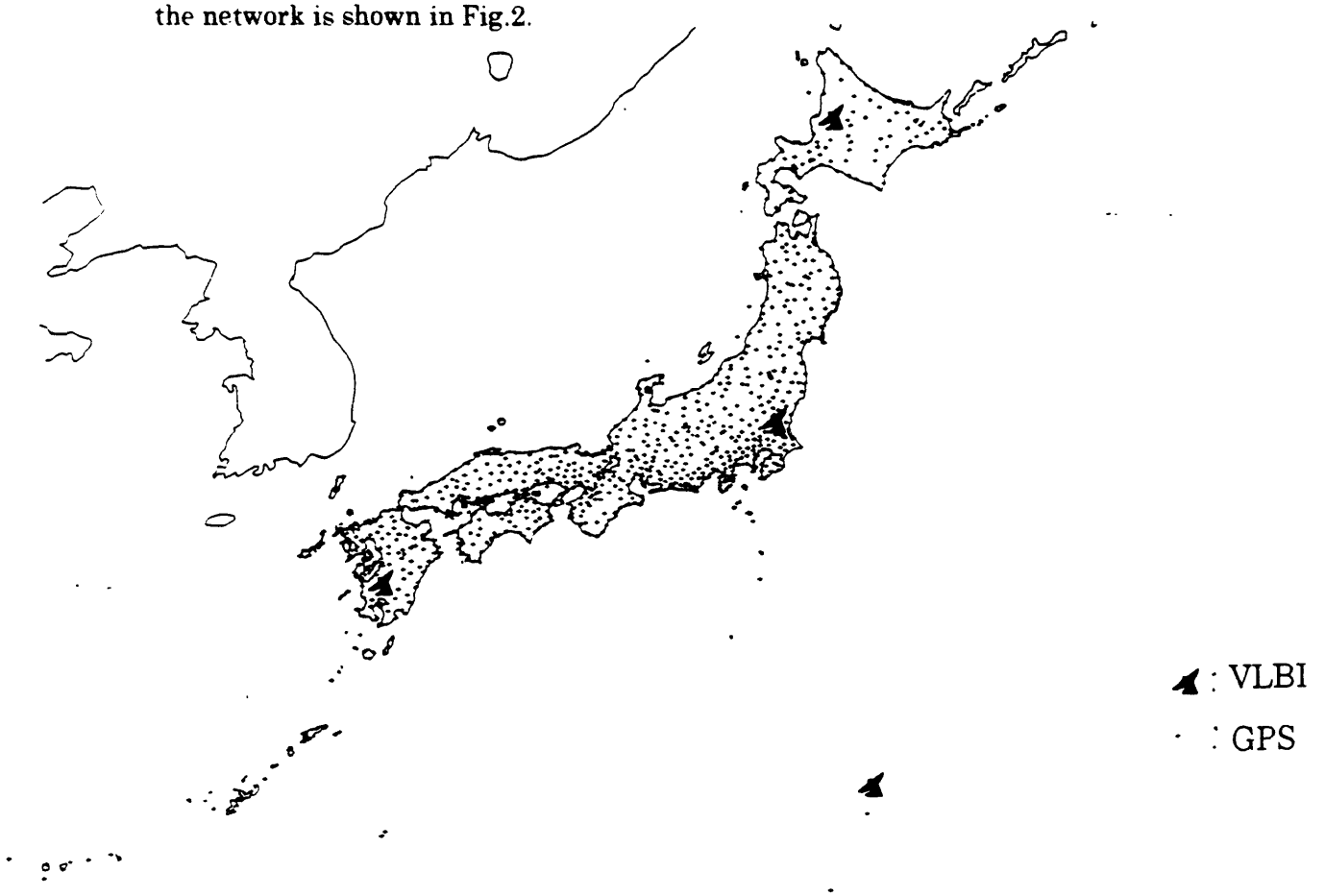

Fig.2 Configulation of Comprehensive Crustal Deformation Monitoring System of GSI as for March 1997.

The system is connected to world wide network through VLBI by DOSE project which is being carried out together with NASA, USA and also through GPS by IGS (International GPS Service for Geodynamics) project under International Association of Geodesy. Each observation revealed tectonic plate motion in and around Japan.

For example, continuous effort by GSI, Communications Research Laboratory, Japan and NASA, USA using Kashima 26m telescope showed relative motion of Pacific Plate against North American (or Okhotsk) Plate. Repeated VLBI survey between Kashima and Chichijima showed motion of Philippine sea Plate relative to North American Plate to be ca. 3.5cm/year which agrees well with theoretical estimation by Nouvel 1 model (Fig.3). Recognizing effectiveness of the kind of observation, GSI is expanding its VLBI permanent stations to 4 stations network which covers Japanese islands.

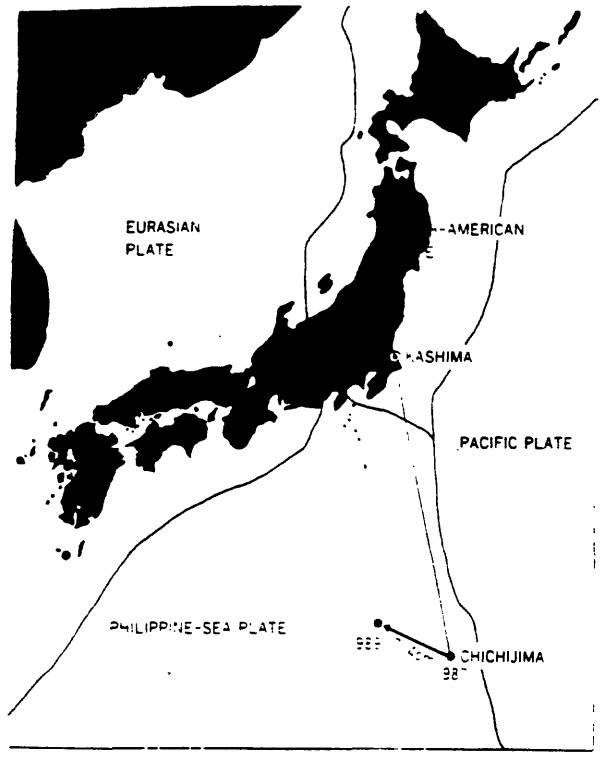

Fig.3 Movement of Chichijima measured by VLBI

Besides VLBI, GPS active arrays has its advantage in relatively low cost and easy operation that we can put more permanent stations to detect regional to local deformation continuously. GSI started to develop nationwide network with 210 stations in 1994. Soon after the system came to operation, eastern part of Hokkaido island was hit by Hokkaido-Toho Oki Earthquake (Shikotan Earthquake). The system revealed in a few days time crustal deformation over Hokkaido at maximum 40cm(Fig.4).

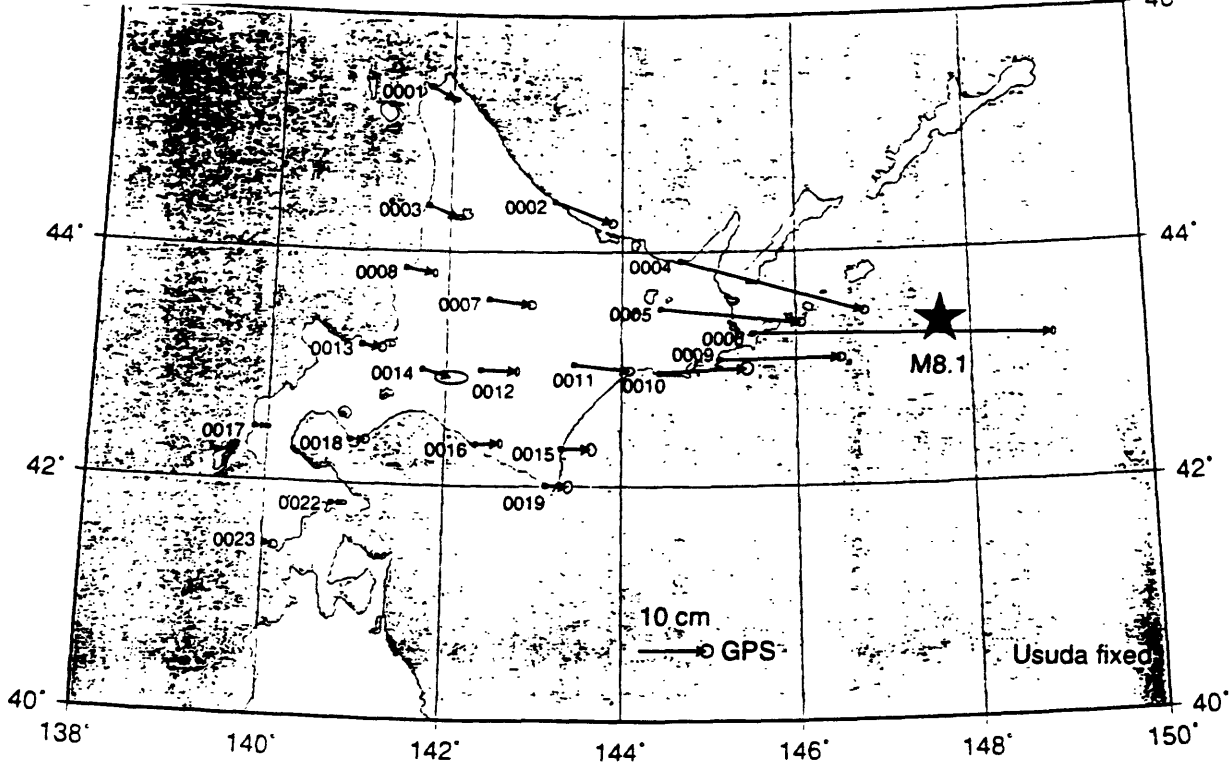

Fig.4 Coseismic displacement of GPS stations associated to 1994 Hokkaido Toho Oki Earthquake. Ellipses at the tip of arrows are error ellipses.

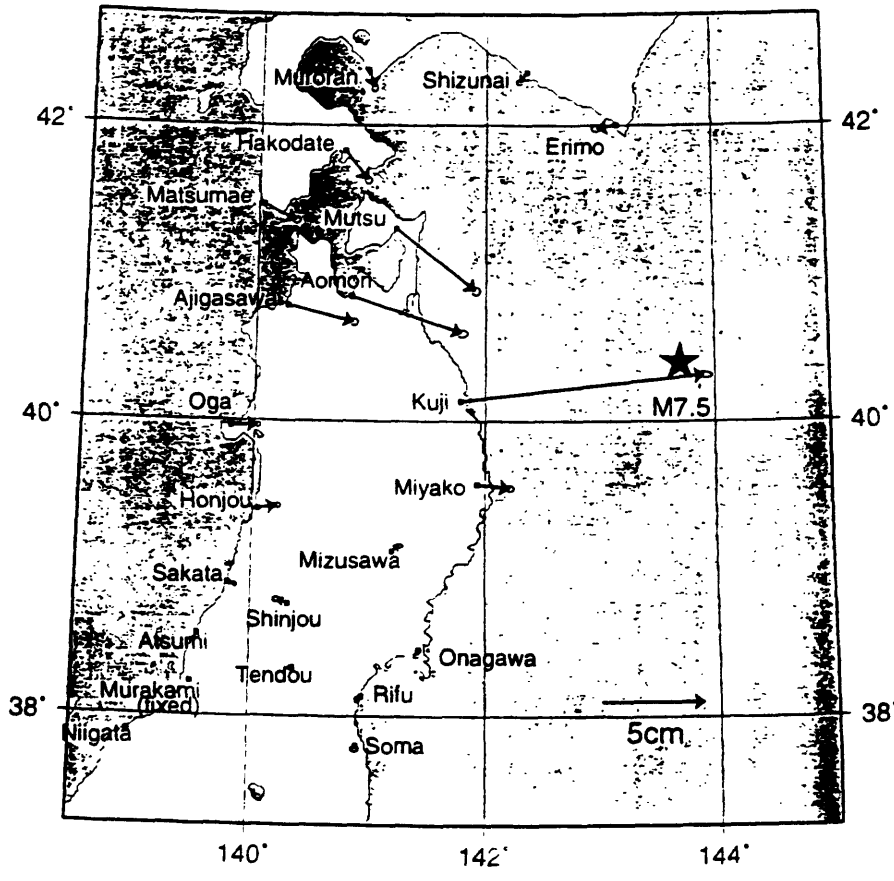

Fig.5 Coseismic displacement of GPS stations associated to 1994 Sanriku Haruka Oki Earthquake.

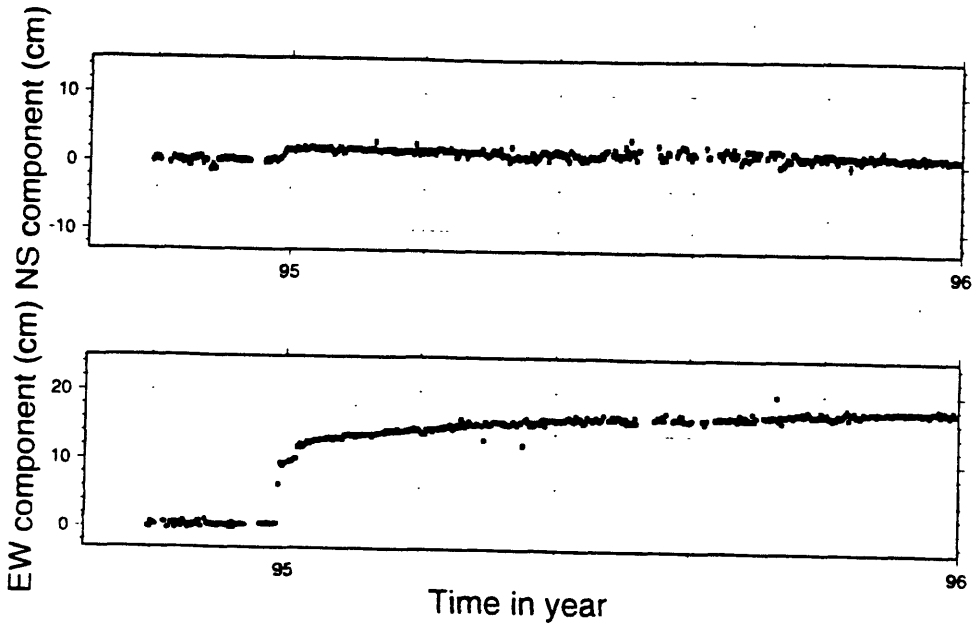

Fig.6 After effect of Sanriku Haruka Oki Earthquake.

Then. northern part of Honshu island was hit by Sanriku Haruka Oki Earthquake at the end of 1994. Again, the system could detect crustal deformation(Fig.5). What was interesting was that the earthquake was associated with long lasting after effect (Fig.6).

In the beginning of 1995. there occurred Hyogo-ken Nambu earthquake (Kobe earthquake). Although the magnitude of the earthquake was only 7.2 in JMA (6.9 by USGS), as the epicenter was close to million population city, more than 5000 casualty was reported.

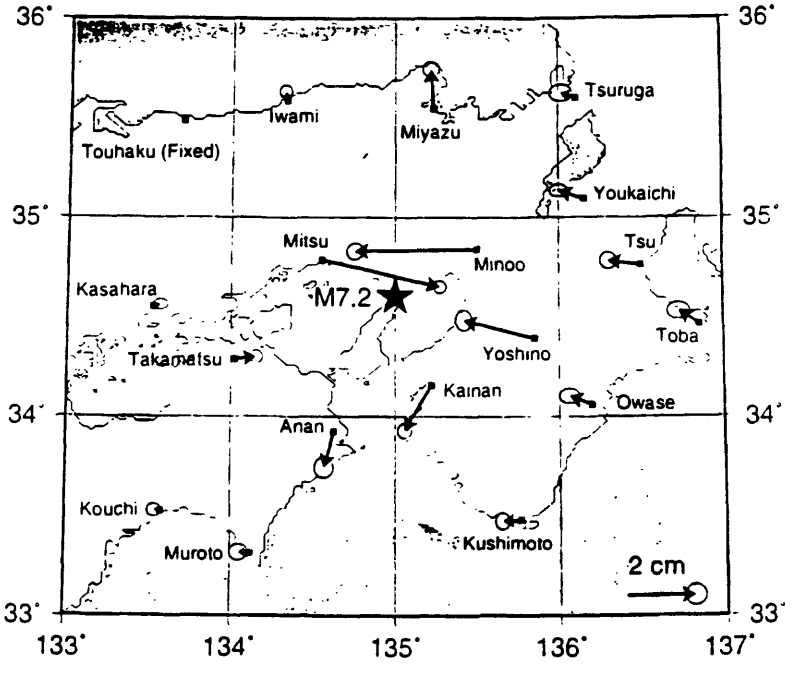

Fig.7 Coseismic deformation associated with Kobe earthquake.

In this occasion. the system reported area of crustal deformation (Fig.7) and played an important role to give reliable reference for reconstruction of infrastructures. GSI provided GPS data through computer network to support engineering survey to help prefectural government and municipalities carry on their recovery process. In August 11, 1996, central part

of Northern Honshu island was hit by M 5.9 (JMA) earthquake. Even for such small earthquake, the system reported crustal deformation within a few days time(Fig.8).

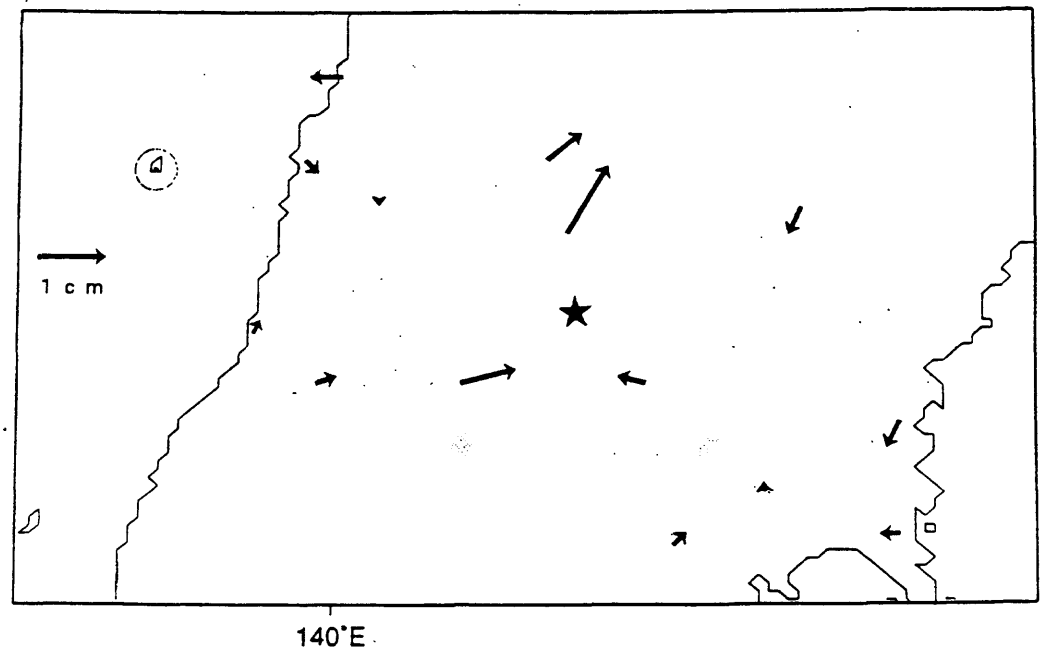

Horizontal Displacement (Tobishima Fixed)

Fig.8 Coseismic displacement of GPS stations associated to earthquakes occured in central part of northern part of Japan in 11th August, 1996.

Besides such brilliant co-seismic achievements, the system shows interesting results so far. One of them is the inter seismic deformation.

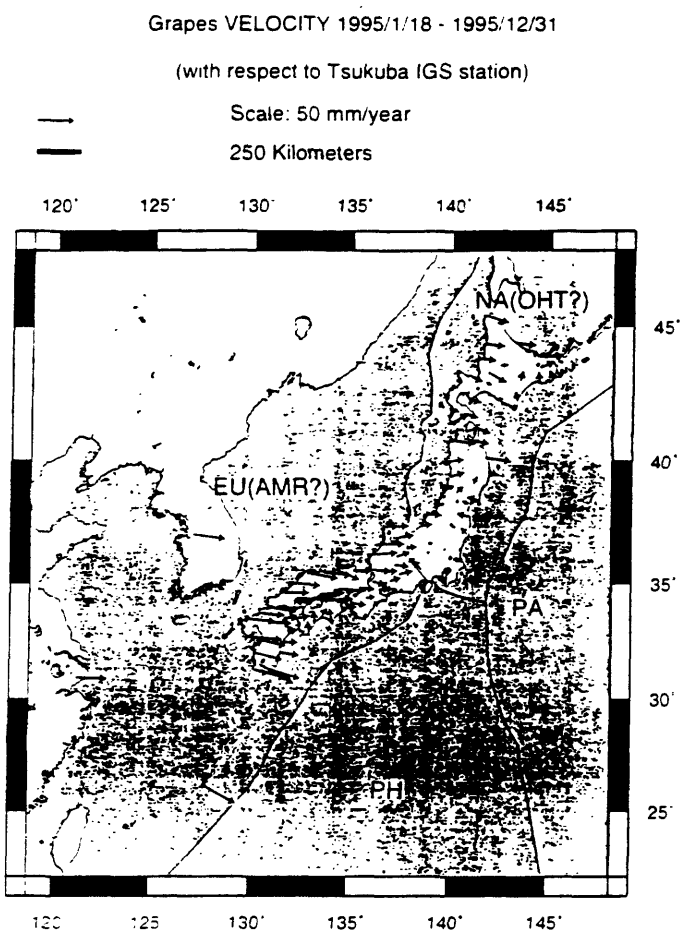

Fig.9 Horizontal velocity of GPS stations in and around Japan.

Figure 9 shows horizontal velocity field in and around Japan in reference to Tsukuba station. We can clearly see the collision between North American Plate and Asian (or Amur) Plate in the very central part of Honshu island. One of the author calculated areal dilatation from this data and found the peak of negative dilatation corresponds to the topographically high region. It suggests the central mountains may supported dynamically. Another interesting phenomena obtained through the system is the slow earthquake. In Boso peninsula near Tokyo, about ten stations start showing anomalous motion in early May, 1996 and such slow but anomalous motion lasted for about a week and returned to normal motion. The motion was equivalent to M7 or so if it has occurred instantly. This phenomena is a key to understand discrepancy between velocity of plate and frequency of seismic event. We are expecting more information of what is really happening in the earth through densified network when the system becomes 885 station network.

Other than space geodetic network, GSI is operating 11 on line electro-magnetic observation post which is fully automated, absolute gravity stations observed by 3 absolute gravity meters (FG5) and 25 tide gauge stations. Together with

conventional survey such as precise leveling. GSI is collecting comprehensive information on crustal deformations. The result is made public through CCEP activity, Earthquake Research Committee, Judgment Committee for the Area of Intencified Countermeasure to Distructive Earthquake, technical publications of GSI itself and so on.

4. GPS regional array in GSI's administration

GPS regional array is playing important role in Japanese Earthquake research. Besides that, the system is also used for daily administration of GSI. As is stated before, the permanent and reliable reference point on which users do not have to occupy themselves is a revolutionary new tools for both scientific and engineering surveys. Users can just occupy targets stations and download data of GSI's regional arrays. Through such system, many users can refer to the same stations instantaneously. This makes survey activities quite efficient and precise. The efficiency was proven in the surveys carried out after Kobe Earthquake. GSI is now preparing the system be used all over Japan. This is also a good reference for precise Geographical Information System(GIS). GIS is a digital system which requires quite high precision to positioning. This is especially so for Land Information System(GIS for cadaster) and Disaster Information System(DIS). Cadaster is related to citizens' property right. In case of DIS, often the area of application is destroyed and coordinates are the final reference. GPS regional array is expected its efficient work both in and between seismic events.

5. Conclusion

As is stated above, Comprehensive Crustal Deformation Monitoring System of GSI is expected to play an important role in the earthquake research in Japan. GSI will take its best effort to maintain the system in the best status and certify good circulation of the data and through that promote researches of tectonics and earthquake occurrence.

The Southern California Integrated GPS Network (SCIGN)

Kenneth W. Hudnut
United States Geological Survey
Pasadena, California
hudnut@usgs.gov

[Note: this abstract is almost entirely excerpted from various WWW pages, reports and proposals that have been prepared by the SCIGN Coordinating Board]

SCIGN is an array of GPS stations distributed throughout the greater Los Angeles metropolitan region. The goal of the experiment is to complement ongoing earthquake hazard investigations in a high-risk metropolitan area with high precision deformation measurements at densely spaced sites.

With its high population density and multi-trillion-dollar infrastructure, metropolitan Los Angeles is susceptible to even moderate earthquakes such as the 1994 Northridge earthquake. Recent studies by the Southern California Earthquake Center (SCEC) suggest that much larger events are possible. Every year, multi-million-dollar corporate and community decisions depend on scientific evaluation of earthquake hazard and risk.

We are vastly enhancing the earthquake monitoring effort in southern California using new geodetic technologies. The new array will measure how the ground deforms during the time interval between earthquakes, and also how it deforms when an earthquake happens. This type of measurement system will complement the newly expanding digital seismic network and provide data that are unattainable with even the most modern broad-band seismic instrumentation.

In a recently published debate, the promise of this initiative has been described (*Prescott*, 1996), as have been some criticisms of it (*Savage*, 1996). Despite the concerns and uncertainties that have been voiced about the SCIGN initiative, the project has gained momentum. A completed array will employ, for the first time, the full potential of GPS in earthquake research and hazard assessment in an active tectonic region particularly suited to this task. To achieve high precision, all new GPS sites will be carefully monumented (e.g., *Wyatt*, 1982; *Wyatt*, 1989; *Johnson & Agnew*, 1995). The array will:

- provide the most promising technique for assessing the earthquake potential of buried thrust faults and other faults that cannot be easily studied by paleo-seismology;
- extend the accuracy and push the ultimate capability of GPS for scientific and practical applications; and
- provide a multiple-use network that will serve the needs of surveyors, engineers, and others.

The Global Positioning System (GPS) array and laser strainmeters we plan to install will allow an unprecedented look at the pattern of crustal deformation throughout southern California. We will see, as never before, the process by which faults are loaded to the point of failure in earthquakes. This improved measurement system will also provide data that are essential to further refining seismic hazard maps of the region.

Our project has several major objectives:

- to provide regional coverage for estimating earthquake potential throughout southern California;
- to identify active blind thrust faults and test the "thin-skin" and "thick-skin" hypotheses of fault behavior in the greater Los Angeles and Ventura regions;
- to measure strain-rate variations to reveal the mechanical properties of earthquake faults;
- after an earthquake, to measure the response of major faults to the regional change in strain;
- after an earthquake, to measure permanent crustal deformation not detectable by seismographs.

GPS is the best new technology for addressing problems related to crustal deformation and earthquake mechanics. This five-year GPS experiment is one component of a much larger effort to address the discrepancy between historical seismicity and geologic rates both across southern California and globally. Measurements from the GPS network will provide a detailed precise velocity field of southern California that will be used to estimate parameters of crustal structure and rheology, and to enable better evaluation of earthquake processes and hazards.

Much has been accomplished with continuous GPS already by investigators in Japan and in the United States. The greatest benefits toward earthquake hazard reduction from these efforts will most likely be obtained at least several years hence, when the high precision velocity field is obtained and incorporated into regional probabilistic hazard maps, and once these measurements are used to address the region's scientific problems.

We are beginning a world class experiment with results that will be applicable to problems globally. With rates of crustal deformation among the highest in the contiguous United States, southern California is an ideal natural laboratory for this experiment: the region is well instrumented and the logistics are straightforward. We will also be able to test the accuracy of GPS in a complex environment and will be able to evaluate campaign style GPS projects run throughout the world. The Southern California Earthquake Center has put a significant investment into the thought behind the network and our resources are in place to expand it. Experts in all aspects of this project, ranging from implementation to data analysis, reside at institutions involved in planning and operating the network.

In addition to the objectives described above, the network will contribute to other aspects of seismic hazard reduction. Geodetic measurements can provide direct measurement of earthquake-induced ground failure, damage to engineered structures, and constraints on the integration of strong-motion records from earthquakes (e.g., *Hodgkinson et al.*, 1996; *Wald et al.*, 1996).

Our project has begun to establish a communications and data processing infrastructure that is already being used by other agencies who study permanent deformation. For example, the Los Angeles County Department of Public Works (Survey Division) has installed 2 GPS receivers on Pacoima Dam and another at nearby Fire Camp 9 on Mount Gleason, and data from these 3 stations are telemetered and processed as part of our data stream. The GPS system for monitoring Pacoima Dam has been fully operational since Sept. 1, 1995. This dam is a 120 meter tall concrete arch structure (built in the early 1930's). It withstood but was damaged by violent shaking during both the

1971 and 1994 earthquakes. The County is responsible for monitoring the structure's stability in response to reservoir loading during floods and future earthquakes. This pilot project has demonstrated how continuous GPS can monitor the integrity of engineered structures. We are finding that other agencies are interested in monitoring such structures as freeway overpasses and buildings using continuous GPS. We are developing partnerships for such multi-use applications of the GPS infrastructure, with the hope that such partnerships may help us support future operational and maintenance costs.

http://www.scecdc.scec.org/scign/

SCIGN is organized under the auspices of the Southern California Earthquake Center (SCEC), with major funding from the National Aeronautics and Space Administration (NASA), the United States Geological Survey (USGS), and the National Science Foundation (NSF).

Date	Description	Total Sites
1997 January 1	SIO, UCSB and JPL receivers installed	50
1997 July 1	Phase I complete	90
1998 January 1	Phase II complete	140
1998 July 1	Phase III complete*	250

* pending W. M. Keck Foundation and other additional funds.

SCIGN Coordinating Board

References:

Blewitt, G., M. B. Heflin, K. J. Hurst, D. C. Jefferson, F.H. Webb and J. F. Zumberge, Absolute far-field displacements from the June 28, 1992, Landers earthquake sequence, *Nature*, v. 361, 340-342, 1993.

Bock Y. et al., Detection of crustal deformation from the Landers earthquake sequence using continuous geodetic measurements, *Nature*, v. 361, 337-340, 1993.

Hodgkinson, K. M., R. S. Stein, K. W. Hudnut, J. Satalich and J. H. Richards, Damage and restoration of geodetic infrastructure caused by the 1994 Northridge, Calif., earthquake, U. S. Geological Survey Open File Report #96-517, 1996.

Hudnut, K.W., Earthquake geodesy and hazard monitoring, *Reviews of Geophysics (Supplement: U. S. National Report to IUGG, 1991-1994)*, pp. 249-255, 1995.

Johnson, H. O. and D. C. Agnew, Monument motion and measurements of crustal velocities, *Geophys. Res. Lett.*, v. 22, pp. 2905-2908, 1995.

King, N. E., J. L. Svarc, E. B. Fogleman, W. K. Gross, K. W. Clark, G. D. Hamilton, C. H. Stiffler, and J. M. Sutton, Continuous GPS observation across the Hayward fault, California, 1991-1994, *J. Geophys. Res.*, v. 100, 20271-20284, 1995.

Prescott, W. H., Will a continuous GPS array for L.A. help earthquake hazard assessment?; Yes: The L.A. array will radically improve seismic risk assessment, *EOS, Trans. AGU*, v. 77, No. 43 (Oct. 22, 1996), pp. 417, 419 and 427, 1996.

Savage, J. C., Will a continuous GPS array for L.A. help earthquake hazard assessment?; No: The L.A. array is not ready for prime time, *EOS, Trans. AGU*, v. 77, No. 43 (Oct. 22, 1996), pp. 417, 419 and 427, 1996.

Shimada, S. and Y. Bock, Crustal deformation measurements in Central Japan determined by a GPS fixed-point network, *J. Geophys. Res.*, v. 97, 12,437-12,455, 1992.

Tsuji H., Y. Hatanaka, T. Sagiya and M. Hashimoto, Coseismic crustal deformation from the 1994 Hokkaido-Toho-Oki earthquake monitored by a nationwide continuous GPS array in Japan, *Geophys. Res. Lett.* v. 22, 1669-1673, 1995.

Wald, D. J., T. H. Heaton, and K. W. Hudnut, The slip history of the 1994 Northridge, Calif., earthquake determined from strong-motion, teleseismic, GPS and leveling data, *Bull. Seis. Soc. Amer.* (Special Issue), v. 86, No. 1, Part B, pp. S49-S70, 1996.

Wyatt, F., Displacement of surface monuments: horizontal motion, *J. Geophys. Res.*, v. 87, pp. 979-989, 1982.

Wyatt, F., Displacement of surface monuments: vertical motion, *J. Geophys. Res.*, v. 94, pp. 1655-1664, 1989.

The Crustal Deformation Monitoring System in the Tokyo Metropolitan Area

By

F.Takahashi, N.Kurihara, H.Kunimori, Y.Koyama, H.Kiuchi, T.Yoshino, T.Ootsubo, Y.Takahashi, M.Imae, S.Hama, T.Kondo, T.Takaba, T.Iwata, Y.Hanado, M.Sekido, J.Nakajima, T.Gotou, R.Ichikawa, E.Kawai, A.Kaneko, C.Miki, J.Amagai, H.Nojiri, M.Hosokawa, and K.Uchida

Communications Research Laboratory, Japan

Abstract

The Tokyo Metropolitan Area is situated above the triple-layered structure of the major tectonic plates: the North American, the Philippine Sea and the Pacific plates. The Communications Research Laboratory (CRL) had developed the Crustal Deformation Monitoring system for the Tokyo Metropolitan Area using both VLBI and SLR. This program is called the "KeyStone Project (KSP)". The four observation stations (Kashima, Koganei, Miura, and Tateyama) in this program are located around the Tokyo Metropolitan Area. This system is characterized by no operator at each station, and by the remote operation system from the center station, and by real time VLBI system. The real time VLBI was realized this summer.

The first 24 hours test experiment was conducted on 29th August in 1994, and we started 5 hours experiments between Kashima and Koganei on every week days since 31th of January in 1995. Since December in 1995, Miura station was participated and the daily 5 hours VLBI experiments have conducted on six baselines among Kashima, Koganei, Miura and Tateyama since September in 1996. Since the VLBI experiments were conducted in 64 Mbps mode as the test period, the observed precision was 6mm in the horizontal movements and 3cm for the vertical movements. The precision was three times worse than the final performance. The VLBI experiments

in the 256Mbps mode will be started in this autumn. The precision in VLBI will be 2mm for horizontal movement and baseline length, and 1cm for vertical movement in the regular 5 hours VLBI experiment, and the half of these precision will be obtained for 24 hours VLBI experiment.

SLR observations will be conducted always in the clear sky. The precision in SLR are expected to be a few mm. The SLR observation will be started at early next year.

Koganei station is moving in rate of 5mm/year towards North-East direction, and Miura station is moving in the rate of 25mm/year towards North-West direction with respect to Kashima station. The Miura station is moving down in the rate of 2cm/year. The movement of Kashima obtained in the global VLBI network was corrected, and the movements at Kashima, Koganei and Miura against the North American Plate were obtained. The direction of movement at Kashima agreed with the pressure of Pacific plate motion, the direction of movement at Koganei and Miura agreed with the motion of Philippine Sea plate.

1. Introduction

Since 1923, we did not have an earthquake in Tokyo as big as the Great Kanto earthquake. Hence it is anticipated that the next disaster may hit Tokyo in the near future considering the history of seismic activities around Tokyo. In this time period, the performance of geodetic instrument is improved dramatically. Space geodesy including VLBI (Very Long Baseline Interferometry), SLR (Satellite Laser Ranging) and GPS (Global Positioning System) made precise geodetic measurement of the globe and the country possible, which allows the crustal deformation and plate motion. Beginning 1993, the CRL started constructing a crustal deformation monitoring system using four VLBI/SLR stations deployed at Tokyo Metropolitan area aiming at detection of the crustal deformation as precursor of a great earthquake. It is named the Key Stone Project (KSP). The observation network consists of four stations (Koganei, Kashima, Miura and Tateyama). The KSP VLBI system is designed so that the unmanned operation may be possible during the observation. Data processing is also easy to perform for the routine work.

The four stations are connected via broadband communication link to start the first real time VLBI. For SLR operation, one operator at the central station in Koganei will control SLR network in the KSP finally.

After the completion of the VLBI system, we started daily observation between four stations using the data recording system. We determined the baseline vector in 24 hours after the last VLBI observation in the quickest case. The results are sent to JMA (Japan Meteorological Agency), and provided to The Coordinating Committee for Earthquake Prediction, regularly.

The result of the KSP is also available via internet as soon as the data analysis is finished.

2. Overview of KSP Observation System

2.1 KSP Four Stations

CRL started the Key Stone Project (KSP) using the space technology from 1993 in order to detect the crustal deformation as of precursor of a earthquake. We construct the both VLBI and SLR new station at four places around the Tokyo Metropolitan Area. The name of KSP stations are "Koganei", "Kashima", "Miura", and "Tateyama" as the respectively. Each VLBI station has an 11m-diameter parabolic antenna and VLBI data acquisition system. These stations have already been available for the daily VLBI observation. Each SLR station has 75-cm optical telescope and laser ranging equipment. The SLR observation is made in cleared up every day. The four remote VLBI and SLR stations' data acquisition facility was automatically controlled from the Koganei central station using the Wide Area Network.

2.2 VLBI System

The KSP-VLBI Observation System (Yokoyama et al, 1996) has been developed with the following aspects in mind.

The system should provide accurate daily observed coordinates of three VLBI stations with respect to the fixed coordinates of the reference VLBI station (Kashima or Koganei) at mm-order level from about 5 hours of observation time every day.

The observations at four VLBI stations should be highly automated. All the necessary operations and system check-outs should be done automatically or remotely from Koganei central station so that almost no human operations at each station should be required. Reliability of the observation system and the data processing system should be highly achieved.

The observed data recorded on tapes should be processed promptly after each experiment and the results should be obtained within about one and a half days from the last observation.

The schematic overview of the entire system of the VLBI part of the KSP is shown in the Figure 2.2.1. The VLBI observation system is consist of :

(1) four VLBI stations equipped with 11m diameter antenna at each site,

(2) the central station at Koganei manages the daily observations and processing tasks

(3) the sub-central station at Kashima to back-up functions of the central station.

In addition to the VLBI observation system.

(4) the real-time VLBI facilities,

(5) the wide area computer networks connecting each sites, and

(6) the software to support the observation system are taking part in the entire system.

The each of four VLBI stations is equipped with a Cassegrain antenna which has an aperture of 11m-diameter parabolic antenna and a dual frequency receiver system for S-band and X-band. The data acquisition system used at each station has been newly developed based on the K-4 VLBI system (Kiuchi et al, 1991) to achieve higher recording speed at 256 Mbps (bit per second). All the observation hardware and software at four stations are almost identical.

Antenna and Receiver System

The antenna is an alt-azimuth-drive and has 11-m modified surface parabolic dish. It is equipped with Frequency Selective Sub Reflector (FSSR) in order to give it high aperture efficiency in both the S and X bands. We designed the antenna's reference position (geodetic VLBI reference point) to be fixed with 3 mm during a year. So the base of the antenna pedestal is firmly connected to the hard ground by long pilings. The receivers are equipped with FET-type low-noise pre-amplifiers and an optical-fiber IF signal transmission system for the S and X bands.

VLBI Data Acquisition System

The VLBI data acquisition system consist of a local oscillator, a video converter, an input interface unit, on output interface unit, a data recorder and digital mass-storage system. The required specifications for the VLBI data acquisition system are:

(1) one and two-bit quantization capability,

(2) sampling rate of up to 64 Mbps,

(3) an image rejection ratio of better than 20 dB for the entire video bandwidth.

These requirements are realized by a 64 Mbps A/D converter with a threshold level control circuit, a digital filter, and a wide bandwidth image rejection mixer.

Reference Signal Distribution System

The reference signal distribution system provides the highly stable signals (1 PPS, 5 MHz, and 10 MHz) and the time code for the VLBI data acquisition system. These reference signal are generated from the hydrogen maser atomic frequency standard which has a frequency stability of about 2-3 x $10^{-13}/\tau$ with regard to the time scale τ (sec). The time code is obtained from the GPS station clock. The basic design concept of the reference signal distribution system is high stability as well as high reliability.

Data Processing System (Correlator)

CRL are developing an XF type VLBI correlation processor by making use of a field programmable gate array, which was specially designed for KSP-VLBI correlator. The outline of the correlator is

(1) Automatic bit synchronization during multi-baseline processing,

(2) Network filing system (NSF) for stored correlated data,

(3) maximum data rate is 256 Mbps,

(4) 2-bit sampled data processing capability,

(5) 16 ch high speed (32 Mbps/channel)processing,

(6) compact and light-weight,

(7) signal provided by VME back plane.

Automatic Monitoring System

The automatic monitoring system at each VLBI station observes the status and error messages of VLBI data acquisition system, effectuating fully reliable automatic VLBI operation with just one operator at the Koganei central station. The system also acquires data used in VLBI data analysis processing and checking of the system.

It regularly acquires data from weather stations, time interval counters for delay calibration, hydrogen masers, etc. by background processing, and writes in log-files for all data every minute. It acquires video data from monitor cameras on command. The information and data are transmitted to the Koganei central station using the computer network.

It also provides an easy-to-use interface for the operator at the Koganei central station and at the Kashima sub-central station. The non-professional operator can monitor the status of the observation system, change various settings to optimize the system, and resolve or at least clarify cases of malfunctions.

Data analysis system

The data analysis system of the KSP was also designed to be easy-to-use, and highly automated. After correlation processing and bandwidth synthesis of all observation data, a single action of the operator causes X band and S band databases to be created and analyzed, and the results are interpreted automatically. Only if errors occur or if the estimated results are not reasonable, the operator is notified and the databases is investigated with the operator-friendly Graphical User Interface. Interested researchers can access the latest result

on the Internet WWW (http://ksp.crl.go.jp). Near 500 daily experiments have been processed with the system, and regular processing began on the daily basis from December 1,1995.

2.3 SLR System

SLR is a space geodetic technology which can measure the distance between a ground station and a satellite most precisely in current methods. A very short laser pulse is transmitted from a telescope in a ground station, and it is retro-reflected vise versa by a corner cube reflector on a satellite and goes back to the station. The round trip time is measured, that is equivalent to measure the distance.

Not only the satellite orbit but also many geodetic parameters such as station coordinates can be determined by analysis of SLR data. In other words SLR measures the absolute time of flight of photon so that the geometry of satellite and laser station can be determined precisely as long as the system calibration error is controlled in a negligible level.

The CRL developed CRLLAS (CRL LASer ranging) system using a 1.5 m diameter telescope and has operated since 1990 (Kunimori, 1991). We also developed analysis software for laser ranging data

(Otsubo, 1994). The new KeyStone system succeeds the system concept in some aspects, but involves many new concepts. Its specifications are shown in Table 2.3.1. The KSP-SLR stations will serve not only a local geodetic motion but also precise geodetic points in the world by constantly providing analysis centers with the range data.

Role of SLR in the KSP

SLR analysis results for the station coordinates ensure that the VLBI results is valid. If the two techniques show similar results, the probability that they detect the crustal deformation becomes stronger. SLR is an optical technique, that is, it can be operated only in clear sky. VLBI hence excels SLR in the continuity of the data generation. However SLR has unique feature that can be cooperated with VLBI. Because geodetic satellites can be tracked from all over the world, the geodetic network is easily expanded worldwide just by adding KSP-SLR data to global data. It means SLR can constantly watch the motion of whole KeyStone network with respect to other stations as well as the motion within the network. SLR will give more accurate solution in the vertical component of station coordinates. This is because the atmospheric delay model is better in optical and because SLR does not need a clock estimation.

New Concept for Automatic and Routine Operation

In the routine observation, the four SLR stations will be remotely operated only by one operator sitting in the central station, unmanned in each station. We are required to generate the station coordinates solution constantly. The KSP system combines the fixed station concept and the mobile station concept; the telescope set is rigidly fixed on the earth but the trailer box which contains laser and measurement facilities is mobile and compatible each other (Figure 2.3.1).

If some instruments fail, the operation can continue only by exchanging the trailer box, not waiting for the system recover. Aircraft detector is equipped to avoid hitting laser beam to a person in sky. A 1.54 micrometer wavelength laser that is safe for human eyes is transmitted just before the main pulse of laser ranging, second harmonics of Nd:YAG, 0.532 micrometer. The main pulse is shut when the eye-safe laser detects an object in air. The 75-centimeter

telescope is never open to the air outside, covered by a waterproof dome. The laser and other lights travel through a window on the dome.

All stations are connected by computer network. Local stations can be remotely operated from the central station. The real-time status of ranging operation, i.e. the data generation information, the health of instruments, the image in local station, etc., is transferred and watched at the central station. Almost all the operations can be done automatically.

It does not require any help of man to detect the return signal from satellites, to reject the noise data, to analyze the ranging data and to find a system failure. The main task of the operator is to watch the sky condition and to solve problems the computer cannot.

New Technology for Higher Accuracy

We are developing this system with a goal of 5-millimeter precision and accuracy in satellite ranging. Several new technologies are introduced in this project: The laser is 30 picoseconds in pulse width (full width at half maximum) though 100 picoseconds pulse width is a typical value for current SLR systems in the world. The short pulse improves the ranging precision significantly. Its repetition rate is variable from 10 to 1000 Hz.

Such a high repetition laser makes the return detection easier and faster, and naturally gives high data productivity. Two kinds of fast-response detector, a micro-channel plate photomultiplier (MCP-PMT) and a single-photon avalanche photo diode (SPAD), are equipped and they can be used simultaneously.

The comparison of the data from the two detector strengthens the accuracy, since they utilize the different techniques. System delay, i.e. the extra internal optical and electrical path, can be monitored accurately. Retro-reflectors are positioned at the reference point of the telescope and it can be ranged during the satellite tracking in real time.

The system delay can firstly directly determined through this. Moreover, three poles outside and two poles below the telescope also have retro-reflectors, whose positions are known in several millimeters precision. The ranging to all the poles secondly gives the system delay. Using the two results, the accuracy of the system delay whose error degrades the ranging data especially in vertical component will be assured.

To shorten the time resolution of the station coordinates determination, the analysis software treats the range data of multiple satellites and gives combined results, whereas generally SLR analysis is done per satellite. Various analysis methods are available, as all the KSP-SLR stations are scheduled to track the same satellite at the same time. The comparison of the results by different methods strengthens the geodetic accuracy. The algorithm and numerical constant are compatible with IERS Conventions 1996 (McCarthy, 1996), and simultaneously they are almost compatible with the VLBI analysis software.

3. Major Results

3.1 Daily VLBI Observations for Two Years

The first VLBI experiment of the Key Stone Project was performed on August 28, 1994. Only two stations, Kashima and Koganei, participated in the first session since the establishment of these two VLBI stations preceded to the other two stations. On January 17, 1995, a special VLBI experiment with Kashima 34m station and the two KSP stations was

performed to make a tie between the KSP VLBI network and a global Terrestrial reference frame. Regular VLBI experiment with about 5.5 hours of duration began on January 30, 1995, at five-days-a-week basis. The duration of 5.5 hours corresponds to about the 200 minutes of recording time which fit one ID1 cassette at 64 Mbps recording rate.

The first experiment with three stations of the KSP network was performed on May 20, 1995, with an addition of the Miura VLBI station. Everyday VLBI observations, literally, began on November 1, 1995. It became possible with the completion of the KSP correlator.

Three-baseline correlator became operational in May, 1996, and the six-baseline correlator became operational in September, 1996. Tateyama VLBI station began its participation in the VLBI experiment on September 1, 1996. hence the full KSP VLBI network was realized

At present on November 9, 1996, 470 independent VLBI experiments have been performed and processed in total. All the experiments were analyzed by using observed group delay values based on the ICRF94 and ITRF94 reference frames, EOP90C04 series of Earth Orientation Parameters, and ocean loading parameters calculated by the GOTIC program (Sato and Hanada, 1984; Sengoku and Sato, 1996).

A set of correction parameters provided in the IERS annual report for 1994 (IERS, 1995) were applied to the EOP90C04 values to maintain the their consistency with the ICRF94 and ITRF94 reference frames. Usually, the coordinates of the Kashima VLBI station were fixed in the data analysis process to the values determined from the results of the special tie experiment and the site velocity of the Kashima 34m antenna station given in the ITRF94. In rare cases when data from Kashima VLBI station are not available, the coordinates of the Koganei VLBI station were fixed.

Figure 3.1.1 shows the estimated baseline lengths between Kashima, Koganei, and Miura VLBI stations and their linear trend estimated by the least-square methods.

The values of reduced chi-squared range from 1.40 to 1.81 reflecting the existence of some outliers and the short-term variation of the estimated baseline lengths. The rates of change of the baseline lengths have been precisely determined with the estimated standard error of 0.58 mm/year for the case of the Kashima-Koganei baseline. Repeatability of the estimates of the baseline lengths can be evaluated with the weighted root-mean-squared of the residuals from the linear trend, and these values range from 5.56 to 6.42 mm.

Figures 3.1.2 and 3.1.3 show the estimated topocentric site position displacements of Koganei and Miura VLBI stations, respectively, projected in the three perpendicular directions. The site velocity of the Kashima VLBI station defined on the ITRF94 reference frame was subtracted, therefore these displacements are the changes of the site positions with respect to the fixed Kashima VLBI station.

If the horizontal motion of each station is focused, the Koganei VLBI station is moving at 4.9 mm/year towards N38 degree E and the Miura VLBI station is moving at 24.8 mm/year towards N24 degree W. Since it is well investigated that the Kashima VLBI station is moving westward with respect to the stable part of the North American Plate and the Eurasian Plate as a result of the contraction caused by the motion of the Pacific Plate (Heki et al., 1990), the eastward velocity of the Koganei VLBI station seen in the Figure 3.1.2 can be considered as a difference of the westward velocity of these two stations.

It seems natural to assume both Kashima and Koganei stations are moving westward and the velocity of Kashima is faster than Koganei since Kashima is closer to the plate boundary. On the other hand, the northward velocities of Koganei and Miura stations can be explained by

the northward contraction of the region caused by the motion of the Philippine Sea Plate Baseline length between Koganei and Miura is decreasing at 9.2 mm/year and this shortening can be regarded as the accumulation rate of the distortion.

It seems very important to monitor these behaviors for better understanding of the mechanisms of huge earthquakes in this area caused by the interactions between these three plates.

3.2 Success of Real-Time VLBI via Giga-bit-rate Optical Fibers

Communications Research Laboratory and NTT Transport Processing Laboratory have developed a new VLBI system, called the KSP (KeyStone Project) real-time VLBI system, using a high-speed ATM (Asynchronous Transfer Mode) network. In real-time VLBI, the cross-correlation processing and data observation are carried out simultaneously, and it takes about three hours to analysis the crustal deformation data after the VLBI observation is completed. This system is one of the most significant technologies in the KSP, and will give us data on crustal deformation in the Tokyo Metropolitan Area quickly.

Real-Time VLBI System

In KSP, the precision of 3 mm is achieved using a tape-based VLBI system. In the current VLBI system, the observed data is recorded on magnetic tapes at the observing site, and the tapes are transported to the correlation site by mail, and the analysis is done the next day. So it takes one day to obtain a measured value of crustal deformation. The major cause of the wasted time is data (tape) transportation, which takes over 18 hours.

This problem is solved by using an ATM network, which has a transmission capability of up to 2.4 Gbps in a basic-optical fiber link. The observed VLBI data is transmitted through the ATM communication network instead of being recorded onto the magnetic tapes. The KSP has four VLBI stations connected by an ATM network and the data transmitted from these remote observing stations to the correlation site in Tokyo, is processed in real time. In ATM, the transmission rate (capacity) can be chosen freely. There is no need changes in the data transfer rate to be controlled on the network side. A block diagram is shown in figure 3.2.1.

Real-time VLBI is expected to be one of the breakthrough technologies for improving VLBI performance. In the KSP real-time VLBI system, it is possible to transmit the signals from the four stations along one transmission path. Signals from the each observation station are multiplexed by the cross-connect switch located in ATM network, and the multiplexed signal is led to the receiver via one transmission path. In the receiver, the multiplex signal is separated into the data of each station and restored in the receiver as a digital signal after the delay fluctuation is absorbed.

The real-time VLBI system also has a function that removes delay of the transmission system in the receiver. An input/output signal of the ATM transmission system is unified to the D-1 standard (same as tape-based VLBI interface), and is adapted to have the same data format as the tape-based K-4/ KSP system. Adoption of the identical data format, enables the tape-based correlation processing system to be used as the real-time system.

The K-4/KSP VLBI data acquisition system consists of a reference distributor, IF distributor, local oscillator, video converter, input interface. The local oscillator synthesizes the local frequency signal for the video converter By the action of this video converter, windows in the IF-signal (500-1000 MHz) input are converted into video signals (32 MHz). The input interface unit samples the video signal from the video converter, and sends the

digital data to the ATM transmitter together with the time data, which is phase locked to an external time reference. Time-code insertion can be selected to be uniformly spaced or at uniform time intervals, or no time-code can be selected. In real-time VLBI, uniformly spaced time-code is adopted. The input interface is adopted as a VSOP

Data acquisition Terminal.

To adopt tape-based VLBI and real-time VLBI with identical formats, it is possible to use the same data-acquisition and correlation systems. The picture of the correlation site is shown in figure 3.2.2. A tape-based 4-station 6-baseline KSP system is used for daily crustal measurement. Good fringes (correlated patterns) are obtained in real-time 4-station 6-baseline KSP system (Figure 3.2.3), and we are making an automatic correlation control software.

3.3 Installation of SLR Stations

The KeyStone (KSP) Satellite Laser Ranging (SLR) system is not only a single instrument but four set of which are composed into a fully integrated network as operates as a single instrument. To achieve its fundamental objective of millimeter accuracy on baseline and heights of the stations, KSP SLR system has had to incorporate a wide range of new technologies, including telescope, dome, laser, timing system, calibration system as well as automation and remote control system.

Following the contract in October 1995, four SLR systems had been designed, manufactured and were delivered in March 1996, and are now installed in Tokyo metropolitan area (See Figure 3.3.1)

This section describes some of new technologies utilized in KSP and presents installation status of the systems.

Telescope and Dome

The KSP telescope and dome are designed for dedicated automatic SLR with the mm accuracy and installed in a KSP observation tower. Figure 3.3.2 shows a schematic and actual view of KeyStone telescope in the observation tower.

The telescope is mounted on a concrete pier with height above ground from 5 m to 8.5 m and with depth under ground from 5 to 10 m depending on how solid ground base of each site is to maintain the pier itself to the fixed crust. The concrete pier is isolated in structure with the observation tower on which dome is located.

Temperature and Humidity of the room inside the observation tower is controlled by air-conditioner to +/–2 degrees C and 50 %, respectively. The reference point of the telescope is the intersection of Azimuth and Elevation axes which is stable in the space within 0.5 mm. This point is set on the surface of the tertiary mirror and measured by a small corner cube located exactly on the plane of collimated laser beam passing on the intersection of the axes.

The KSP dome is fully sealed and optical interface is through a ranging window made of high quality glass. Because of no possibility of weather intrusion, it reduces mechanical corrosion in dome, and to be fail-safe under power fail conditions and stabilize temperature, lower humidity and dust proof which are crucial to telescope optics performance and for maintenance.

Laser and Electronics

All the optics and electronics except for telescope and dome needed in SLR is set in a temperature controlled trailer box dimensioned by 7.5m x 2.4m x 2.2m. It aims the trailer box can be exchanged by spare box when repair is needed and multiple boxes can be collocated at an observation tower with common telescope for test and calibration.

A diode-pumped laser oscillator is adopted as KSP laser subsystem for stable operation with high performance of laser pulse and energy and for longer mean time between maintenance break. Laser has multi-stage operation mode in pulse energy and repetition rate which enable us not only to scale a variety of targets from low orbit satellite to geosynchronous satellite in the standard receiving condition, but also to perform the search and go observation by intervening multiple satellite.

Ranging electronics consists of a single photon receiver, a custom epoch timing unit, GPS receiver and calibration electronics which has accuracy of as much as a few picoseconds to ensure any system bias and its drift except systematic error due to atmosphere and target shape effect is within 1 mm. Kashima station has capability of optional two color laser ranging for calibration of atmospheric excess path down to a few mm.

Network and Software

Koganei has the function of control and monitoring of all the KeyStone stations using a dedicated 128 kbps communication network. While the Koganei central station deliver the schedule and orbit information, each station observes satellites automatically and send the observation data and instrument status. An operator at Koganei station can override any command to initiate and stop observation by monitoring weather information, alarm status as well as video information from multiple cameras in the station. Figure 3.3.3 shows a overview of the control and monitoring room of the Koganei central station.

Analysis center is located at Koganei, where all the orbital prediction and determination and baseline analysis are conducted by commercial Geodyne II based analyzer and CRL short arc analyzer (Otsubo, 1994) working on three Windows NT based high performance PCs.

Schedule of Installation

The project commenced in October 1995 with contracts awarded for delivery 4 complete mm SLR stations. The phase one in which the equipment installed on sites was completed in March 1996. The phase two in which initial integration and single baseline measurement is completed in October 1996. Phase 3 which activates a full operation of 4 stations will be completed in May 1997.

4. Future Plan

At first, the VLBI experiments in the 256Mbps on the 6 baselines in the real time VLBI and SLR full observations will be conducted in the early next year. We will be able to obtain the movements of four stations with the precision of 2-3 mm. Geographic Survey Institute (GSI) and we have GPS receivers on the same 4 sites. The position change will be obtained by VLBI, SLR and GPS, and the data will be checked by the three different methods. Therefore, the movements of these four stations should be very reliable data. The reliability of data is important for the research of the inland earthquakes.

Furthermore, we will compare the data among VLBI, SLR and GPS system, and we investigate the difference between them (for example, the movements by VLBI is agreed with the movements by GPS or not).

The variations of positions in the short term are noticed. The short term variations appear in KSP daily observations. We will compare the short term variations observed by VLBI, SLR and GPS. When all data has the similar behavior, the short term variation clearly exists. However, if the behavior of position change is different, the short term variation is caused by the estimation method.

The next future target is the real time VLBI system in the rate of 1 or 2 Gbps. The noise error decreases half or one third of 256Mbps mode (current final target). In this case, we can use weaker sources and it is possible to reduce the measurement error. Moreover the continuous running average correlation will create new VLBI data analysis horizon.

In KSP experiments, the correlated amplitudes are obtained everyday, and we can monitor the change of the correlated flux density for several quasars. If we can detect the bust change of the flux density of radio source, we announce the information and we will propose the concentrated observation. Therefore, our system is also useful for the astronomy.

Furthermore, we are now planning to evaluate the tropospheric path delay correction based on numerical prediction data at KSP sites. Precise correction of tropospheric path delay is indispensable to detect seismic precursors and coseismic movements by using KSP network.

VLBI geodesy can avoid uncertainties of satellite orbit determinations and can independently estimate the tropospheric path delay at each site by long distance measurements. Thus, it is expected that the residual delay estimated by VLBI will be more precise using the correction based on numerical prediction data. The estimated delay is available in the analysis of GPS data as a priori delay. As a result, we can reduce an unknown parameter in the GPS analysis. In addition, real-time VLBI analysis will be more effective and challenging. Consequently, more precise monitoring of crustal movements by VLBI and GPS will be carried out with sub-daily temporal resolution.

Figure 2 shows time series of the zenith delay estimated by VLBI and GPS analyses at Koganei and Kashima during 8 - 14 July, 1996 (JST). Both plots by VLBI and GPS increase during 9 - 11 July (JST) and extremely decrease during 11 - 12 July (JST) in a similar manner. According to the infrared images by a geostationary meteorological satellite of JMA (GMS5), a typhoon moved northward in the Western Pacific during the concerned period (see Figure 3).

It seems that the variations of the zenith delay are attributed to the water vapor variation caused by the typhoon movement though it is a roughly qualitative comparison. For more detailed interpretation another investigations are required; comparisons with numerical prediction data and radiosonde data sets, recalculations of parameter estimations in VLBI and GPS analyses.

R & D observations will be conducted in our project. For example, we will observe the extra sources, or by extra observation mode. In SLR system, the new techniques, such as two laser methods, will be developed using KSP system. We will obtain the new results not only of crustal deformation but also in the other fields.

5. Concluding Remarks

Starting with the Koganei and Kashima baseline, daily VLBI observation is conducted with 64 Mbps recording rate since the end of January in 1995. The 256 Mbps mode operation will start soon. This improves the precision by the factor of 2. Eventually the precision available by the KSP system is 3-4 millimeter in baseline length. According to the analysis, we see the influence of the motion of Pacific plate and Philippine Sea plate. The distance between Koganei and Kashima is -4 mm/yr.

After the successful "Kamikaze" system installation, the SLR observation is under test. It will also start observation between the Koganei and Kashima station. The results determined by SLR are compared with that of VLBI. Not only the control of SLR network assisted by only one operator, but also the quick capture of the geodetic satellite by exchanging the information of the satellite orbit via digital communication lines will be established. Since VLBI and SLR system are closely colocated at the KSP stations, which is the first case in the Asia, improvement of reference frame is expected. Under the cooperation with GSI, dense GPS network and KSP will offer very fruitful results.

Modern communication technology allows us to send VLBI data directly to the data processor. The KSP utilizes high-speed communication networks in Tokyo to conduct the real time VLBI data processing. We succeeded in getting fringe in the test experiment at 256 Mbps data rate which is as fast as the K-4 data recording. The high speed data link between the KSP stations is provided by the NTT by the agreement .

In future, the data rate will be increased to 600Mbps and more to have higher sensitivity. The real time VLBI data processing allows a quick and continuous running average report of the crustal deformation and unmanned operation. This also suggests one of the ways to overcome the compatibility problems between international VLBI data recording. Furthermore, less number of mechanical parts in the system may provide higher reliability.

KSP system has two aspects in the technical concept. Firstly, the observing system must always work reliably with minimum manpower. Secondly, advanced technology should be adopted in the system design to produce the best results. To the first requirement, we have used the technical knowledge we learned in the past. We plan to review the compiled geodetic results in the near future. In the second point, we may have a risk. However, a data recording system in VLBI may be a redundant system in the case of real time VLBI. We also have one spare equipment each for VLBI and SLR. Advanced technology will provide some interesting applications as by-products.

References

IERS Annual Report for 1994, Central Bureau of IERS - Observatory of Paris, 1995.

Heki K., Y. Takahashi, and T. Kondo, Contraction of northeastern Japan: evidence from horizontal displacement of a Japanese station in global very long baseline interferometry networks, Tectonophysics, 181, 113-122, 1990.

Kiuchi, H., S. Hama, J. Amagai, Y. Abe, Y. Sugimoto, and N. Kawaguchi, K-3 and K-4 VLBI Data Acquisition Terminals, J. of the Communications Res. Lab., 38, 435-457, 1991

Kunimori, H. et al, New development of satellite laser ranging system for highly precise space and time measurements, J. of Communications Res. Lab., 38, 2, 303--317, 1991.

McCarthy, D. D., IERS Conventions (1996), IERS Technical Note 21, International Earth Rotation Service, 1996.

Otsubo, T. et al, Error control of numerical integration in SLR analysis software CONCERTO, Journal of the Geodetic Society of Japan, 40, 4, 1994.

Sato T. and H. Hanada, A Program for the Computation of Ocean Tidal Loading Effects 'GOTIC', Publ. of the International Latitude Obs. of Mizusawa, 18, 29, 1984.

Sengoku A. and T. Sato, Site Displacements due to Solid Earth Tide and Ocean Loading at SLR, VLBI and GPS Observation Sites in Japan, J. of the Japan Soc. for Marine Surveys and Technology, 7, 1-7, 1995.

Yokoyama et al, Crustal deformation monitoring system for the Tokyo Metropolitan Area, Special Issue, J. of the Communications Res. Lab., Vol.42, No.1, 1-219, 1996 (in Japanese).

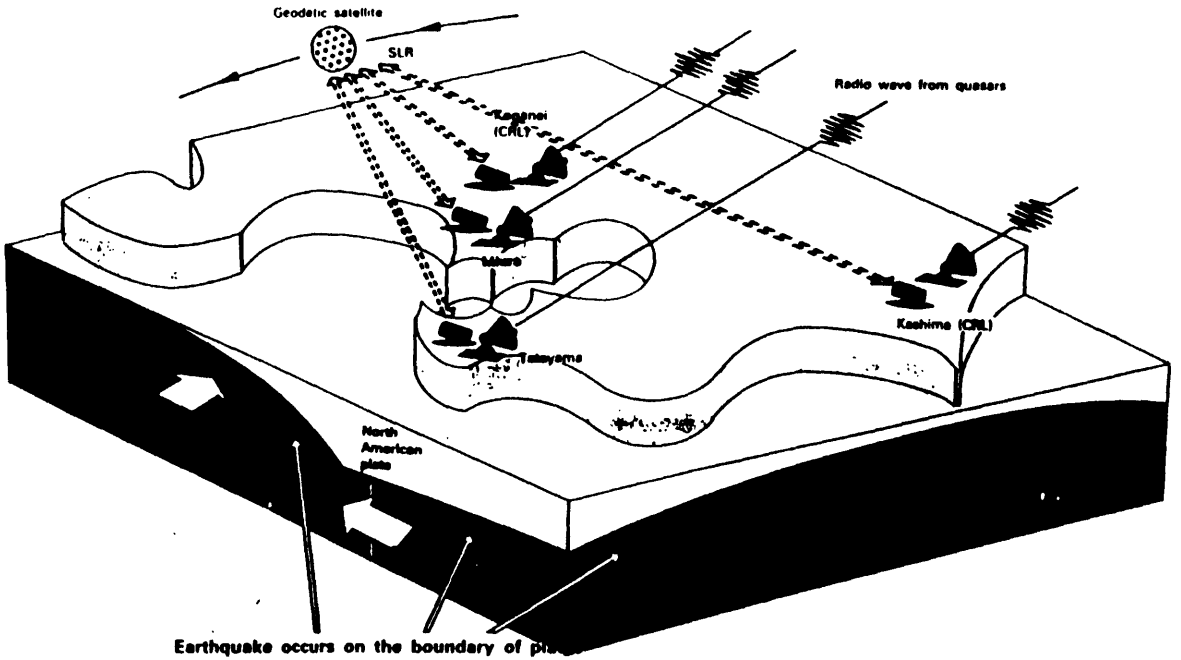

Figure 2.1.1 The configuration of VLBI/SLR station (Koganei, Kashima, Miura, Tateyama) constructed in KSP. A illustration of 3-dimensional plate structure beneath the Tokyo Metropolitan Area.

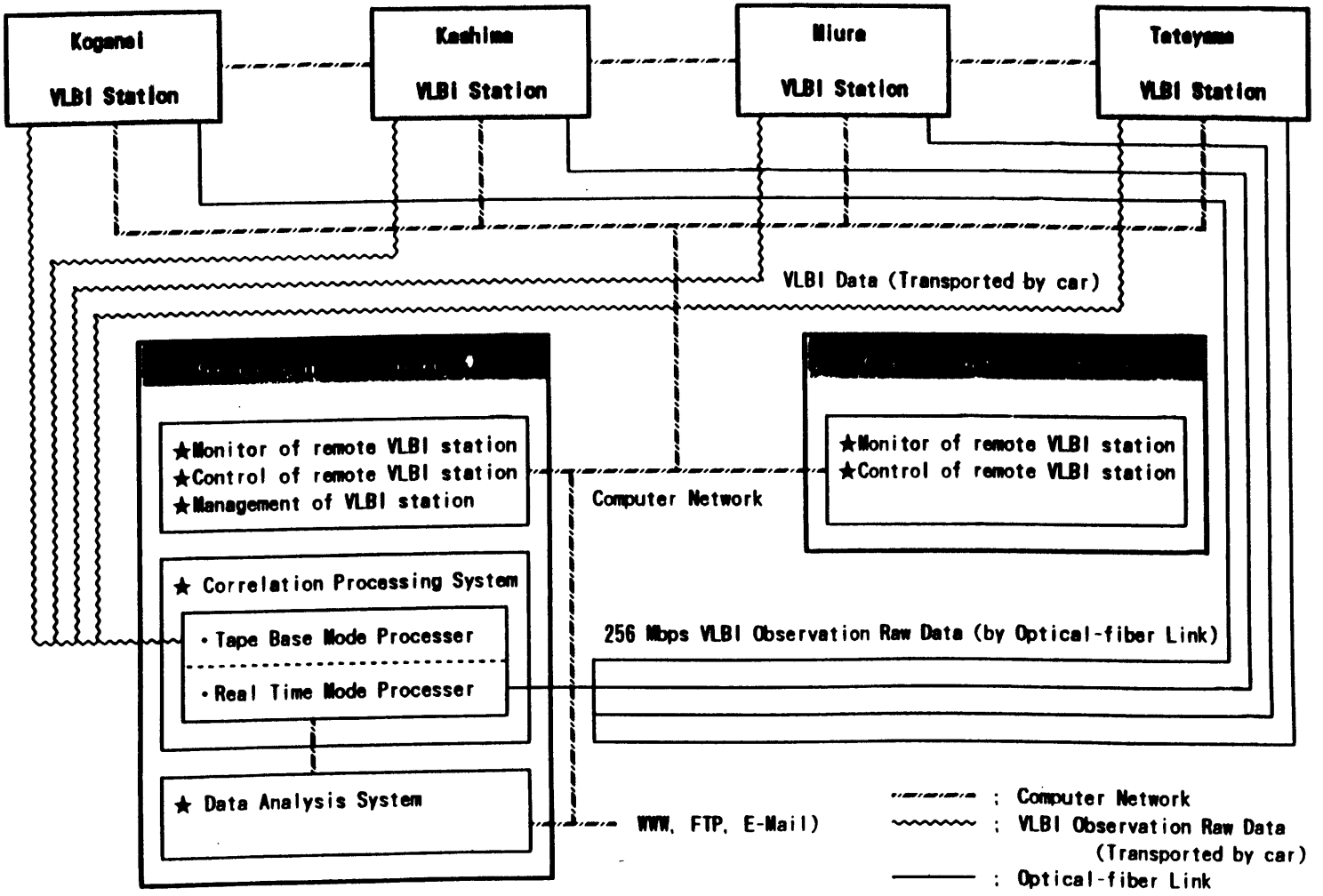

Figure 2.2.1 Block diagram and VLBI data flow of the KSP-VLBI system

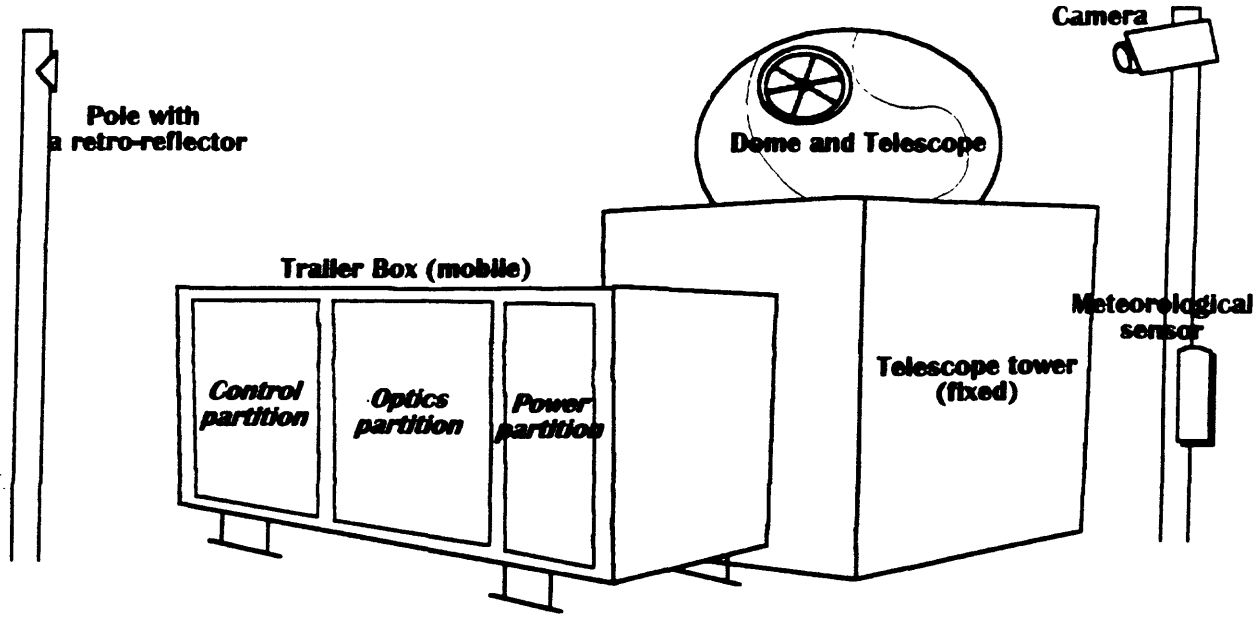

Figure 2.3.1 Sketch of a KSP-SLR system.

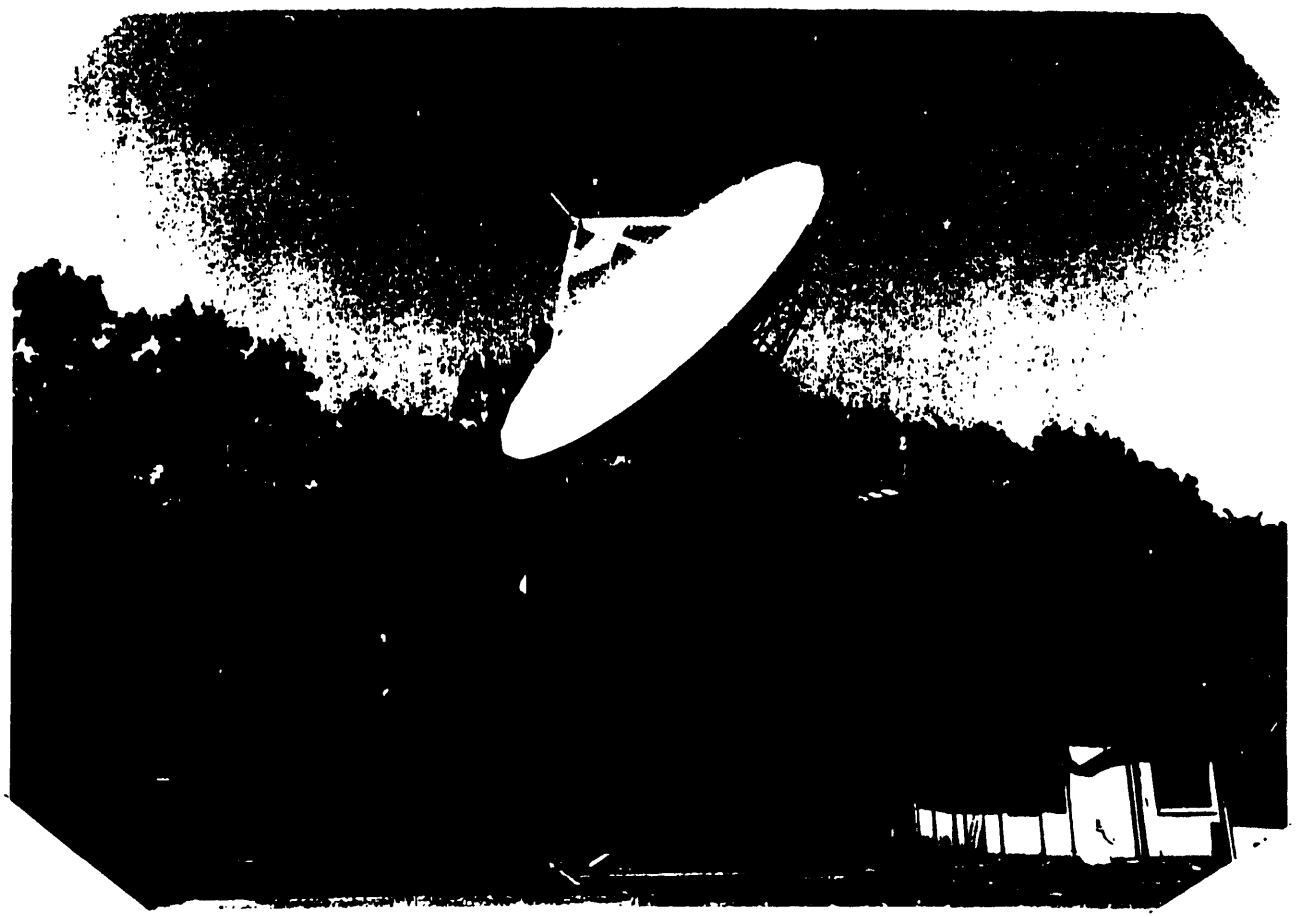

Photo 2.1.1 An 11-m antenna at Koganei VLBI station

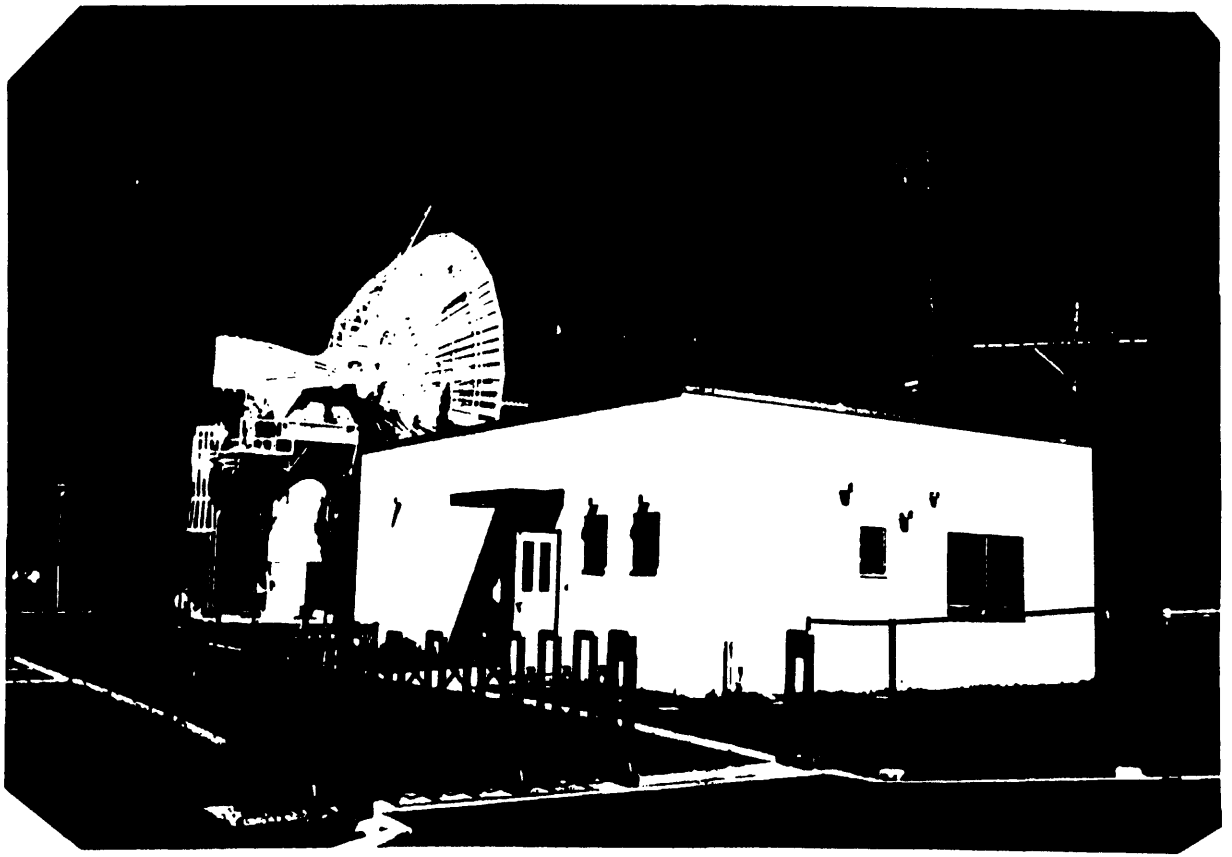

Photo 2.1.2 Kashima VLBI Station

Photo 2.1.4 Miura VLBI Station

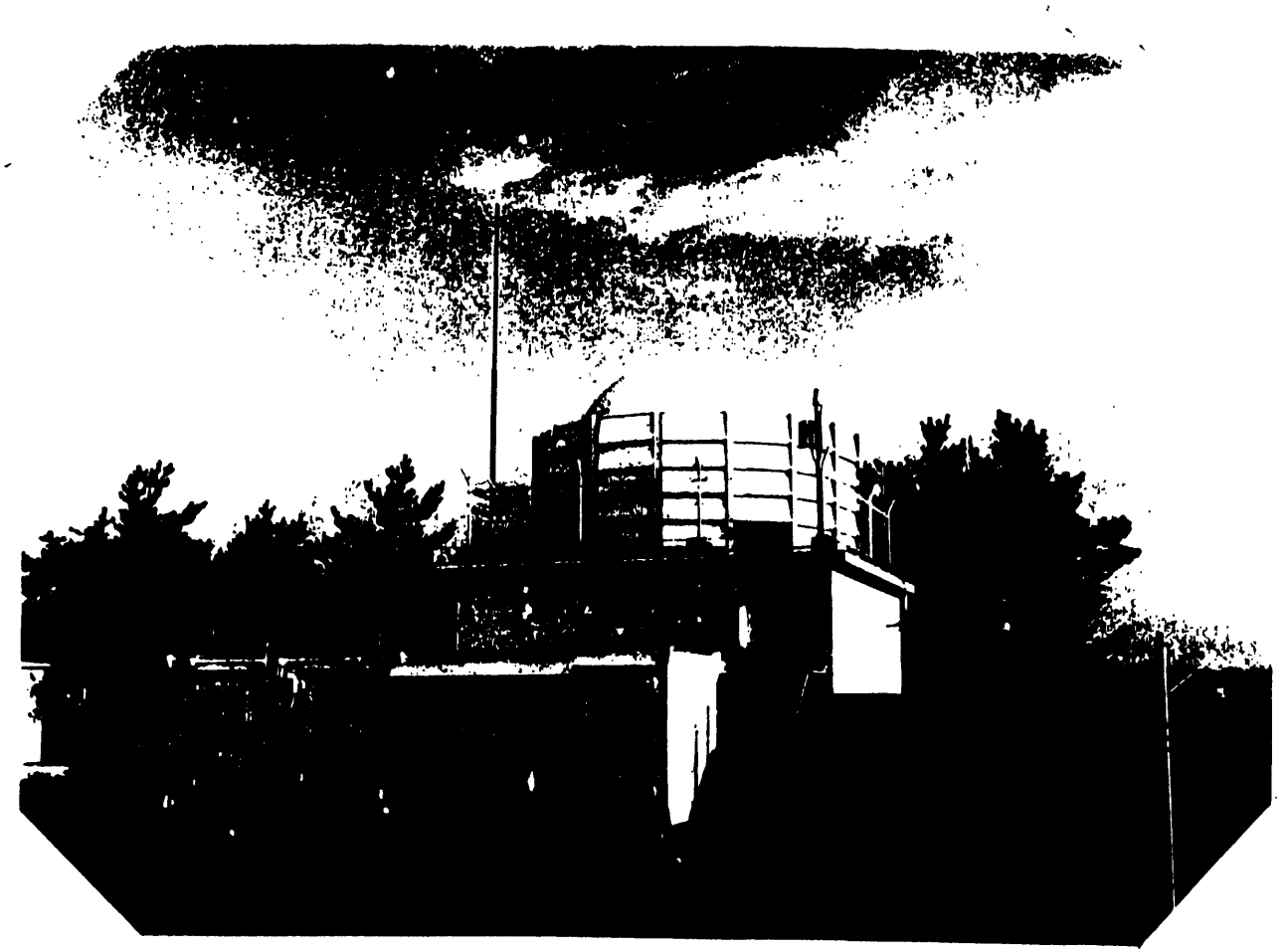

Photo 2.1.3 Kashima SLR Station

Figure 3.1.1 Estimated baseline lengths between Kashima, Koganei, and Miura VLBI stations. Uncertainties are shown by vertical error bars with ± 1 standard deviation of the estimated formal errors. Linear trend was estimated from the least square estimation.

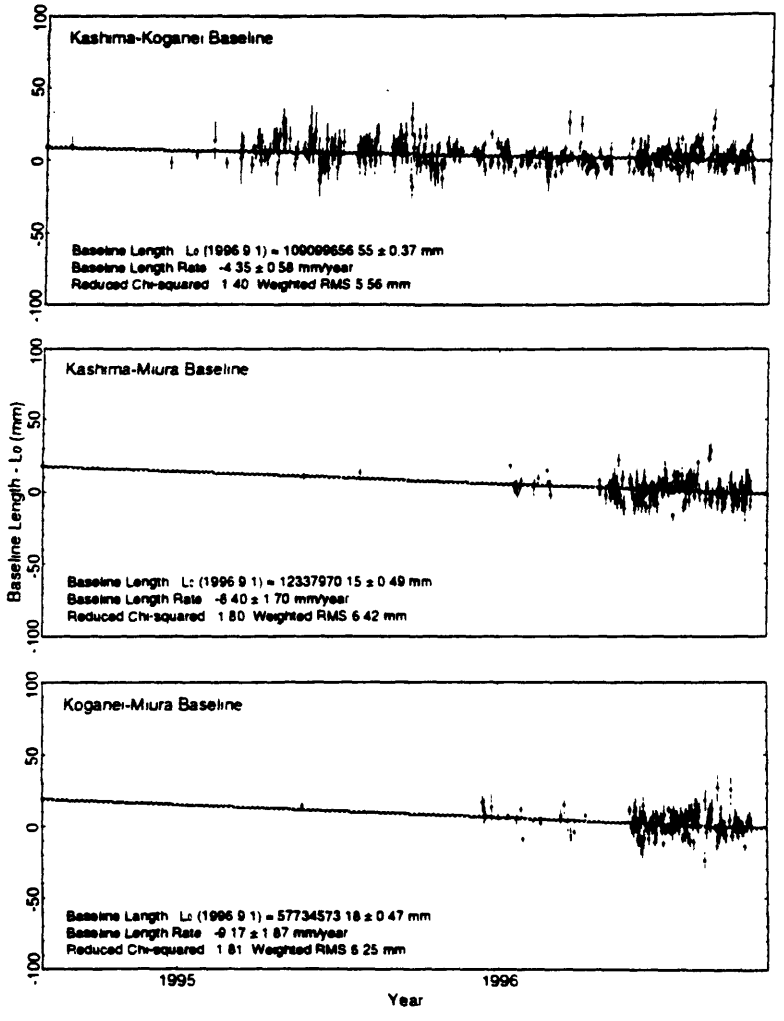

Figure 3.1.2 Topocentric site position displacements of the Koganei VLBI station in three perpendicular directions. Uncertainties are shown by vertical error bars with ± 1 standard deviation of the estimated formal errors. Linear trend was estimated from the least square estimation.

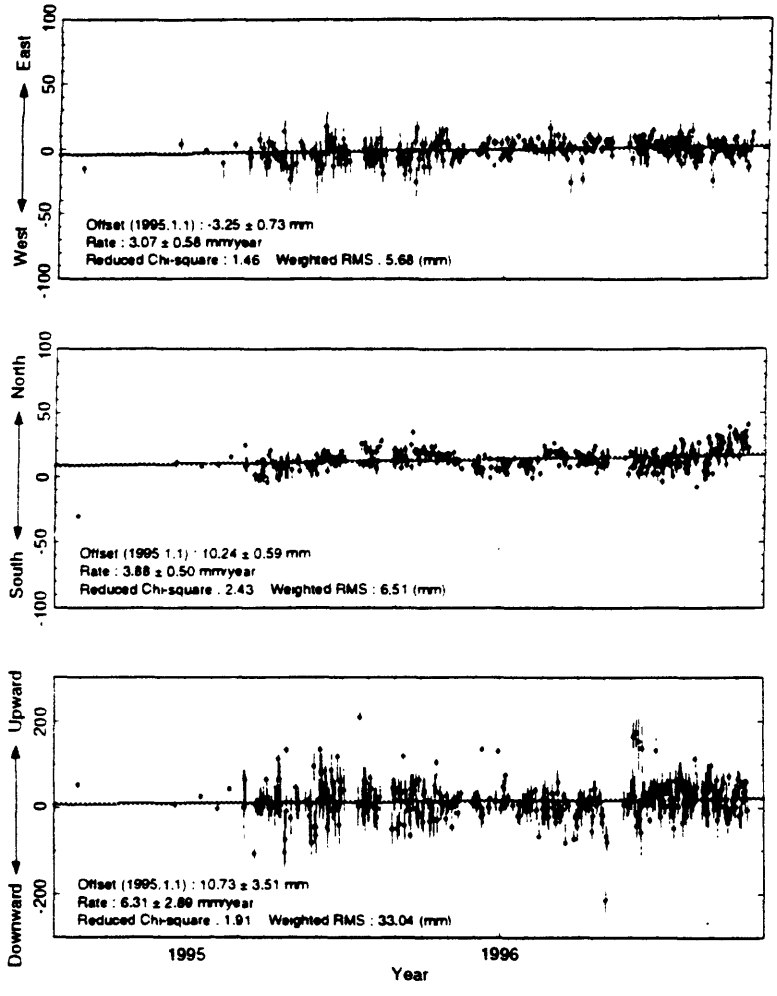

Figure 3.1.3 Topocentric site position displacements of the Miura VLBI station in three perpendicular directions. Uncertainties are shown by vertical error bars with ± 1 standard deviation of the estimated formal errors. Linear trend was estimated from the least square estimation.

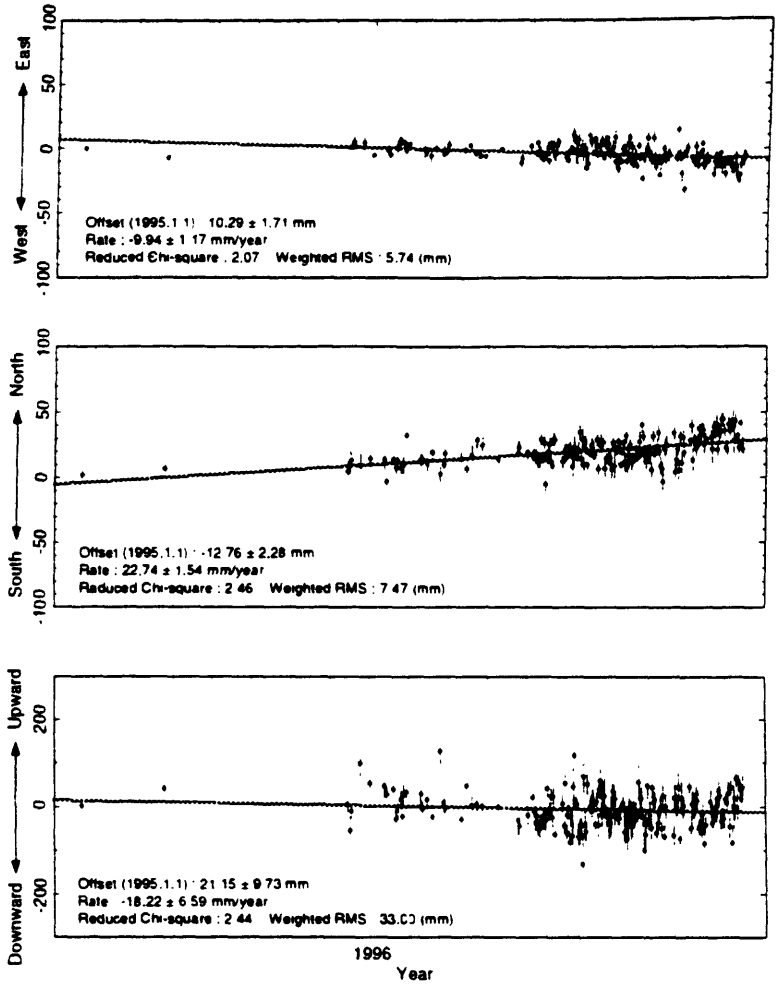

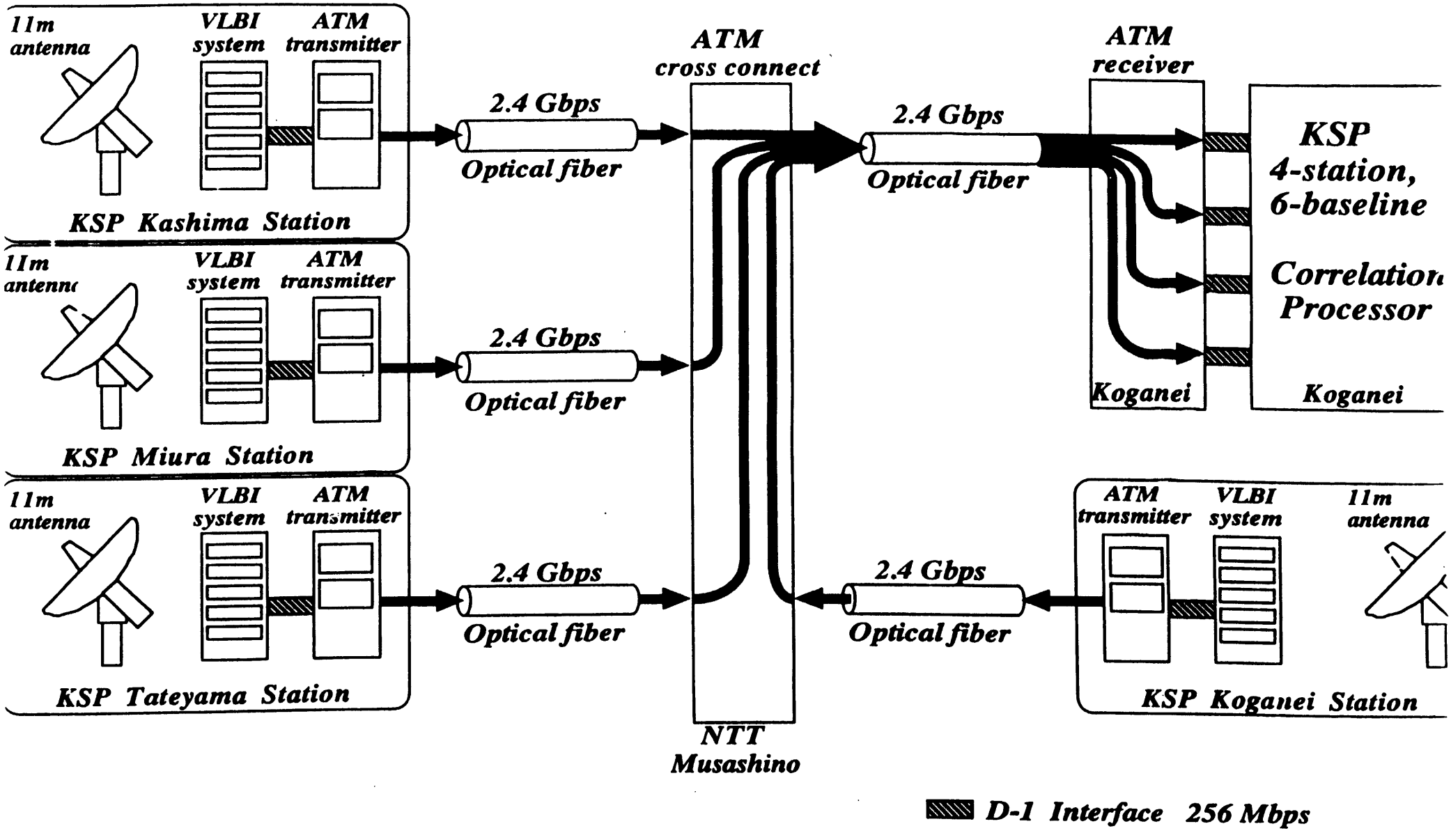

Figure 3.2.1 A block diagram of KSP ATM network. Signals from the each observation station are multiplexed by the cross-connect switch located in ATM network, and the multiplexed signal is led to the receiver via one transmission path. In the receiver, the multiplex signal is separated into the data of each station and restored in the receiver as a digital signal after the delay fluctuation is absorbed.

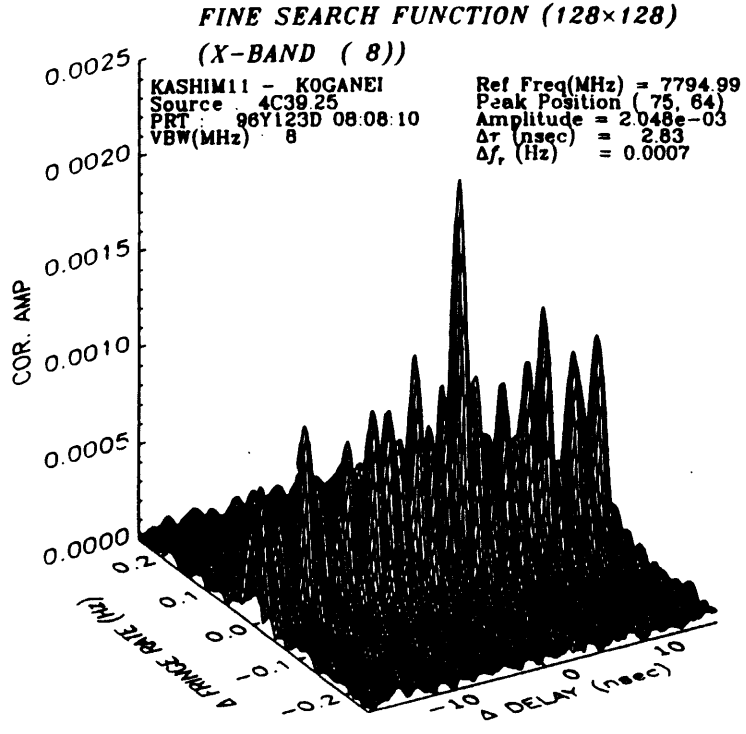

Figure 3.2.3 Obtained fringe (a result of fine delay search function)

The Crustal Deformation Monitoring of the Tokyo Metropolitan Area

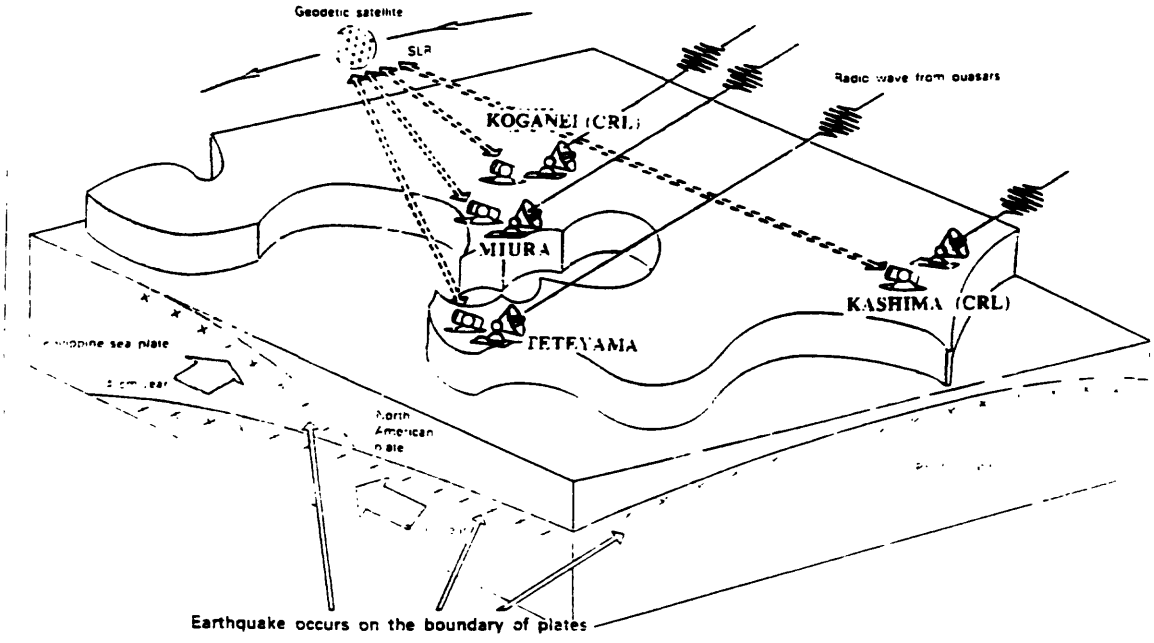

KOGANEI (CRL)

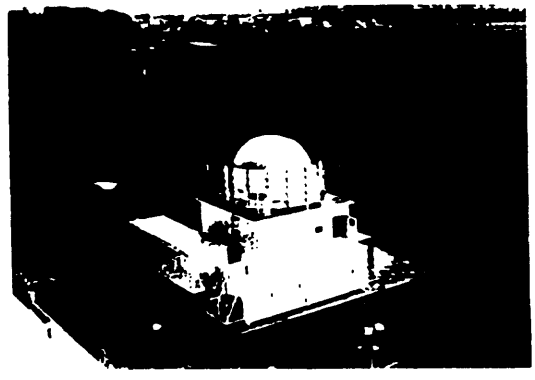

KASHIMA (CRL)

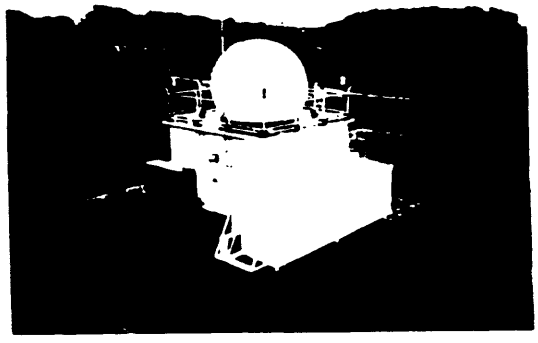

MIURA

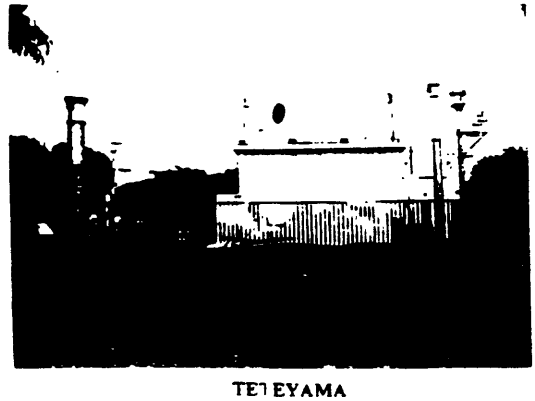

TETEYAMA

Figure 3.3.1
Map of Tokyo Metropolitan Area and delivered SLR systems.

Figure 3.3.3
The control and monitoring room
at the Koganei central station

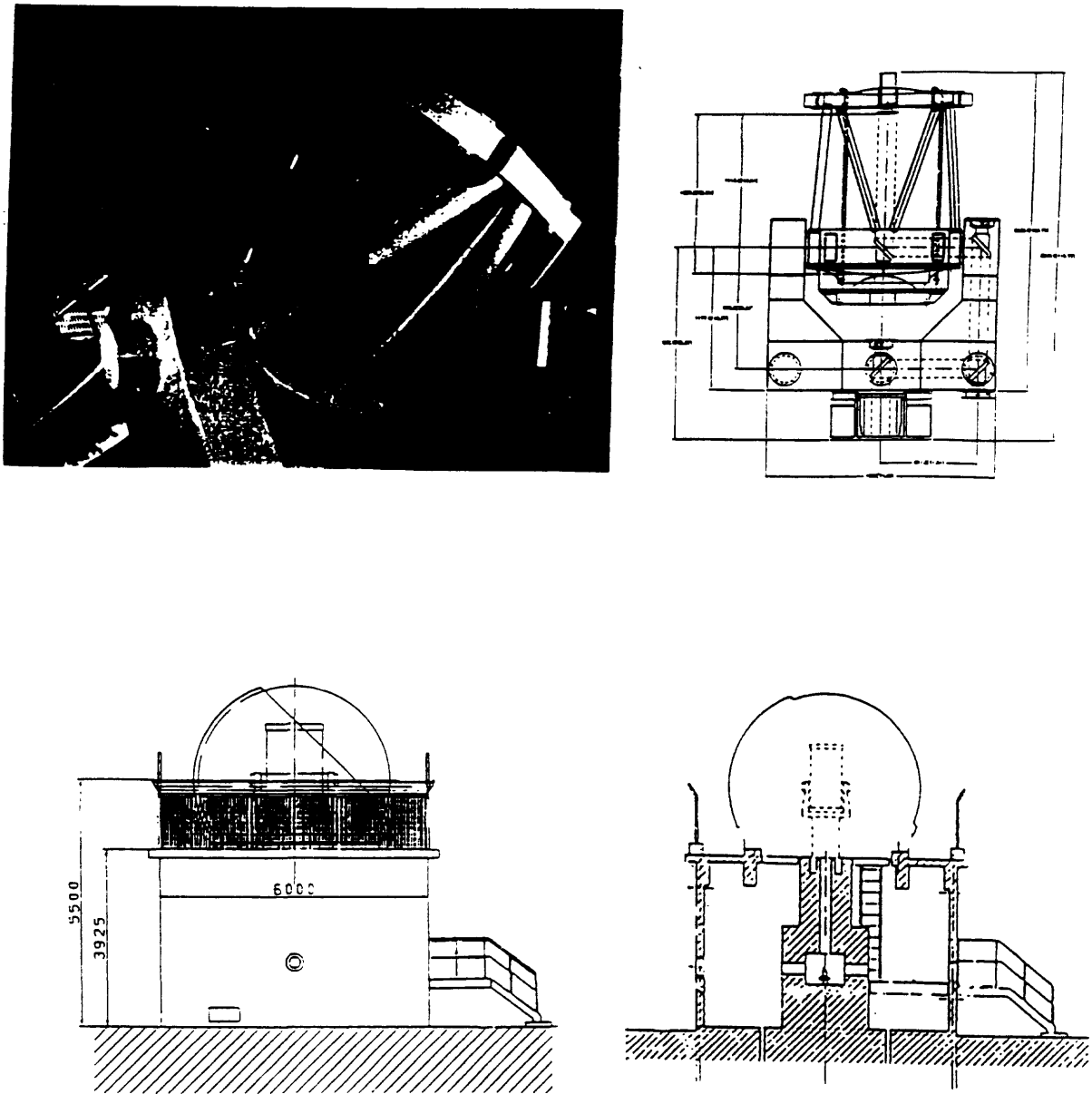

Figure 3 3 2
Schematic and actual view of Keystone telescope in observation tower.

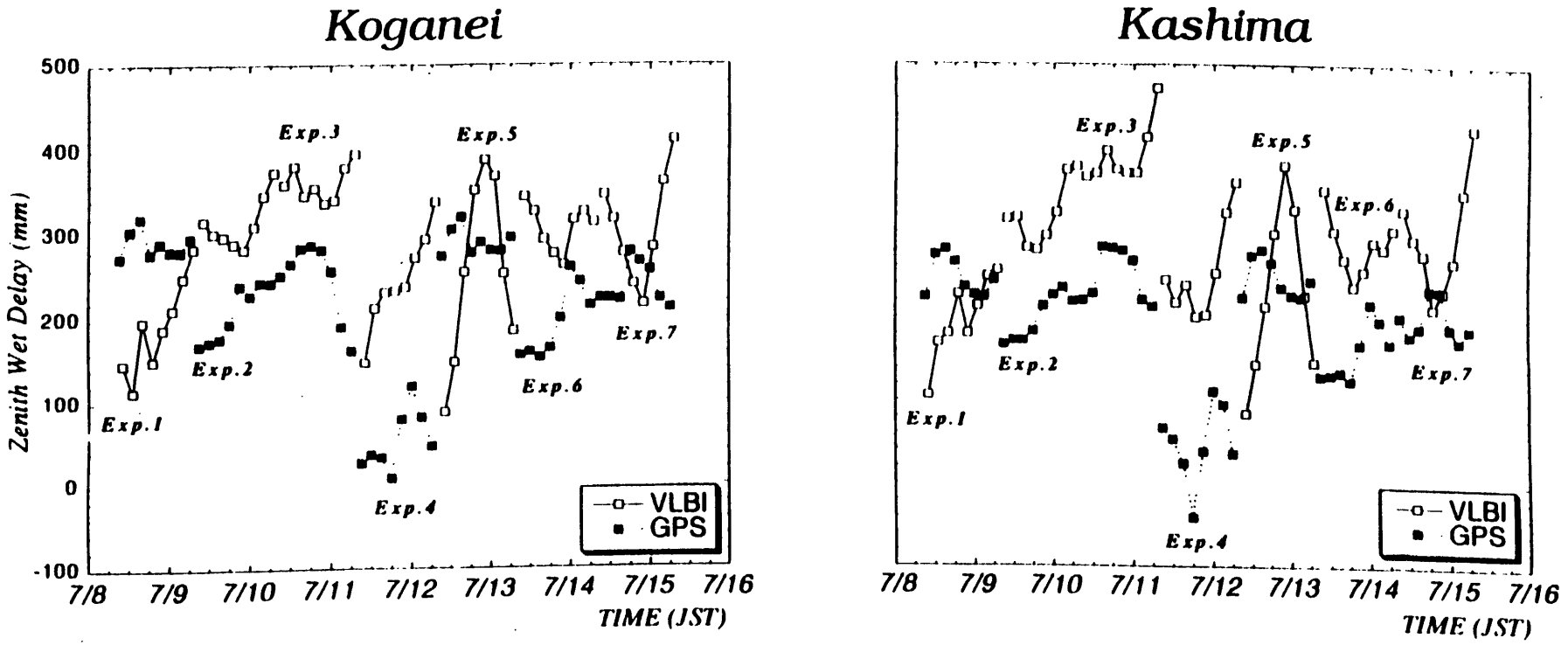

Figure 4.1 Time series of zenith tropospheric delay estimated by VLBI and GPS analyses at Koganei - Kashima baseline (about 109 km) during 8 - 14 July, 1996. Since a priori delay is not used in this analyses for both VLBI and GPS, the absolute values are not confident. However, similar characteristics are shown for both plots by VLBI and GPS; increasing in Exp.2 (July 9) and Exp. 3 (July 10), and decreasing in Exp. 4 (July 11).

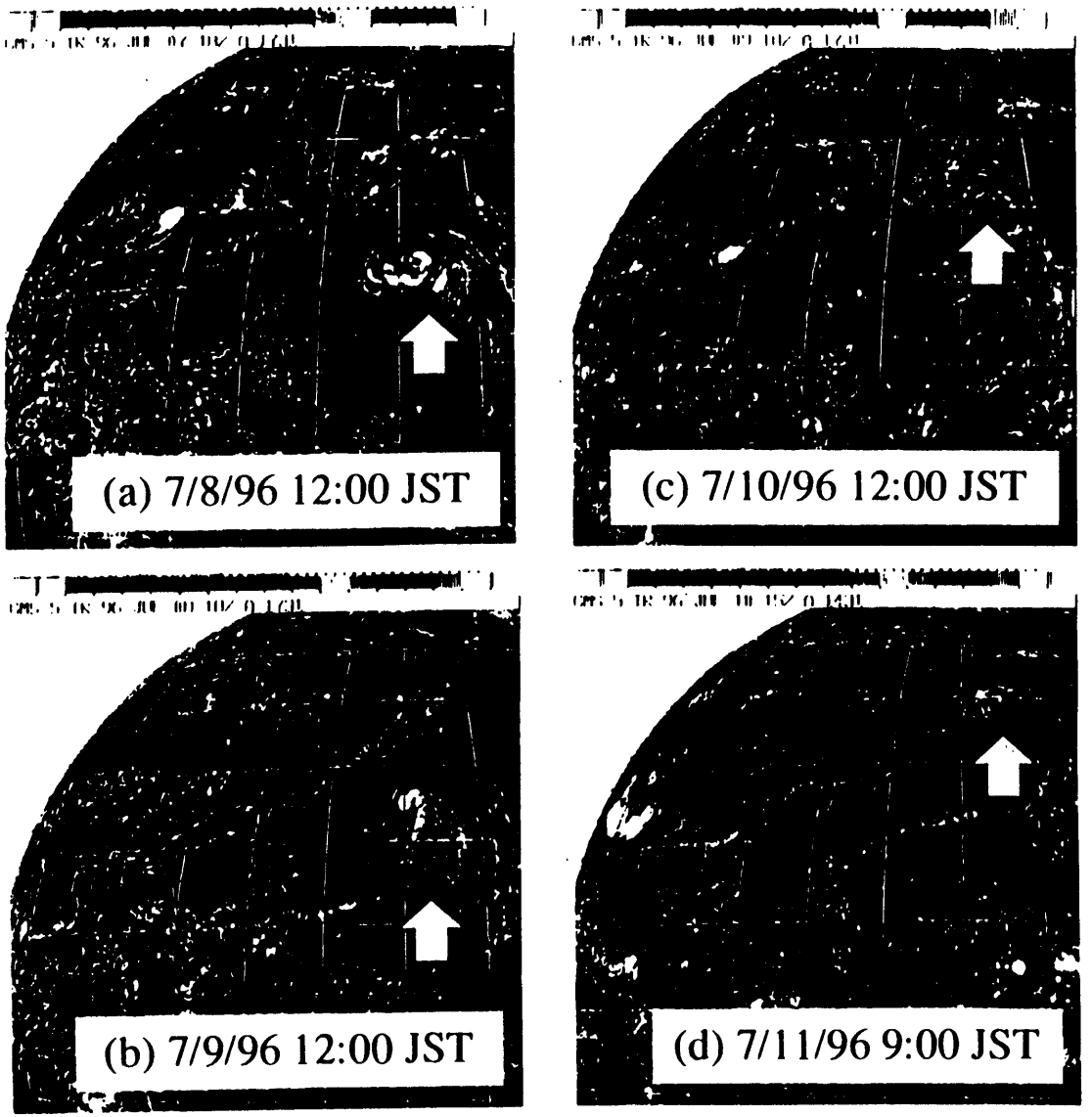

Figure 4.2

Infrared images by GMS5 of JMA. Arrows as shown in these figures indicate typhoon. It is inferred that the variation of water vapor related to the typhoon causes the temporal variations of zenith delay as shown in Figure 2.

Table 2.2.1 Performance of KSP-VLBI System

Antenna Diameter:	11 m
Driving Speed:	AZ and EL 3 deg./sec.
Drive Range:	AZ: +/- 270 deg., EL: 0-90 deg.
Receiving Frequency	
S band:	2200 - 2500 MHz
X band:	7700 - 8600 MHz
System Noise Temperature	
S band:	90 K (EL=90 deg.)
X band:	110 K (EL=90 deg.)
IF signal Frequency	
S band:	500 - 900 MHz
X band:	XL:500-1000 MHz, XH:500-1000 MHz
IF Signal Transmission:	Optical-fiber method
Video Converter :	1 KHz-32 Mhz, 16 ch.
Input Interface:	16 Mbps, 16ch.
Data Recorder:	Rotary-Head Type, L-Cassette Tape
	Recording Rate 256 Mbps
Tape Exchanger:	Automatic Tape-Exchanger Unit
Reference Signal Source:	Hydrogen Maser
Frequency Stability:	2-3 x 10(-13)/τ (τ=1 sec)
Reference Signal:	5MHz, 1 PPS, IRIG-B
Station Clock:	GPS System

Table 2.3.1 Specification of a KSP-SLR system

Laser	
Pulse width	30 ps
Repetition Rate	10 - 1000 Hz
Maximum Energy	50 mJ
Wavelength	532 nm
Timing Measurement	
Detector	SPAD (single photon avalanche diode) and MCP-PMT (micro-channel plate photomultiplier)
Filter	3Å filter and spatial filter
Time supply	GPS and H-maser from VLBI
Telescope	
Clear Aperture	75 cm
Mount	Alt-Azimuth Mount
Tracking Accuracy	2.5 arcseconds
Azimuth Range	> 540 degrees
Elevation Range	-20 to 95 degrees
Maximum Driving Speed	12 degrees / second
Focus	Coude

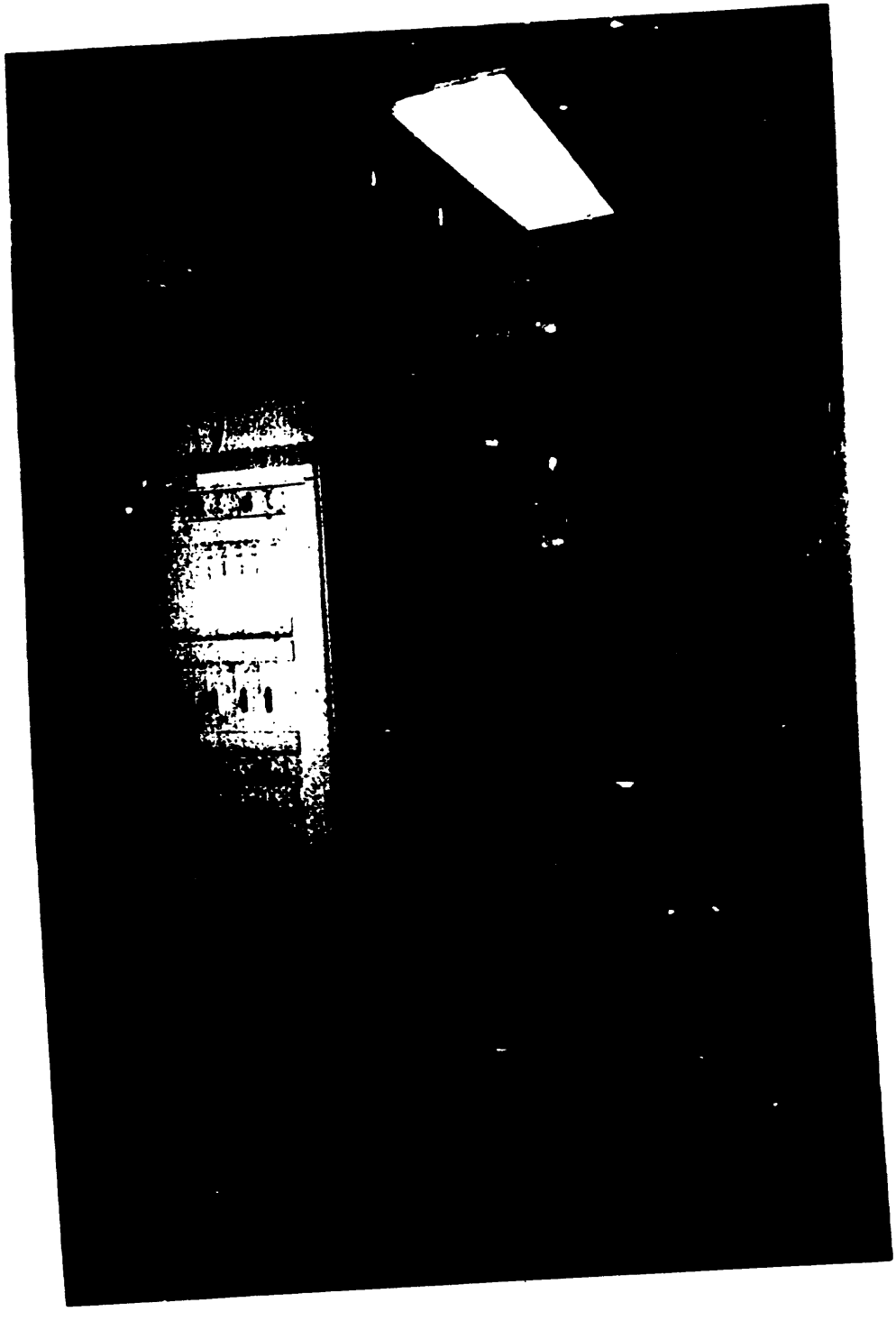

Figure 3.2 : A view of the correlation site. Left side : ATM receiver. Center and right side : 4-station 6-baseline correlator.

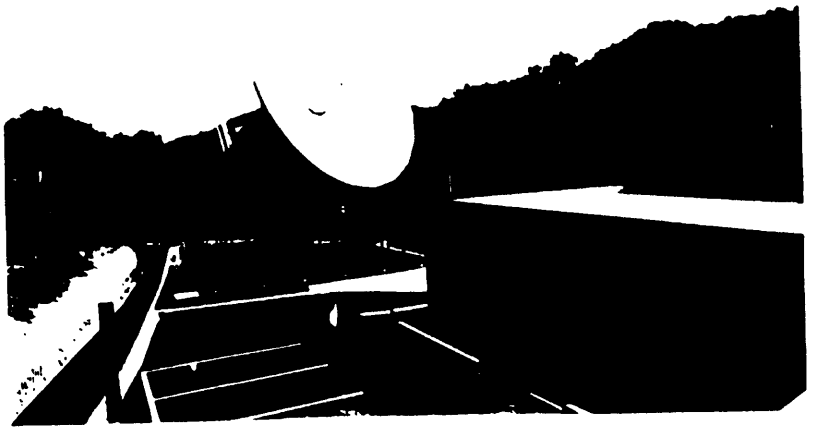

Photo 2.1.5 Tateyama VLBI Station

Photo 2.2.1 KSP-VLBI data acquisition system(Kashima station). From left: Reference signal distribution rack, weather station rack, antenna front-end control rack, IF signal distribution and calibration rack, back-end terminal rack, automatic tape exchange unit(DMS24), and antenna control computer.

Modeling Crustal Deformation - Application to the Northridge Earthquake

Andrea Donnellan and Gregory A. Lyzenga
Jet Propulsion Laboratory
California Institute of Technology
Pasadena, CA

Geodetic measurements collected before and after the 1994 Northridge earthquake provide an excellent opportunity for understanding earthquake processes throughout the earthquake cycle. Measurements collected before the earthquake indicate high strain associated with the seismogenic thrust faults and lower strain away from those faults. Measurements collected following the earthquake indicate that rapid post-seismic motions occurred for two years following the earthquake near the source of the earthquake. The post-seismic motions are about 10% of the coseismic motions. They are best modeled by afterslip on the rupture plane and relaxation of a 5 km thick soft upper crust. The models indicate that viscoelastic relaxation of the lower crust dominates late in the earthquake cycle while fault afterslip and deformation of the upper sediments dominate early in the cycle.

Integrated Analysis of Crustal Activity

Manabu Hashimoto and Yoshimitsu Yoshimura,
Crustal Dynamics Department,
Geographical Survey Institute

Introduction

Recent development of space techniques in geodesy allows us to monitor regional and global deformations of crust or lithosphere in nearly real time. Geographical Survey Institute have been deploying continuous GPS observation sites for these 4 years. This nation-wide array will consist of more than 800 stations with average spacing of 20 - 30 km by the end of next March. This array may accumulate bunch of invaluable data of deformations of crust or lithosphere as well as conventional geodetic works and show us several phenomena which we have never seen before. GSI have provided information on crustal activity in and around the Japanese islands. However the public seeks for the prediction based on the observations. So far we could give only qualitative and phenomenological interpretation to the public. However such a phenomenological way of thinking, which depends on "experience", will be on dead rock because of accelerated accumulation of data. Therefore we must develop methods to understand the mechanism of such phenomena in a more objective way.

Recently study of friction of rocks is developed and several formula, which can be incorporated in computer simulation, are presented. Structure of crust and mantle have been clarified with remarkable resolution. Movements of plates are being observed every day. Furthermore computing technology is developing with incredible speed. We can solve huge structure mechanics problems which we had never dreamed. Considering these issues, GSI decided to start a project, the Integrated Analysis of Crustal Activity, by using a supercomputer.

Outline of Project

The Integrated Analysis of Crustal Activity (hereafter IACA) consists of three major parts. Schematic image of this project is shown in Fig. 1.

First, we compile geological and geophysical data for the construction of three-dimensional numerical tectonic model. We collect information on the structure of crust and upper mantle such as distribution of micro earthquakes, results of seismic tomography, results of seismic soundings, distribution of active faults, etc. Referring to these information we construct a numerical model with three-dimensional

heterogeneity of crust and upper mantle.

Second, we analyzes geodetic data, including continuous GPS . GSI now operates more than 600 continuous GPS stations and is going to deploy about 250 stations by the end of next March. With IGS ephemerides we analyze phase data from all GPS stations and obtain daily movement of each station. We combine these GPS velocity data with those obtained by conventional geodetic surveys and present crustal deformation in the Japanese islands in detail in space and time. This deformation should be an input or referring data to the numerical simulations as below. However this deformation includes several kinds of noise or local movements. Therefore we must incorporate some smoothing techniques. Inversion techniques based on kinematic block-fault model by Matsu'ura et al. (1986) or back-slip model by Yabuki and Matsu'ura (1992) are useful to estimate back-slip rate or slip deficit of interface of plates or active faults and are easily implemented. It may be more practical to input back-slip rate or slip deficit to numerical model.

Third, the core of this project, we try to forecast of crustal activity with numerical tectonic model. There are several numerical techniques in the analysis of crustal activity. In this project we adopt following four techniques. The first is the finite element modeling with visco-elastic rheology. We try to model crust and upper mantle in and around the Japanese islands with FEM and calculate time-dependent variation in stress and strain with several boundary conditions. The second is simulation of seismic cycle with rate and state dependent friction law. So far this technique can handle 2 dimensional model of thrust. We try to develop 3 dimensional model and simulate seismic cycle of the Nankai trough. The third is the finite element spring model (FESM), which can treat discontinuous material much easier than conventional FEM, developed by Hamajima (1995). We try to simulate sequence of rupture events over the Japanese islands. The fourth is "2.5 dimensional" modeling of earth's plates developed by Bird (1994) in order to simulate stable plate motions as boundary conditions of regional model.

Above techniques have advantages and disadvantages in each and can simulate only part of all the characteristics that real earth has. We try to integrate these techniques to develop a mid- to long-term forecast techniques of crustal activity for the purpose of mitigation of seismic hazards in future.

References

Bird, P., 1989, New finite element techniques for modeling deformation histories of continents with stratified temperature-dependent rheology, *J. Geophys. Res.*, **94**,

3967-3990.

Hamajima, R., 1994, Crustal movement analysis, Research Report of Dept. Civil & Environmental Eng., Saitama Univ., 24, 207-237.

Matsu'ura, M., D.D. Jackson, and A. Cheng, 1986, Dislocation model for aseismic crustal deformation at Hollister, California, *J. Geophys. Res.*, **91**, 12661-12674.

Yabuki, T., and M. Matsu'ura, 1992, Geodetic data inversion using a Bayesian information criterion for spatial distribution of fault slip, *Geophys. J. Int.*, **113**, 363-375.

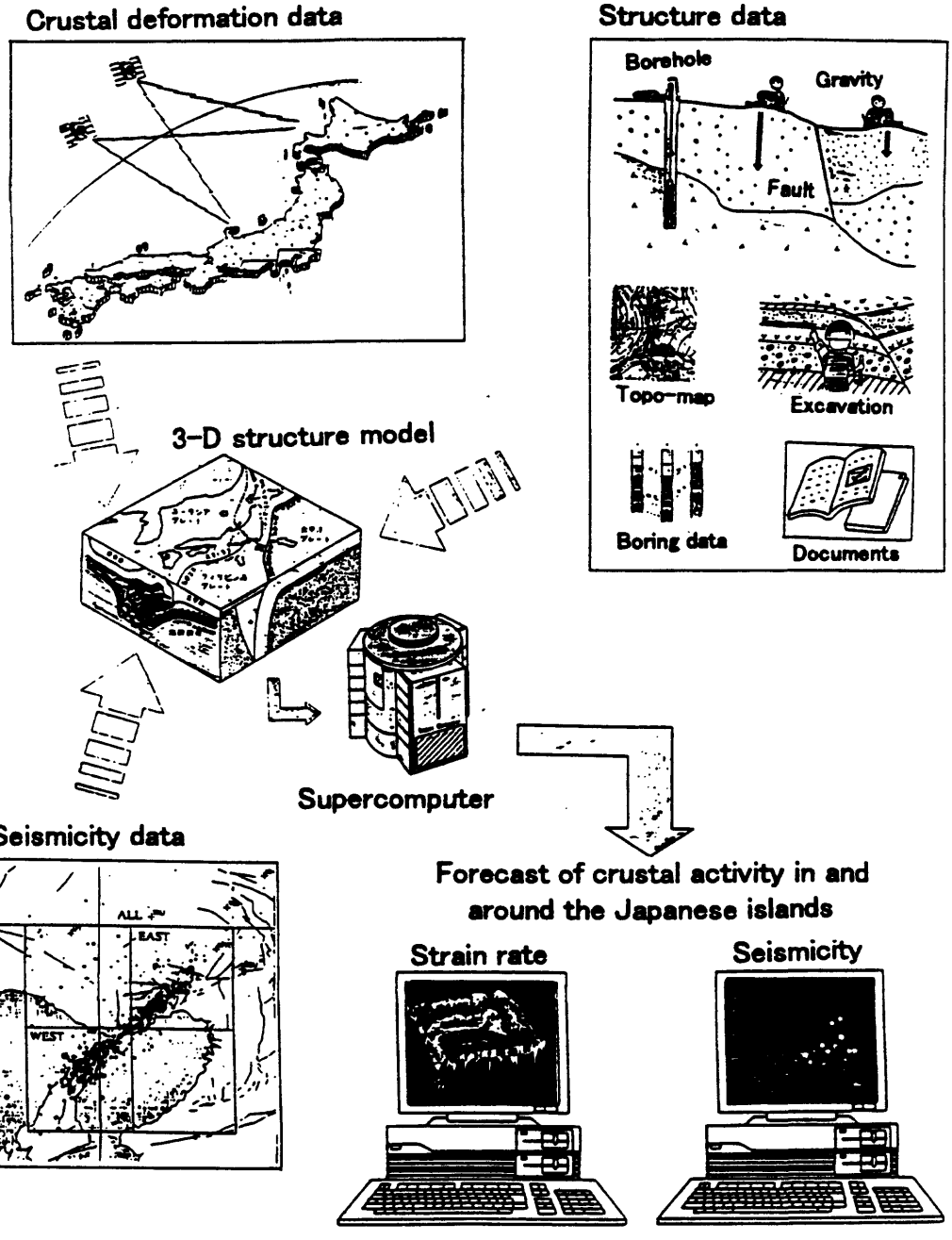

Fig. 1 Schematic diagram of concept of the Integrated Analysis of Crustal Activity

DETECTION OF POSTSEISMIC DEFORMATION FOLLOWING THE 1992 M7.3 LANDERS CALIFORNIA EARTHQUAKE USING SATELLITE RADAR INTERFEROMETRY

Wayne Thatcher*, Didier Massonnet**, and Hélène Vadon**

* United States Geological Survey, 345 Middlefield Road, Menlo Park, CA.94025,USA
** Centre National d'Etudes Spatiales, 18 Ave. E. Belin, 31055 Toulouse, France

Stress changes caused by earthquake faulting induce transient aseismic crustal movements in the earthquake source region that continue for months to decades following large events (Okada and Nagata, 1952; Thatcher, 1983, 1986; Savage and Plafker, 1991). These motions reflect aseismic fault zone adjustments and/or bulk deformation of its surroundings in response to applied stresses and supply information on the inelastic behaviour of the Earth's crust. These processes are imperfectly understood because it is difficult to infer what occurs at depth using only surface measurements, poorly sampled in general. Pushing radar interferometry close to its typical artefact level permits us to densely map the postseismic deformation field in the 3 years following the 28 June 1992 M_W=7.3 Landers, California earthquake. We use this mapping to identify two distinct deformation mechanisms, including a hitherto poorly-understood process involving closure of dilatant cracks and fluid expulsion from a transiently over-pressured fault zone.

We measure the deformation around the 1992 rupture zone over three years by producing interference patterns from the difference of two synthetic aperture radar (SAR) images acquired by the ERS-1 satellite. This geodetic technique can reveal surface phase changes (Gabriel et al., 1989) and displacements due to earthquakes (Massonnet et al., 1993), glaciers (Goldstein et al., 1993) or volcanoes (Massonnet et al., 1995) with a centimeter, and sometimes millimeter, accuracy. The interferogram is a contour map of the change in range, or the component of the displacement vector which points toward the satellite. The techniques used to calculate the interferograms

require a digital elevation model (DEM) to calculate the effect of topography and can obtain a result using any pair of radar images from the same orbital position.

A location map is shown in Figure 1, indicating the ERS-1 satellite radar swath, the regional faults, and the 1992 Landers epicenter and surface rupture. Five separate interferograms have been obtained for varying intervals following the earthquake (Figure 2), although we show results from only one of them in contoured form in Figure 3.

Two distinct patterns of deformation are highlighted in Fig. 3. Pattern 1, on the northern and central parts of the surface rupture, consists of a region of range increase southwest of the fault and range decrease to the northeast. It resembles the coseismic fringe pattern (Massonnet et al., 1993), but at much reduced amplitude and without any discontinuity across the fault, immediately suggesting continued fault slip that does not reach the earth's surface. Pattern 2, on the southern half of the 1992 fault, shows a much more localised region of range decrease lying within a few kilometers of the Landers fault zone.

Adjacent range change profiles, located in Fig. 3, that pass through each of these deformation patterns are shown in Fig.4 along with model profiles that have been fit to them. Profile 1 is matched well by a model (Model 1) with 90 cm of right-lateral slip on a 5-km wide fault strip lying between 6 and 11 km on the same plane that ruptured in the 1992 earthquake. The slight mismatch between model and data near the southwest edge of the profile is due to an offset across the Lenwood fault. It is caused by the small amount of postseismic surface slip on this fault. The profile lies in the region where coseismic displacement was a maximum, suggesting continued slip on the same fault patch. Movements must be dominantly aseismic because slippage is much more than can be accounted for by aftershocks of the 1992 event. Postseismic slip at depth has been observed for many earthquakes but it is

commonly confined to the down dip edge of the coseismic rupture plane rather than the rupture plane itself (e.g. Thatcher, 1986).

Profile 2 is fit acceptably by a conceptually very different model. Following recent models of fault zone crack growth and fluid flow (Sleep and Blanpied, 1992; Byerlee, 1993), and similar postseismic deformation modeling (Savage et al., 1994), we imagine that earthquake motions open dilatant cracks in a fluid saturated fault zone, resulting in time-dependent post-earthquake crack closure and fluid flow. Such crack closure and fluid expulsion may be crudely modelled by elastic dislocation models in which the "slip" is normal to the fault surface, approximating postseismic collapse (volume decrease) within the fault zone. In Fig. 4b we apply such a model, with 30 cm of fault closure on the same fault strip used in model 1 (5km wide lying between 6 and 11 km depth). However, as Profile 2 also includes movements due to Model 1 (see Profile 2 location in Fig. 3), we must superpose a fraction of the Model 1 motion onto Profile 2; in Fig. 4b we have added 70% of the model 1 deformation to that of Model 2. The procedure is clearly subjective and non-unique, indicating some uncertainty in the derived parameters of Model 2, particularly the depth and slip magnitude of the equivalent dislocation. Recent work by Peltzer et al. (1996) has nicely shown that maximum range changes are concentrated in fault jog regions, where coseismic dilatant volume changes are greatest. The along-strike continuity of the near-fault range decrease shown by the pattern 2 deformation may be due to smaller right-stepping jogs on this reach of the fault.

The selected profiles of Fig. 4 can easily be obtained for all the postseismic interferograms computed in this area, although the postseismic pattern is of low amplitude and is not recognised easily in any of them. We plotted the amplitude of range change between the points where it is maximum (points A and B on Fig 4a and 4b). If we exclude the interferograms using the acquisition of 28 August 1993, where a large propagation path contribution has been already described, we observe that the

data fit a logarithmic law reasonably well, with a general shape given by X log(t)+Y, where t is the time elapsed since the Landers event in days. Since interferograms give only a difference between two, or more, radar acquisition dates, Y cannot be determined . The total amplitude X is found to be 22.5 mm (resp. 30 mm) for Profile 1 of Fig. 3a (resp. Profile 2 of Fig. 3b). The rms uncertainty of X is 5 mm for both profiles.

Our models are consistent with the Global Positioning System (GPS) data gathered at 19 ground stations in the 6 months following the Landers earthquake (Shen et al., 1994). However, only a limited subset of these data are relevant to our models. Horizontal displacement vectors derived from the GPS data and corrected for inferred interseismic movements are plotted for the 8 stations located within the frame of Fig. 3. The 5 stations that lie within 20 km of the Landers rupture show general features of the postseismic deformation, with roughly fault-parallel movements except near the ends of the rupture. Because of end effects, near-fault complexities, and likely along-strike variations in postseismic slip, station displacements both close to the rupture (Lazy) and near its termination points (7000, Sand, Paxu) are of limited utility in comparing with our model results. Station 7001, which lies close to our profiles and about 8 km from the fault, provides the most definitive check. We first use the maximum amplitudes observed on the 03Jul-25Dec92 interferogram profiles (Fig. 2) to infer the contributions of Models 1 and 2 in the 6 months following the earthquake. Assuming equal contributions from each model we compute a horizontal displacement at station 7001 of 49 mm on an azimuth of 162°, which compares with the GPS values of 36 mm along 171°, acceptable agreement considering the assumptions used in both calculations. Model 1 has three times the slip of Model 2, so the effect of Model 2 is to rotate the displacement vector slightly (20°) towards the fault, as is observed. The fault-normal displacement of station Lazy is consistent with fault zone collapse (Model 2), but the site does lie within a few km of a secondary splay of the surface rupture. In addition,

any Model 1 slip required to explain fault-parallel movements of station Sand would introduce a more northerly component into the displacement field at station Lazy.

We found that synthetic interferograms computed using the postseismic slip model derived from inversion of the GPS data are quite inconsistent with our SAR images. This disagreement is not surprising given the admitted non-uniqueness of the model (see Shen et al., 1994) and the very incomplete spatial sampling of the deformation field by the GPS measurements. The comparison illustrates the difficulty of unravelling the mechanisms responsible for observed deformation with necessarily limited conventional survey measurements, especially when, as here, more than one process is operating. Our result not only shows the unique capability of SAR interferometry to provide the necessary complete mapping of the postseismic deformation field but, as importantly, it casts new light on poorly understood lithospheric relaxation processes. Given the demonstrated sensitivity of the method, we can expect that new SAR measurements of postseismic deformation will play an important role in more fully elucidating these processes. The result also provides grounds for optimism that the even fainter deformation signal associated with inter-earthquake elastic strain accumulation can also be detected using radar interferometry.

FIGURE CAPTIONS

Figure 1. Location map. Thin lines denote known faults; heavy lines, the surface rupture. Large, inclined box delimits the 120 X 275 km area covered by the interferograms. The radar antenna, at 785 km altitude, points across this swath at an azimuth of N77°W with an average angle of incidence of 23°. The interferometric sensitivity to various ground displacements is expressed by the unitary vector (East, North, Up): E = 0.333; N = -0.07; U = 0.94. The smaller box is the location of Fig. 2.

Figure 2. Bar chart showing the interferograms used in this study as a function of time. The number on each bar is h_a, the altitude of ambiguity, equal to the amount of error in the DEM which produces one artefact fringe. The elevation model was produced by the U.S. Defense Mapping Agency which calls it a Digital Terrain Elevation Data, Level 1 (DTED-1), and is distributed by the U.S. Geological Survey.

Figure 3. Detail of contours for the "Combined" interferogram constructed by adding two interferograms made of radar images acquired: (1) On 3 July 1992 and 2 April 1995, and (2)On 7 August 1992 and 18 June 1993. No pair of radar images could create this interferogram. The effective altitude of ambiguity is more than 16000m, suppressing all topographic residuals. . Thin lines denote Landers fault. Locations of two deformation patterns discussed in the text are outlined by dotted rectangles and locations of profiles plotted in Fig. 3 are shown. Triangles locate GPS stations and arrows show inferred displacements during the 6 months following the Landers earthquake.

Figure 4. *(a)* Profile 1 *(b)* Profile 2. See locations in Figure 3. Solid jagged lines denote data, dasshed lines show models fit to them. The maximum amplitude was obtained between points A and B in the profiles.

REFERENCES

Byerlee, J., *Geology*, **21**, 303-306, 1993.

Gabriel, A.K., Goldstein, R.M. & Zebker, H.A. *J. Geophys. Res.* **94**, 9183-9191, 1989.

Goldstein, R.M., Engelhardt, H., Kamb, B. & Frolich, R.M. *Science* **262**, 1525–1530, 1993.

Massonnet, D., *et al. Nature* **364**, 138-142, 1993.

Massonnet, D., Briole, P. & Arnaud, A. *Nature* **375**, 567-570, 1995.

Okada, A., and Nagata, T., Bull. Earthq. Res. Inst. Tokyo Univ., **31**, 151-167, 1953.

Peltzer, G., P. Rosen, F. Rogez, and K. Hudnut, Science, 273, 1202-1204, 1996.

Savage, J. C., and Plafker, G., J. Geophys. Res., **96**, 4325-4335, 1991.

Savage, J.C., Lisowski, M., and Svarc, J.L., *J. Geophys. Res.* **99**, 13757-13765, 1994.

Sleep, N.H., and Blanpied, M.L., *Nature*, **359**, 687-692, 1992.

780-791, 1994.

Shen, Z., Jackson, D., Feng, Y., Kim, M. & Cline, M. *Bull. Seism. Soc. Amer.* **84**,

Thatcher, W., J. Geophys. Res., **88**, 5893-5902, 1983.

Thatcher, W., *Roy. Soc. N.Z., Bull.* **24**, 245-272, 1986.

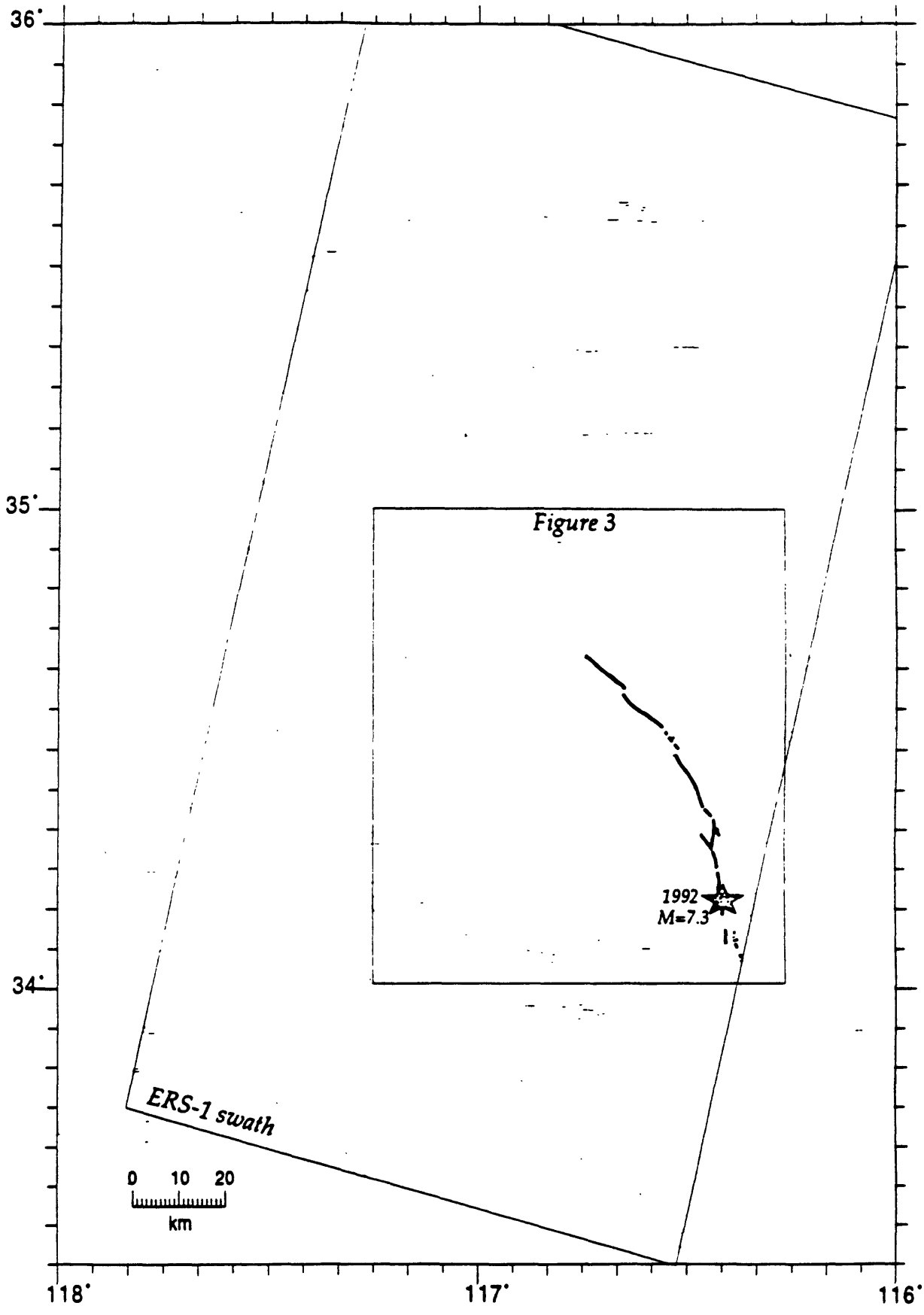
LOCATION MAP
36°
35°
34°
118°
117°
116°
Figure 3
1992
M=7.3
ERS-1 swath
0 10 20
km

Figure 1

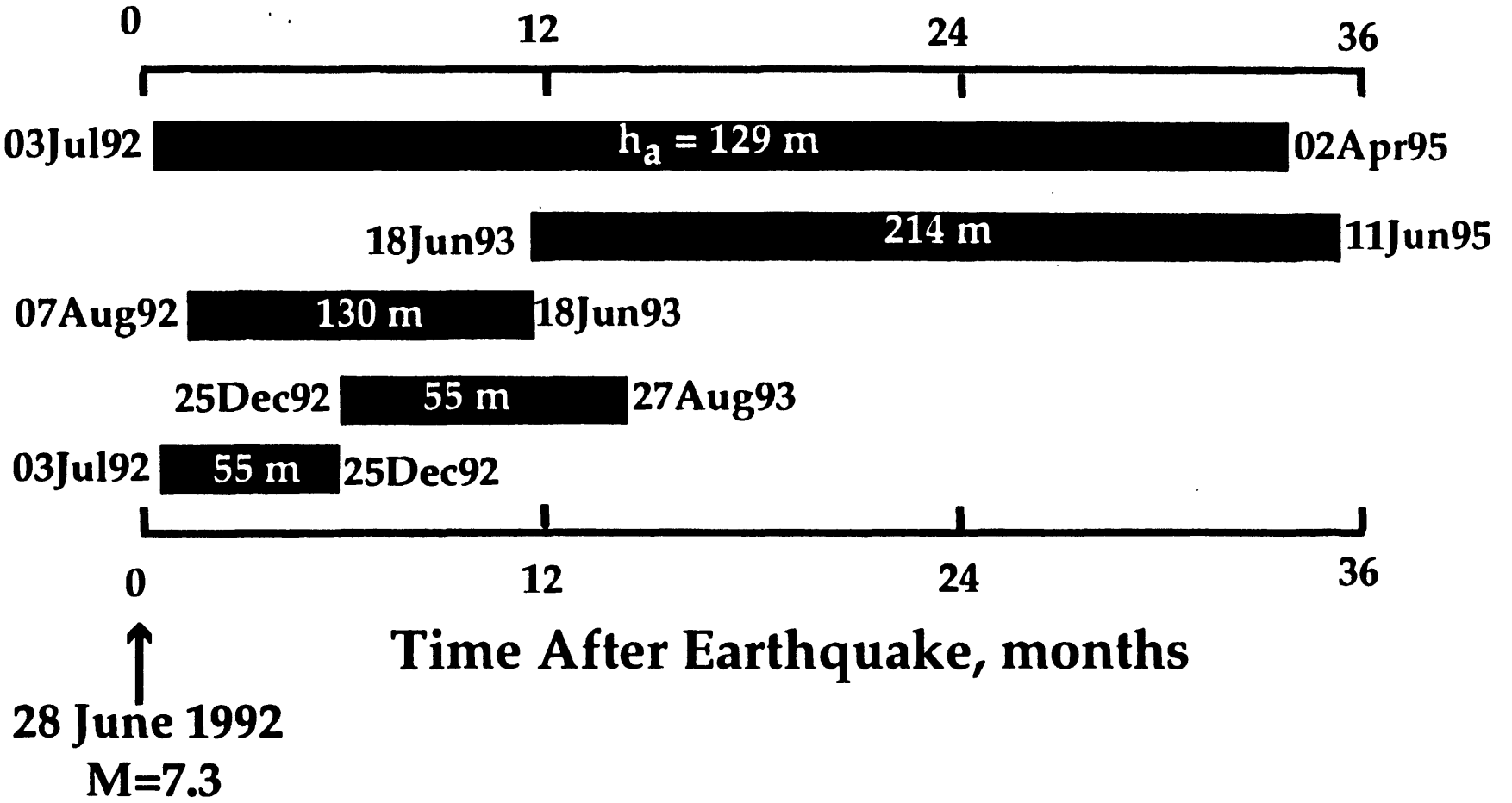
0
12
24
36
03Jul92
h_a = 129 m
02Apr95
18Jun93
214 m
11Jun95
07Aug92
130 m
18Jun93
25Dec92
55 m
27Aug93
03Jul92
55 m
25Dec92
0
12
24
36
Time After Earthquake, months
28 June 1992
M=7.3

Figure 2

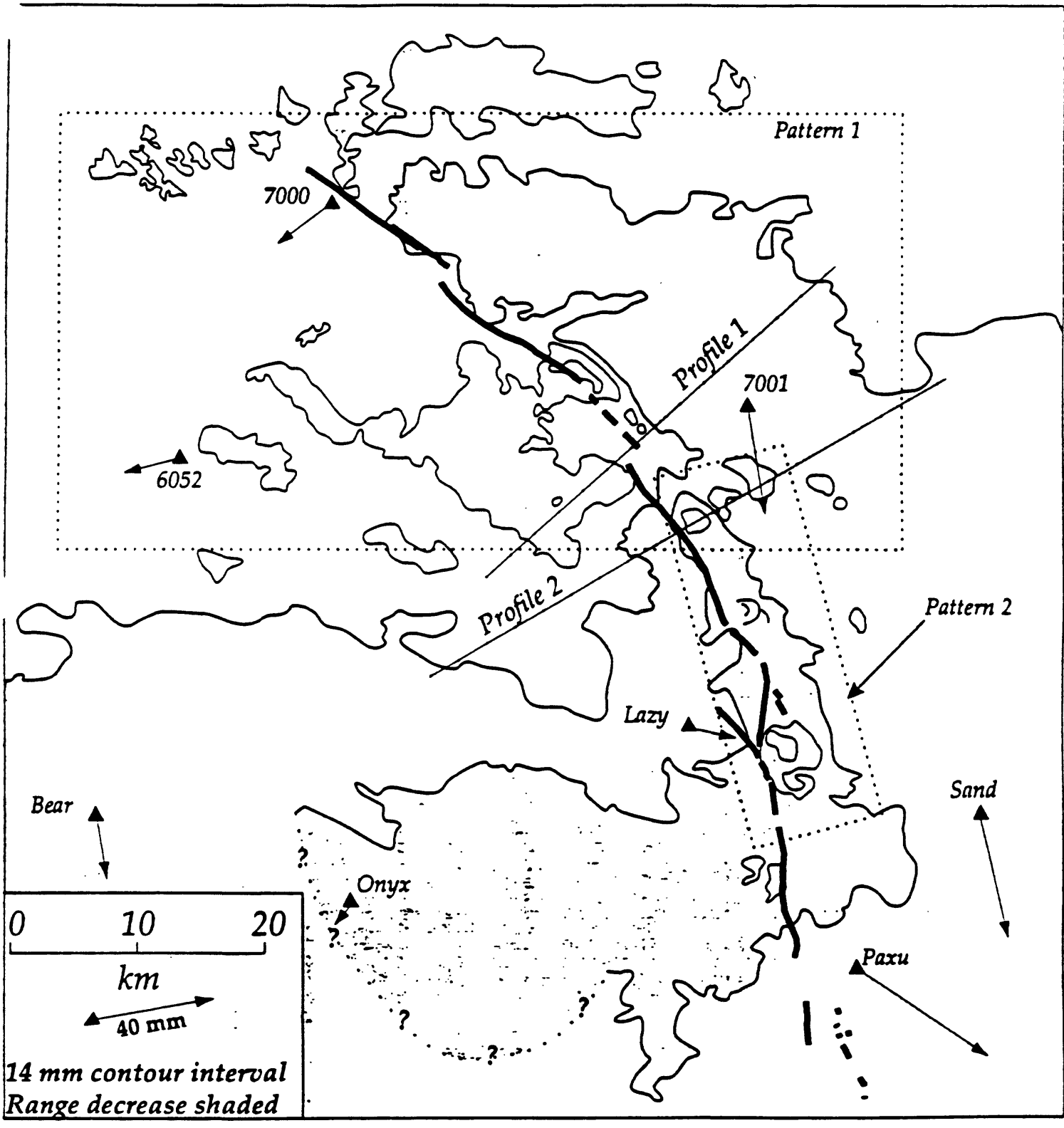
Pattern 1
7000
Profile 1
7001
6052
Profile 2
Pattern 2
Lazy
Bear
Sand
Onyx
Paxu
0
10
20
km
40 mm
14 mm contour interval
Range decrease shaded

Figure 3

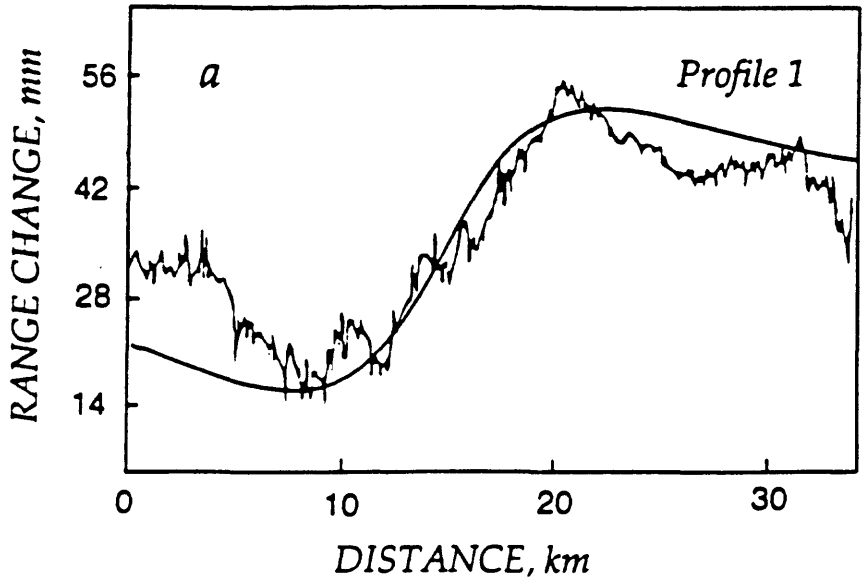
a
Profile 1
RANGE CHANGE, mm
56
42
28
14
0
10
20
30
DISTANCE, km

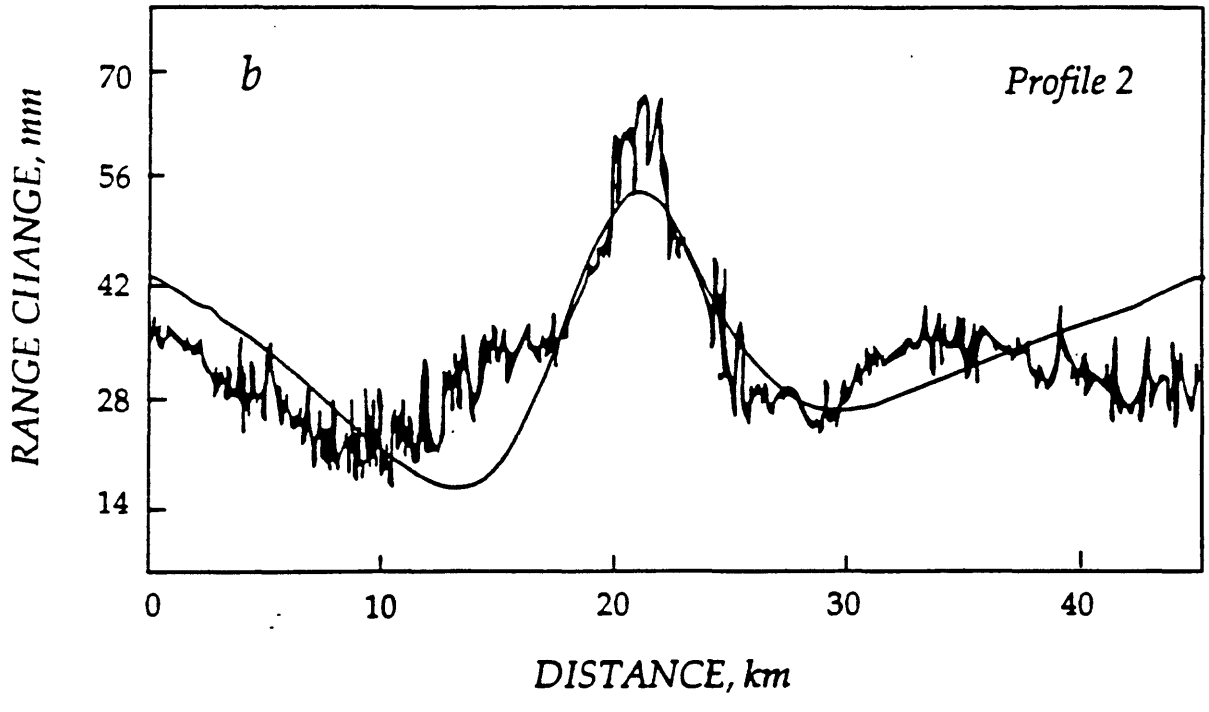
b
Profile 2
RANGE CHANGE, mm
70
56
42
28
14
0
10
20
30
40
DISTANCE, km

Figure 4

Recent seismic activity around Tokyo area

by

Yoshimitsu OKADA

Earthquake Research Center, National Research Institute
for Earth Science and Disaster Prevention
Tennnodai 3-1, Tsukuba, 305 Japan
okada@geo.bosai.go.jp

Abstract

A large number of artificial earthquakes contaminate the catalog of shallow earthquakes in the Kanto-Tokai area, central Japan due to quarry blasts or large-scale public works. To distinguish between them, the occurrence time distributions were examined for each of 193 earthquake clusters shallower than 20 km, and 81 clusters were identified as artificial ones. They occupy 25%-30% of the total number of shallow events in the catalog and are mainly located around big cities such as Tokyo and Nagoya. Based on the data excluding artificial events, a volume of seismic quiescence was found at the north of Tokyo.

Among the recent seismic activity around Tokyo area, there were two noteworthy events. One is the M6.2 earthquake which occurred off Cape Inubo with a depth of 50km and with a normal fault type focal mechanism. This event seems to be generated in the Pacific plate due to the bending effect. The other is the small-scale earthquake swarm beneath the eastern coast of Boso Peninsula in May, 1996. Compared to the earthquake size, it was deteted a considerable crustal deformation, from which we can infer the occurrence of a slow earthquake.

1. Distribution of artificial earthquakes around Tokyo and temporal changes

Since the occurrence of disastrous Kobe earthquake of Jan., 1995, many seismologists in Japan are thinking better of shallow seismic activities in their fields. When we study such a work, it often becomes a big problem how we can eliminate the artificial earthquakes due to quarry blasts or large-scale public works.

It is known that a large number of artificial events are contaminated in the catalog of shallow microearthquakes in the Kanto-Tokai area, central Japan. We have tried to distinguish between these events by the following procedure [Okada, 1996].

(1) Count the number of events contained in a 1-km cubic mesh for the earthquakes shallower than 20km in the Kanto-Tokai area within a 16.5-yr. period, Jul., 1979 to Dec., 1995.

(2) Sum up the number of events contained in a 2-km block, shifting 1-km to NS, EW and vertical directions.

(3) Select the 2-km blocks which contain 10 or more events, and combine them if the blocks are connected each other. Thus, 193 earthquakes clusters are automatically extracted.

(4) Make a diagram like Figure 1.1 to show occurrence time distributions.

(5) Judge from the pattern of the diagram whether the cluster is composed of natural earthquakes or artifitial ones.

As the result, we could identify 81 earthquake groups as artifitial ones out of 193 clusters(Figure 1.2). They are mainly located around big cities such as Tokyo and Nagoya. Based on this work, we can classify all the earthquakes into three categories, i.e. (a) blast clusters, (b) natural clusters, and (c) non-clustered earthquakes. Figure 1.3 shows diagrams showing occurrence time distributions for the assembled earthquakes in each category stated above.

In Figure 1.3(c), it still remains both features of blast clusters and natural clusters. It seems due to marginal distributions of corresponding events in which the number of earthquakes in 2-km block did not reach to 10.

The artifitial events occupy 25% to 30% of the total number of shallow events in the catalog. Figure 1.4 shows the relation between magnitude and cumulative frequencies for the events in three categories above.

Each cluster of artificial earthquakes has its own distribution in regard to occurrence time within a day, usually showing a pattern of single or double peaks. We can also find wide varieties in the time series of artificial events, showing continuous, intermittent, or only temporary patterns. The distribution of artificial earthquakes has a close relation to industrial activities. It was found that the change in the total number of the artificial earthquakes roughly corresponds with changes in economic trends in Japan(Figure 1.5).

2. Seismic quiescence around Tokyo

Figure 2.1 shows epicentral distribution of the earthquakes around Tokyo shallower than 35km. Here is plotted the earthquakes which occcurred only during a nighttime (from 19h to 07h) to avoid the contamination of artificial earthquakes such as quarry blasts. Bold lines in the figure indicates the distribution of active faults. It is impressive that four clusters form in a line along 36N in latitude with an almost constant spacing of 35km. Furthermore, they locate around the northern ends of the major active faults by chance.

Figure 2.2 shows cross section of the hypocenters in a rectangle region, AB, indicated in FIgure 2.1, together with a space-time plot. The depths of the clusters become deeper from west to east, and we can find clear seismic quiescence in the third cluster from the west which is located at the depth of about 25km.

Wyss and Wiemer(1996) discussed quantitatively the seismic quiescences around Tokyo to find out three current quiescent volumes including the one stated above. They suggest that this may be a sign of M6.5 earthquake, although they also argue that such a hypothesis may be denied if they take account of high b-values estimated for these volumes.

3. M6.2 earthquake off Cape Inubo of Sep.11,1996

On Sep.11, 1996, an earthquake of M6.2 took place at 40km ESE off Cape Inubo, Chiba Prefecture, with a depth of 55km and a mechanism solution of normal fault type with T-axis in NNE-SSW direction. The epicenter of this earthquake is indicated with a large triangle in Figure 3.1, where the events in Kanto area shallower than 80km are shown. Figure 3.2 shows the cross section of the hypocentral distribution down to the depth of 150km in a rectangle, AB, indicated in Figure 3.1. The M6.2 events locates within the Pacific plate and is near to the crest of bending, from which we can infer that this event was generated due to the bending effect of the plate. The occurrence modes of recent moderate earthquakes belonging to the intraplate events in the Pacific plate is illustrated in Figure 3.3.

4. Earthquake swarm beneath the eastern coast of Boso Peninsula of May,1996 and the occurrence of a possibe slow earthquake

In May, 1966, a small-scale earthquake swarm was generated beneath the eastern coast of Boso Peninsula with the largest event of M3.9 at a depth of about 25km. Successive seismic activity was followed off the peninsula at deeper zone. Including this event, the tectonic setting of this region is realized as shown in Figure 4.1 [Okada and Kasahara, 1990].

Associated to this seismic swarm, it was found horizontal displacement of about 1cm to ESE direction by GPS at several stations in the eastern Boso Peninsula as well as 0.5microradian westward tilting at nearby borehole tiltmeter station, Katsuura(Figure 4.2). Both of the crustal deformation data were too large compared to the expected static deformation by a M3.9 earthquake. We can speculate the occurrence of a slow earthquake of M5-6 at a shallow depth to explain the observation. Looking back to the tiltmeter record at Katsuura station, we found that the similar phenomenon might occur in May, 1983, at when an extensive seismic swarm also appeared including a M5 earthquake [Noguchi, 1984].

References

Noguchi, S. (1984) Seismic activity near east coast of Boso Peninsula in May, 1983, Rep. Coord. Comm. Earthq. Pred., 31, 159-164. (in Japanese)

Okada, Y. (1996) Distribution of artificial earthquakes in the KAnto-Tokai area and temporal changes, Rep. Natl. Res. Inst. Earth Sci. Dissa. Prev., 57, (in press; in Japanese with English abstract).

Okada, Y. and K. Kasahara(1990) Earthquake of 1987, off Chiba, central Japan and possible triggering of eastern Tokyo earthquake of 1988, Tectonophysics, 172, 351-364.

Wyss, M. and S. Wiemer(1996) Two current seismic quiescences within 40km of Tokyo, Geophys. J. Int., (in submit).

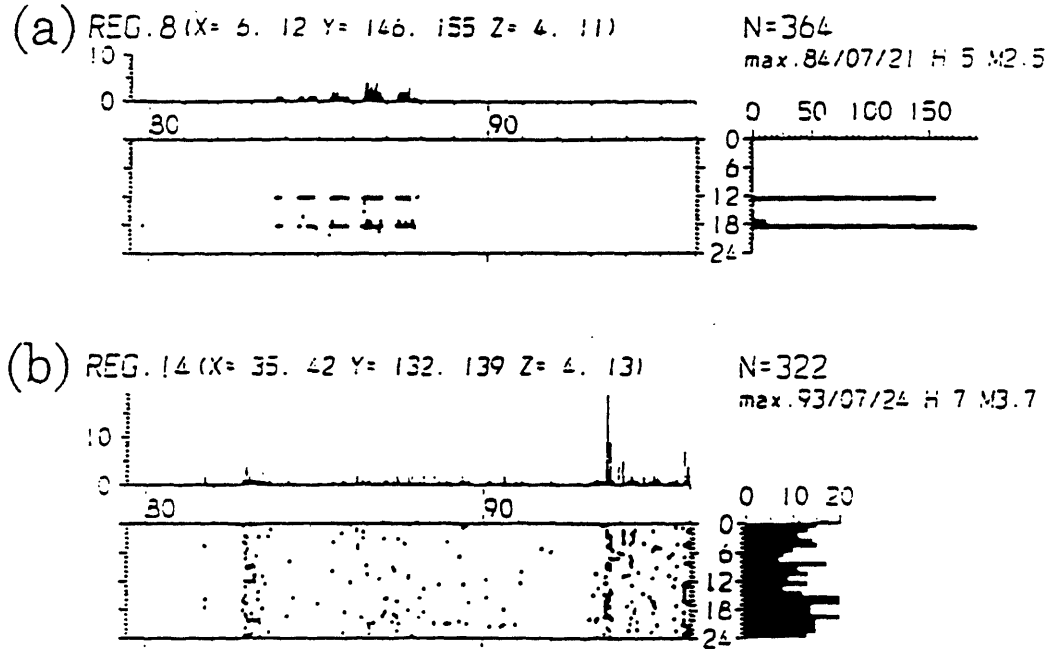

Figure 1.1 A sample of diagram showing occurrence time distribution. Daily earthquake numbers and hourly frequency of the occurrence times within a day are also plotted together with number of earthquakes and a list of maximum event. (a) represents the cluster of artificial events, while (b) is for natural ones.

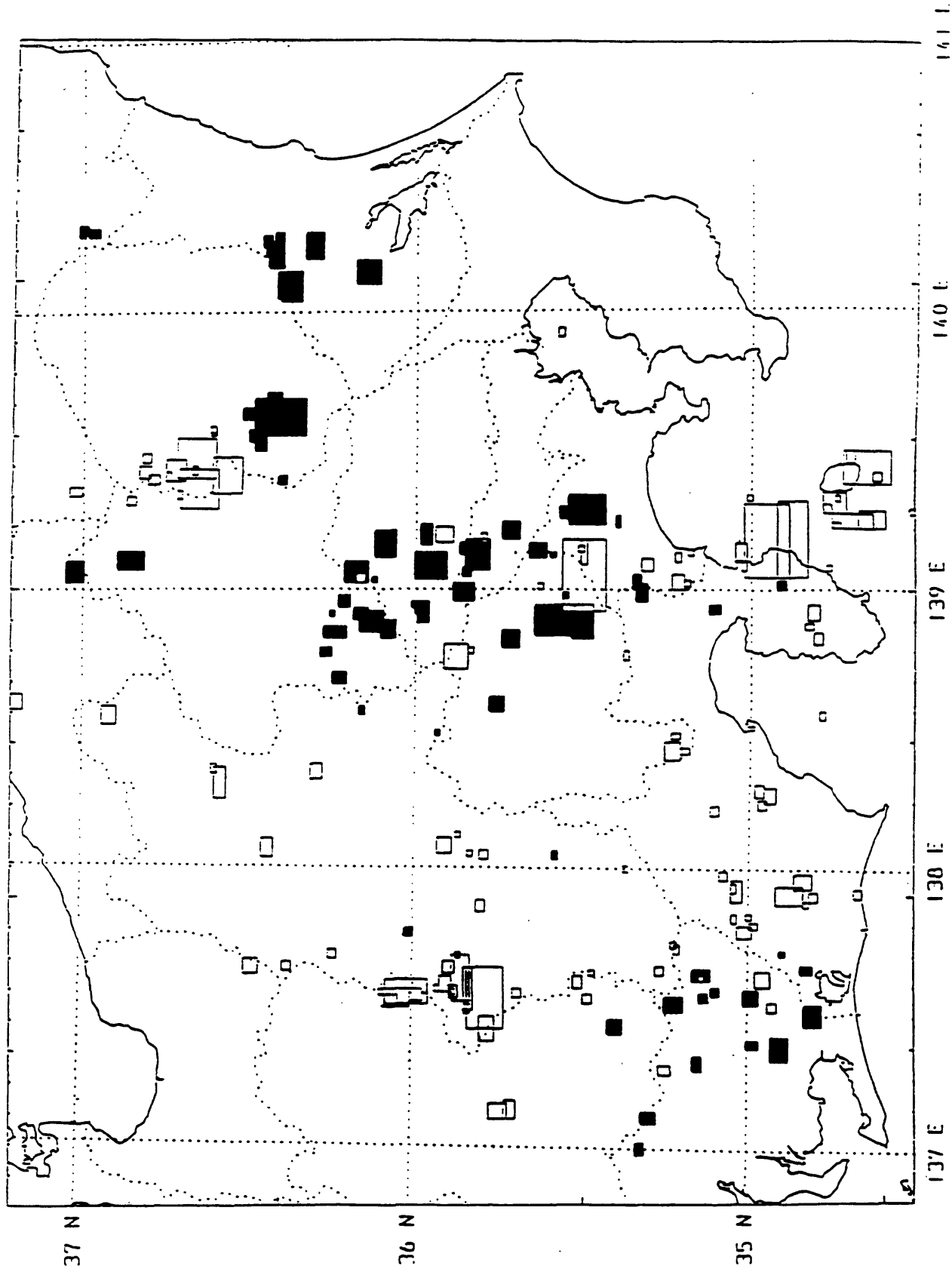

Figure 1.2 Classification of the earthquake clusters. 81 clusters(closed rectangles) were identified as artificial ones, while the remaining 112 clusters(open rectangles) were judged as natural ones.

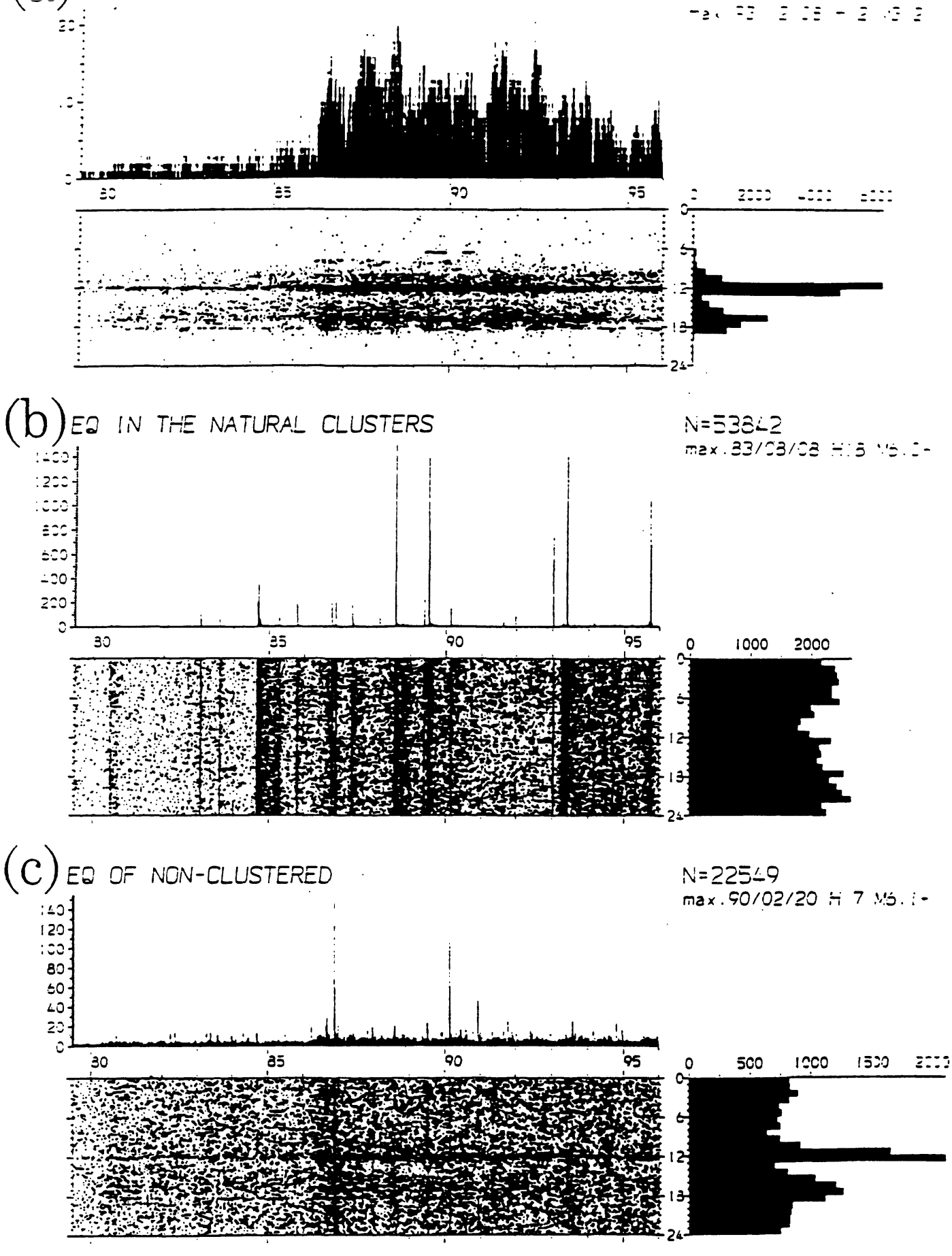

Figure 1.3 Diagrams showing occurrence time distributions for assemblies of (a)blast clusters, (b)natural clusters, and (c)non-clustered earthquakes. Increase of registered events in Apr. 1986 is due to the updating of the routine data processing system.

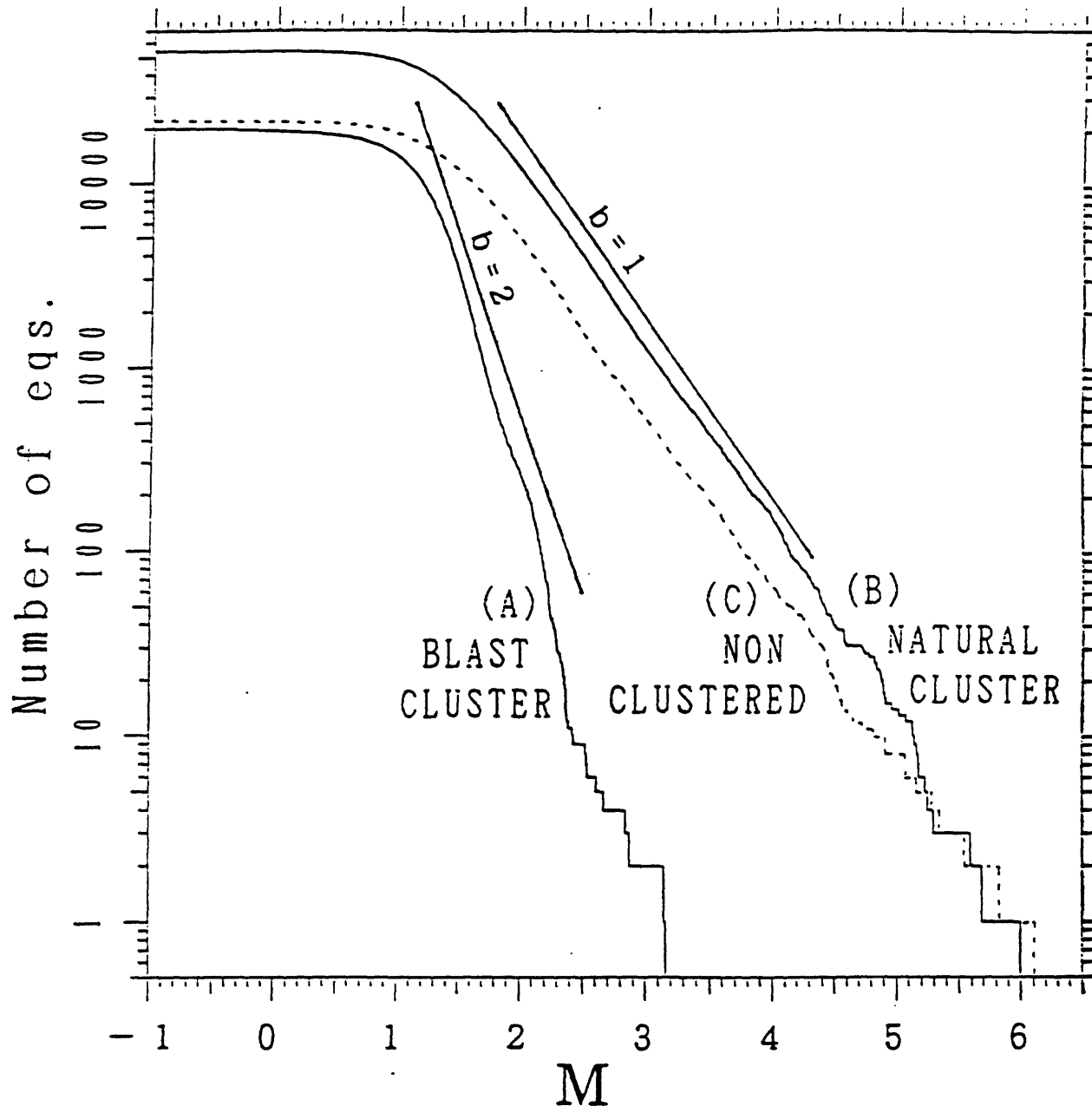

Figure 1.4 Distribution of magnitude-cumulative frequencies for (a)blast clusters, (b)natural clusters, and (c)non-clustered earthquakes.

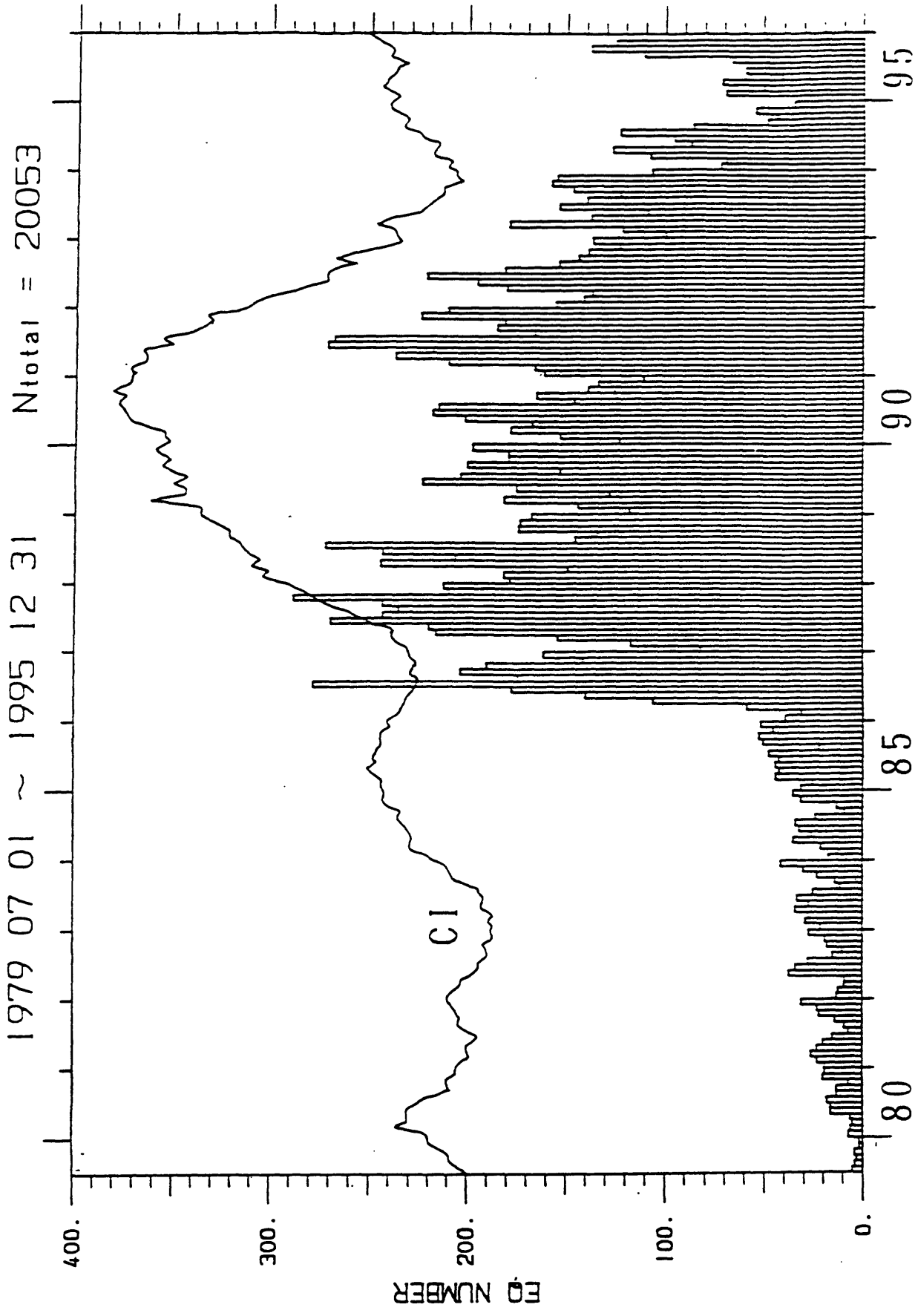

Figure 1.5 The change in monthly earthquake numbers for the blast clusters, compared with the economic composite index(CI) of Japan.

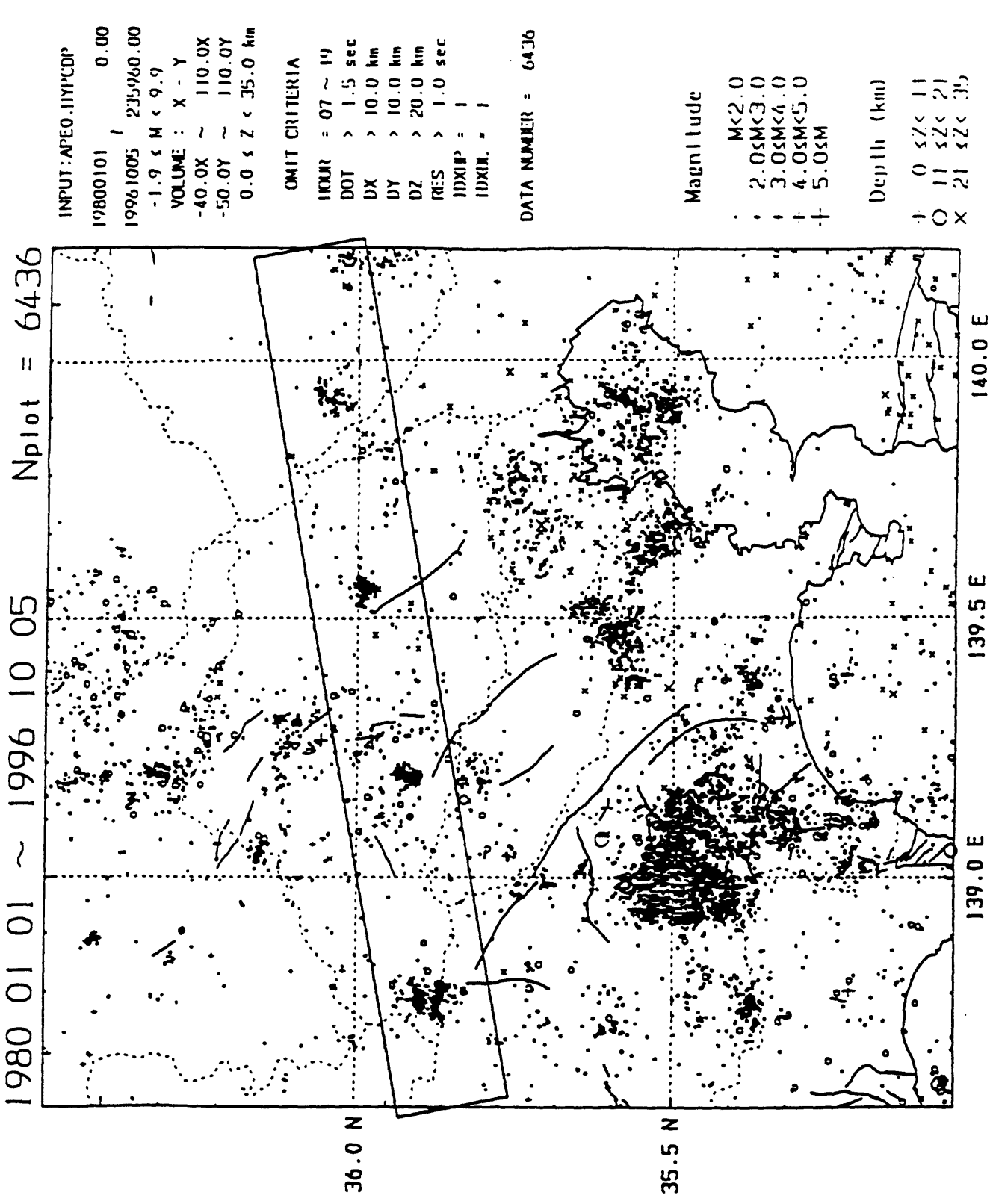

Figure 2.1 Epicentral distribution of earthquakes shallower than 35km around Tokyo. Only the events occurred during nighttime(19:00-07:00) are plotted to avoid the contamination of artificial earthquakes.

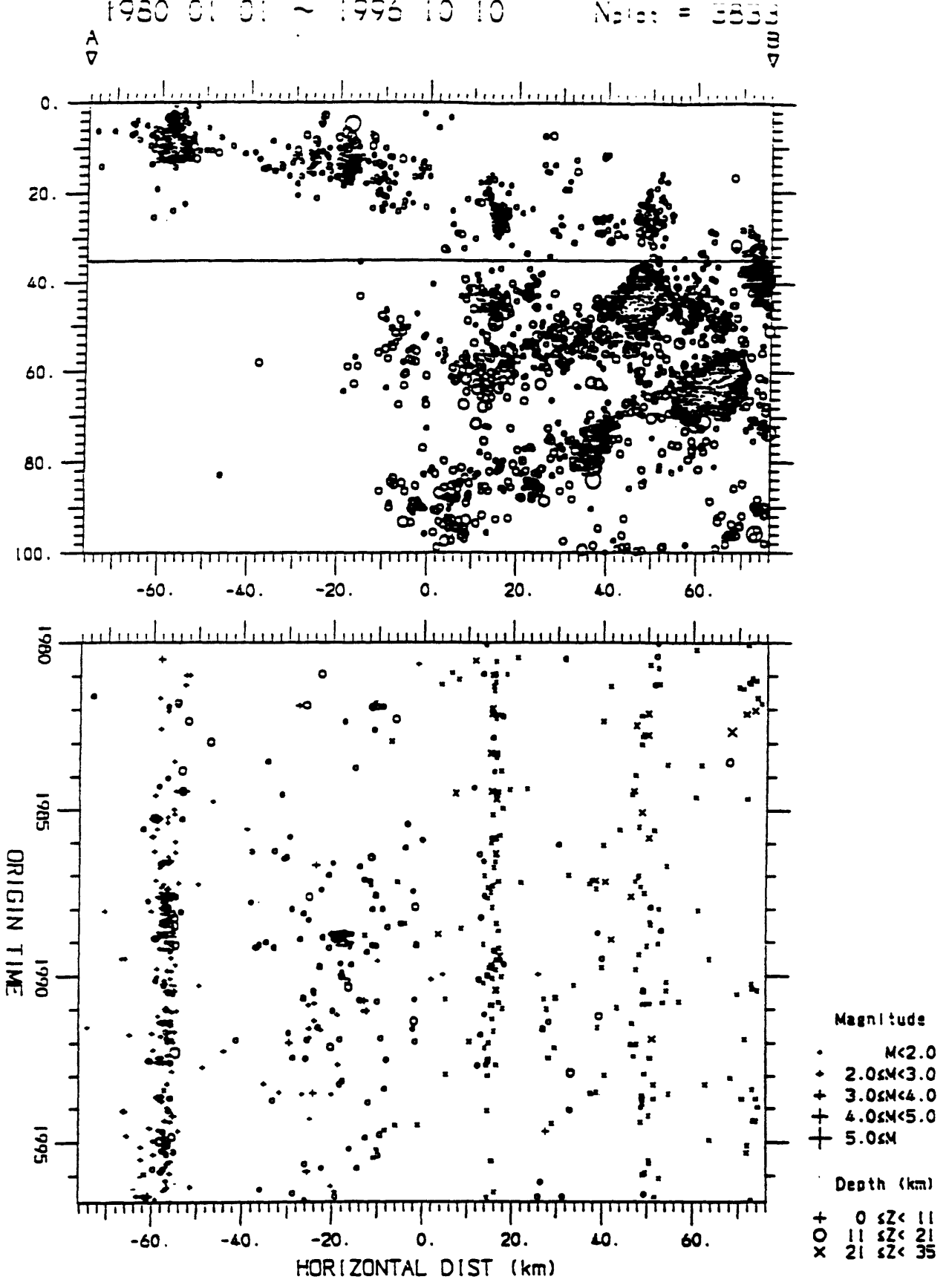

Figure 2.2 Cross section of the hypocentral distribution down to the depth of 100km in a rectangle shown in Figure 2.1, together with a space-time plot of the earthquakes shallower than 35km. The 3rd cluster from the west shows a seismic quiescence in recent.

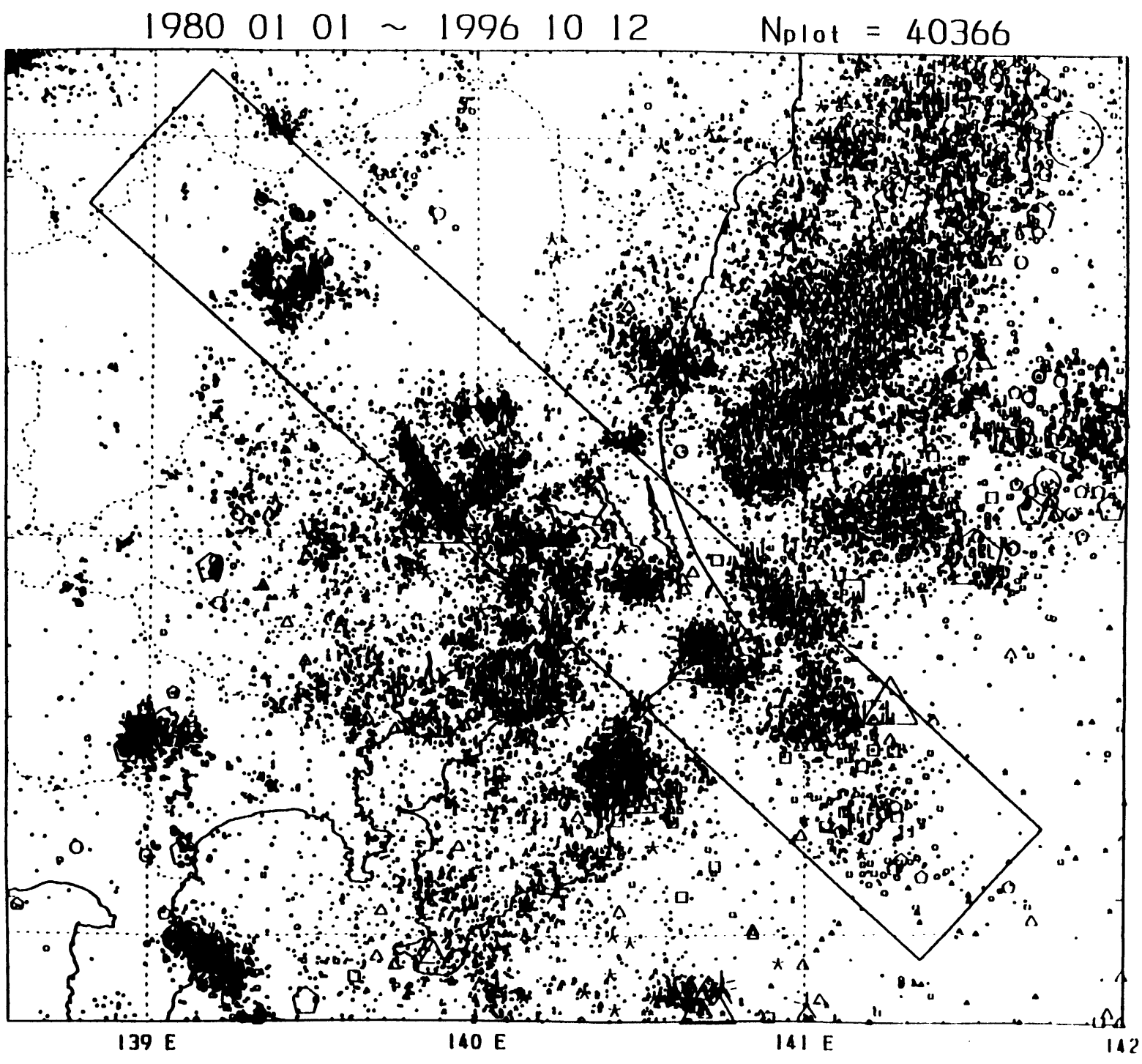

Figure 3.1 Epicentral distribution of Earthquakes shallower than 80km with magnitude 2 or larger in the Kanto area, central Japan. A large triangle ESE off Cape Inubo shows the earthquake of M6.2 on Sept. 11, 1996.

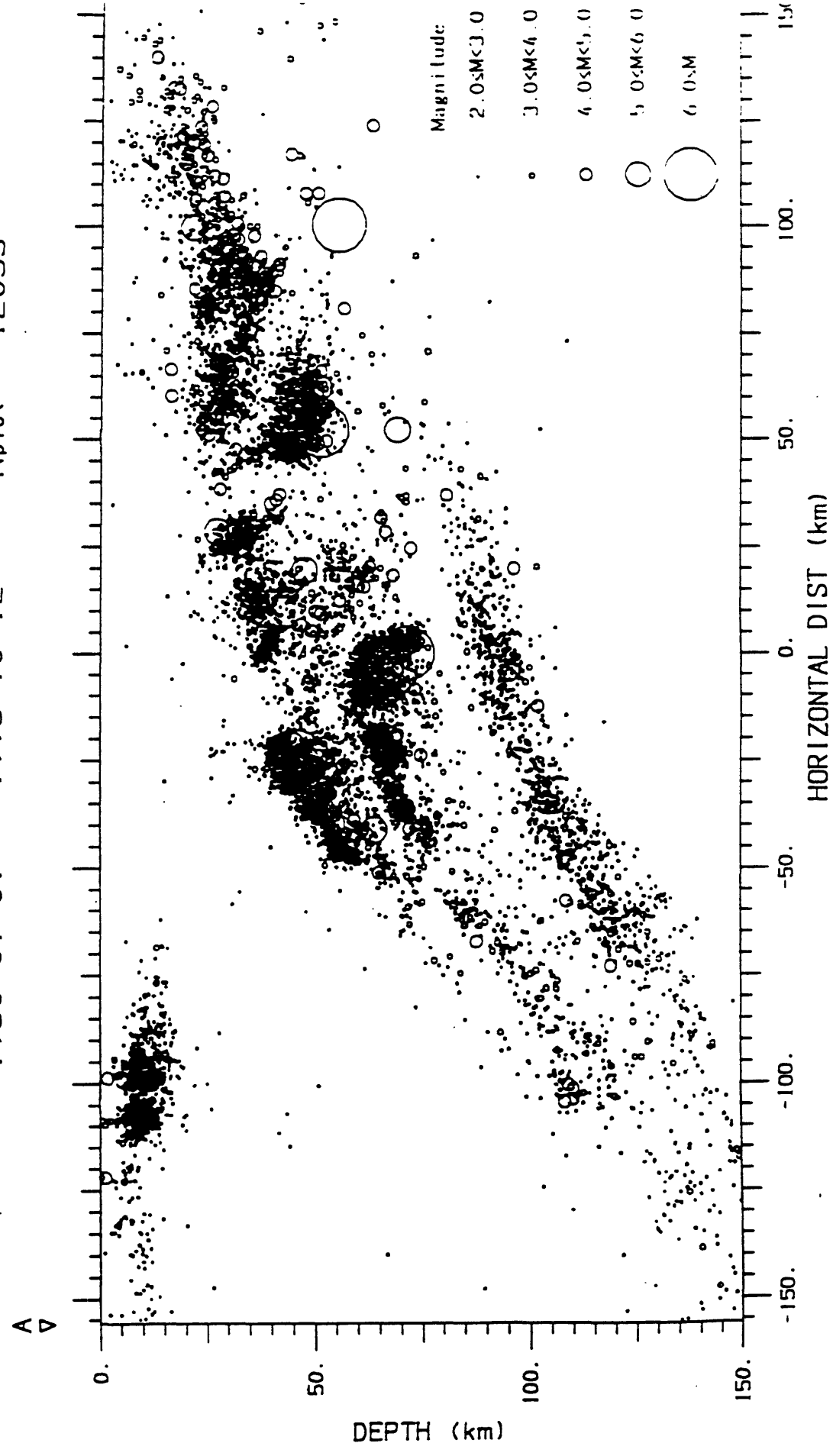

Figure 3.2 Cross section of the hypocentral distribution down to the depth of 150km in a rectangle, AB, indicated in Figure 3.1.

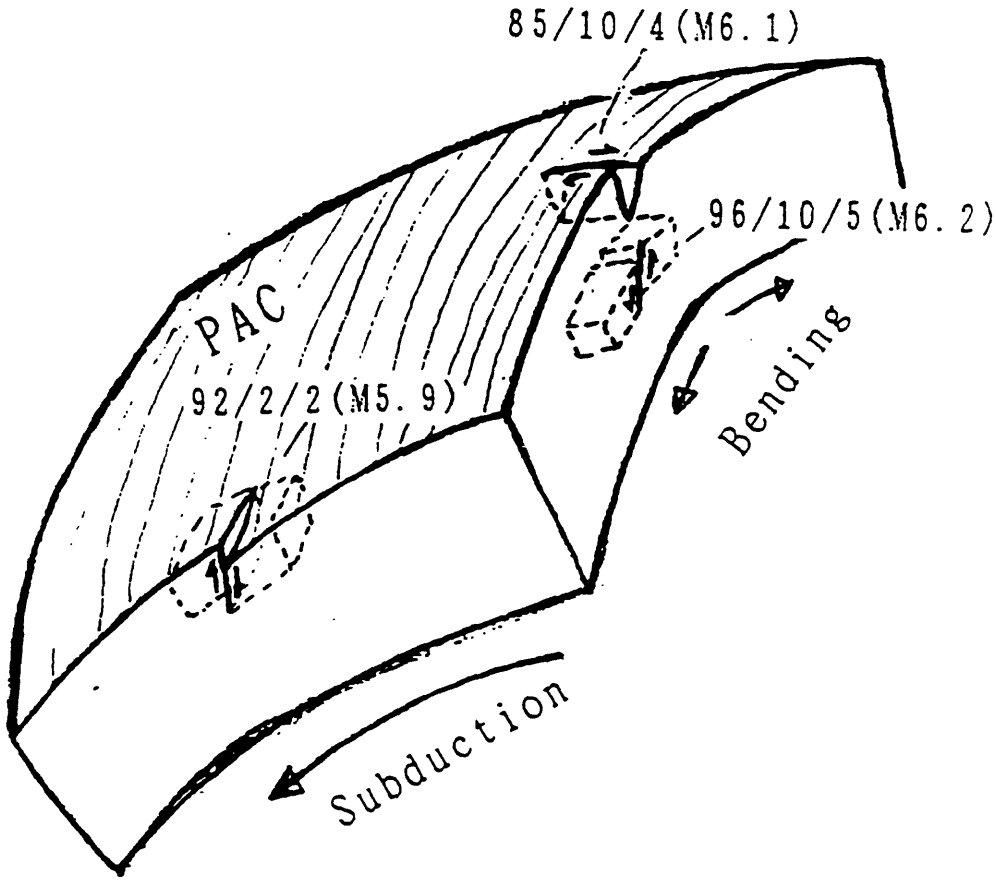

Figure 3.3 The occurrence modes of recent moderate earthquakes belonging to the intraplate events in the Pacific plate.

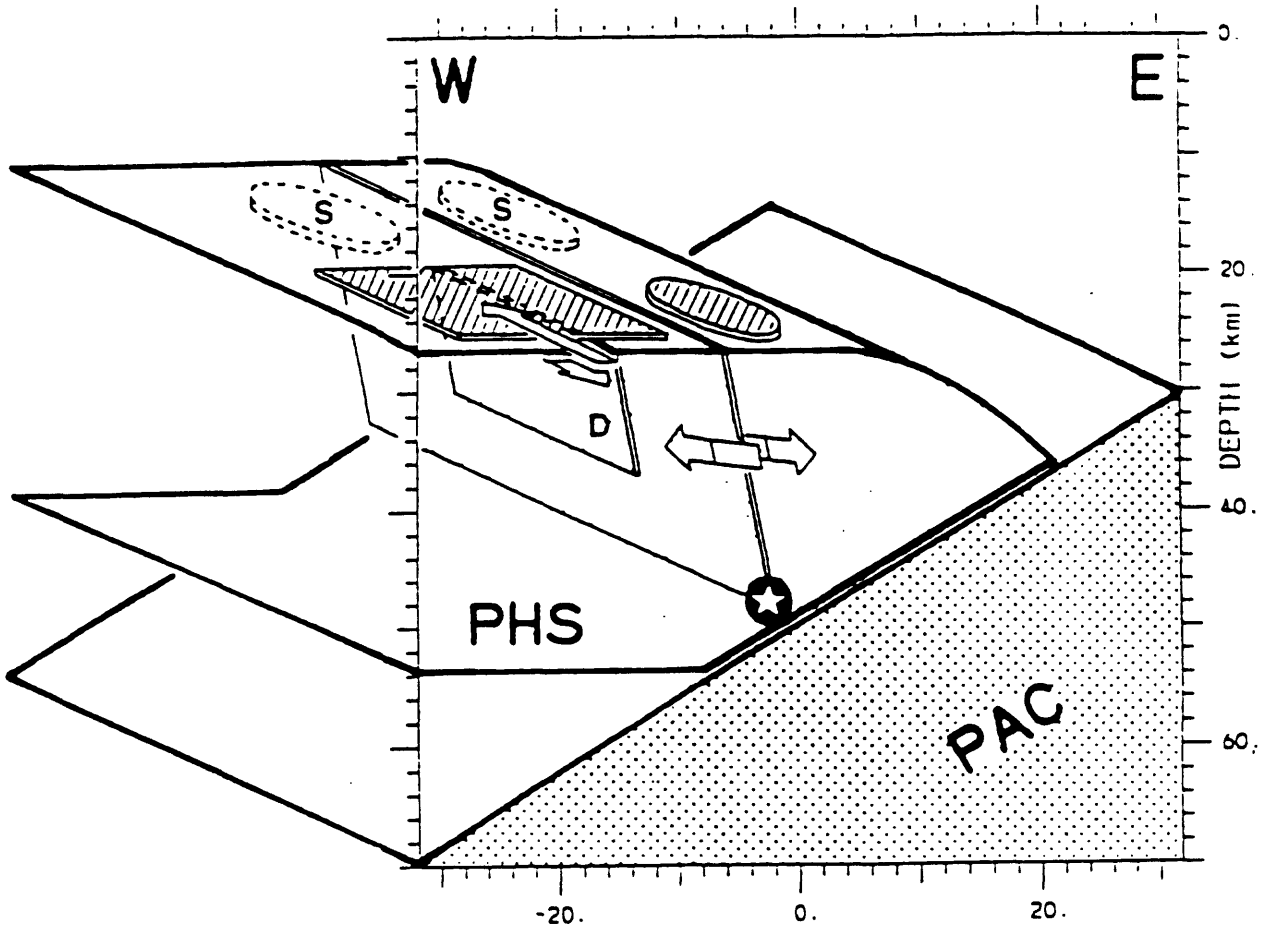

Figure 4.1 Tectonic setting of the region beneath the eastern coast of Boso Peninsula [Okada and Kasahara, 1990].

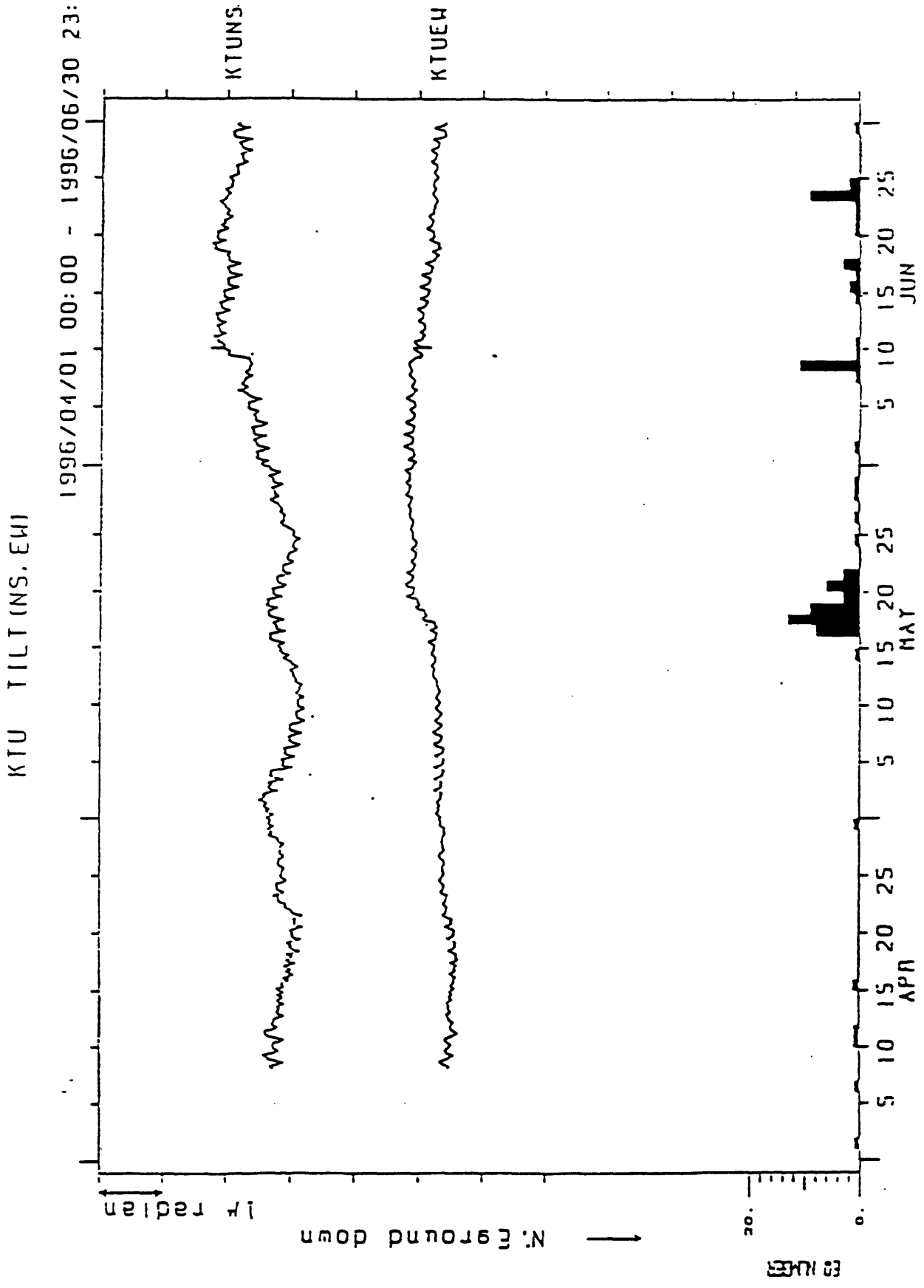

Figure 4.2 A tilimeter record associated to the seismic activity beneath the eastern Boso Peninsula on May, 1996.

Earthquakes, Faults, and Stress in Los Angeles: Seismotectonic Review

Egill Hauksson
California Institute of Technology, Pasadena, CA 91125

L. M. Jones
US Geological Survey, Pasadena, CA 91106

Los Angeles lies within a geologically complex region at the intersection of the strike-slip faulting of the San Andreas fault system in the Peninsular Ranges and the reverse and thrust faulting of the Transverse Ranges. A transition zone of left-lateral strike-slip faults and south dipping reverse faults forms the southern edge of the Transverse Ranges at the center of the city. Over one hundred faults pose a risk to the metropolitan region, including the San Andreas fault itself. Moderate to large earthquakes occur on all those faults while major earthquakes are possible on more than a dozen faults.

The three-dimensional crustal structure of the Los Angeles area provides images of tectonic structures associated with both surficial and concealed faults. Surficial faults such as the Newport-Inglewood, Santa Monica, and the Whittier faults coincide with strong velocity contrast along the basin edges. In contrast, the upthrown side of blind faults appear to be associated with uplift of high velocity blocks. These observations suggest that surficial faults may play a predominant role in the deformation of the upper crust while deep-seated blind faults also accommodate the deformation of the lower crust.

The maximum horizontal stress changes direction across the Los Angeles region with northeasterly trends to the south and northerly trends in the Transverse Ranges. This rotation of the maximum horizontal stress may be influenced by the incipient subduction beneath the Transverse Ranges as well as the San Andreas fault itself, which may be a stress refractor. In addition to affecting the deformation of tectonic structures the stress state also may change at the time of major earthquakes in southern California. The rate of small earthquakes ($M \geq 3$) in the Los Angeles basin suddenly decreased both following the M7.4 Kern County and the M7.3 Landers earthquakes suggesting regional strain release. Following the 1952 earthquake the strain reaccumulation took more than 15 years suggesting lower seismicity rate for the Los Angeles area for the next several years.

CHASE : A method for quantitative evaluation of seismic quiescence before large earthquakes

Akio Yoshida, Kohji Hosono and Hidemi ITO

Earthquake Prediction Information Division

Seismological and Vocanological Department

Japan Meteorological Agency

1-3-4, Otemachi, Chiyoda-ku, Tokyo 100, Japan

Abstract

We propose a method for quantitative evaluation of seismic quiescence before large and moderate earthquakes. An essence of the method exists in the point that increase or decrease of seismicity is more clearly detected by taking difference of occurrence rate of earthquakes between former and later periods. We call the method CHASE. Long-term trend of seismic activity is canceled in the analysis, and seismicity change of any specific time scale can be extracted effectively by choosing the former and later periods properly. That is an advantage of the CHASE method. By taking the observational facts into consideration that the period of the precursory quiescence is more or less several years for great interplate earthquakes and a few months for moderate intraplate earthquakes, we show precursory seismic quiescence for both of great earthquakes and moderate earthquakes is effectively detected using the CHASE method..

§ 1. Introduction

Whether seismic quiescence could be a useful precursor for the prediction of large earthquakes or not has been a controversial problem for a rather long time (Kanamori, 1981; Ogata, 1992; Reasemberg and Matthews, 1988; Wiemer and Wyss, 1994; Wyss and Habermann, 1988). In general seismicity changes in various spatial and time scales. Among the causes of the seismicity change, occurrence of great earthquake is contained, but it is merely one of them. That situation seems to be a main factor that makes the problem complicated. The important might be to extract quiescence related to the occurrence of large earthquakes from various types of seismic quiescence. We, here, taking into consideration characteristics of precursory quiescence, propose a practically useful method to detect the quiescence before large and moderate earthquakes.

§ 2. CHASE method

Before introducing the CHASE method, I first note some characteristics of seismicity change.

Figure 1 shows epicentral distribution of earthquakes with $M \geqq 5.3$ in northeastern Japan and its east-off sea region, occurred during the period 1926 through 1995, and the cumulative number of earthquakes. A tendency which the inclination of the cumulative curve is small in recent years indicates that occurrence rate of earthquakes has been decreasing in a long time scale. That feature is clearly seen in Figure 2, where are plotted number of earthquakes which occurred during the time interval of preceding 15 years for each year, and that during the time interval of preceding 5 years. The mean number of earthquakes in recent years is only a half of that in the years before 1940s.

One more feature which should be noted is that seismicity level became

low several years before two great earthquakes, that is the 1952 Tokachi-oki earthquake and the 1968 Tokachi-oki earthquake, compared to that in the immediately preceding time period. The feature can be seen in the cumulative number of earthquakes in Figure 1.

A noteworthy thing which we can derive from the above-mentioned features is that the low level seismicity itself does not have much meaning in relevance to the precursory quiescence, but the important is the decrease of the seismicity relative to the immediately former period.

Figure 3 shows epicentral distribution of earthquakes with $M \geqq 5.5$ in the Kanto and its south-off region, occurred furing the period 1926 through 1995 and the cumulative number of earthquakes. In this region two tectonically significant earthquakes occurred in 1953, the off Boso Peninsula earthquake, and in 1972, the east-off Hachijojima eartqhuake. Before those earthquakes we can also recognize decrease of seismicity for the period of more or less several years compared to the seismicity in the preceding periods. The seismicity in the south-off Kanto region has a tendency to decrease in a long time scale as well. The feature is seen in Figure 4, where the change of number of earthquakes as that in Figure 2 is shown. The high activity until the mid of 1950s is considered to be due to the influence of the 1023 great Kanto earthquake by some Japanese seismologists.

Figure 5 shows the space-time distribution of earthquakes during 15 years before the 1968 Tokachi-oki earthquake and Figure 6 is a similar plot of earthquakes during 15 years before the 1972 east-off Hachijojima earthquake. We can see from these space-time diagrams that the quiescence before each of the two large earthquakes occurred in really wide areas: the area extended to whole of the region investigated.

The CHASE method, which we propose here, takes advantage of the above shown characteristics of the precursory quiescence, that the duration

is more or less several years commonly, and the quiescence appears in a wide area, much wider areas than the focal regions. The term CHASE is an abbreviation of CHAnge of SEismicity, amd the CHASE value is defined as the following.

$$\mathrm{CHASE}(i) = \sum_{j=0}^{m-1} \frac{N_{ij}}{m} - \sum_{j=m-1}^{m+n-1} \frac{N_{ij}}{n}$$

As is seen from the definition CHASE represents difference of average occurrence rate of earthquakes between the preceding and the succeeding periods. In other words, CHASE is the difference of the average inclination of the cumulative curve between the former and the later periods. An advantage of taking difference between occurrence rates of the preceding and the succeeding periods is that the decrease or increase of seismicity in any specific time scale which w want to see, in this case decrease in a time scale of several years, could be extracted effectively. Another advantage of taking the difference is that trending change of seismicity in long-time scale is canceled out.

We show some examples of the CHASE analysis in the next section.

§ 3. Quiescence before great earthquake

(a) east-off northeastern Japan

Figure 7 shows a result of CHASE analysis applied to the seismicity in east-off northeastern Japan. We took 10 years for the former period and 4 years for the later period, respectively. Note that the CHASE value was remarkably small before both of the 1952 Tokachi-oki earthquake and the 1968 Tokachi-oki earthquake. Figure 8 is a result of the CHASE analysis using the data after 1935. Omitting the data before 1935 has a reason in the meaning that the seismicity in the early 1930s was extraordinarily high

because of the occurrence of the 1933 off Sanriku earthquake, and that it is very difficult to remove its aftershocks or influenced activity properly.

A similar result as above is obtained, if the investigated region is changed somewhat. The reason is because the decrease of seismicity do occur in a wide area before great earthquakes. This characteristic of the quiescence makes the CHASE method a robust one.

Figure 9 shows the spatial pattern of CHASE values just before the 1968 Tokachi-oki earthquake. The CHASE value is calculated for each grid point of 15 minutes interval in latitude and longitude using 100 earthquakes occurred around the point during the investigated period. Areas of blue and green colors represent where seismicity during 4 years just before the 1968 Tokachi-oki earthquake was lower than that in the preceding period. It is clear from Figure 9 that the seismicity actually had decreased in a wide area before the 1968 Tokachi-oki earthquake. As shown in Figure 10 the same pattern was observed before the 1952 Tokachi-oki earthquake. In that case the decrease was most conspicuous in the focal region.

(b) south-off the Kanto region

Figure 11 shows a result of CHASE analysis applied to the seismicity in the rectangular region specified in Figure 3. We took 10 years for the former period and 4 years for the later period. CHASE value became noticeably small, exceeding the standard deviation, before both of the two large earthquakes, the 1952 off Boso Peninsula earthquake and the 1972 east-off Hachijojima earthquake.

Figure 12 shows the spatial pattern of CHASE values before the 1972 east-off Hachijojima earthquake. Areas of blue and green colors represent where seismicity during 4 years just before the earthquake was lower than that in the preceding period. It is seen that the quiescence before the 1972 east-off Hachijojima earthquake had actually occurred in an extensive area.

As is observed in Figure 13 the seismicity before the 1953 off Boso Peninsula earthquake was also remarkably quiet in a wide region, and the decrease was most conspicuous around the focal region.

It should be noted here that the recent seismicity in the sea region south-off the Izu and the Boso Peninsula seems to indicate an appearance of quiescence as seen in Figure 14. We do not have a confidence as yet to say that it is a precursory quiescence for a great earthquake, however, we think it is necessary to watch cautiously seismicity change in this region in the coming several years.

§ 4. Quiescence before moderate inland earthquake

We show an example of CHASE analysis applied to the seismicity in the southern coastal area of the central part of Honshu island. The epicentral distribution and the cumulative number of earthquakes in the investigated region are shown in Figure 16. During the period from Jan. 1989 through Jun. 1996 earthquakes larger than M4 occurred three times in this region. The occurrence times are indicated by arrows. Note that the occurrence rate of earthquakes just before the arrows turned down somewhat. Figure 17 shows a result of the CHASE analysis applied to the seismicity. We took one year for the former period and four months for the later period, respectively. The decrease of activity before the occurrence of these moderate earthquakes is clearly seen from the CHASE diagram. This suggests the effectiveness of the CHASE method for the detection of quiescence before inland moderate earthquakes as well.

Figure 18 is a spatial pattern of CHASE values just before the earthquake on May 27, 1996, with a magnitude of 4.2, and Figure 19 is that before the earthquake on August 8, 1993 with a magnitude of 4.2. It is observed from these Figures that a rather wide area compared to the focal regions of the

moderate earthquakes became quiet before their occurrence. This is the same feature as that observed in the quiescence before great earthquakes in the subduction zones.

§ 5. Summary

Seismicity changes in various time scales, and the characteristic duration time of the quiescence before great interplate earthquakes is more or less several years and that before moderate inland earthquakes is several months for most cases. Area where quiescence appears is much larger than the focal region of the relevant earthquake for both of the types of earthquakes. The CHASE analysis that takes advantage of these characteristics of the seismicity change is considered a practically effective method to detect the precursory quiescence before earthquakes.

References

Kanamori, H., The nature of seismicity patterns before large earthquakes, in *Earthquake Prediction (Maurice Ewing Series, 4)*, edited by D.W.Simpson and P.G. Richards, pp1-19, AGU, Washington, D. C., 1981.

Ogata, Y., Detection of precursory relative quiescence before great earthquakes through a statistical model, *J. Geophys. Res.*, *97*, 19845-19871, 1992.

Reasenberg, P.A., and M.V. Matthews, Precursory seismic quiescence: a preliminary assessment of the hypothesis, *Pure Appl. Geophys.*, *126*, 373-406, 1988.

Wiemer, S., and M. Wyss, Seismic quiescence before the Landers (M=7.5) and Big Bear (M=6.5) 1992 earthquakes, *Bull. Seism. Soc. Am.*, *84*, 900-916.

Wyss, M., and R.E. Habermann, Precursory seismic quiescence, *Pure Appl. Geophys.*, *126*, 319-332.

Figure Captions

Fig.1 Left panel: Epicentral distribution of earthquakes with M≧5.3 in the northeastern Japan and its east-off sea region during the period 1926-through 1995.

Right panel: Cumulative number of earthquakes in the rectangular region. Arrows indicate the occurrence times of the 1952 Tokachi-oki earthquake and the 1968 Tokachi-oki earthquake.

Fig.2 Top panel: Number of earthquakes occurred during the time period of preceding 15 years for each year in the rectangular region shown in Fig.1

Bottom panel: Number of earthquakes occurred during the period of preceding 5 years for each year in the same region.

Fig.3 Left panel: Epicentral distribution of earthquakes with M≧5.5 in the Kanto and its south-off sea region during the period 1926 through 1995.

Right panel: Cumulative number of earthquakes in the rectangular region. Arrows indicate the occurrence times of the 1953 off-Boso Peninsula earthquake and the 1972 east-off Hachijojima earthquake.

Fig.4 Top panel: Number of earthquakes occurred during the time period of preceding 15 years for each year in the rectangular region shown in Fig.3

Bottom panel: Number of earthquakes occurred during the period of preceding 5 years for each year in the same region.

Fig.5 The right panel is a space-time plot of earthquakes, occurred during 15 years before the 1968 Tokachi-oki earthquake in the rectangular region shown in the epicentral map.

Fig.6 The right panel is a space-time plot of earthquakes, occurred during

15 years before the 1972 east-off Hachijojima earthquake in the rectangular region shown in the epicentral map.

Fig.7 A result of CHASE analysis applied to the seismicity in east-off northeastern Japan. 10 years are taken for the former time period and 4 years for the later time period.

Fig.8 A result of CHASE analysis applied to the seismicity in east-off northeastern Japan when the data after 1935 are used.

Fig.9 Spatial pattern of CHASE values just before the 1968 Tokachi-oki earthquake. Areas of blue and green colors represent where seismicity during 4 years just before the 1968 Tokachi-oki earthquake was lower than that in the preceding period.

Fig.10 Spatial pattern of CHASE values just before the 1952 Tokachi-oki earthquake. Areas of blue and green colors represent where seismicity during 4 years just before the 1952 Tokachi-oki earthquake was lower than that in the preceding period.

Fig.11 A result of CHASE analysis applied to the seismicity in the south-off Kanto region. 10 years are taken for the former time period and 4 years for the later time period.

Fig.12 Spatial pattern of CHASE values just before the 1972 east-off Hachijojima earthquake. Areas of blue and green colors represent where seismicity during 4 years just before the 1972 east-off Hachijojima earthquake was lower than that in the preceding period.

Fig.13 Spatial pattern of CHASE values just before the 1953 off Boso Peninsula earthquake. Areas of blue and green colors represent where seismicity during 4 years just before the 1953 off Boso Peninsula earthquake was lower than that in the preceding period.

Fig.14 Spatial pattern of CHASE values at the end of 1995.

Fig.15 An area where the seismicity change is investigated using the CHASE

method.

Fig.16 Left panel: Epicentral distribution of earthquakes with M≧2.0 in the southern coastal area of the central part of Honshu island, occurred during the period Jan. 1989 through Jun. 1996.
Right panel: Cumulative number of earthquakes in the rectangular region. Three arrows show the times when moderate earthquakes with M4.9, M4.2, M4.2 occurred.

Fig.17 A result of CHASE analysis applied to the seismicity in the coastal area shown in Fig.16.

Fig.18 Spatial pattern of CHASE values before the earthquake on May 27, 1996 with a magnitude of 4.2. Areas of blue and green colors represent where seismicity during 4 months just before the earthquake was lower than that in the preceding one-year period.

Fig.18 Spatial pattern of CHASE values before the earthquake on Aug. 8, 1993 with a magnitude of 4.2. Areas of blue and green colors represent where seismicity during 4 months just before the earthquake was lower than that in the preceding one-year period.

Fig 1

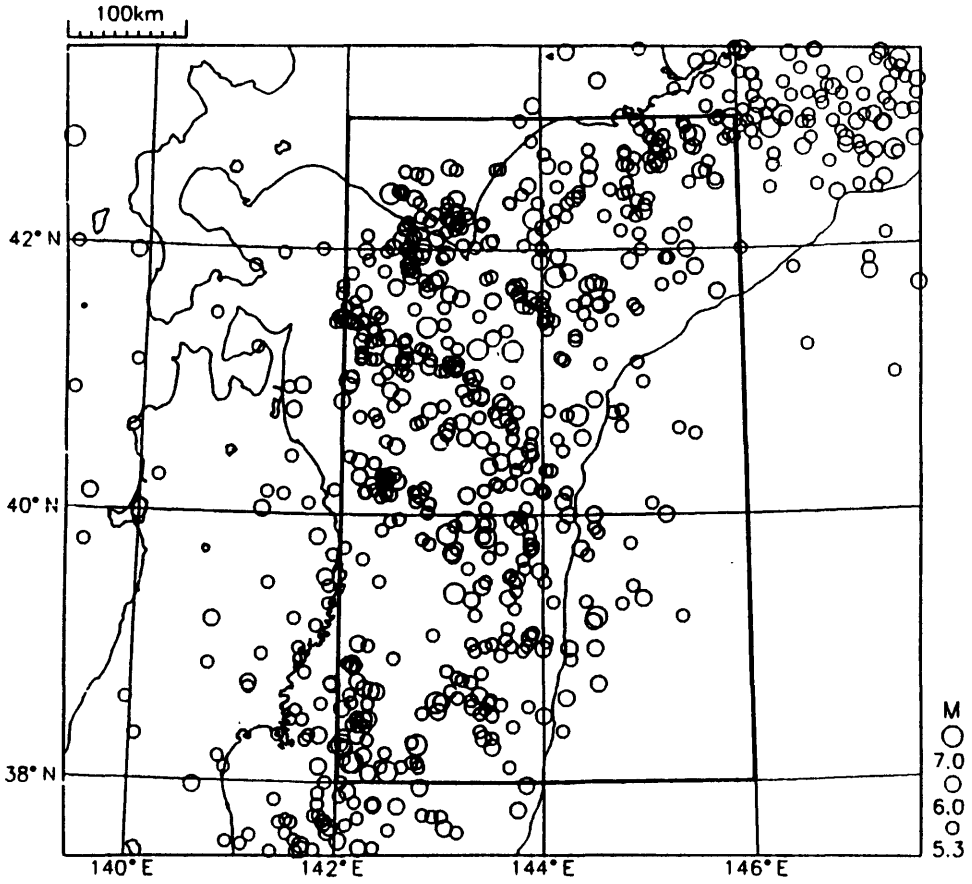
100km
42° N
40° N
38° N
140° E
142° E
144° E
146° E
M
7.0
6.0
5.3

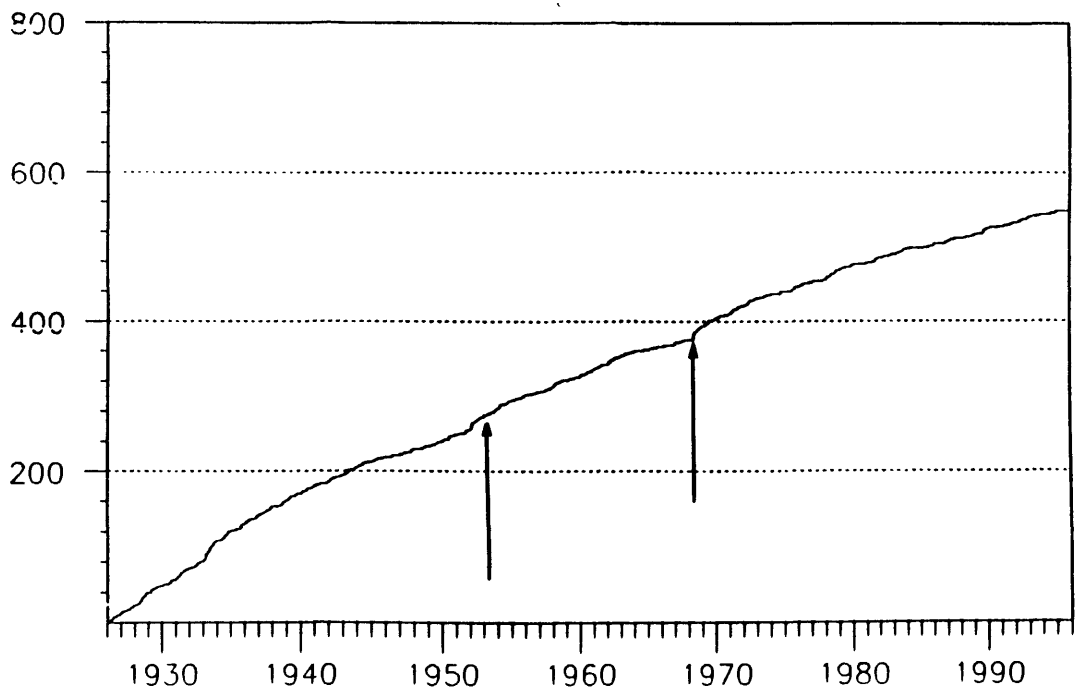
800
600
400
200
1930
1940
1950
1960
1970
1980
1990

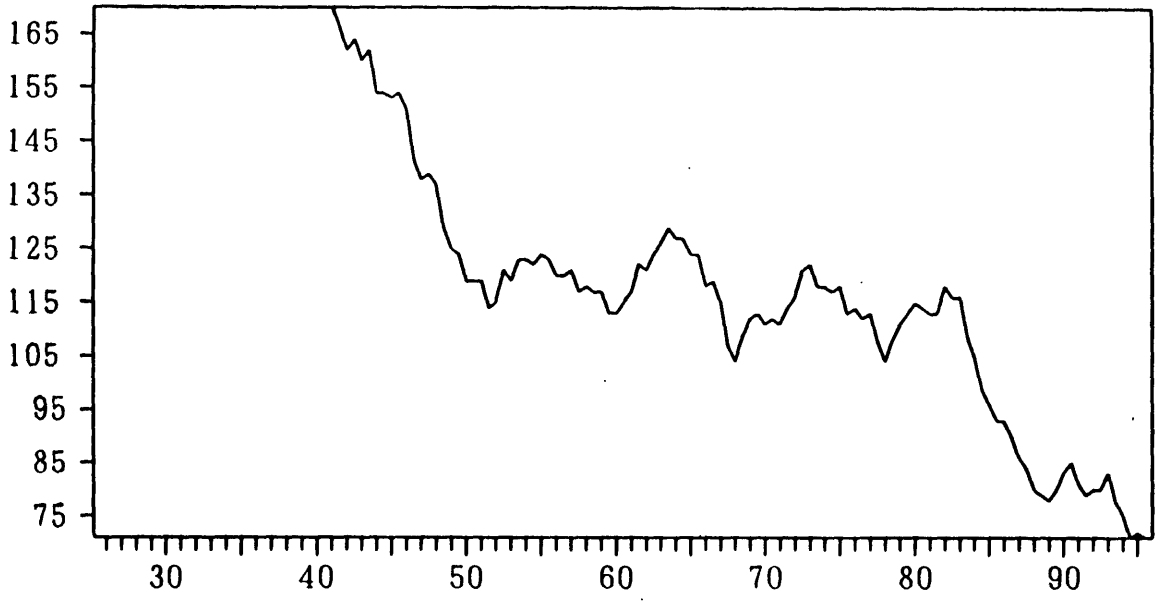
165
155
145
135
125
115
105
95
85
75
30
40
50
60
70
80
90

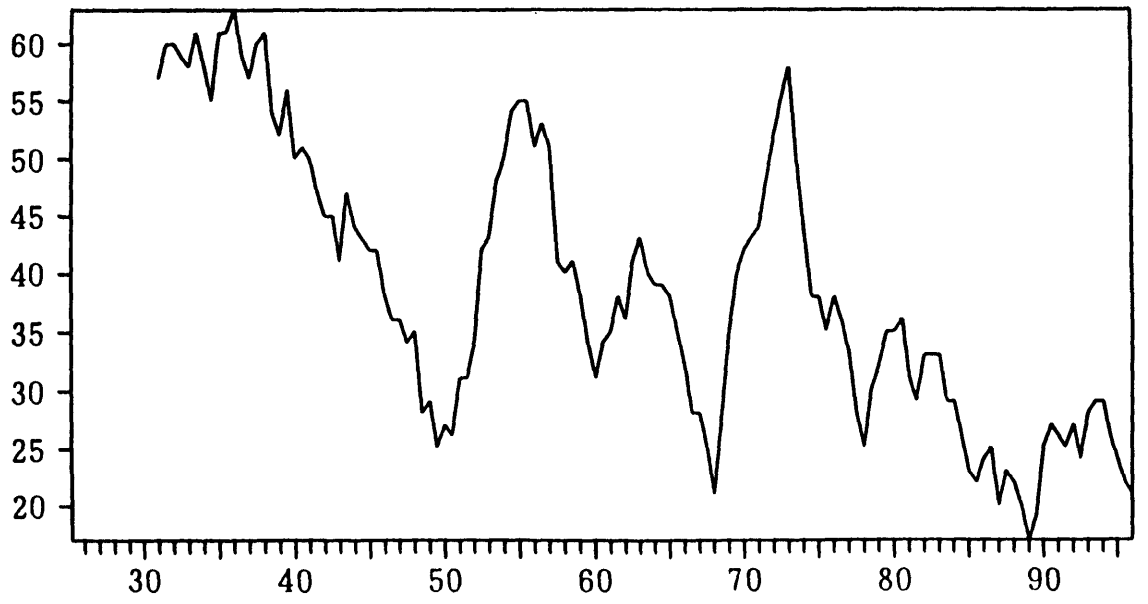
60
55
50
45
40
35
30
25
20
30
40
50
60
70
80
90

Fig.

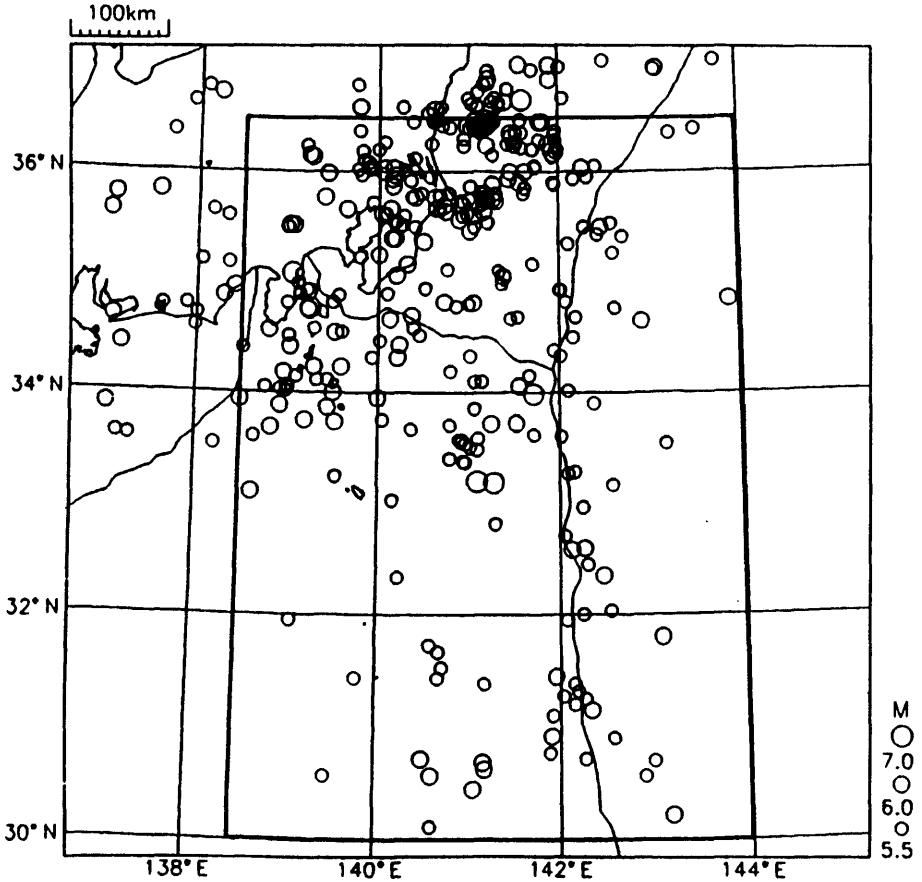
100km
36° N
34° N
32° N
30° N
138° E
140° E
142° E
144° E
M
7.0
6.0
5.5

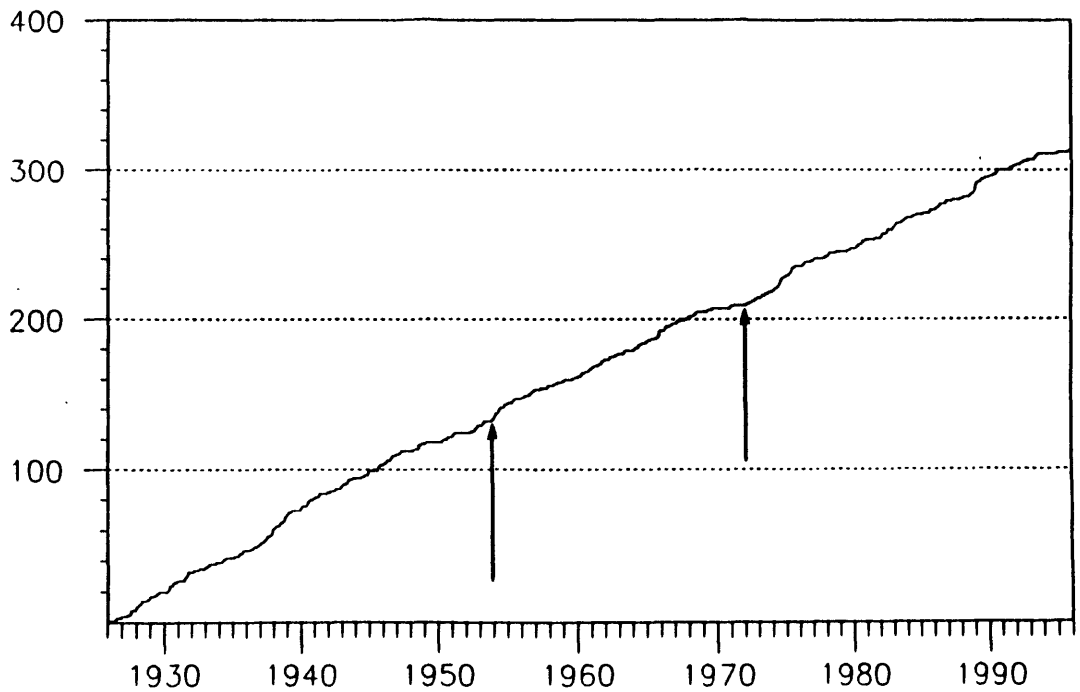
400
300
200
100
1930
1940
1950
1960
1970
1980
1990

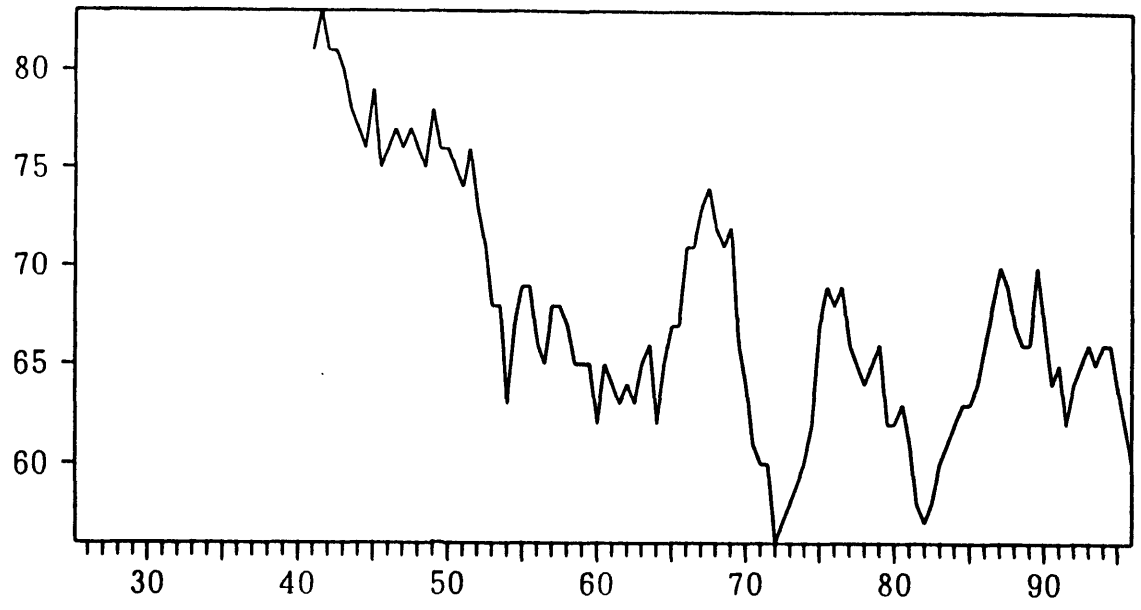
80
75
70
65
60
30
40
50
60
70
80
90

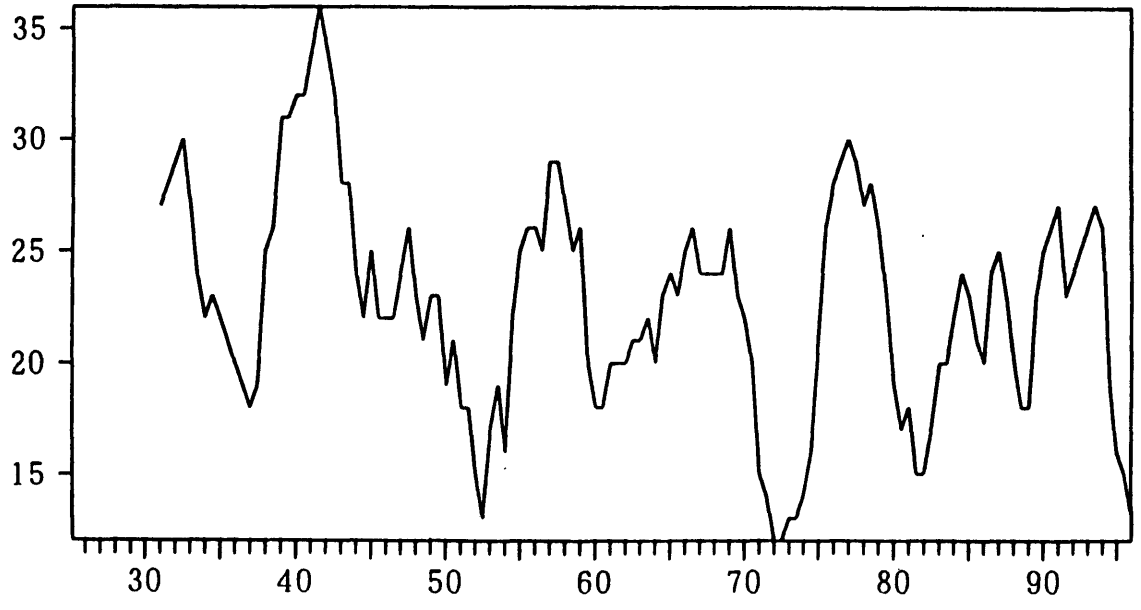
35
30
25
20
15
30
40
50
60
70
80
90

Fig. 5

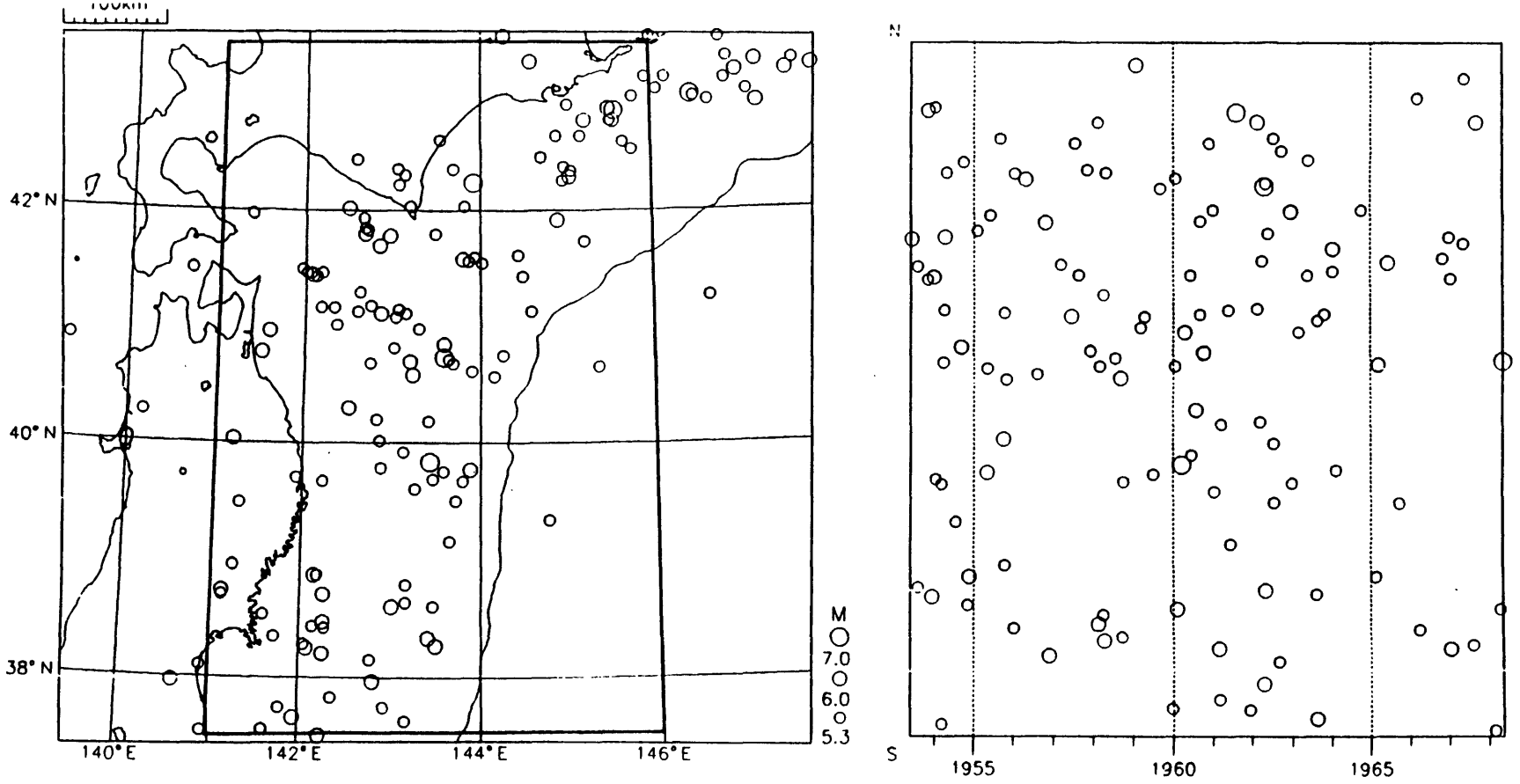
100KM
42° N
40° N
38° N
140° E
142° E
144° E
146° E
M
7.0
6.0
5.3
N
S
1955
1960
1965

Fig. 6

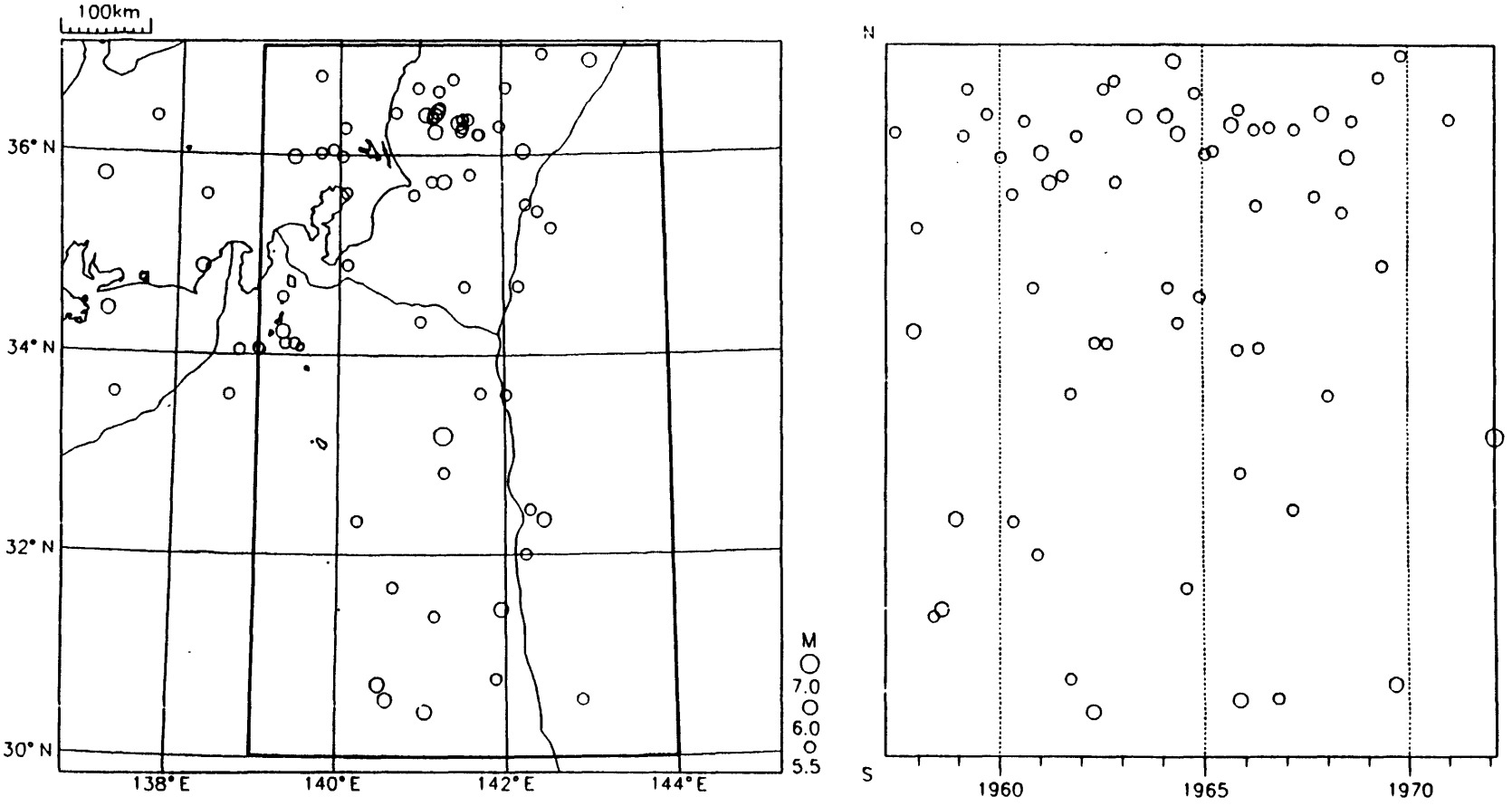
100km
36° N
34° N
32° N
30° N
138° E
140° E
142° E
144° E
M
7.0
6.0
5.5
N
S
1960
1965
1970

Fig.

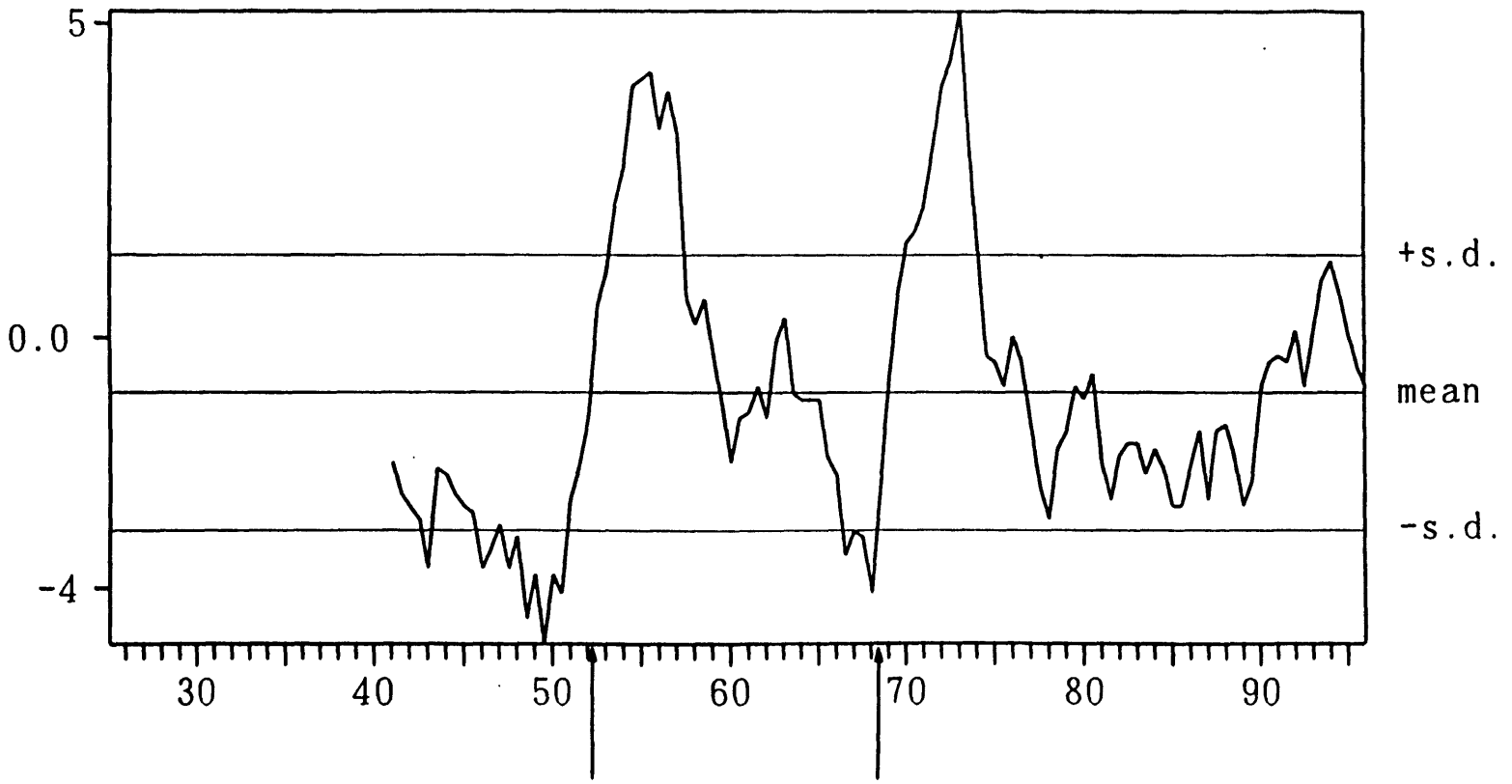

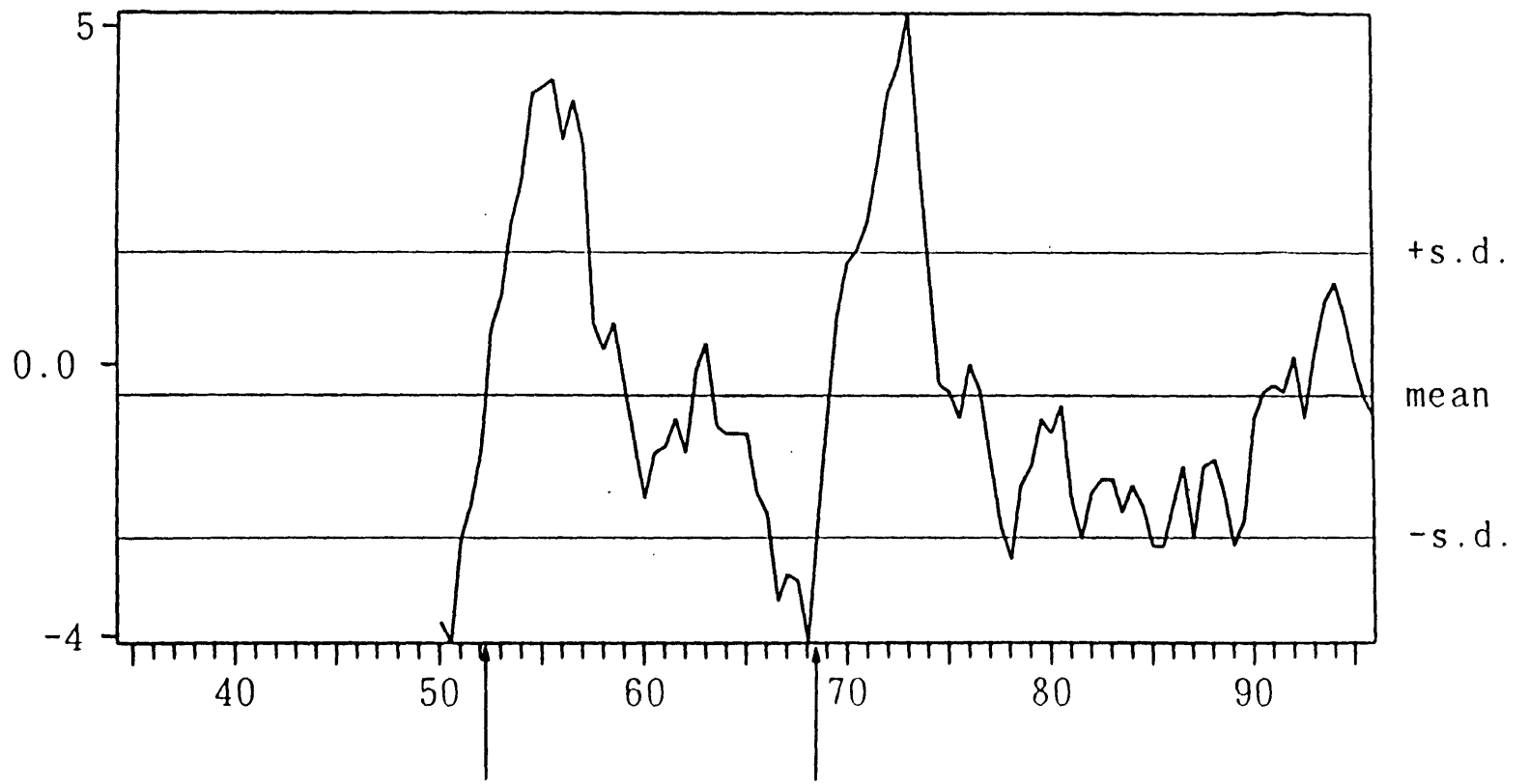
5
0.0
-4
40
50
60
70
80
90
+s.d.
mean
-s.d.

500km

500km

Fig

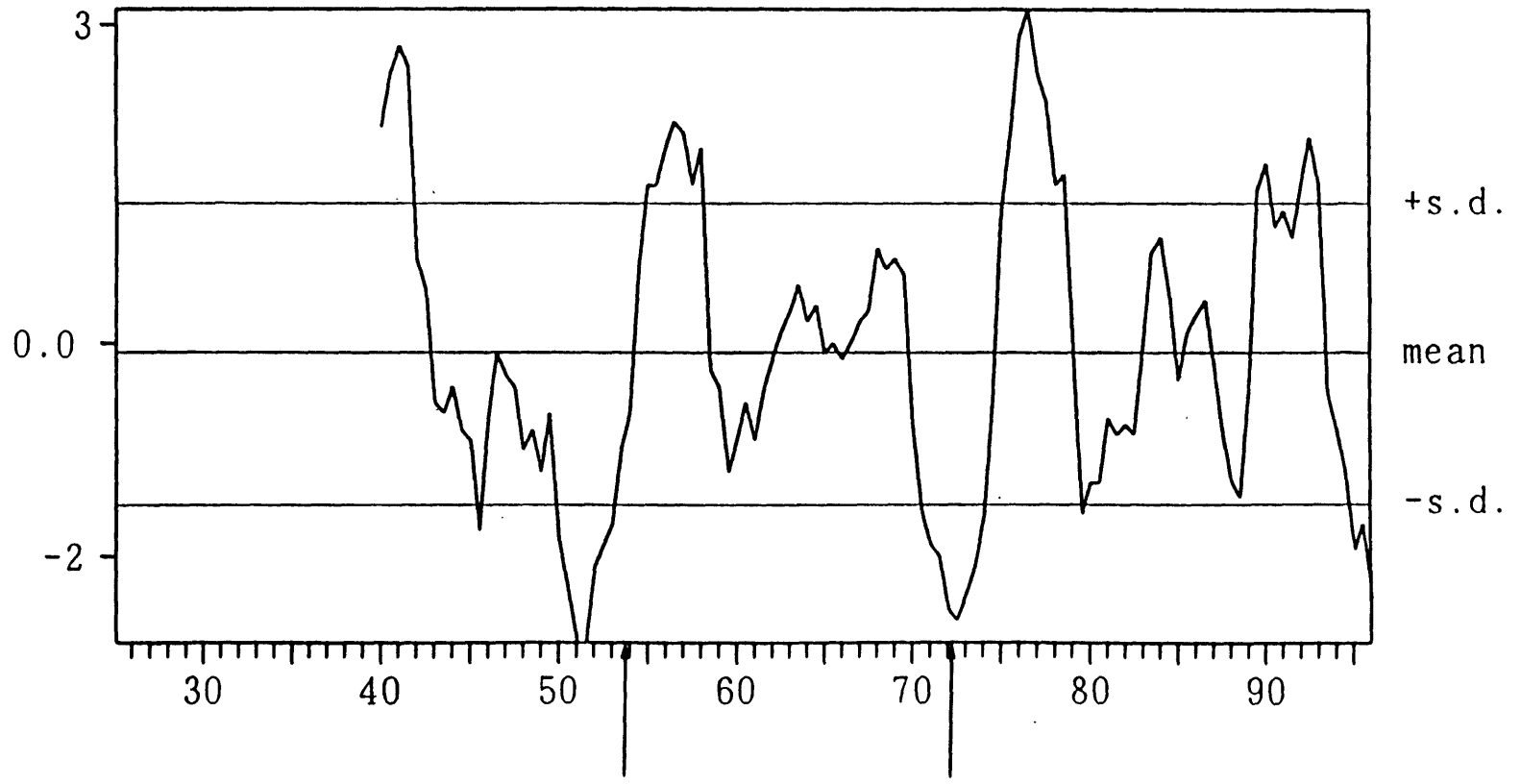

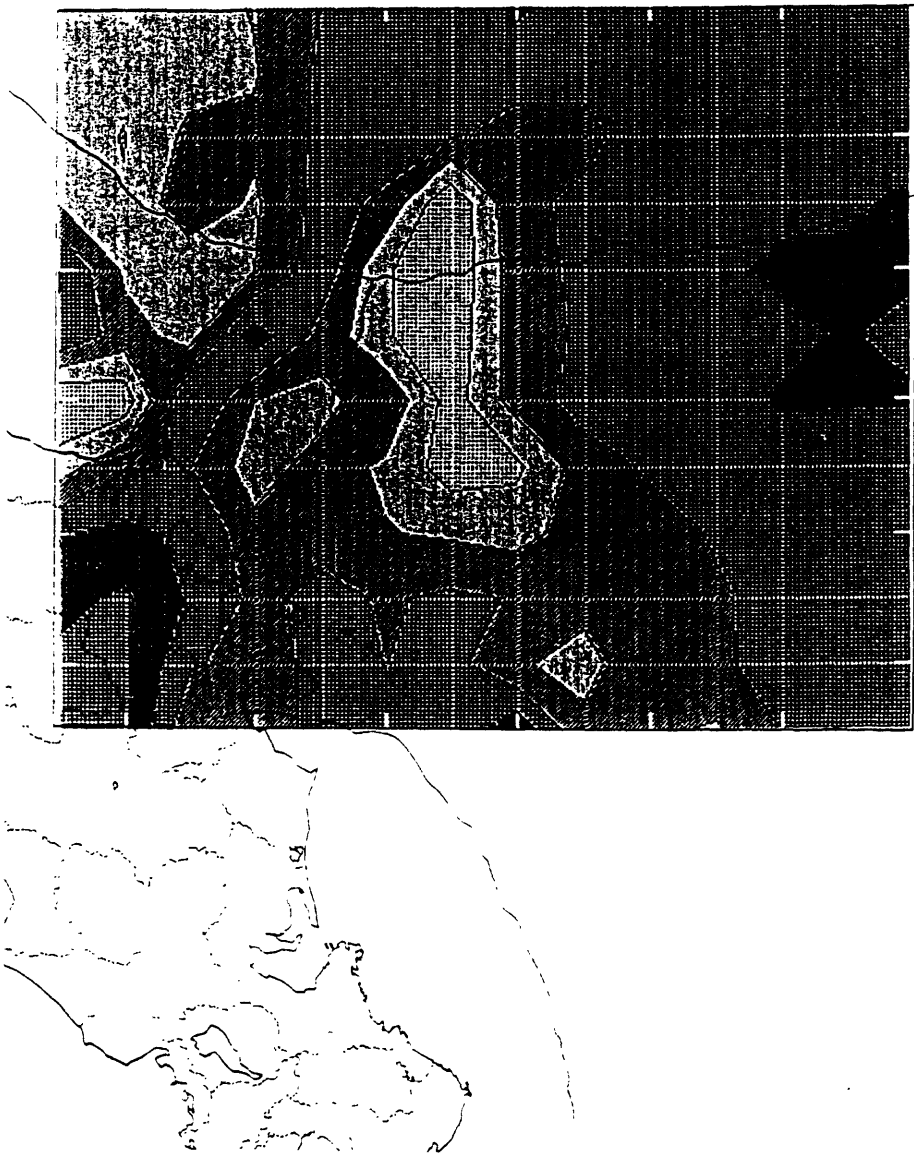

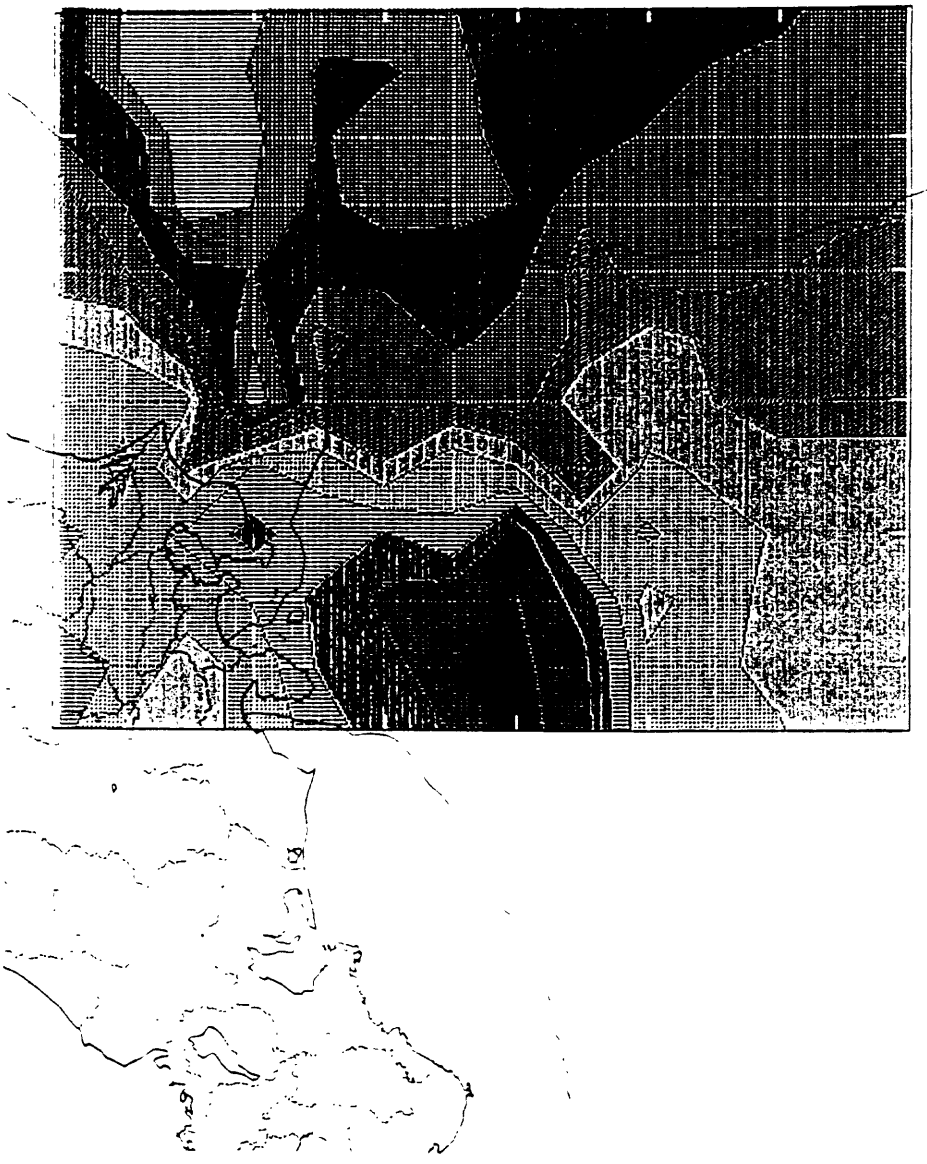

Fig 1

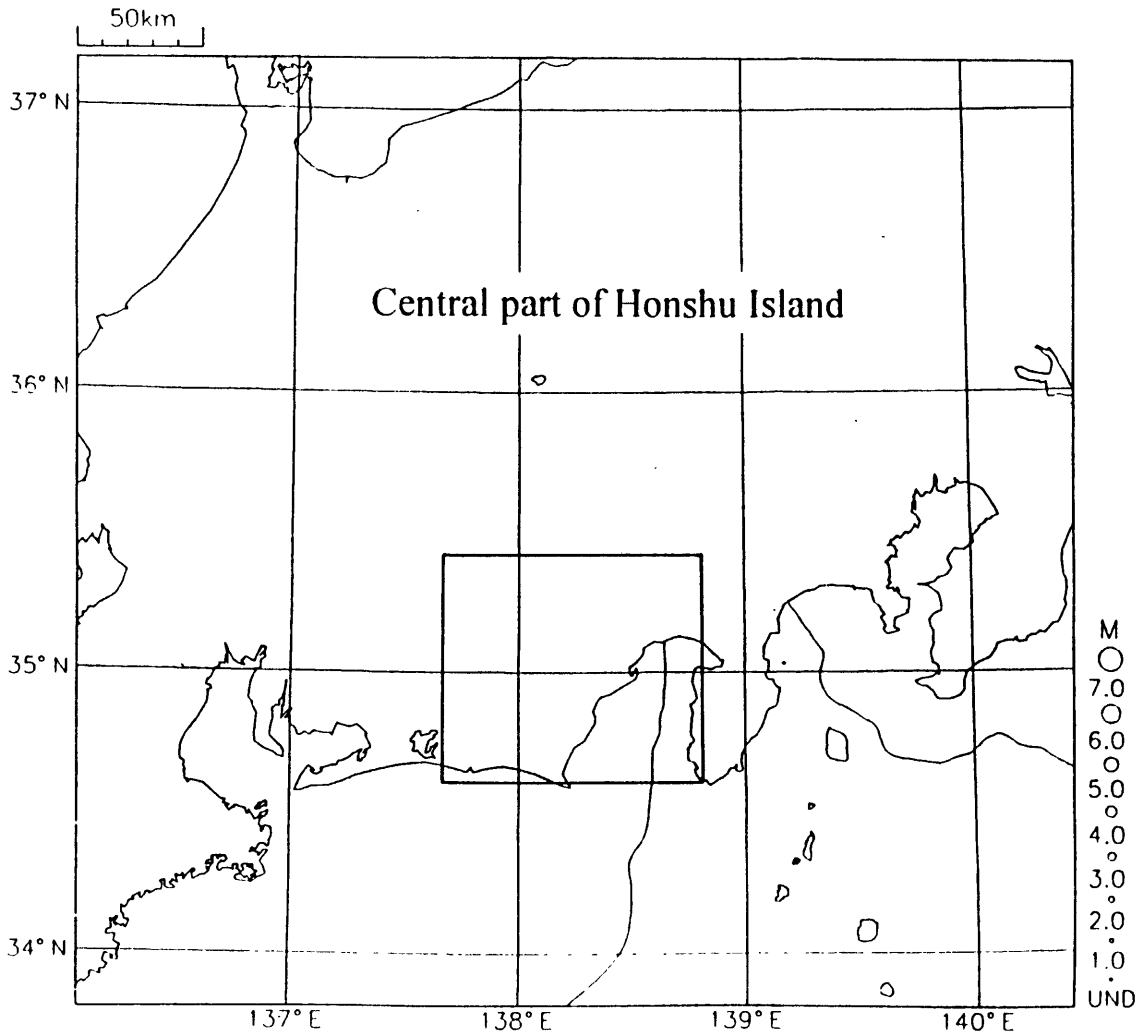
50km
37° N
36° N
35° N
34° N
137° E
138° E
139° E
140° E
Central part of Honshu Island
M
7.0
6.0
5.0
4.0
3.0
2.0
1.0
UND

Fig. 11

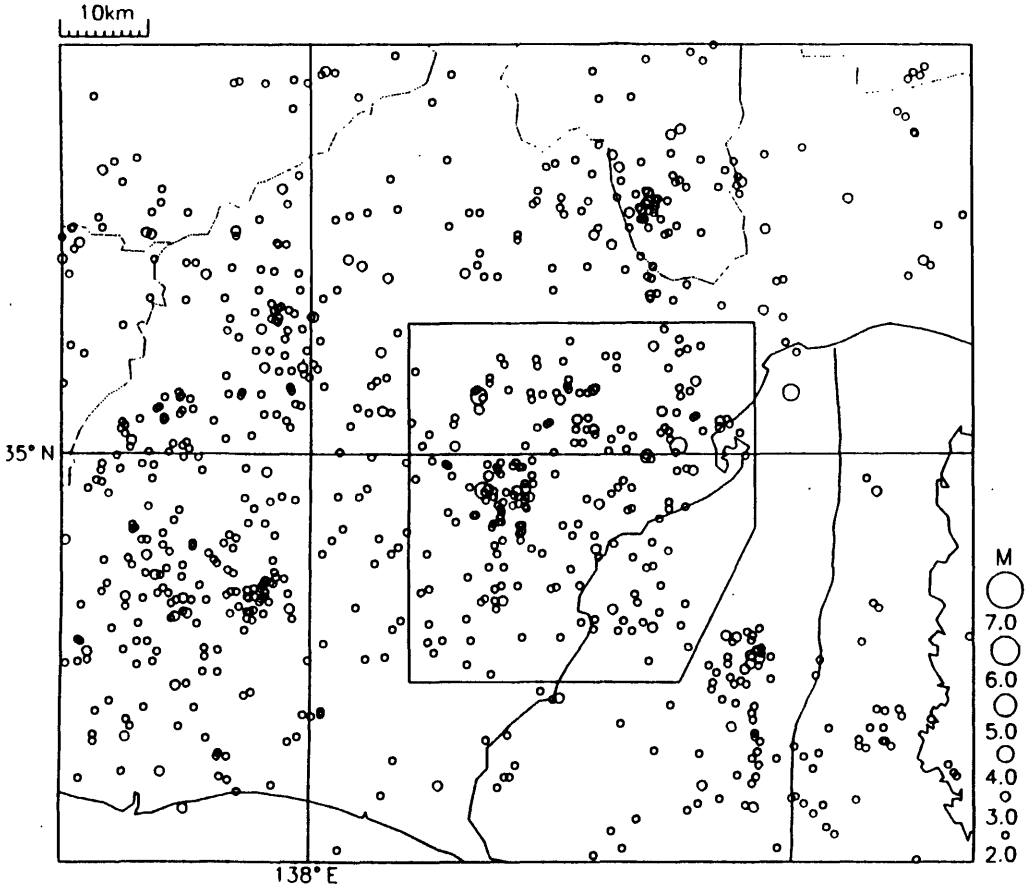
10km
35° N
138° E
M
7.0
6.0
5.0
4.0
3.0
2.0

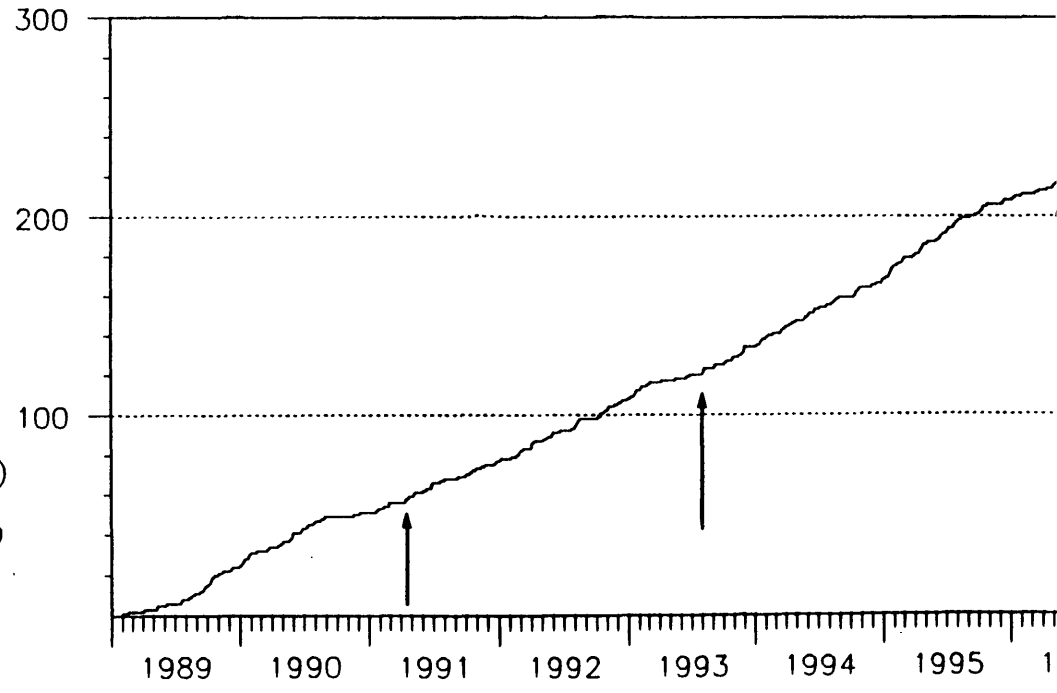
300
200
100
1989
1990
1991
1992
1993
1994
1995

Fig. 17

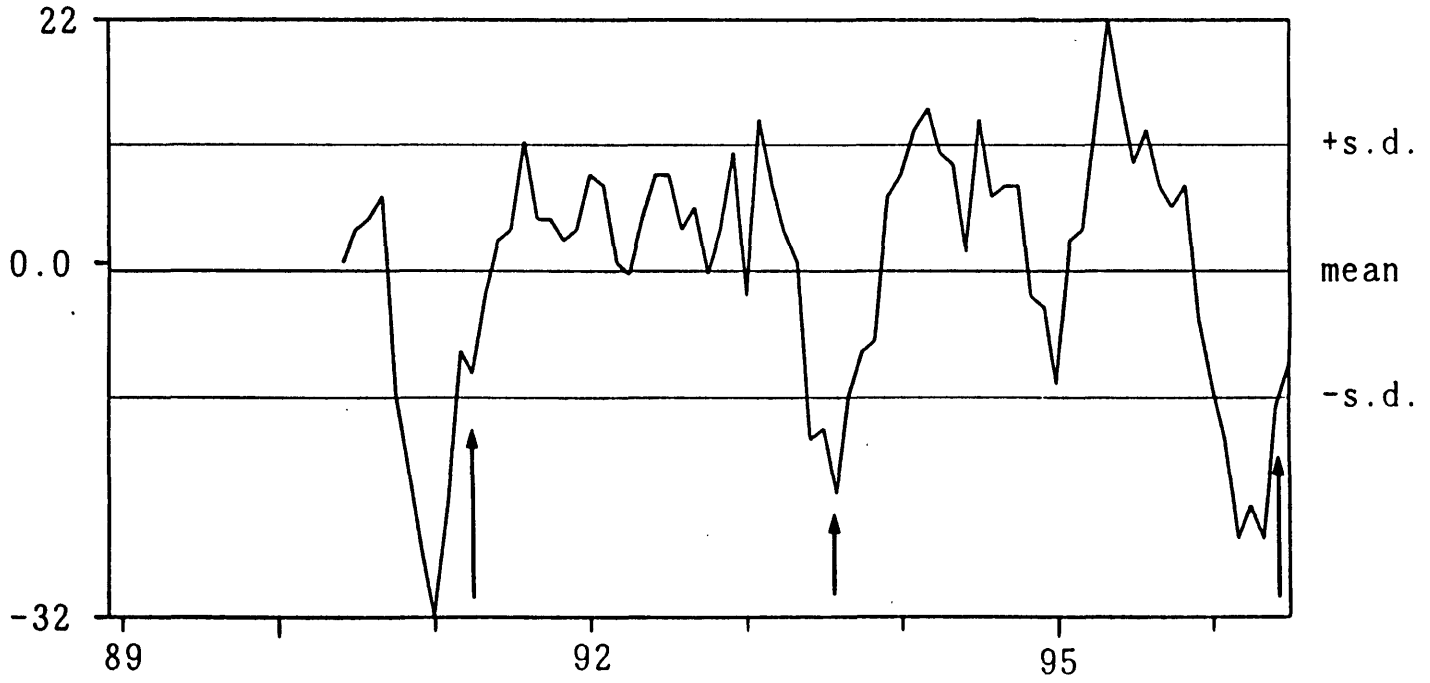

5.0
4.0
3.0
10km

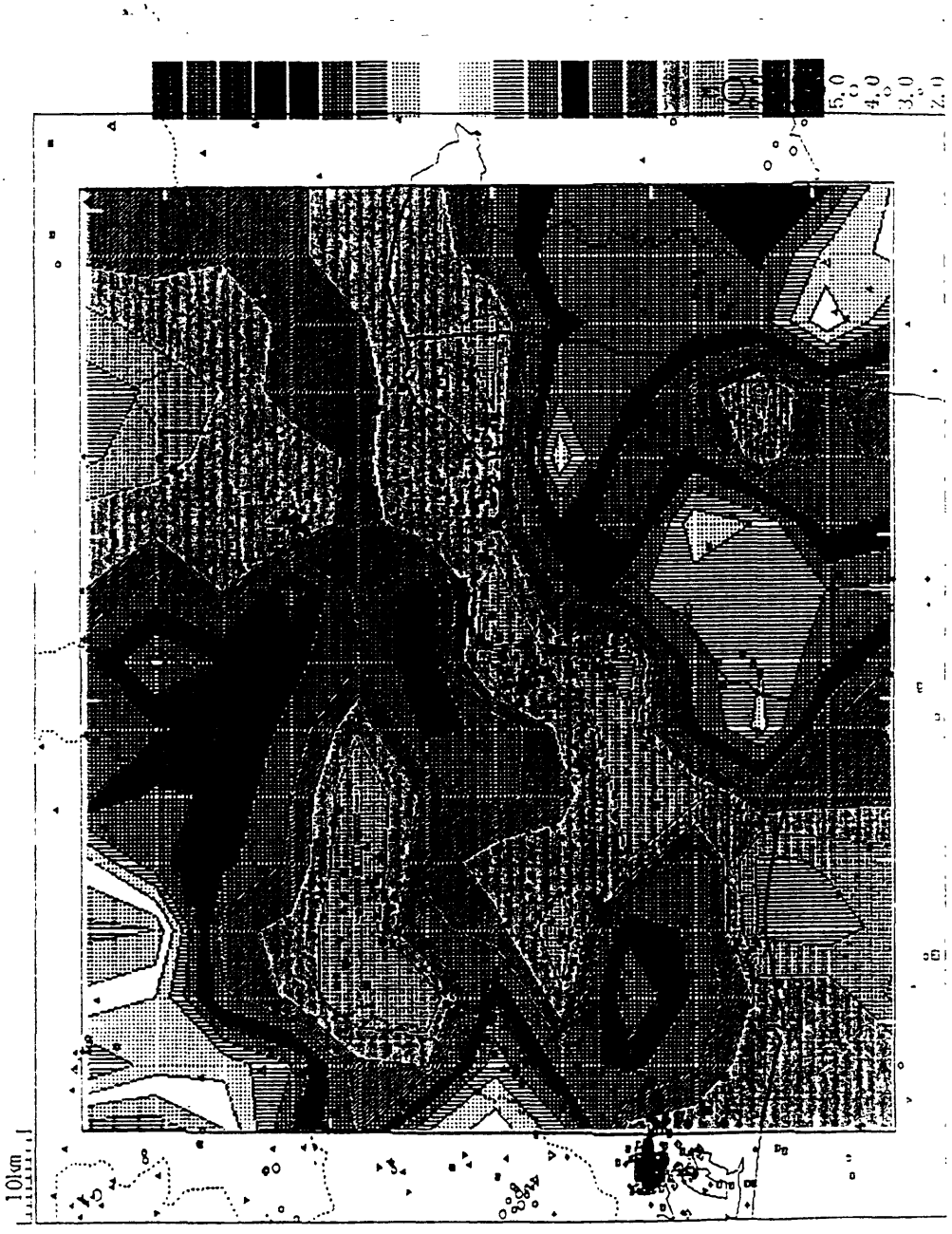
6.0
4.0
3.0
2.0
10km

Southern California Permanent GPS Geodetic Array: Continuous Measurements of Regional Crustal Deformation between the 1992 Landers and 1994 Northridge Earthquakes

Y. Bock, S. Wdowinski, P. Fang, J. Zhang, J. Behr, J. Genrich, S. Williams, D. Agnew, F. Wyatt, H. Johnson, et al.
University of California, San Diego

K. Hudnut
U.S. Geological Survey, Pasadena

W. Young
Riverside County Flood Control and Water Conservation District

The southern California Permanent GPS Geodetic Array (PGGA) was established in 1990 across the Pacific-North America plate boundary in southern California to continuously monitor crustal deformation. Array data, in combination with precise satellite ephemerides derived from a global network, provide a regional anchor for determining positions with respect to a reference frame external to this diffuse plate boundary. We describe the development of the array, the components of the system developed by us to collect and analyze data every twenty-four hours, and the time series of daily positions estimated for the first ten sites in the 19-month period between the 28 June 1992 (M=7.3) Landers and 17 January 1994 (M=6.7) Northridge earthquakes. Focusing on this particular data span allows us to approximate by linear regression long-term, non-linear, postseismic deformation induced by the Landers earthquake at sites 65-100 km from the earthquake epicenter. A comparison of the post-Landers site velocities with those derived from GPS and VLBI measurements collected over nearly a decade prior to the Landers earthquake indicates changes in displacement rate at three sites which are significant at the 95% confidence level. We observe that velocity differences range between 3-5 mm/yr in magnitude and are oriented in a clockwise direction at angles between 20-45 with respect to the directions of coseismic surface displacements. These observations are consistent with a post-earthquake fault-normal contraction component that is superimposed on right-lateral slip at depth along the Landers fault trace. This is the first recorded geodetic determination of a change in regional displacement rates after a major earthquake, and suggests a region-wide non-linear viscoelastic response of the crust rather than merely a continuation of slip at depth on faults ruptured by the event. These observations may also be explained by a change of deformation across neighboring locked faults due to changes in the regional stress field. In particular, our measurements support the conclusion of others that there was a shear stress drop on the SAF fault north of the Los Angeles basin after the Landers earthquake. Our results also suggest that convergence of the Los Angeles basin with respect to the Pacific plate was reduced by about 3 mm/yr after the earthquake which is consistent with a drop in SAF-normal compressional stress across the basin prior to the Northridge earthquake.

Foreshock Activities Associated with the Nucleation of the 1995 Off Etorofu Earthquake

N. Hurukawa and B. Shibazaki (both at International Institute of Seismology and Earthquake Engineering, Building Research Institute, Tsukuba 1, Japan: e-mail: hurukawa@kenken.go.jp)

Abstract.

Predominant foreshock activities preceded the Ms 7.9 (Mw 7.9) off Etorofu earthquake in the Kurile Islands on Dec. 3, 1995. Using the method of the modified joint hypocenter determination (Hurukawa, 1995), we relocated foreshocks, a main shock and aftershocks of the 1995 off Etorofu earthquake simultaneously to study foreshock activities in detail in view of the nucleation process of the large earthquake.

Distribution of relocated earthquakes and their focal mechanisms suggest that the 1995 off Etorofu earthquake is an interplate earthquake at the boundary between the North America (or Okhotsk) and Pacific plates. Its source area overlaps with those of the 1958 off Etorofu (m 8.1) and the 1963 Kurile (Mw 8.5) earthquakes.

Nine days before the occurrence of the mainshock, a first foreshock of magnitude 6.4 occurred at the deepest point of the foreshock area. Then many foreshocks including three more magnitude 6.0 or greater events occurred east or southeast of the first foreshock with expanding the foreshock area to the trench axis with a velocity of several to several tens cm/s. A number of events per day is also increasing day by day. The final size of the foreshock area is about 80km x 20km. Then the rupture of the mainshock started at the deepest point of the foreshock area.

These observational facts are consistent with recent theoretical studies and laboratory experiments (Shibazaki and Matsu'ura, 1995; Ohnaka, 1993), in which foreshocks are regarded as the rupture of localized asperities in a broad weak zone where the nucleation of the large earthquake started.

References

Hurukawa, N., 1995, Quick aftershock relocation of the 1994 Shikotan earthquake and its fault planes, *Geophys. Res. Lett.*, **22** , 3159-3162.

Ohnaka, M., 1993, Critical soze of the nucleation zone of earthquake rupture inferred from immediate foreshock activity, *J. Phys. Earth*, **41**, 45-56.

Shibazaki, B. and M. Matsu'ura, 1995, Foreshocks and pre-events associated with the nucleation of large earthquakes, *Geophy. Res. Lett.*, **22**, 1305-1308.

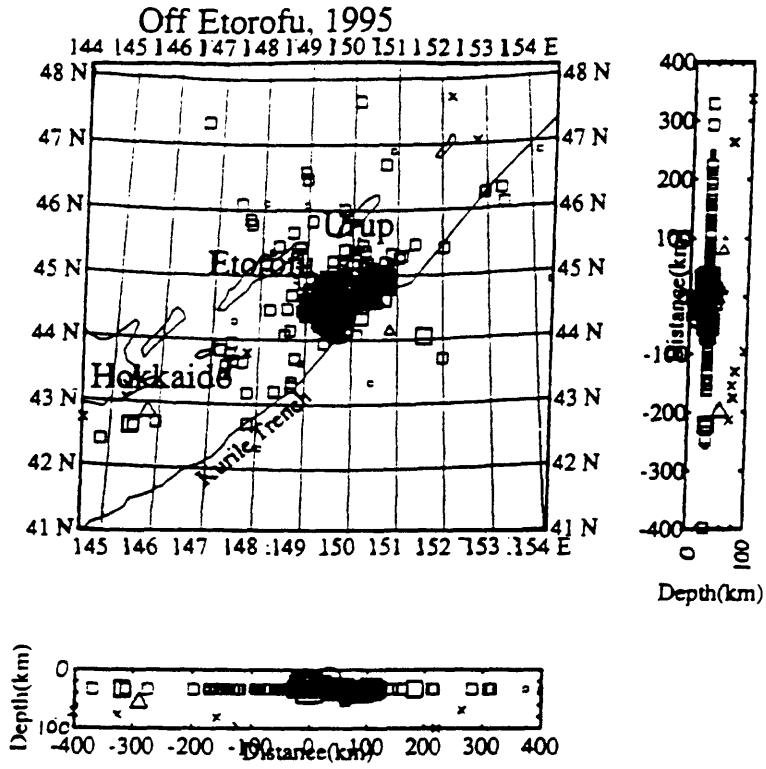

Fig. 1 Hypocenter distribution of the 1995 off Etorofu earthquake during Nov. and Dec. 1995 determined by NEIC, USGS. Note that focal depths of almost all earthquakes are fixed to 33 km.

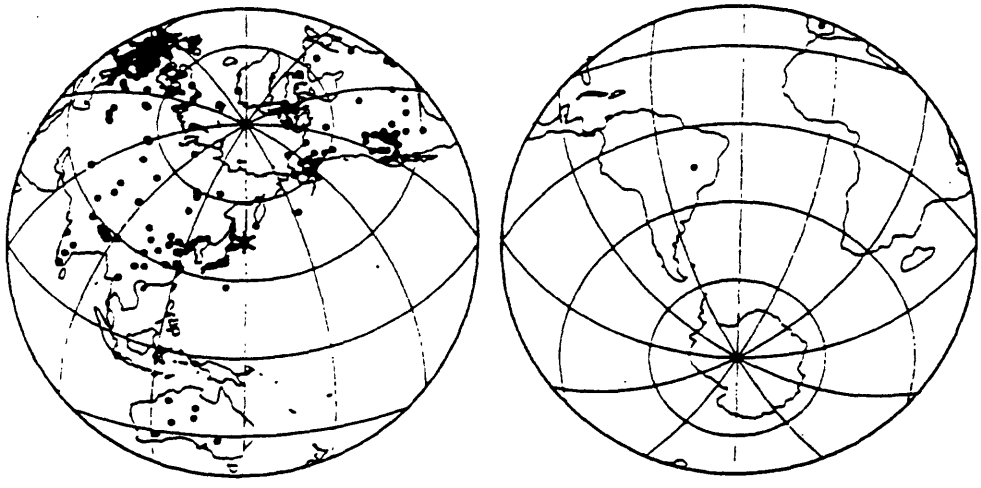

Fig. 2 Stations used in relocation of foreshocks and the mainshock of the 1995 off Etorofu earthquake in this study. A total number of stations is 307. An asterisk represents the epicenter of the mainshock.

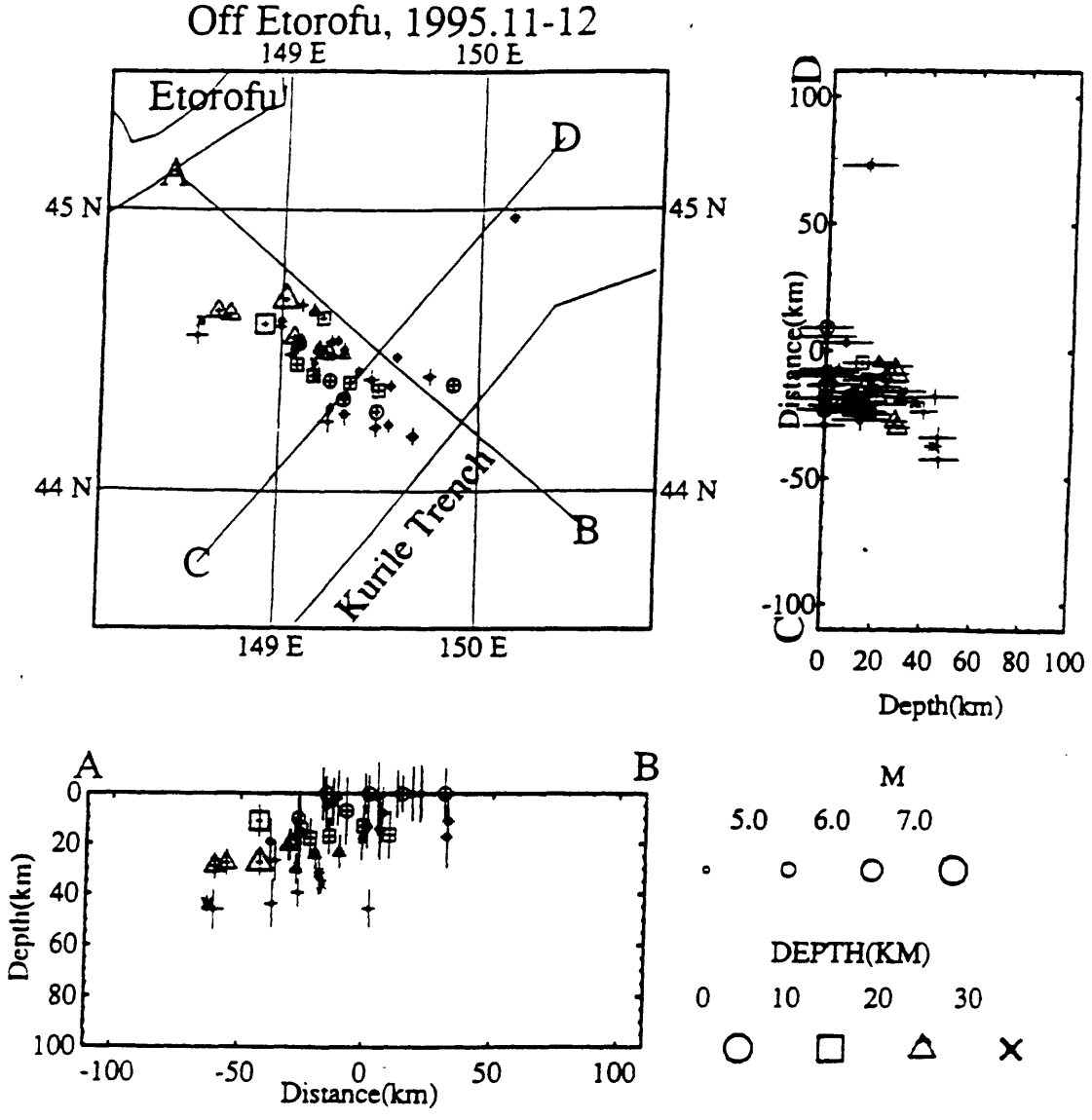

Fig. 3 Hypocenter distribution of relocated foreshocks and mainshock of the 1995 off Etorofu earthquake during Nov. and Dec. 1995. Epicentral distribution and two vertical cross sections along lines AB (N50°W-S50°E) and CD (N40°E-S40°W) are shown. Hypocenters were determined by the method of Joint Hypocenter Determination by Hurukawa (1995) on following conditions: A minimum number of stations that observed each event is 20. A minimum number of events observed at each station is 10. Earthquakes of which magnitude is less than 4.0 and of which epicentral distance to a nearest station is greater than 20° are not included. Fifty seven earthquakes were well determined with errors of focal depths within 20 km and with root-mean square errors less than 2 s.

It is clear that all earthquakes occurred along a plane dipping northwestward with a gentle angle. This plane is almost parallel to one of the nodal planes of the mainshock and large foreshocks. Therefore we can conclude these low-angle nodal planes are planes of these earthquakes and that they occurred along the boundary between the North America and Pacific plates.

Although we didn't show aftershock distribution here, they also occurred along the plate boundary.

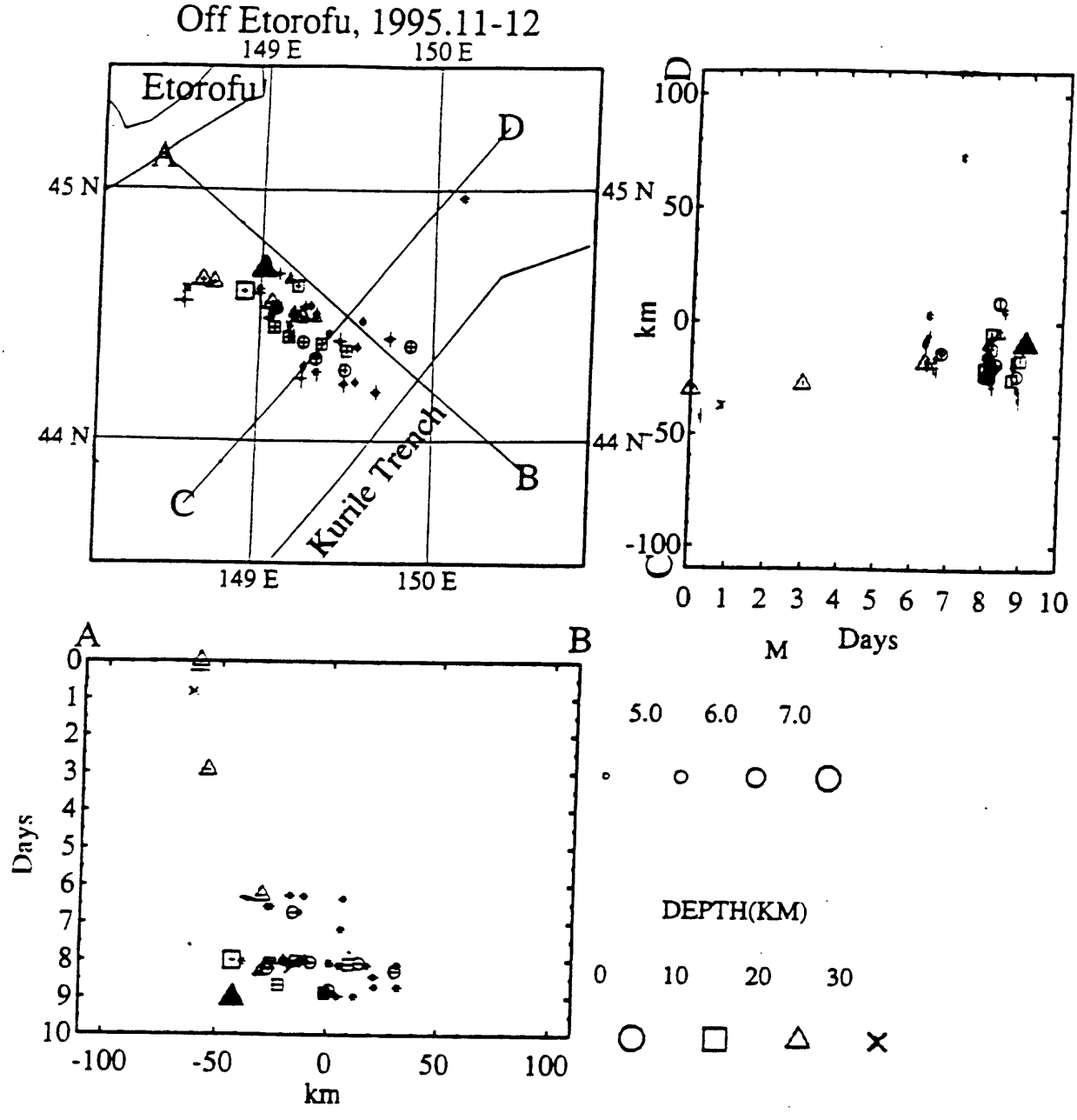

Fig. 4 Space-time plot of relocated foreshocks and the mainshock of the 1995 off Etorofu earthquake along lines AB (N50°W-S50°E) and CD (N40°E-S40°W) during Nov. and Dec. 1995.

The first foreshock occurred on Nov. 24, 9 days before the mainshock. Then the foreshock area extended to southeastward and toward shallower part to the Kurile trench. The expanding speed increase rapidly, that is from several to several tens cm/s. Finally the mainshock (solid triangle) occurred on Dec. 3.

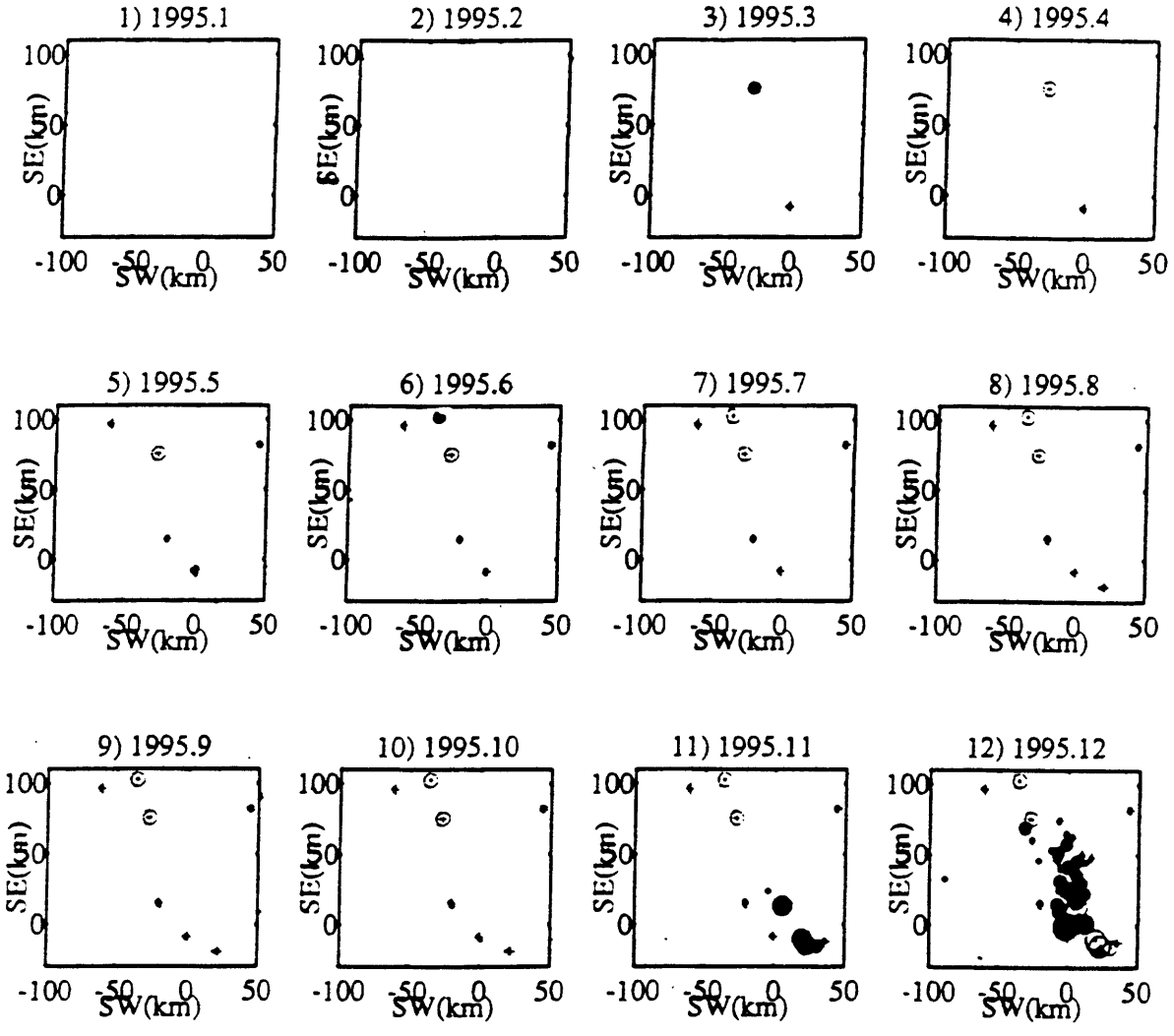

Fig. 5 Epicentral distribution of relocated foreshocks and the mainshock of the 1995 off Etorofu earthquake each month from Jan. to Dec. 1995. Solid and open circles represent earthquakes occurred on that month and previous months, respectively.

Although immediate foreshocks started to occur on Nov.24 as shown in Fig. 4, several foreshocks already occurred just northeast side of the immediate foreshock area.

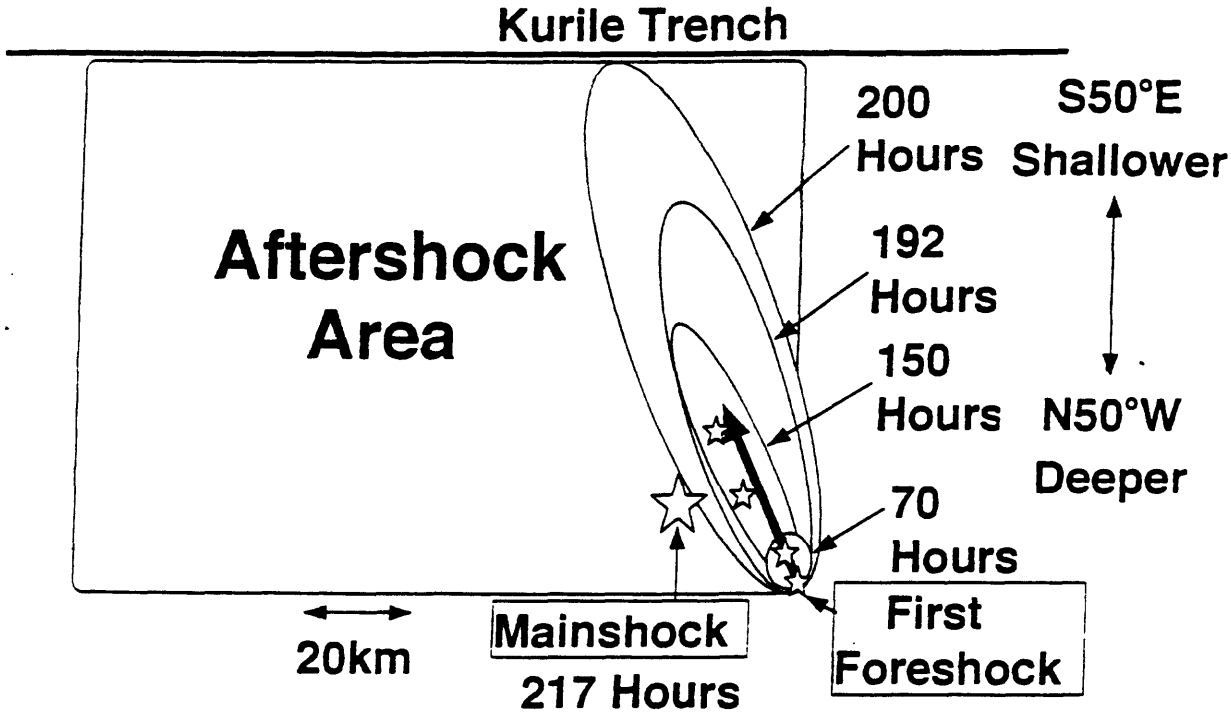

Fig. 6 A schematic illustration of the foreshock activity of the 1995 off Etorofu earthquake. The first immediate foreshock occurred at the deepest and point. This is the western edge of the both foreshock and aftershock areas. The foreshock area expanded to south-southeastward. The rupture of the mainshock started edge of the foreshock area at deeper part. Asterisks represent magnitude 6 or more earthquakes.

Some features of seismic activities before the recent large earthquekes in and near Japan - the 1995 Kobe earthquake and the 1955 Iturup-oki earthquake -

by

Kiyoo Mogi

College of Industrial Technology, Nihon University
Narashino, Japan

Some characteristic features of the seismic activities before the Kobe (Hyogoken-nanbu) earthquake of M 7.2 and the Iturup-oki earthquake of Mw 7.7 which occurred in 1995 in and near Japan are discussed from the standpoint of the long-term forecasting of large earthquakes.

1. 1995 Kobe earthquake

1.1 Long-term forecasting

As shown in Figure 1, the Kobe earthquake occurred in the Areas of Specified Observation designated by the Coordinating Committee for Earthquake Prediction(CCEP) since 1970. The areas of Specified Observation are regions in which the occurrence of M 7-class inland (including coastal region) earthquakes should be apprehended during the coming 20-30 years. This designation was made on the basis of the past seismic activity, crustal deformation, active faults, social activity, etc. The map of the areas has been published and distributed formally by the National Land Agency, Goverment of Japan, yearly since 1981 (e.g. National Land Agency, 1985). However, it was unfortunate that this designation of the areas in western Japan has not been considered sufficiently by the Goverment and the Local goverment for disaster prevention.

Figure 2 shows locations of shallow of M 6.5 and above which occurred in land areas and coastal regions since 1978, and the Areas of Intensified and Specific Observation designated by CCEP in 1978. 80% of these earthquakes occurred in the areas.

Figures 3 and 4 are mostly reproduced from the previous paper (Mogi, 1994) presented in the 1994 UJNR meeting at Kyoto. The top

figure of Figure 3 indicates the number of deaths caused by large earthquakes in and near Japan against to time in the past 200 years. Numerals in this figure are number of deaths of several major earthquakes. Disastrous earthquakes of number of deaths 1000 and over occurred frequently during the period from 1800 to 1950, but no destructive earthquake occurred in the recent time until 1994. In the previous paper, I stated as followings :"However, since the 1948 Fukui earthquake (M 7.3), no such destructive earthquake occurred in the past 50 years. Now an abnormal state is continuing and we must expect a more dangerous period in near future". Figure 4 shows that the Kinki district in western Japan has been particularly quiet in the past 50 years until the 1995 Kobe earthquake. Thus, it is not the fact that a dangerous earthquake in western Japan occurred quite unexpectedly, and it may be stated that its occurrence has been forecasted in a broad sense.

1.2 Seismic activity

In western Japan, great shallow earthquakes of M-8 class have occurred repeatedly along the Nankai Trough at fairly regular intervals of 100 to 150 years. Inland earthquakes follow after the great earthquake and gradually decrease, then begin to increase about 50 years before the next great earthquake (Mogi, 1985). Figure 5 shows the simplified earthquake cycle along the Nankai Trough.

After the 1946 Nankaido earthquake of M 8.0, the seismic activity in western Japan gradually decreased and the wide area became very quiet in 1970's, and the activity began to increase from about 1985, as shown in Figures 6 and 7. Figure 6 shows the temporal change in seismic activity by M-T graph in western Japan after the 1946 Nankaido earthquake. Figure 7 shows the epicentral locations of major earthquakes in successive periods after the 1944 Tonankai earthquake and the 1946 Nankaido earthquake. In these figures, the increase to some degree in the seismic activity in the recent years can be seen in the wide area. The 1995 Kobe earthquake seems to be one major event in this increase of seismic activity in western Japan.

On the other hand, the seismic activity in the focal region of the Kobe earthquake has been relatively low before the Kobe earthquake. Figure 8 shows epicentral locations of shallow earthquakes of M 4.0 and above in the successive two periods

(1935-1965) and (1966-1994). The quiescence in the focal region of the 1995 Kobe earthquake is remarked in the latter period. Figure 9 shows M-T graphs of earthquakes of M 4.0 and above in the focal region of the 1995 Kobe earthquake and those in the surrounding regions. Although the seismic activity is nearly constant in the surrounding regions, the activity in the focal region clearly decreased before the Kobe earthquake. Similar changes were recognized in the case of the 1983 Hokkaido-nansei-oki earthquake of M 7.8 and others. This seismic quiescence is regarded as a long-term precursor of the Kobe earthquake.

2. 1995 Iturup-oki earthquake

The seismic belt along the southwestern part of the Kurile Trench and the northern part of the Japan Trench was comletely covered by the focal regions of interplate earthquakes of Mw 7.7 and above, which occurred successively during the period from 1952 to 1973, as shown in Figure 10. However, very recently great shallow earthquakes have occurred successively in this seismic belt as shown also in Figure 10. The 1993 Kushiro-oki earthquake and the 1994 Hokkaido-toho-oki earthquake are intraplate earthquakes. However, the 1995 Iturup-oki earthquake is an interplate earthquake of Mw 7.7, which occurred at the focal region of the 1963 Iturup-oki earthquake of Mw 8.5. The time interval of these two interplate shallow earthquake is shorter than the recurrence time expected in this seismic belt. This result may bring out the question on the seismic gap theory.

Here it is discussed that this short time interval may be attributed to the change of stress condition caused by the occurrrence of a large deep earthquake and shallow intraplate earthquakes, which occurred recently in the adjacent regions.

I pointed out that large shallow earthquakes along the Kurile Trench and the Japan Trench were sometimes preceded by large deep earthquakes which occurred in a subducting slab (Mogi, 1973, 1994). Figure 11 shows a close relation between great shallow earthquakes and deep earthquakes in the Hokkaido-Sakhalin region along the Kurile Trench. The 1952 Tokachi-oki earthquake and the 1993 Kushiro-oki earthquake were preceded by several major deep earthquakes including large earthquakes of M 7.8. These large deep

earthquakes are of the down-dip compression type, and the directions of the maximum compression are nearly parallel to the direction of plate subduction.

The top figure of Figure 12 shows M-T graph of large deep and shallow earthquakes. After the 1950 large deep earthquake, a number of large shallow interplate earthquakes occurred successively and covered the seismic belt completely, but a number of large shallow earthquake have occurred again in this seismic belt just after the 1990 large deep earthquake. The bottom figure of Figure 12 schematically explaines the possible mechanism of the relation between large deep and shallow earthquakes.

Figure 13 shows a possible relationship between the 1995 Iturup-oki earthquake and large intraplate earthquakes in the adjacent region. The subduction of the plate in this region was accelated by the occurrence of the 1990 Sakhalin deep earthquake (1) of down-dip compression type, and it triggered the intraplate shallow earthquakes of down-dip extension type: the 1993 Kushiro-oki earthquake (2) (Hokkaido University,1993) and the Hokkaido-toho-oki earthquake (3) (Kikuchi,1994). It is noted that the 1995 Itutup-oki earthquake (4) occurred on the line of the eastward migration, as shown in the bottom figure. From these results, it is deduced that the change of stress condition caused by the eastward migration of the large shallow intraplate earthquakes of down-dip extension type triggered the 1995 Iturup-oki earthquake.

Referrences

Hokkaido University (1993). On the 1993 Kushiro-oki earthquake (1) -Aftershock sequence-, Rep. Coord. Comm. Earthquake Predict., 50 17-22. (in Japanese)

Kikuchi, M. (1994). Focal mechanism of the 1994 Hokkaido-toho-oki earthquake, reported at the meeting of the Coord. Comm. Earthquake Prediction.

Mogi, K. (1973) Relationship between shallow and deep seismicity in the western Pacific region, Tectonophysiics, 17, 1-22.

Mogi, K. (1993). Deep seismic activity preceding the 1993 Kushiro-oki earthquake, the 1952 Tokachi-oki earthquake and the 1933 Sanriku-oki earthquake, Rep. Coord. Comm. Earthquake Predict., 50, 27-33. (in Japanese)

Mogi, K. (1994) Some features of seismic activities before recent three large earthquakes in and around Hokkaido, Proc. 9th Joint Meeting UJNR, Panel on Earthquake Prediction Technology, 1-23.

Captions of Figures

Figure 1 Areas of Intensified and Spesific Observation desinated by the Coordinating Committee for Earthquake Prediction.
Left: areas designated in 1970; Right: revised one in 1978.
Open circle: 1995 Kobe earthquake.

Figure 2 Locations of shallow earthquakes of M 6.5 and above which occurred in land areas and coastal regions since 1978, and the Areas of Intensified and Specific Observation by CCEP.

Figure 3 Number of deaths caused by large earthquakes in and near the Japanese islands (top figure) and M-T graph of large earthquakes of M 7 and above. The 1995 Kobe earthquake is added to the figure in Mogi(1944). Numerals in the top figure indicate the number of deaths of major earthquakes.

Figure 4 Locations of large shallow earthquakes of M 7 and above during the two periods (1900-1949) and (1950-1994)(Mogi,1994). A number of destructive earthquakes occurred in the former period, but no such destructive earthquake occurred in the latter period. In the latter period, large earthquakes mainly occurred in sea areas. The 1995 Kobe earthquake is shown by a recangular solid symbol.

Figure 5 Simplified earthquake cycle in the subduction zone along the Nankai Trough in western Japan.

Figure 6 Temporal change in seismic activity shown by M-T graph in the area shown by the region A in western Japan after the 1946 Nankaido earthquake. Broken curve in the left figure: Nankai Trough. The gradual increase in the seismic activity is recognized before the 1995 Kobe earthquake.

Figure 7 Temporal change in seismic activity shown by space distributions of major earthquakes in the successive periods after the 1944 Tonankai earthquake and the 1946 Nankaido earthquake. The increase to some degree in the seismic activity in the recent period (before the 1995 Kobe earthquake) can be seen in the wide area.

Figure 8 Locations of shallow earthquakes of M4.0 and above in the

successive two periods (1935-1965) and (1966-1994). The quiescence in the focal region of the 1995 Kobe earthquake is remarked in the latter period.

Figure 9 M-T graph of earthquakes of M 4.0 and above in the focal region of the 1995 Kobe earthquake (Region A) and those in the surrounding regions (Regions B, C, D). The seismic activity in B, C and D is nearly constant, but the activity in the focal region (A) clearly recreased before the 1995 Kobe earthquake. This seismic quiescence is regarded as a long-term precursor of the Kobe earthquake.

Figure 10 The top figure shows the activity during the period from 1950 to 1969 in and around Hokkaido. In this peiod, the seismic belt along the southwestern part of the Kurile Trench and the northern part of the Japan Trench was covered completely by the focal regions of great interplate shallow earthquakes of Mw 7.7 and above. The bottom figure shows the activity during the period from 1990 to 1995. The 1993 Kushiro-oki earthquake and the 1994 Hokkaido-toho-oki earthquake are intraplate earthquakes, but the 1995 Iturup-oki earthquake is a interplate earthquake. It is noted that great deep earthquakes occurred in Sakhalin in both periods.

Figure 11 Relation between great shallow earthquakes and deep earthquakes in the Hokkaido-Sakhalin region along the Kurile Trench. The 1952 Tokachi-oki earthquake and the 1993 Kushiro-oki earthquake were preceded by several major deep earthquakes including large shocks of M 7.8 (Mogi,1994).

Figure 12 M-T graph showing the relation between great shallow earthquakes and deep earthquakes (Top figure), and the possible mechanism that large deep earthquakes trigger great shallow intraplate and interplate earthquakes in a subduction zone.

Figure 13 Relation between the 1995 Iturup-oki earthquake and large intraplate earthquakes in the adjacent region. The subduction was accelated by the occurrence of the 1990 Sakhalin deep shock (1) of down-dip compression type, and it triggered the intraplate shallow earthquakes: the 1993 Kushiro-oki earthquake (2) and the Hokkaido-toho-oki earthquake (3). The 1995 Iturup-oki earthquake (4) seems to have a close relation with the successive occurrence of these intraplate earthquakes, as seen in the space-time graph in the bottom figure.

Areas of Intensified Observation and Specific Observation disignated by Coordinating Committee for Earthquake Prediction

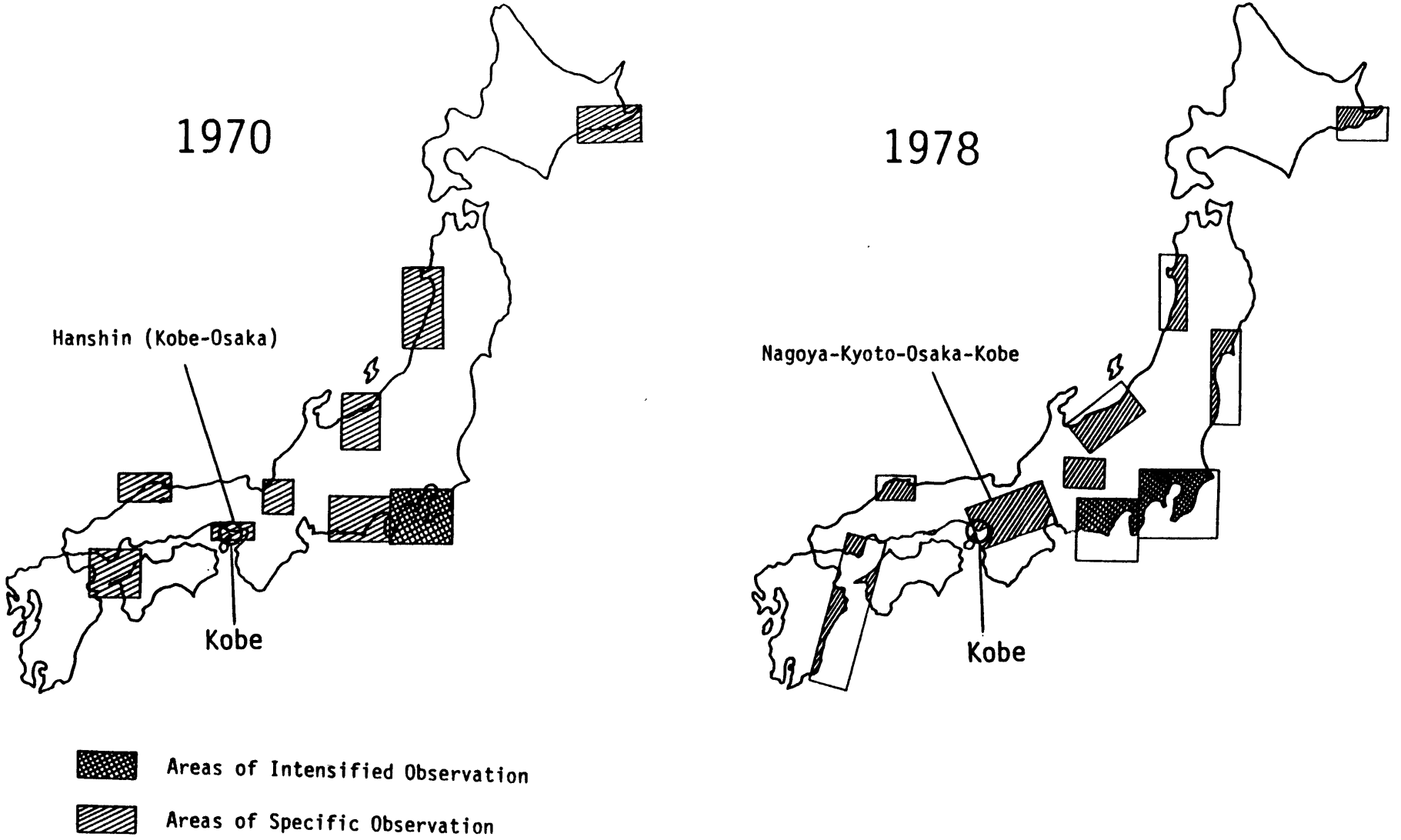

Fig. 1

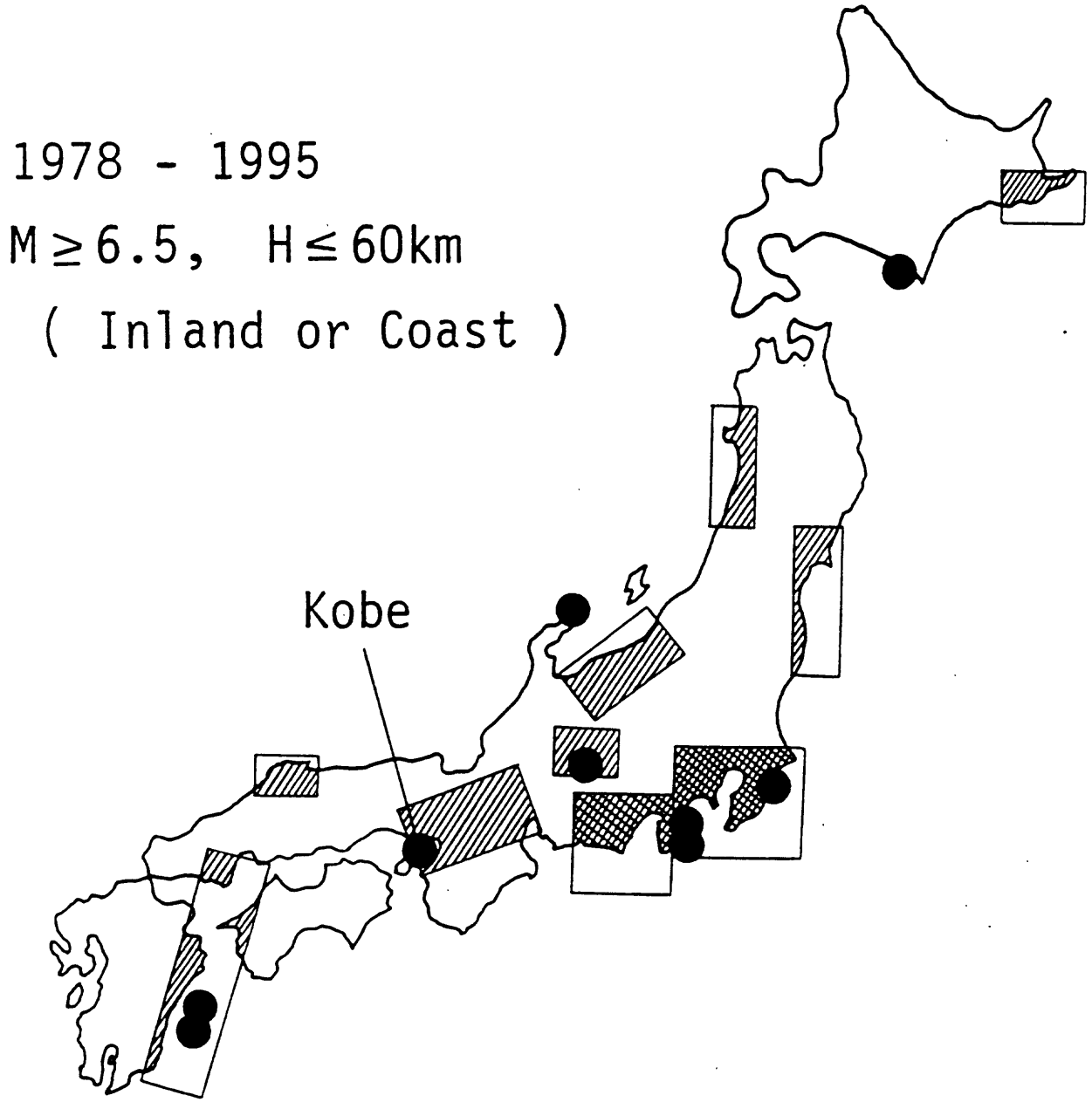

Fig. 2

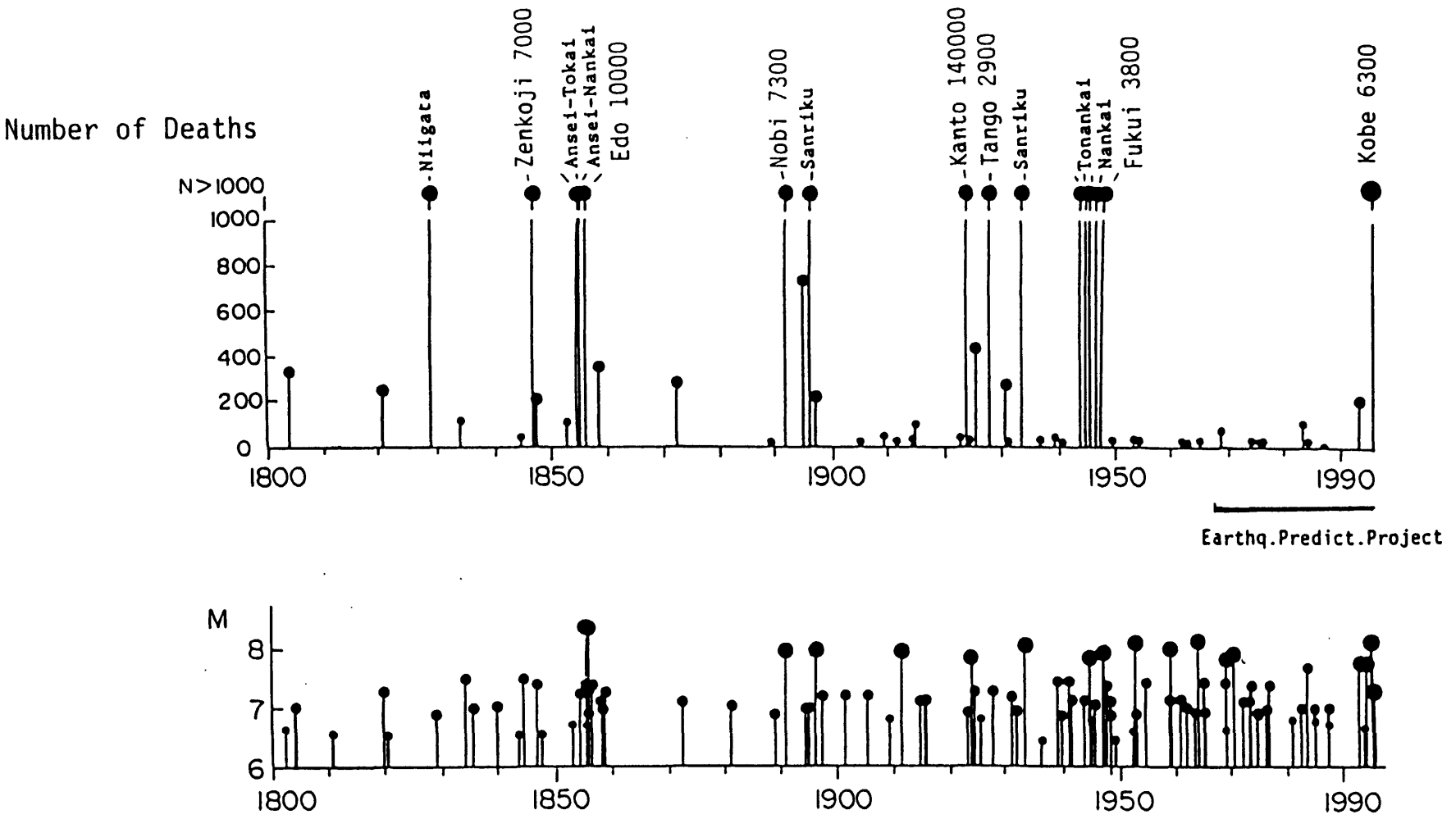
Number of Deaths
N>1000
1000
800
600
400
200
0
-Niigata
-Zenkoji 7000
-Ansei-Tokai
-Ansei-Nankai
Edo 10000
-Nobi 7300
-Sanriku
-Kanto 140000
-Tango 2900
-Sanriku
-Tonankai
-Nankai
Fukui 3800
Kobe 6300
1800
1850
1900
1950
1990
Earthq.Predict.Project
M
8
7
6
1800
1850
1900
1950
1990

Fig. 3

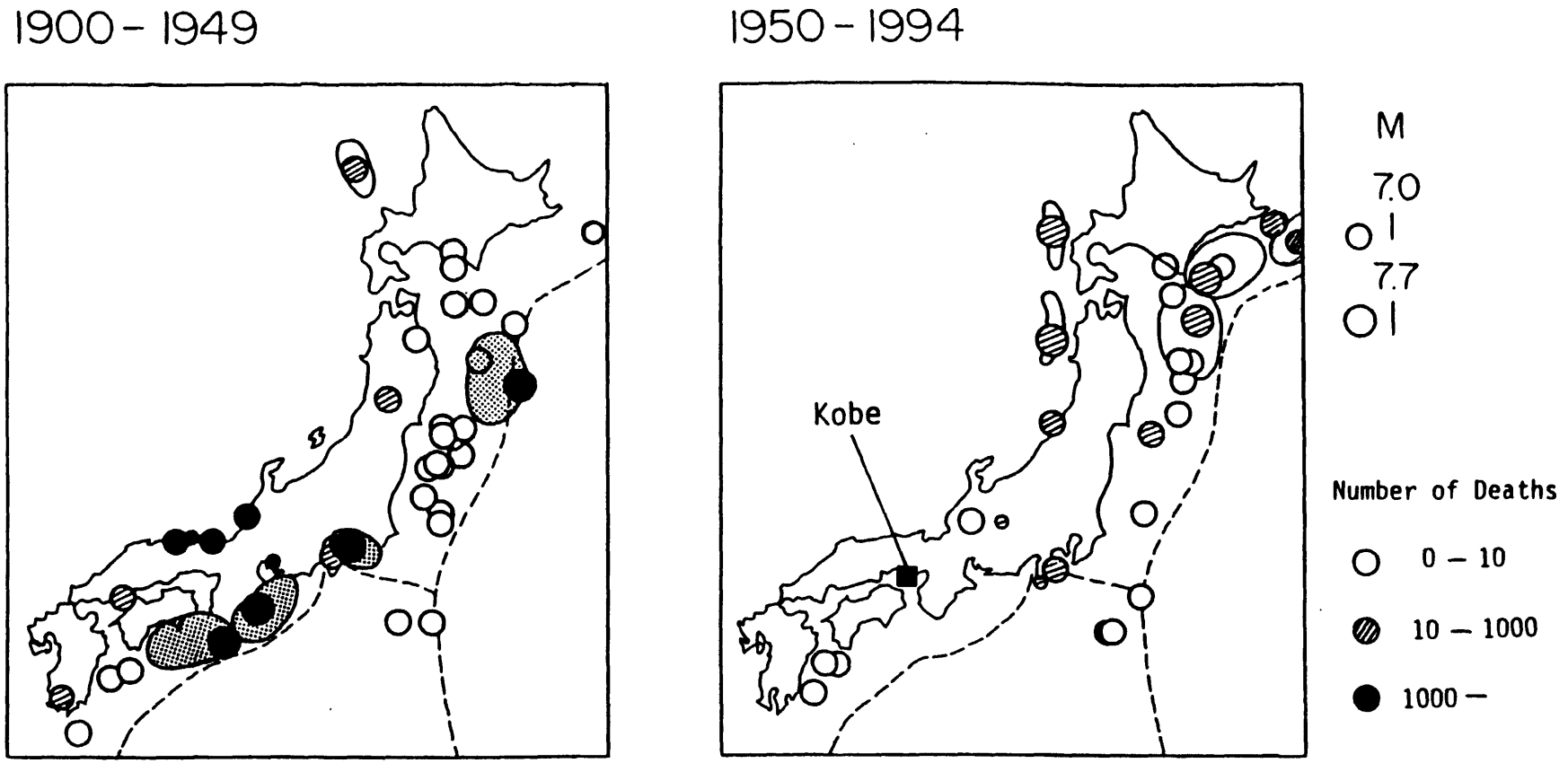
1900 - 1949
1950 - 1994
Kobe
M
7.0
7.7
Number of Deaths
0 — 10
10 — 1000
1000 —

Fig. 4

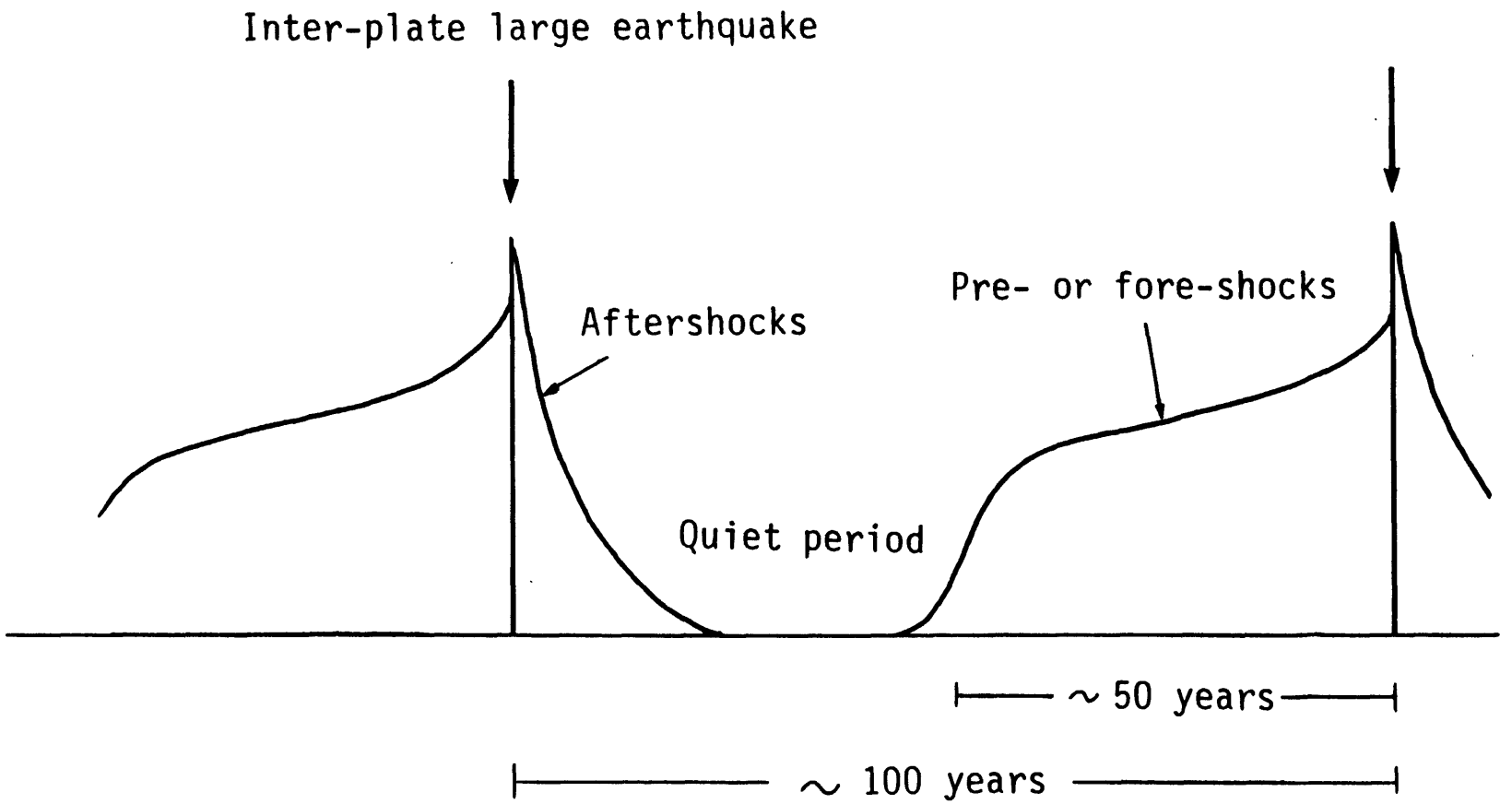
Inter-plate large earthquake
Aftershocks
Pre- or fore-shocks
Quiet period
~ 50 years
~ 100 years

Fig. 5

Seismic activity in western Japan after the 1946 Nankaido earthquake

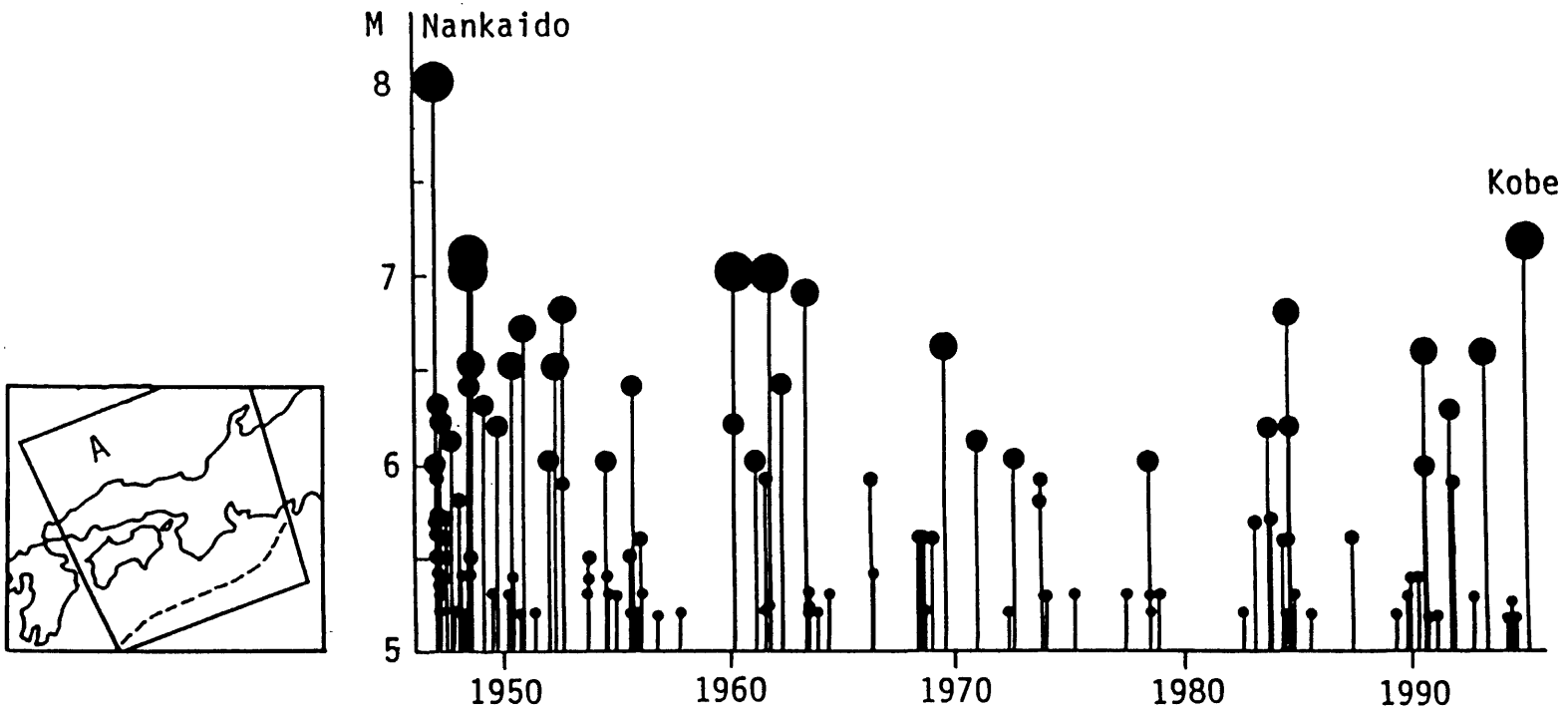

Fig. 6

Seismicity before
the 1995 Kobe earthquake

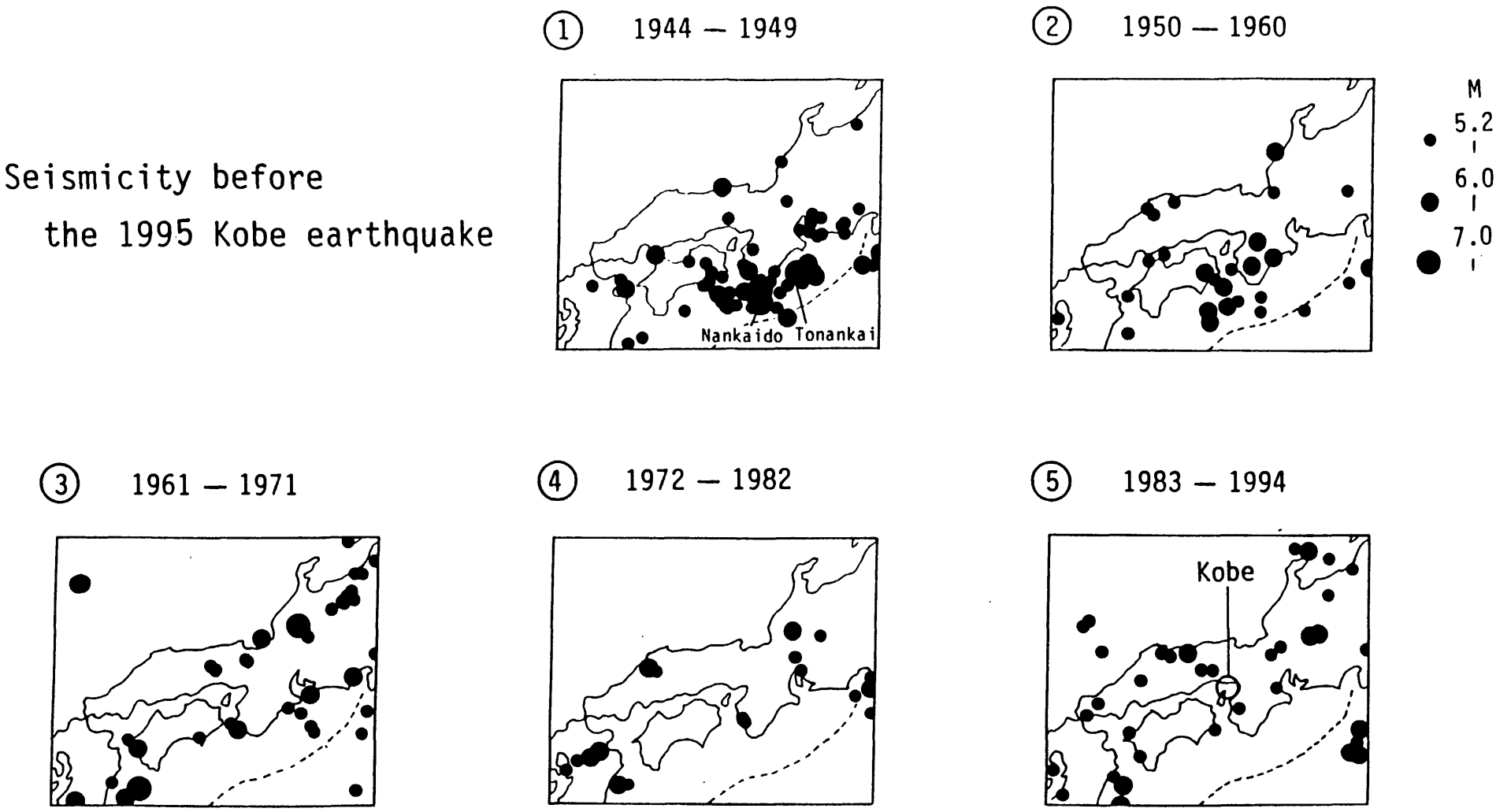

Fig. 7

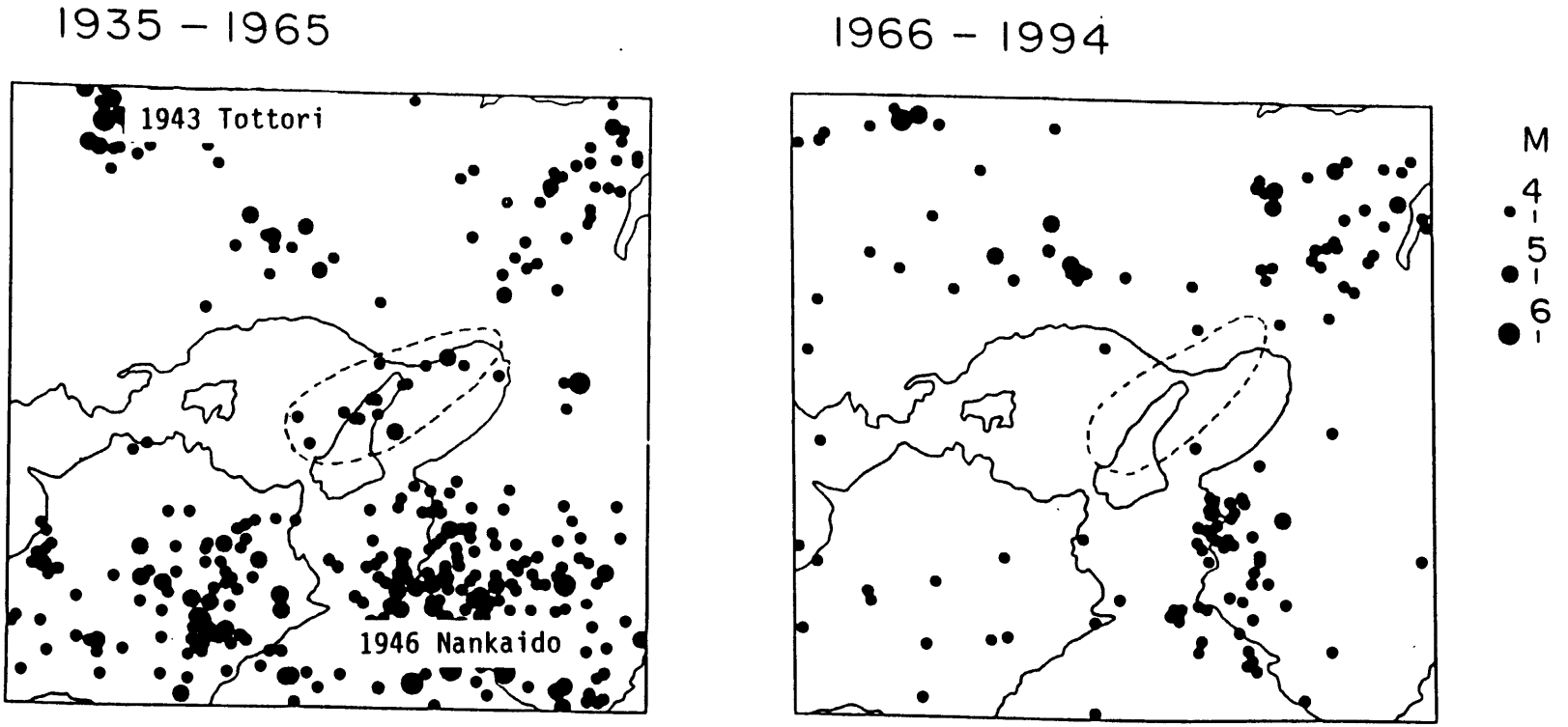

Fig. 8

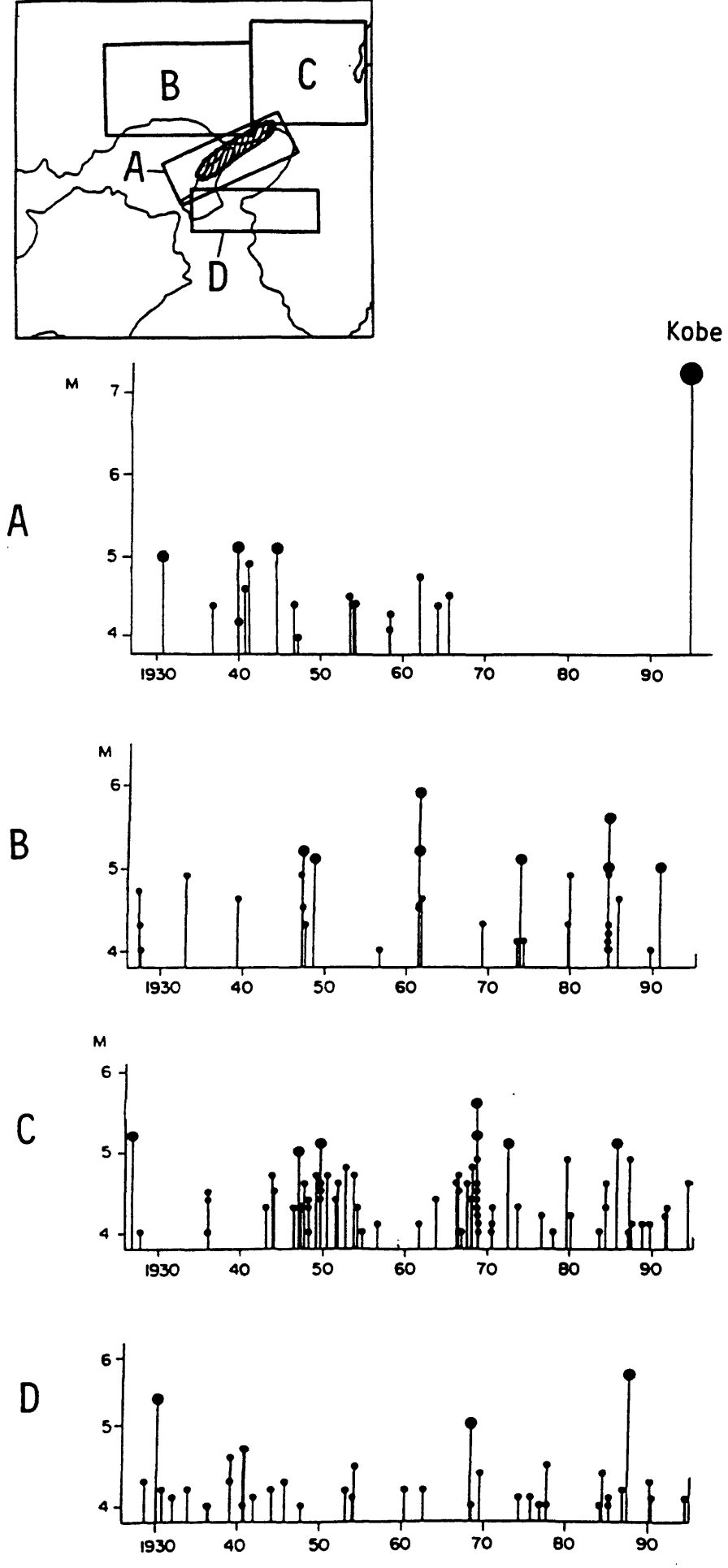
B
C
A
D
Kobe
M
7
6
5
4
A
1930
40
50
60
70
80
90
M
6
5
4
B
1930
40
50
60
70
80
90
M
6
5
4
C
1930
40
50
60
70
80
90
6
5
4
D
1930
40
50
60
70
80
90

Fig. 9

1950 – 1989

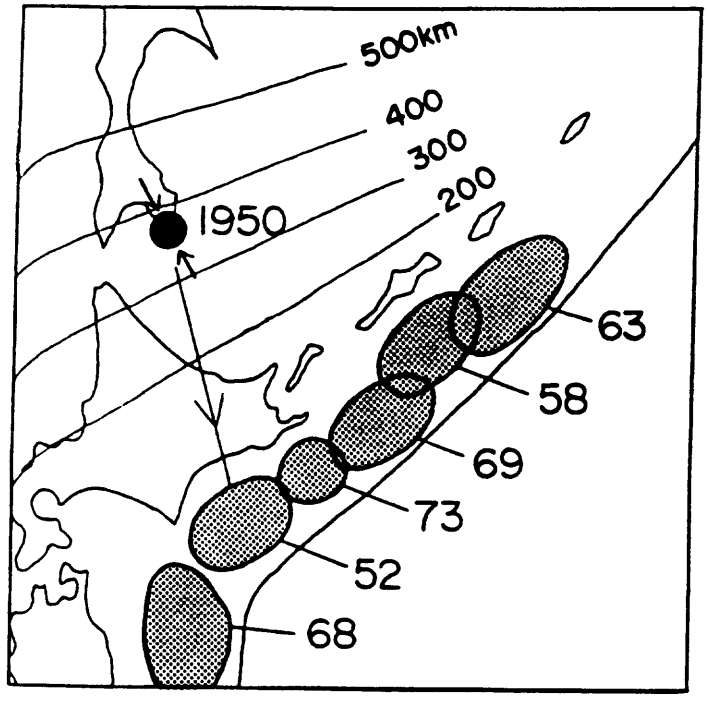

1990 – 1995

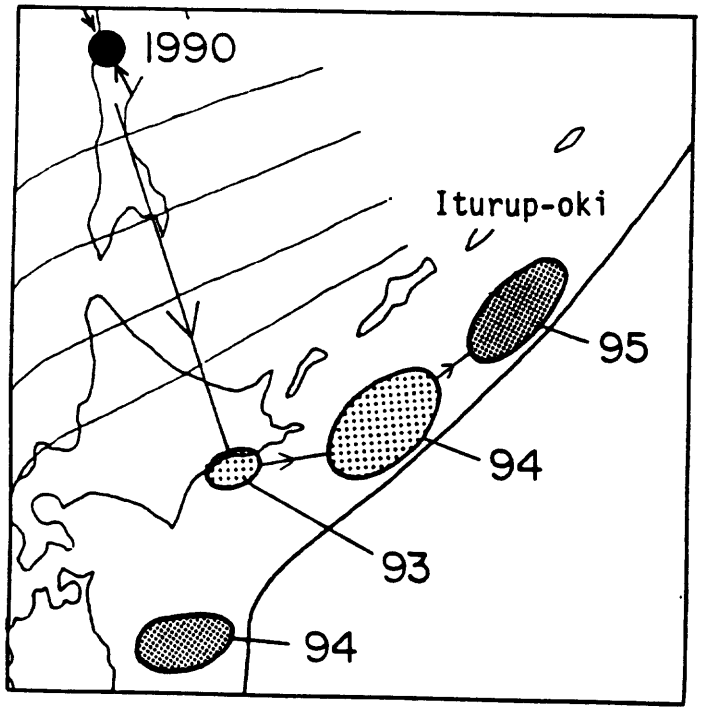

Fig. 10

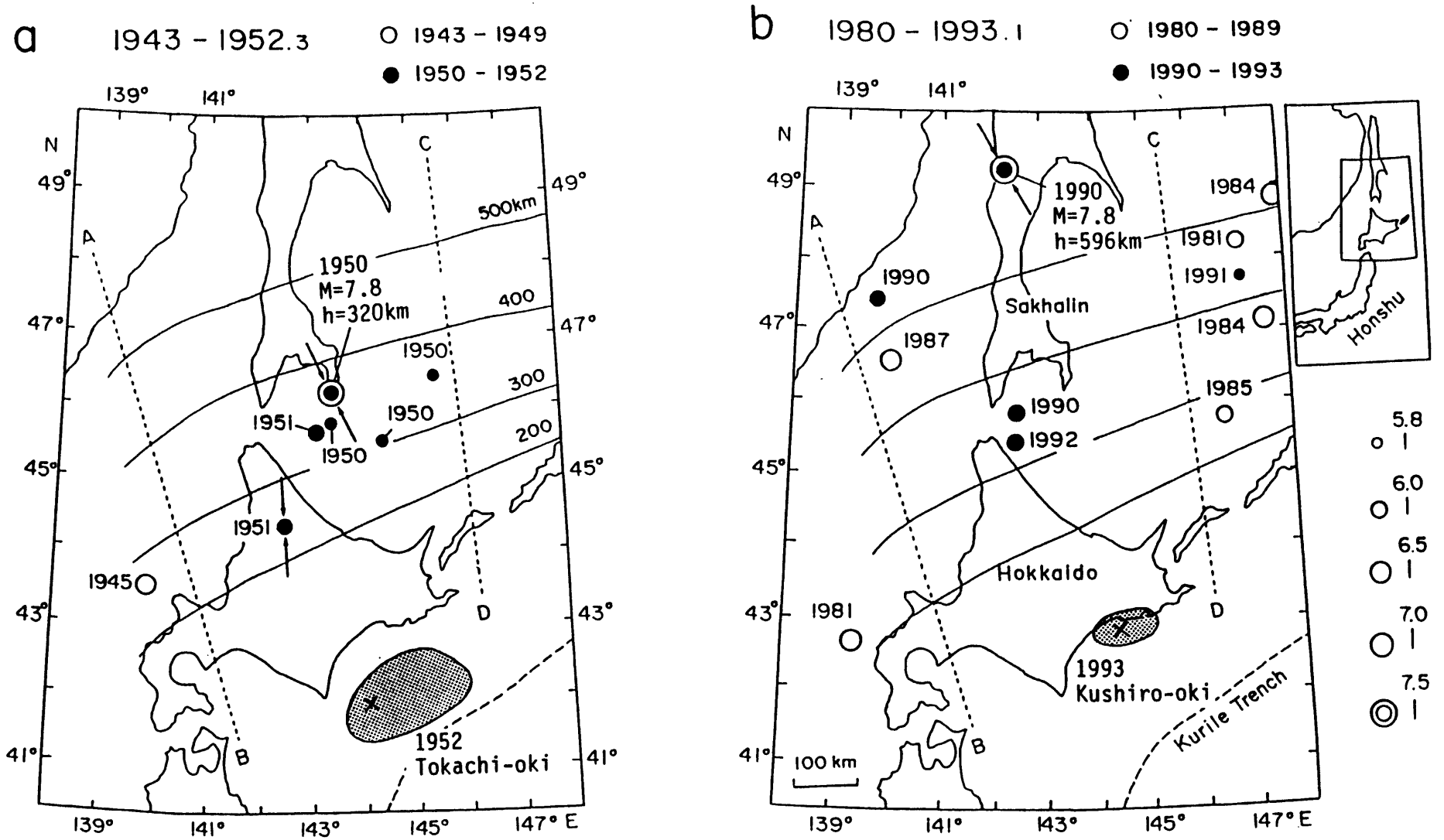
a
1943 - 1952.3
○ 1943 - 1949
● 1950 - 1952
139°
141°
N
49°
47°
45°
43°
41°
A
B
C
D
500km
400
300
200
1950
M=7.8
h=320km
1950
1951
1950
1950
1951
1945
1952
Tokachi-oki
139°
141°
143°
145°
147° E
b
1980 - 1993.1
○ 1980 - 1989
● 1990 - 1993
1990
M=7.8
h=596km
1984
1981
1991
1990
1984
1987
Sakhalin
1985
1990
1992
Hokkaido
1981
1993
Kushiro-oki
Kurile Trench
100 km
Honshu
5.8
6.0
6.5
7.0
7.5

Fig. 11

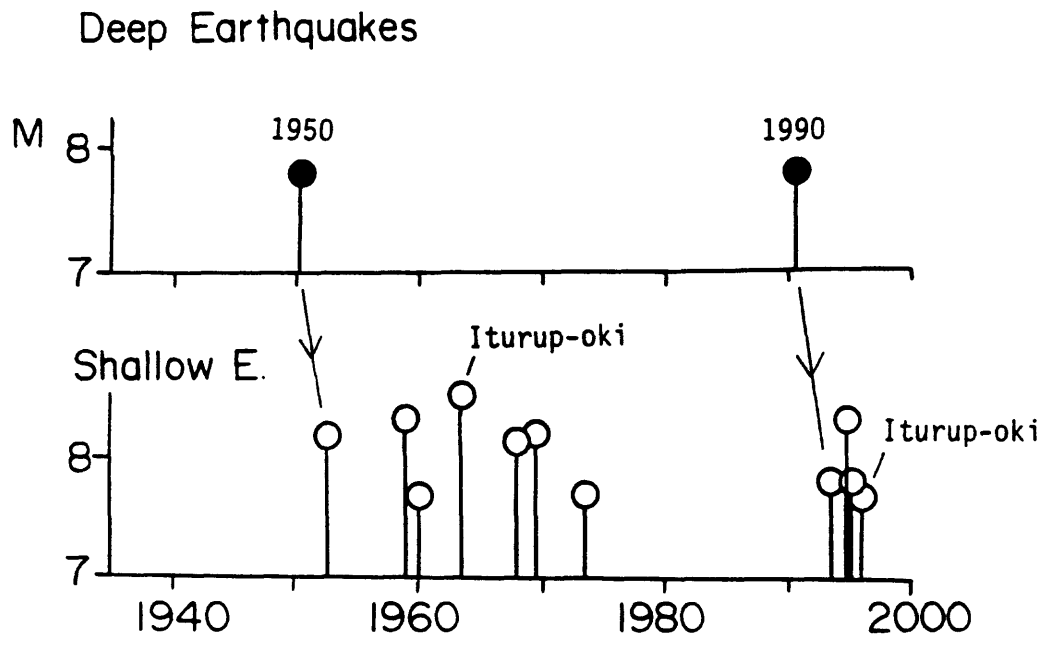
Deep Earthquakes
M
8
7
1950
1990
Shallow E.
Iturup-oki
Iturup-oki
8
7
1940
1960
1980
2000

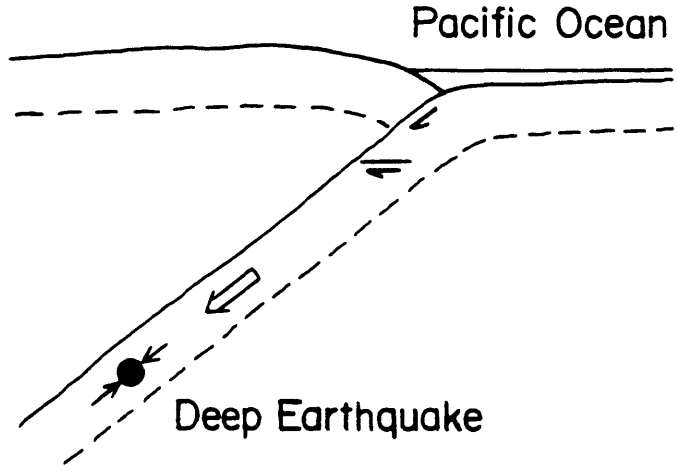
Pacific Ocean
Deep Earthquake

Fig. 12

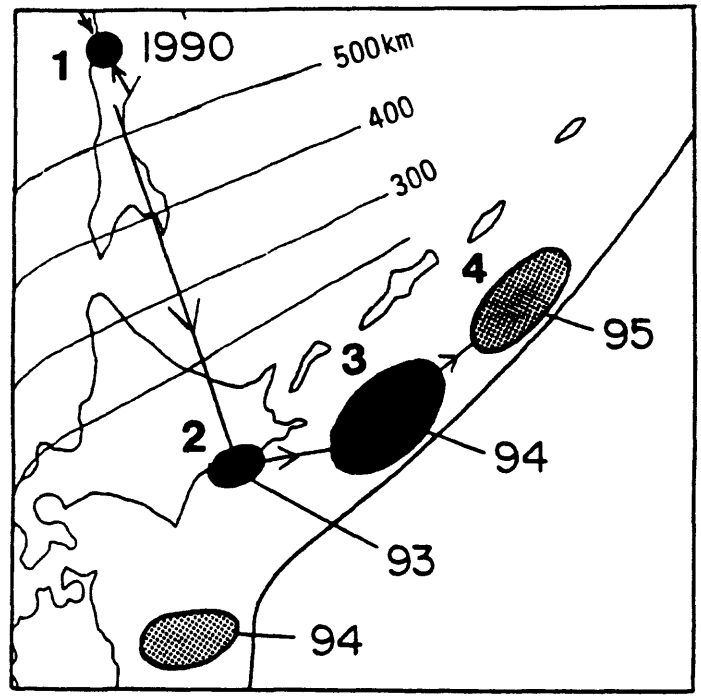
1
1990
500km
400
300
4
95
3
2
94
93
94

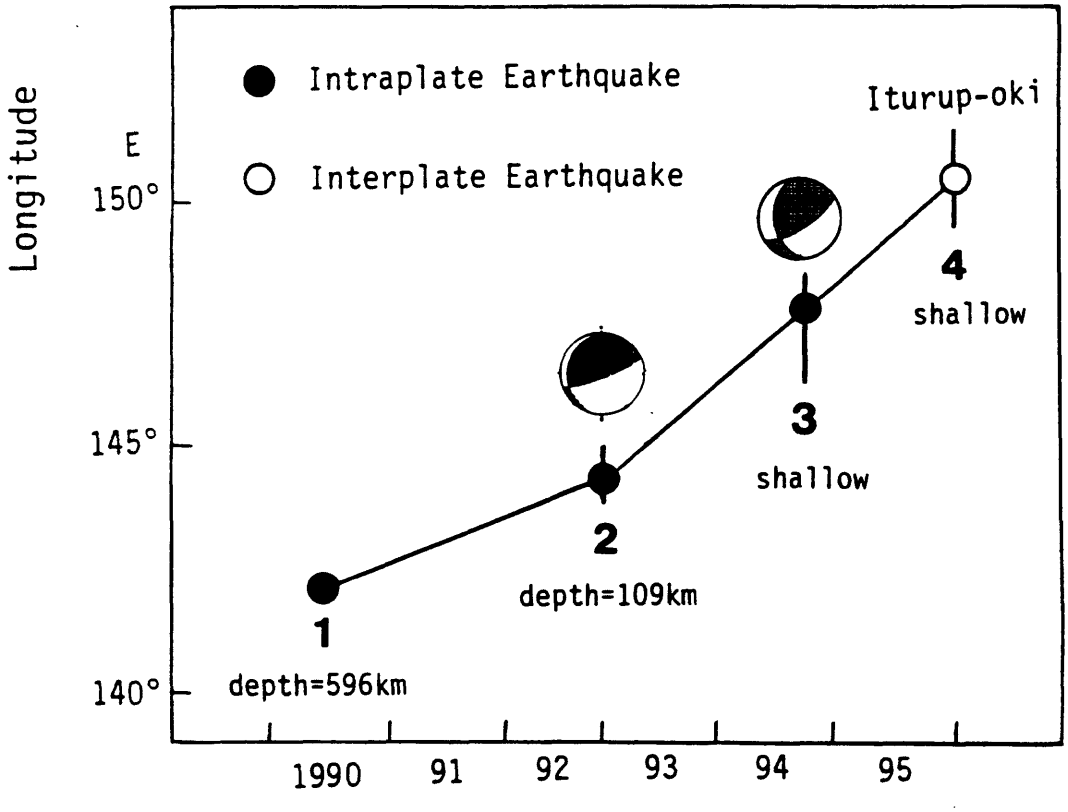
Intraplate Earthquake
Interplate Earthquake
Iturup-oki
Longitude
E
150°
145°
140°
4
shallow
3
shallow
2
depth=109km
1
depth=596km
1990
91
92
93
94
95

Fig. 13

The Los Angeles Basin Response in Simulated and Recorded Ground Motions

David J. Wald
U.S. Geological Survey, Pasadena

Vince Quitoriano
Caltech, Pasadena

Rob Graves
Woodward-Clyde Federal Services, Pasadena

The 1992 Landers earthquake provides an excellent set of strong motion data to study the long-period excitation of the Los Angeles Basin and its sensitivity to both earth structure and source parameterization. We are using a numerical modeling approach to make a systematic study of the importance of a variety of source and propagational effects on the estimation of ground motions produced during the Landers event. Although such a task is computationally demanding, the 3D finite-difference (FD) algorithm of Graves (1996) allows multiple realizations to be computed using a desktop workstation. As a calibration of the 3D FD, finite-fault implementation, we first reproduced the time histories of Wald and Heaton (1994) for their three-fault, variable-slip, source model using their same source and 1D velocity structure. We then analyzed how variations in source-slip heterogeneity and earth structure affect the waveform amplitudes and fit to the data. We have modeled the Magistrale (1996) 3D Los Angeles Basin model, a 3D model derived by Graves, and we are currently modeling the 3D structure of Hauksson and Haase (1996), derived from travel-time tomography. Analyses of observed and simulated ground motions for station profiles across the basin indicate peak displacements at sites in the central basin are 3-5 times larger than sites at comparable distances located outside the basin. This relative amplification (inside-to-outside basin) is quite variable over small distances (a few km), even at long periods ($T > 2$ sec). While some of the general ground motion characteristics are matched by the 3D simulations, there are exceptions, and the predicted amplification ratio and spatial variability is less than that observed. We are currently conducting further investigations to evaluate the accuracy and range of usefulness of existing earth structures for predicting basin effects on long-period ground motions.

THREE-DIMENSIONAL WAVE PROPAGATION IN THE LOS ANGELES BASIN

Ralph J. Archuleta[1,2] and Kim B. Olsen[1]

Institute for Crustal Studies[1] and Department of Geological Sciences[2]
University of California, Santa Barbara

We have used a 3-D finite-difference method to simulate ground motion from elastodynamic propagating ruptures with constant slip on faults in and near the metropolitan area of Los Angeles, California (Olsen and Archuleta, 1996; Olsen et al., 1995). Simulations are carried out for hypothetical earthquakes: (1) **M** 7.75 earthquake along the 170 km section of the San Andreas fault between Tejon Pass and San Bernardino (2) **M** 6.75 strike-slip earthquake on the Palos Verdes fault, (3) **M** 6.75 blind thrust earthquake on the Elysian Park fault, (4) **M** 6.7 blind thrust earthquake on the Oak Ridge fault—an approximation to the 1994 Northridge earthquake, (5) **M** 6.75 thrust earthquake on the Santa Monica fault. Simulated ground motions are restricted to the frequency range 0.0–0.4 Hz; thus the ground motion represents the long-period response of the metropolitan area.

Ground motion time histories show that, in general, sites associated with the largest particle velocities and cumulative kinetic energies are located 1) near the fault, 2) above the deepest parts of the basins and 3) near the steepest edges of the Los Angeles basin. We find maximum particle velocities in the Los Angeles basin for the San Andreas, Palos Verdes, Elysian Park, Northridge and Santa Monica simulations of 1.4 m/s, 0.44 m/sec, 0.67 m/sec, 0.58 m/s, and 0.3 m/s, respectively. In all cases, both the directivity of the rupture and the lower impedance of the basins significantly amplifies the ground motion. Although the gross radiation pattern from these ruptures is observable, the 3-D structure distorts the wavefield and becomes a source for edge generated waves. Signal durations at some basin sites last beyond 90 s due to Love waves and refracted S waves that propagate into the sediments from the basin edges.

One of the most difficult problems with predicting ground motion in the Los Angeles area is the three-dimensional nature of the velocity structure, especially the deep sedimentary basins. Until recently, almost all ground motion studies that simulated earthquakes as propagating ruptures on a finite fault have been limited to a one-dimensional velocity model that did not account the more realistic basin structure. As a first attempt to integrate the full 3-D regional velocity structure of the Los Angeles we use a complex 3-D geological model of the Los Angeles area

Evidence of Focusing Effects in Aftershock Seismograms of the Northridge

Paul M. Davis
Department of Earth and Space Sciences
UCLA
Los Angeles CA 90024
pdavis@cyclop.ess.ucla.edu

Several areas in southern California experienced greater damage than was expected at the time of the Northridge earthquake, given their distance from the epicenter. Because the geology in neighboring, less-damaged areas appeared to be the same it was not obvious that site effects were the cause. We investigated two such areas, Sherman Oaks and Santa Monica with a seismic array aftershock study. Over 100 digital seismographs were installed in the damaged and surrounding areas in order to compare amplitudes as a function of angle of incidence, frequency content, and damage caused by the main shock. When corrections are made for radiation pattern, geometric spreading and attenuation, we find that aftershock amplitudes are larger in the damaged zones. For Santa Monica, amplitudes in the damaged zone are, in extreme cases, 17 times that in the neighboring area. We attributed this difference to focusing by a small sub-basin lying beneath the city which concentrates the seismic energy in the focal region leaving the surrounding region in the shadow zone. Such a sub-basin has been mapped geologically where the reverse-dipping Santa Monica fault down drops an elliptical basin of sediments on the southern side of the Santa Monica mountains. This extreme basin-edge effect probably required a localized structure to have formed along the northern edge of the Los Angeles basin that gave rise to a three dimensional convex lens. Higher velocity basement surrounding a basin of lower velocity sediments appears to be the best explanation at present. For Sherman Oaks, the explanation is less clear. The region of high damage lies in a valley of Holocene sediments laid down by the Los Angeles river. Both coda waves and site amplifications support the view that near-surface site effects gave rise to higher than normal shaking at the time of the main event. However significant damage occurred in the foothills of the Santa Monica mountains, out of the region of river sediments. There is also evidence in the aftershock data of amplitude focusing by structural effects. Thus at this level of our understanding it appears the Sherman Oaks enhanced damage was a combination of focusing and site effects, but further testing, including mapping of the basement-sediment interface, is necessary to resolve the relative importance of each. In either case, it appears that constructive interference of seismic waves in the sedimentary structures near the edges of basins is a significant hazard that will require greater understanding of both the structures themselves and wave propagation through them.

Studies of active faults in Japan since the Kobe earthquake

Yoshihiro KINUGASA
<king@gsj.go.jp>
Geological Survey of Japan

The Hyogo-ken-nanbu (Kobe) earthquake of 17 January, 1995 caused massive damages including more than 6,000 casualties, the worst consequence of earthquake in Japan since the Great Kanto earthquake of 1923.

Distribution of aftershocks coincides with pre-existing active faults, namely, the Nojima fault in the Awaji island and other active faults at foothill of Mt. Rokko on the Kobe side. Surface ruptures are observed along the Nojima fault in the Awaji island. The maximum net slip reached as much as 2 meters right-laterally with some southeast up component.

An extensive effort has been carried out to reveal the paleoearthquake along the Nojima fault as well as to reveal future earthquake potentials along other active faults in the epicentral region.

Since the Kobe earthquake public interests on active faults increased dramatically and the Geological Survey of Japan has set up a new project "100 Faults in 10 Years" to evaluate earthquake potential nationwidely. After completion of this project, regional characteristics of fault activity in the past as well as in the future will be revealed.

Besides the GSJ's project, the Science and Technology Agency of Japanese Government starts supporting active fault surveys by local governments. To help local governments technically, experienced geologists of the GSJ and universities are involved in such active fault surveys by local governments as advisors.

Results of these surveys including those by the GSJ are reviewed by the member of Active Fault Sub-Committee under the Earthquake Research Committee and the Earthquake Research Committee takes responsibility of dissemination of information on active faults to the general public.

Tree-ring Dating of an Earthquake at the Cascadia Subduction Zone To Within Several Months of January 1700

David K. Yamaguchi* , Gordon C. Jacoby† , Brian F. Atwater‡ , Daniel E. Bunker†, Boyd E. Benson§ , Marion Reid, Connie Woodhouse

A tsunami that damaged Japan in January 1700 may have originated across the Pacific Ocean at the Cascadia subduction zone[1], where an earthquake attended by a tsunami (or a series of such earthquakes) has been radiocarbon dated to about that time[2,3]. We checked this proposed origin by studying annual rings of trees at Cascadia that were probably killed or disturbed by the earthquake (or series). Among seven killed redcedar retaining bark despite centuries of decay, six contain a complete 1699 ring but no younger ring. At least four surviving spruce contain disturbed rings from 1700, and in several other survivors such rings begin in 1701 or 1702. By converging so narrowly on the time of the tsunami in Japan, these tree-ring dates confirm that an earthquake known from geologic inference in North America left a mark in the written history of Asia.

The proposed Cascadia origin for the January 1700 tsunami[1] hinges on dating of the most recent earthquake (or series) that lowered much of the Pacific coast between southern British Columbia and northern California[4] and which left forests submerged by more than a meter of tidewater in Washington[5]. Such earthquakes are not part of the region's written history, which begins with European explorers in the 1770s. They remained unknown to seismology until the 1980s, when they were deduced from geophysics[6] and recognized in coastal geology[7]. The most recent of the earthquakes (or series) was soon dated, through tree-ring work described below, to a time shortly after the 1680s. Subsequent radiocarbon dating gave a range of 1680-1720 and, upon averaging of six ages, suggested an interval as narrow as 1695-1710 (ref. 2). Within these windows Satake *et al.*[1] found the January 1700 tsunami, for which they inferred no source in Japan, Russia, Alaska, or Latin America. Correction of a radiocarbon time scale[8], however, shifts the narrow interval to 1703-1715, and additional radiocarbon ages imply a slightly broader range that barely includes 1700 (ref 3). Did the January 1700 tsunami nonetheless originate at Cascadia? Tree-ring evidence now suggests that it did.

Our tree-ring work began during logging of old-growth western redcedar (*Thuja plicata*) rooted 50 m above sea level on Long Island, Washington (Fig. 1). Radial pieces cut from 19 of the stumps share enough variation in ring widths to match one another. Matches were initially inferred from graphing of narrow rings, which are especially useful in tree-ring dating[9,10]. Matches were then confirmed by statistical correlation of width measurements, from which long-term trends were first removed by fitting of growth-decay curves and cubic splines[11,12,13]. The result is a ring-width pattern that extends from 991 to 1986 and resembles a pattern previously obtained[14] from redcedar 150 km to the north.

* 3616 N.E. 97th Street, Seattle, Washington 98115, USA <TrRingzRUs@aol.com>
† Tree-Ring Laboratory, Lamont-Doherty Earth Observatory, Palisades, New York, USA <druid@ldeo.columbia.edu>
‡ U.S. Geological Survey, Department of Geological Sciences, University of Washington, Seattle, Washington 98195-1310 USA <atwater@u.washington.edu>
§ GeoEngineers, Inc., 8410 154th Avenue N.E., Redmond, Washington 98052, USA

With the Long Island samples in hand, we cut wedges from the trunks of 73 redcedar that stand dead, as snags, in tidelands of Copalis River, Grays Harbor, Willapa Bay, and Columbia River. Each of 19 snags yielded a long series of rings that matches only one part of the Long Island pattern. The probability of obtaining this match by chance is less than .001 for all but one of the 19 snags (Table 1). Resulting ring dates accord with graphical similarities in ring-width patterns (Fig. 2) and with the sole radiocarbon age obtained from the snags (Table 1, PX-782).

The dated trunk wood shows that many of the redcedar died sometime after the 1670s and 1680s (Table 1), consistent with death in 1700. At least one redcedar snag from each estuary retains a trunk ring from 1680 or later, and a Columbia River snag extends to 1691. Still younger rings, however, have been lost to three centuries of exposure that has left the trunks barkless, charred, and pitted.

We recently sought better-preserved wood in roots of redcedar snags, in hopes of narrowing the time of tree death. We found bark on roots of eight previously dated snags and two additional snags. Although convergent rings in three snags gave only maximum ages for death, concentric rings in seven snags gave the time of death more exactly (Table 1). We dated roots directly in seven snags by cutting vertical slices that allowed distinctive, previously dated rings to be traced from trunk to roots. For three other snags we used tree rings more conventionally, matching ring-width patterns between isolated samples of a root and its trunk.

Dates from the roots accord with January 1700 as the time of tree-killing submergence (Table 1). The most secure of these dates comes from roots that stopped growing after completing a 1699 ring. This evidence implies death between August 1699 and May 1700. It is compelling because it comes from six trees and four estuaries along 80 km of the central part of the subduction zone, and because it is based on Long Island and trunk-wood dating done before proposal of January 1700. The only potential discord is a 1708 ring at the Copalis River. But the 1708 ring comes from the highest of the dated roots (Table 1); height above tides may explain why this root outlived the others.

In related work begun in 1992 we cored 108 of the largest living trees in tidelands between the Copalis and Columbia Rivers. Most of these trees originated a few years to more than a century after 1700; they colonized emerging mudflats and marshes that had replaced forests killed by tidal submergence[15]. But among a few tidal areas transitional to floodplains we found 34 living trees established before 1700 (Fig. 1b). All but one of these survivors are Sitka spruce (*Picea sitchensis*), which tolerates flooding more than western redcedar[16].

At least one-third of the survivors were probably flooded, tilted, or both during or soon after 1700 (Table 2). Decreases in ring width, an easily delayed response to flooding[17], begin in 1700 (WL-79; Fig. 3a), 1701 (WL-81, PR-4; Fig. 3b), or 1702 (BS-3). Traumatic resin canals, which can also result from flooding[17], appear in 10 survivors by 1702. Compression wood[18]—marked by thick-walled cells and attributable to tilting or flooding[19]—forms part of the 1700 ring in WL-83 and PR-4. Temporary increases in ring width (Fig. 3c)—paradoxically, another response to flooding[17]—affect at least six trees by 1702, followed in most cases by decades of decline. Rings in survivors thus strengthen the linkage between the January 1700 tsunami in Japan and an earthquake at the Cascadia subduction zone.

[1] Satake, K., Shimazaki, K., Tsuji, Y. & Ueda, K. *Nature* **379**, 246-249 (1996).

[2] Atwater, B.F., Stuiver, M. & Yamaguchi, D.K. *Nature* **353**, 156-158 (1991).

[3] Nelson, A.R., *et al.*, *Nature* **378**, 371-374 (1995).

[4] Atwater, B.F., *et al.*, *Earthquake Spectra* **11**, 1-18 (1995).

[5] Hemphill-Haley, E. *Geol. Soc. America Bull.* **107**, 367-378 (1995).

[6] Heaton, T.H. & Hartzell, S.H. *Science* **236**, 162-168 (1987).

[7] Atwater, B.F. *Science* **236**, 942-944 (1987).

[8] Stuiver, M. & Becker, B. *Radiocarbon* **35**, 35-67 (1993).

[9] Stokes, M.A. & Smiley, T.L. *An Introduction to Tree-Ring Dating* (Univ. Chicago, 1968).

[10] Fritts, H.C. *Tree Rings and Climate* (Academic Press, New York, 1976).

[11] Cook, E.R. & Briffa, K.R. in *Methods of Dendrochronology, Applications to Environmental Sciences* (eds Cook, E.R. & Kairiukstis, L.A.) 97-162 (Kluwer, Boston, DATE).

[12] Yamaguchi, D.K. & Allen, G.L. *Can. J. For. Res.* **22**, 1215-1221 (1992).

[13] Yamaguchi, D.K. *Can. J. For. Res.* **24**, 427-429 (1994).

[14] Jozsa, L.A., Parker, M.L., Johnson, S.G., & Bramhall, P.A. *Ozette Dendrochronological Studies* (ed Gleeson, P.F.) 27-56 (Laboratory of Anthropology, Wash. State Univ., Pullman, Wash., 1983).

[15] Atwater, B.F. *U.S. Geol. Surv. Prof. Pap. 1560* (in the press).

[16] Brink, V.C. *Ecology* **35**, 94-95 (1954).

[17] Kozlowski, T.T., in *Flooding and Plant Growth* (ed Kozlowski, T.T.), 129-163 (Academic Press, New York, 1984).

[18] Timell, T.E. Compression Wood in Gymnosperms, v. I, II, III (Springer-Verlag, New York, 1986).

[19] Kozlowski, T.T., Kramer, P.J & Pallardy, S.G. *The Physiological Ecology of Woody Plants* (Academic Press, San Diego, 1991).

ACKNOWLEDGEMENTS. We thank Lorin Amidon, Patricia Atwater, Ken Bevis, Judy Boughner, Marco Cisternas, Skye Cooley, Laura Davis, Stephanie Fritts, Nancy Jacobson, José Morales, Peter Raskind, Kathleen Sayce, John Shulene, Yumei Wang, Karl Wegmann, and Andrew Zachery for help with field work; Erich Eipert for sanders; Minze Stuiver for radiocarbon advice; and AAA, BBB, and CCC for manuscript reviews. Most of the work was funded by the U.S. Geological Survey through the National Earthquake Hazards Reduction Program.

TABLE 1 Dating of redcedar snags

Estuary	Tree	Trunk				Root	
		Sample length (yr)	Outer preserved ring (yr AD)	Mean correlation with other trees at estuary	Correlation with Long Island*	Height (m, relative to high tide)†	Outer ring against bark (yr AD)
Copalis River	CP-789	348	1667	.35	.21 (<.05)	+0.1 to -0.2	after 1680‡
	CP-790	328	1632	.38	.27 (<.0005)	--	--
	CP-791	285	1680	.43	.32 (<.0001)	+0.2 to -0.3	1708§
	CP-793	328	1664	.40	.26 (<.001)	--	--
	CP-794	274	1599	.44	.28 (<.001)	--	--
	CP-GF2	--	--	--	--	-0.5	1699
Grays Harbor	CH-764	151**	1682	.30	.35 (<.005)	--	--
	JN-560	297	1674	.34	.28 (<.0005)	-0.5 to -1.0	after 1689‡
	JN-561	266**	1678	.27	.42 (<.0001)	-0.5 to -1.0	1699
	JN-566	229	1685	.33	.33 (<.0001)	--	--
Willapa Bay	BN-915	288	1684	.42	.28 (<.0005)	--	--
	PX-nt778	358**	1684	.41	.31 (<.0001)	-0.1 to -0.3	after 1670‡
	PX-779	292	1677	.41	.44 (<.0001)	-0.4 to -0.8	--
	PX-782††	241**	1682	.63	.46 (<.0001)	-0.2 to -0.6	1699
	PX-783	343	1675	.43	.29 (<.0001)	-0.2 to -0.7	1699
	PX-J6	--	--	--	--	-0.8 to -1.2	1699
Columbia River	GR-578	338	1676	.46	.26 (<.0005)	--	--
	GR-580	224	1658	.50	.42 (<.0001)	--	--
	GR-582	223**	1691	.59	.30 (<.005)	--	--
	GR-776	245	1675	.50	.29 (<.001)	--	--
	GR-777	381**	1671	.41	.30 (<.0001)	-0.7 to -0.9	1699

--, not determined.

* Number in parentheses gives probability of obtaining correlation by chance. This probability (p) is calculated from student's t value that weights correlation (r) for sample length (n, in years): $t = r\sqrt{[(1-r^2)/(n-2)]}$; $p = 1-(1-\alpha)^m$, where α is the significance level from statistical tables and m is the number of dating positions between AD 1190 and 1720. Each correlation is highest obtained along entire 996-year Long Island ring series and corresponds to the position that gives the highest within-estuary correlation.

† High tide denotes present mean higher high water, as estimated from depth below present tidal wetland surface (all sites), from leveling tied to one (CP, GR) or three (PX) tidal cycles, and from tide tables.

‡ Bark preserved only on parts of roots where outer rings taper, some to the point of disappearance. Such rings gave various, probably limiting dates for death that are youngest where the rings are widest and most nearly concentric. Date listed is youngest obtained.

§ Upper part, probably fed by a smaller root entirely above present high tide. Lower part of main root, fed by a root entirely below modern mean higher high water, gave an outer-ring date of 1701.

** Combined length from 2 or 3 samples on different radii. Mean ring-width indices from these samples were used for correlation with Long Island. Longest sample only was used for correlation with other trees at estuary.

†† Rings assigned dates of 1645-1655 gave a radiocarbon age 241±11 ^{14}C yr B.P. (QL-4411), which corresponds to 1648-1671. The latter range, calculated from calibration data of Stuiver and Becker[8], includes the 95-percent confidence interval if the quoted error exceeds 0.6 standard deviation.

TABLE 2 Annual ring-width changes and anatomical features in cores from living trees

Estuary	Tree*	Oldest ring seen	No. cores †	Growing season (May to September)											
				1698 dtci	1699 dtci	1700 dtci	1701 dtci	1702 dtci	1703 dtci	1704 dtci	1705 dtci	1706 dtci	1707 dtci	1708 dtci	After 1708
Copalis River	CP-1	1667	3	----	----	----	1---	----	----	----	----	----	----	--1-	c to 1730s
	CP-3	1675	2	-1--	----	-1--	----	----	----	-2--	-1--	-1--	----	-1--	t common to 1750
Willapa Bay	WL-77	1651	7	----	----	1---	-42-	-112	--1-	--1-	-11-	--1-	-11-	--1-	d in 1709, all cores
	WL-79	1621	7	----	----	5---	5---	5---	6---	----	----	4---	----	---1	d to 1760
	WL-81	1652	9	-2--	----	-1--	75--	45--	1---	----	-1--	1---	----	-1--	--
	WL-83	1659	5	----	----	--3-	----	-42-	---1	---1	----	----	----	----	t in 1709, all cores
Columbia River	PR-3	1618	3	----	----	-2--	----	-2--	--1-	----	1---	3---	-1--	12--	d to 1730
	PR-4	1624	4	--1-	--1-	-22-	321-	-1--	31--	1---	1---	31--	----	----	d to 1745
	PR-19	1611	3	-2--	----	-1-1	----	-1-1	-2--	----	-1-1	11--	----	12--	d to 1740
	PR-31	1649	4	----	----	1---	11--	-1-1	---1	21--	1---	2---	----	----	d to 1750
	PC-1	1484	3	----	----	----	----	-113	-113	-1--	-2--	11--	1---	1---	d to 1800
	PC-2	1604	3	----	----	---1	--11	--22	-111	--11	--1-	--1-	----	--1-	--
	BS-2	1552	3	----	----	----	-1--	-1-2	-1-1	-111	131-	211-	----	1---	d to 1725
	BS-3	1624	2	----	----	----	----	2---	2---	2---	----	----	----	----	d to 1740
	BS-4	1603	2	----	----	----	-1--	-111	--11	--11	--11	--11	--2-	-11-	d to 1715

d, decrease in ring width relative to previous year; t, traumatic resin canals, tabulated only for rings containing two or more in a core where most other rings have none; *c*, compression wood; i, increase in ring width relative to previous year, eventually followed (except in PC-2) by persistent decrease in ring width; 1, 2, etc., number of cores in which change or feature was observed.

* BS-3 is western redcedar that retains a strip of live wood on an otherwise long-dead trunk. All other trees are Sitka spruce. Dating was done by statistical correlation with Long Island (BS-3) and by statistical correlation, graphical comparisons, and microscopic core-to-core comparisons within trees and among trees and sites, independently by two investigators (other trees).

† Diameter 5 mm (all trees) or 12 mm (1 or 2 cores from each tree except WL-83).

Figure 1

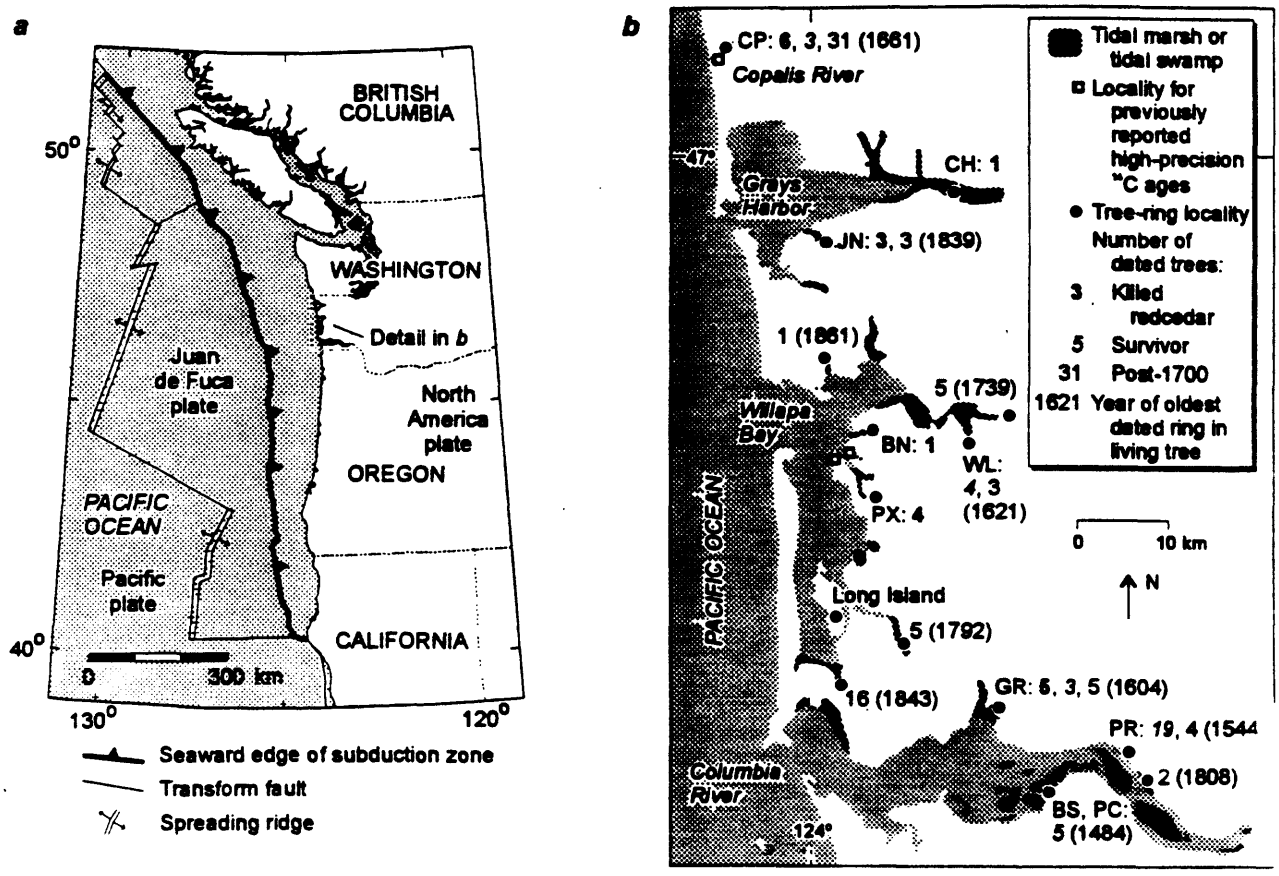

FIG 1 Index maps of Cascadia subduction zone (a) and estuaries of southern Washington (b).

Figure 2

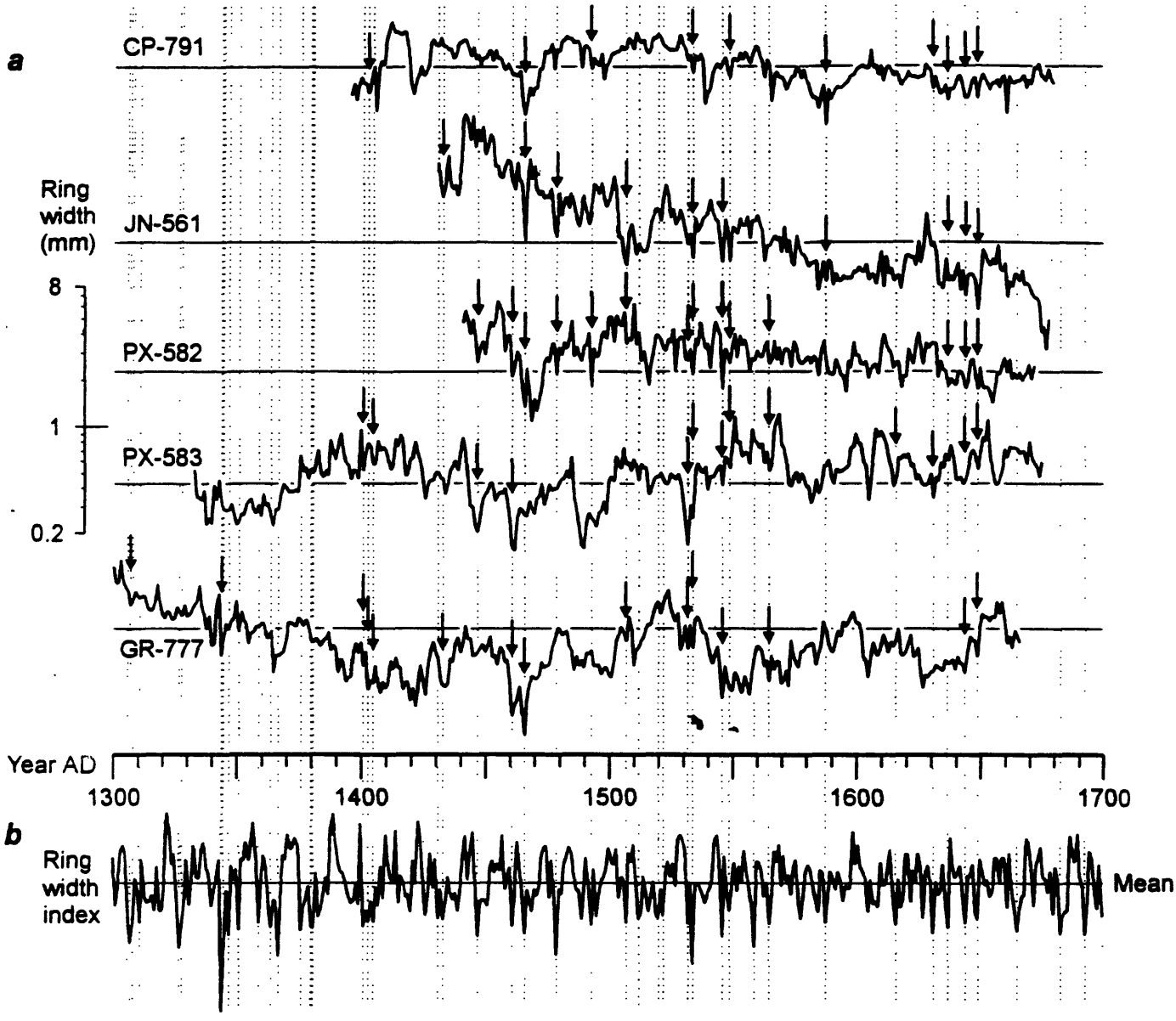

FIG 2 Correlation of ring widths in redcedar snags (a) with dimensionless index computed from detrended ring widths in 19 old-growth redcedar at Long Island (b). Vertical lines highlight narrow rings that are more than 1 standard deviation below the Long Island mean; arrows mark corresponding minima in snags. Snags plotted are most of those sampled successfully for year of death as recorded in bark-bearing roots (Table 1). These snags are at Copalis River (CP), Grays Harbor (JN), Willapa Bay (PX), and Columbia River (GR) (Fig. 1b).

Figure 3

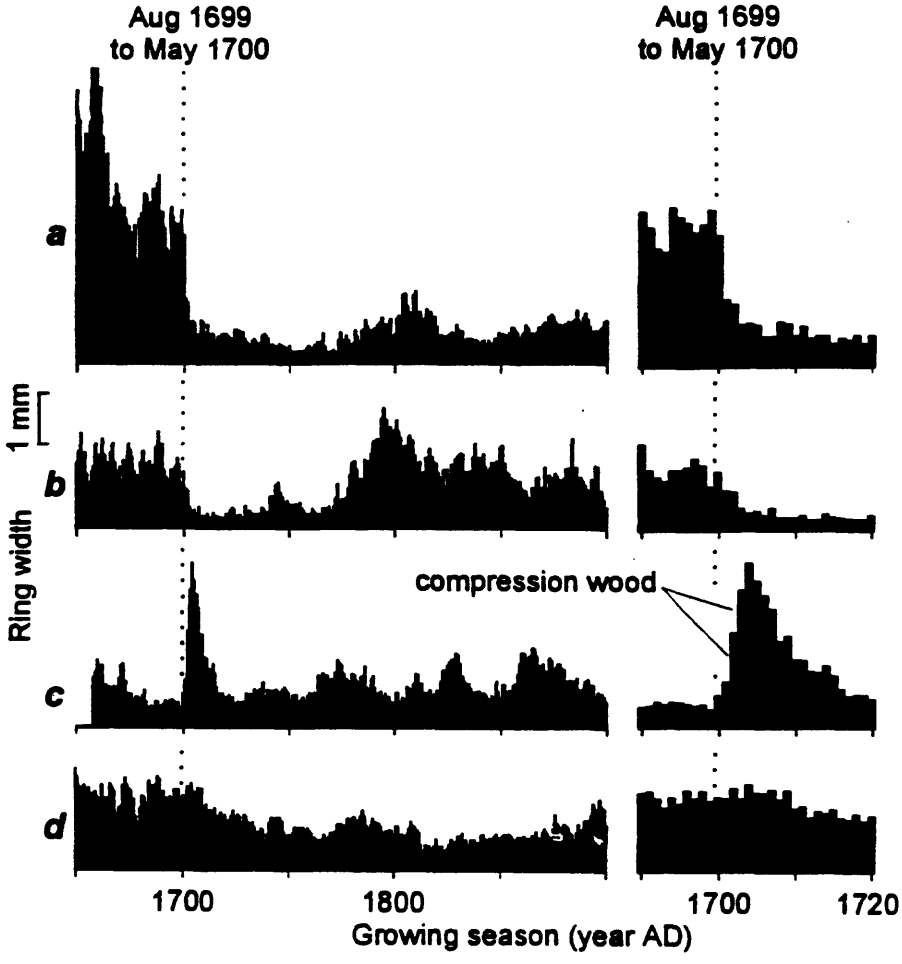

FIG 3 Ring widths in tideland spruce that lived through the decades before and after January 1700. Graphs at left give long-term context for changes between 1690 and 1720, which are shown at right. Upper graphs show evidence for disturbance in single cores from Willapa Bay locality WF (a) and Columbia River localities PR (b) and PC (c) (Fig. 1b). Bottom pair of graphs shows mean of five trees, at Columbia River locality PR, that show little if any sign of disturbance.

Seismotectonic Background for Tsunami Risk Assessments

Kenji Satake
Geological Survey of Japan

Tsunami hazards are unique in several aspects: time delay before tsunami arrival after an earthquake, damage limited to coastal area although it can be very wide, and possibility of trans-Pacific damage. In addition, hazards from unusual "tsunami earthquakes" or secondary sources such as landslides or submarine slumping triggered by earthquakes can be significant. In order to assess tsunami risk and reduce hazards, long-term assessment and effective tsunami warning system are both critical. While the tsunami warning system in Japan is improving, the long-term assessment is mostly based on empirical data from relatively short time period (typically a few tens of years).

Seismotectonic studies of tsunamigenic earthquakes can help us better understand the tsunami generation process and contribute to improve tsunami warning system and long-term hazard assessments. I will review recent studies on tsunami generation process from subduction-zone earthquakes, unusual "tsunami earthquakes" and the secondary sources, and discuss how these studies can contribute tsunami risk assessments.

For typical subduction-zone earthquakes, the probability for future occurrence has been estimated on the basis of "seismic gap theory", although recent examples (e.g., the 1994 E off Hokkaido earthquake) showed that non-subduction earthquake generates a similar tsunami. Tsunami generation, propagation and run-up are computed for a "characteristic earthquake" for hazard assessment purpose in the Tokai area and the U.S. Pacific Northwest.

"Tsunami earthquakes" generate much larger tsunamis than expected from seismic waves; examples include the 1896 Sanriku, 1946 Aleutian, and 1992 Nicaragua earthquakes. There was no damage from ground shaking for these events, but the tsunami damage was devastating. Recent studies of the above three events revealed that a narrow and shallow faulting beneath accretionary wedge is responsible for the tsunami generation. Further, the location of tsunami earthquakes seems to be related to submarine geological structure. Studies of recent tsunamigenic earthquakes in other regions (e.g., the 1992 Flores and 1994 Mindoro earthquakes) indicate that tsunamis from local and secondary sources, presumably due to landslide or submarine slumping triggered by ground shaking, causes significant damage.

Survey of Active Faults in the Coastal Areas

Shigeru Kasuga and Yo Iwabuchi
(Hydrographic Department of Maritime Safety Agency, Japan)

1. Introduction

Active faults are the relicts of large inland earthquakes. It is important to reveal the distributions of active faults in order to estimate the potentials of large earthquakes. The distributions of active faults on the land area of Japan are described in the catalog which was compiled by the Research Group for Active Faults of Japan (1980, 1991). According to this catalog, there are about two thousands of active faults and lineaments on the land area in Japan.

Distribution of the faults in the sea is not well described in the catalog because most of the coastal area is unsurveyed or poorly surveyed. Most of Japanese metropolises are located on the coast, however, the bays such as the Tokyo Bay and the Osaka Bay were scarcely surveyed because coastal area close to megalopolis is not suitable to the field of seismic survey. As the multi-channel seismic profiling requires a long streamer cable and straight truck line, it is difficult to operate in the heavy traffic water. Besides, noisy water spoils resolution of seismic records. There remain other problems to estimate the potentials of earthquakes by the active faults in the sea area.

Hydrographic Department of Japan (JHD) has been conducting bathymetric and seismic survey in the sea areas around Japan for the past 30 years. Main purpose of the surveys is to provide the basic data for utilization and exploitation of the ocean. In addition to these, we have started a new project of active-fault survey in bays and inland seas, following the occurrence of the Hyogoken-Nanbu Earthquake of M7.2 in 1995 which caused severe damage in Kobe and the neighboring area. The main purposes of this surveys are, 1) to detect the buried active faults in the coastal area, 2) to reveal the geologic structures around the area, 3) to provide the acoustic profiles at the extension of the active faults on land to estimate the whole length and seismic potential of the active faults, 4) to estimate the event intervals and the latest event of the active faults which provide useful information on a long-term risk assessment of the earthquake.

We will report the outline of the JHD's ongoing project of active faults survey and preliminary results of our survey conducted in the Osaka Bay.

2. Survey method

Geographical approaches are widely applied to detect active faults on land. However, tectonic landforms caused by active faults will not be well preserved in the coastal area, because erosions by waves and swells are prominent in the shallow seas. Therefore, geographical approaches are not suitable, whereas the seismic surveys using sub-bottom profiler or airgun, sparker system, etc., are very important in the coastal sea (Fig. 1). Seismic surveys are usually carried out with line spacing of about 500 m to 900 m in the coastal area.

Vertical resolution depends on the frequency and pulse length of seismic waves. However, horizontal resolution in the shallow waters mainly depends on the density of shot points of seismic survey. Horizontal resolution depends on the ping intervals and speeds of research vessels. Since it is impossible to control the vessels at very low speed, seismic surveys are carried out at least more than 2 to 3 knots. We make much of the horizontal resolution than power or wave shape of seismic source. Therefore, conventional sparker system is used as the source of low frequency ranges.

In addition to this, it is also important to reveal the deep geological structure to clarify whether the detected geological structures in shallow layers reflect the movements of basement or not. Therefore, multi-channel seismic surveys using air-gun should be carried out in the area where the prominent faults in shallow layers were detected.

The detected faults are judged if they are active faults or not. We regard them as active faults if seismic records have the following characteristics. a) the fault displacement reaches to the surface layers, b) the fault displacements or offset at each layer are larger as layers becomes deeper. A typical example of seismic profile recognized as an active fault is shown in Fig.1.

3. Examples of active fault survey in the sea

1) Survey of buried faults in coastal seas

A fault that was named as the Osaka Bay Fault (Iwasaki et al., 1994), was found in the Osaka Bay, close to metropolises such as Osaka and Kobe (Fig.2). However, the details of the fault were unknown because the fault was detected from only one truck line. There seems to be no other fault in the Osaka Bay according to the previously published catalog (Research Group of active Faults of Japan, 1991) as shown in Fig.2.

Hydrographic Department of Japan (JHD) carried out seismic survey in the Osaka Bay in 1995 immediately after the Hyogoken-Nanbu Earthquake occurred. The survey revealed that the Osaka Bay Fault reaches to the south of Kobe, and its entire length is more than 30 km. In addition to this, many faults are detected as shown in Fig.4. A comparison of Fig.2 and Fig.4 indicates that density of the active faults in the Osaka Bay is no less lower than that in the surrounding land area.

2) Survey of coastal area at the seaward extension of active fault on land

It is pointed out there are distinct empirical relations between a length of active fault and magnitude of earthquakes (e.g., Matsuda, 1975). Therefore, it is significant to reveal overall length of the fault on land which extends to the sea to estimate the potential of earthquakes. Figure 3 shows Kikukawa Fault in western Japan. The Kikukawa Fault can be traced to 27 km on land. The earthquake potential of Kikukawa fault is estimated by Matsuda's expression (Log L = 0.6M - 2.9, L:km; Matsuda, 1975). This expression shows its magnitude is 7.2 based on fault length on land. Besides, according to seismic records, the fault is traced at least 25 km in northwest extension of coastal area. Whole length of the fault on land and sea is more than 52 km. The potential (possible maximum magnitude) of the fault is estimated as magnitude 7.7 according to the whole length of the fault. This example shows the importance of survey in the sea at the extension of the fault on land to estimate the earthquake potential.

3) An attempt to estimate the activity of fault by a combination of seismic survey and boring

There are about two thousands of active faults on land in Japan. However, the event intervals and last event are known only for few dozens of faults. The studies on the event intervals and the last event by piston-corer in the coastal area were carried out since 1986 (e.g., Nakata and Shimazaki, 1993, Okamura,1995).

The Osaka Bay fault is located close to metropolises. Considering its neighboring high populations, it is very important to reveal the event intervals and the latest event in order to assess seismic risk. JHD carried out borings at the both sites of the Osaka Bay fault to the off Kobe. Multi-channel seismic survey using airguns was conducted crossing the two boring sites (Fig.5). Preliminary core analyses are being carried out. Thus, tentative results will be reported

here.

Borings were carried out by a private company under contract across both sides of the fault to the 6 km southwest of Kobe port. Water depth of the two sites are about 25 m. Cores were recovered to 100 m from the sea floor respectively. The fault is flexure at the site. Both boring sites across the fault are 1 km apart from each other. These sites were not best sites in terms of the clearness of seismic profiles across the fault because the sites were selected setting high priority on the security from sea traffic. After all, fortunately or unfortunately, drilling rig was turned over and sank under the see by a collision of a reckless cargo boat just on the next day when all core samples were landed.

Core samples of both sites were compared by rock faces, magnetism, tephra, C^{14} dating, thermoluminescent dating, microfossils etc. Tentative comparison of cores and seismic profile is shown in Fig.6 and Fig.7. Difference in depth of each layers between the both sites must be reflecting vertical movements of the faults, if there were no hiatus of deposition. Offset or difference in depth of each layer increase as the layer becomes deeper and its age becomes older (Fig.8). As a result of tentative comparison, an average rate of the vertical displacement of the fault is about 0.8 mm/y during the past 6300 years and about 0.3 - 0.5 mm/y during the past 120,000 years. The difference in the rate of vertical displacement may be attributed to the change in the activity of the fault or the change in sedimentation environment. Estimation of the event intervals and the latest event of the faults are being carried out by analyzing core samples in detail. The analysis also requires consideration of the complicated change in sedimentation rate and the effect of erosion at the two sites.

4. Future Plan

It is important to provide the information about active faults to estimate the potentials of earthquake. JHD is planning to carry out systematic survey project to detect buried active faults in the other coastal area, placing high priority to the area close to the large cities. So far, JHD have conducted the survey at Osaka Bay, Tokyo Bay, Ise Bay, and we are conducting seismic surveys at Fukuoka Bay and Hiroshima Bay, all of which are close to large cities. In addition to this, JHD will re-analyze accumulated seismic profiles around Japan, which have been obtained since 1967 as a part of its mapping project. Besides, attempts to reveal event intervals and the latest event for major active faults will be carried out cooperating with other institutions in order to provide useful information on a long-term risk assessment of the earthquake.

References

The Research Group for Active Faults of Japan (1980): Active Faults in Japan. Tokyo Univ. Press.

The Research Group for Active Faults of Japan (1991): Active Faults in Japan. Revised edition. Tokyo Univ. Press.

Matsuda, T. (1975): Zisin, 28, 269-283.

Nakata, T and Shimazaki, K. (1993): Kagaku, 63, 593-599.

Okamura, M. (1995): Earth Monthly, 17, 536-540.

Iwabuchi, Y., Kasuga, S., Kokuta, S., Okino, K., Shimura, E. And Nagata, S. (1995): Jour. Japan. Soc. Marine Surv. Tech.,7, 11-19.

Iwasaki Y., Kagawa, T., Sawada, S., Matsuyama, N., Oshima, K., Ikawa, T. and Onishi, M. (1994): Zisin, 46,395-404.

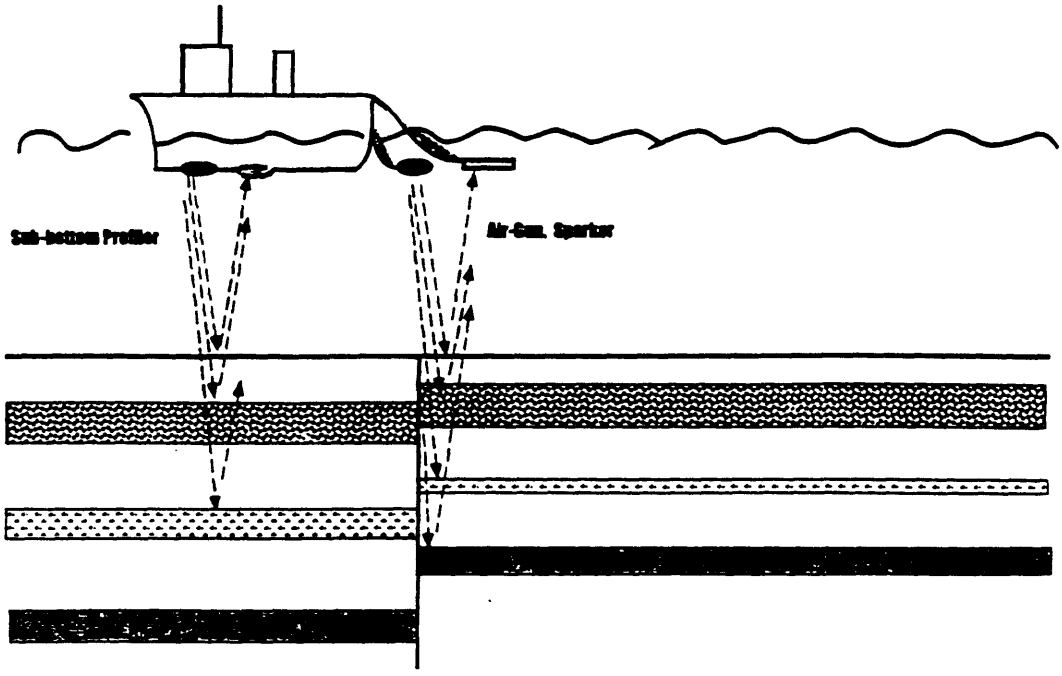

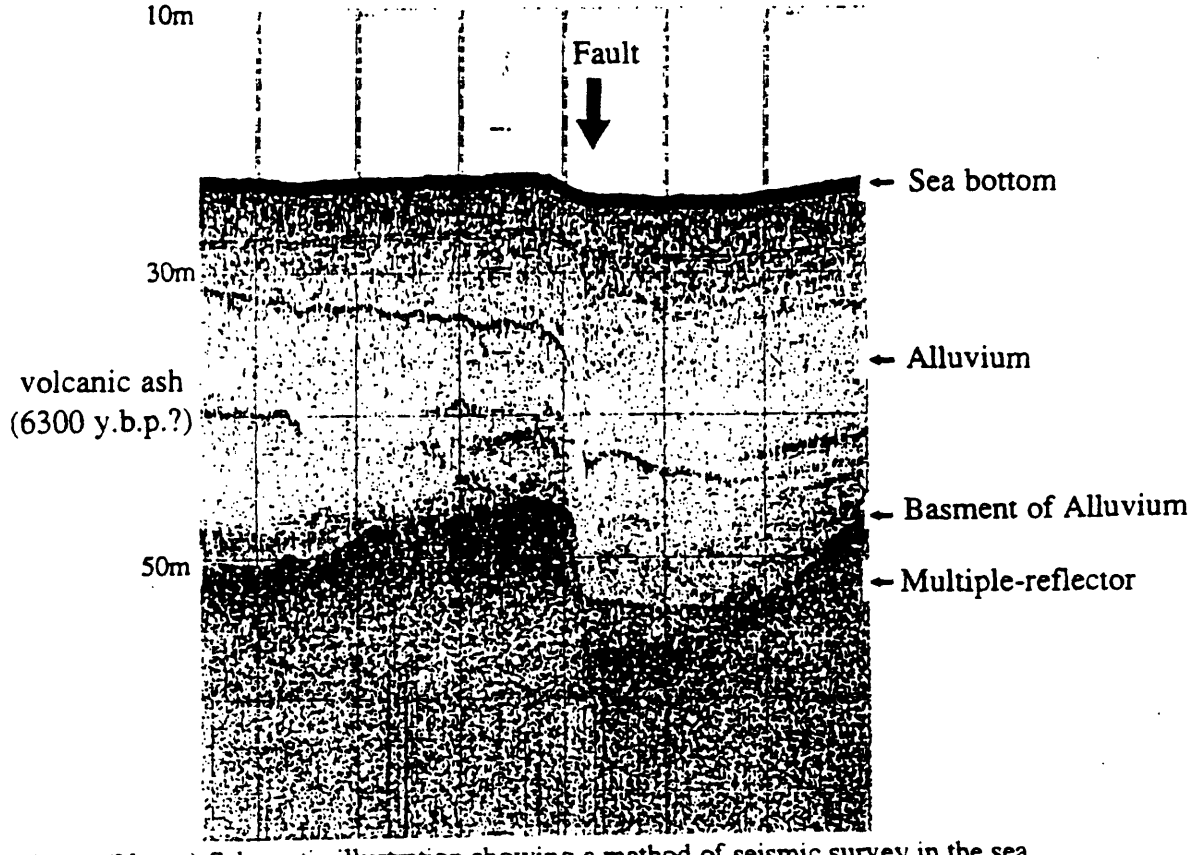

Fig.1 (Upper) Schematic illustration showing a method of seismic survey in the sea .
(lower) and an example of seismic profile of active fault, Median tectonic line off Shikoku.
(Chirp sonar record, frequency:3 to 7 kHz, ping interval: 0.25sec.)

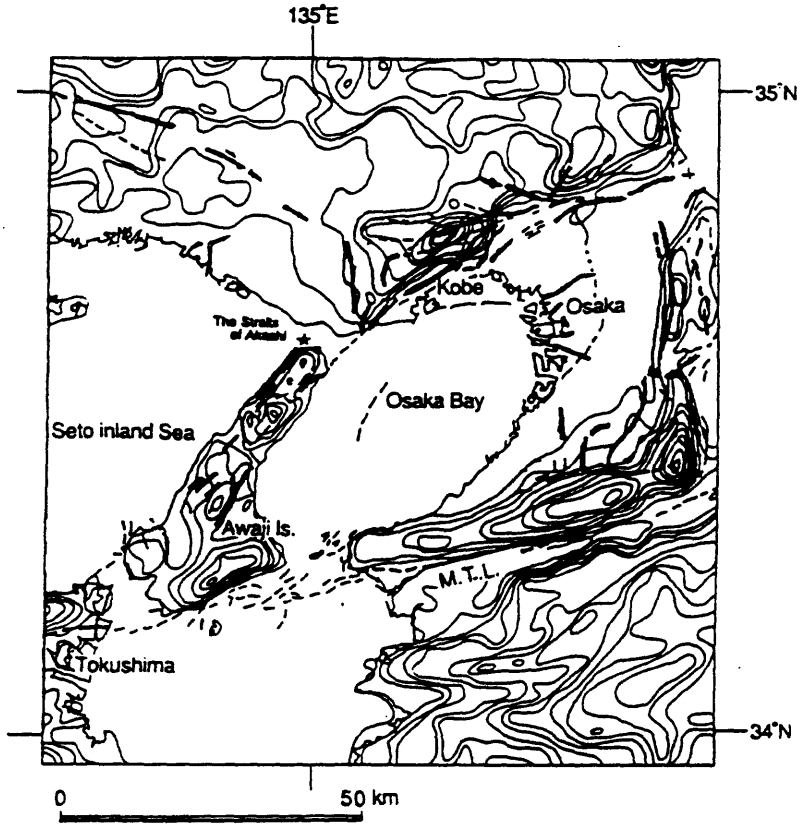

Fig. 2 Distributions of active faults adjacent to the Osaka Bay. (after The Research Group for Active Faults of Japan, 1991).

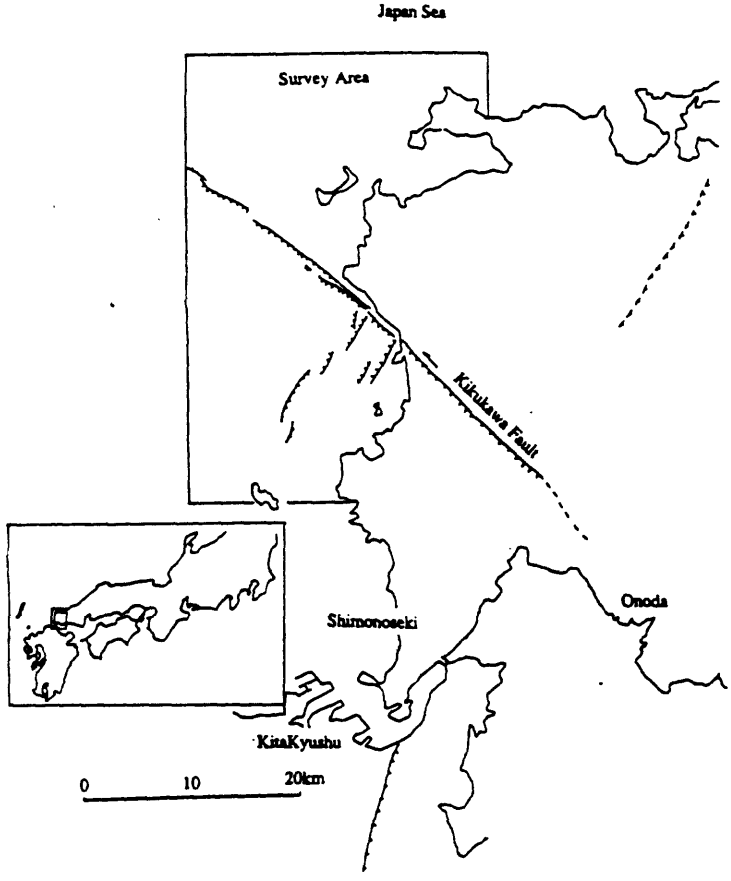

Fig. 3 Kikukawa fault, Southwest Japan. The fault is able to be traced on land toward coastal sea.

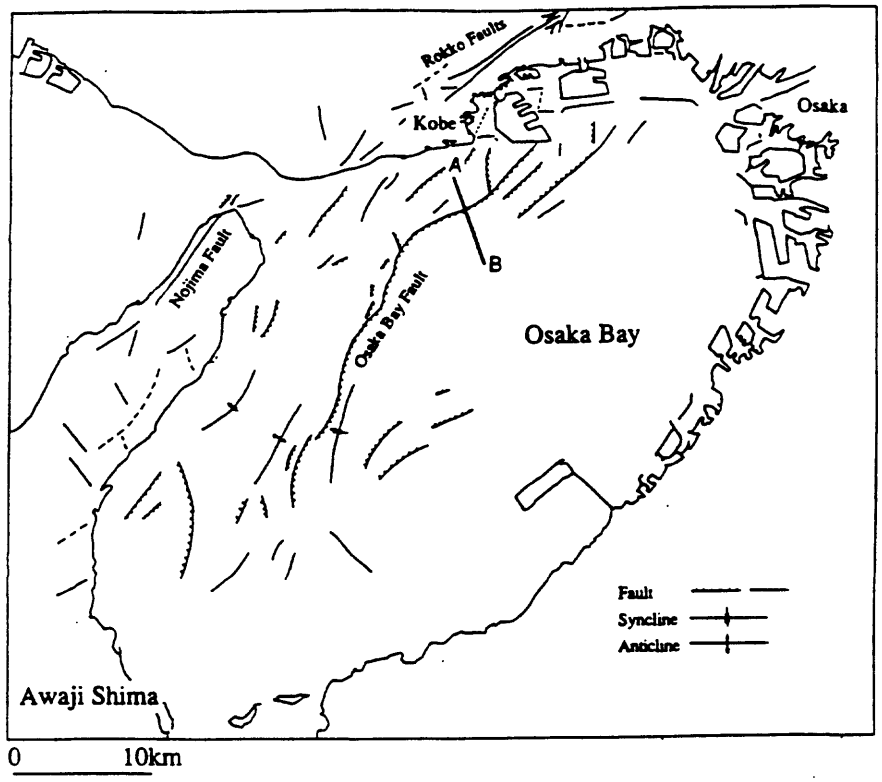

Fig. 4 Distributions of active faults in the Osaka Bay (after Iwabuchi et al., 1995)

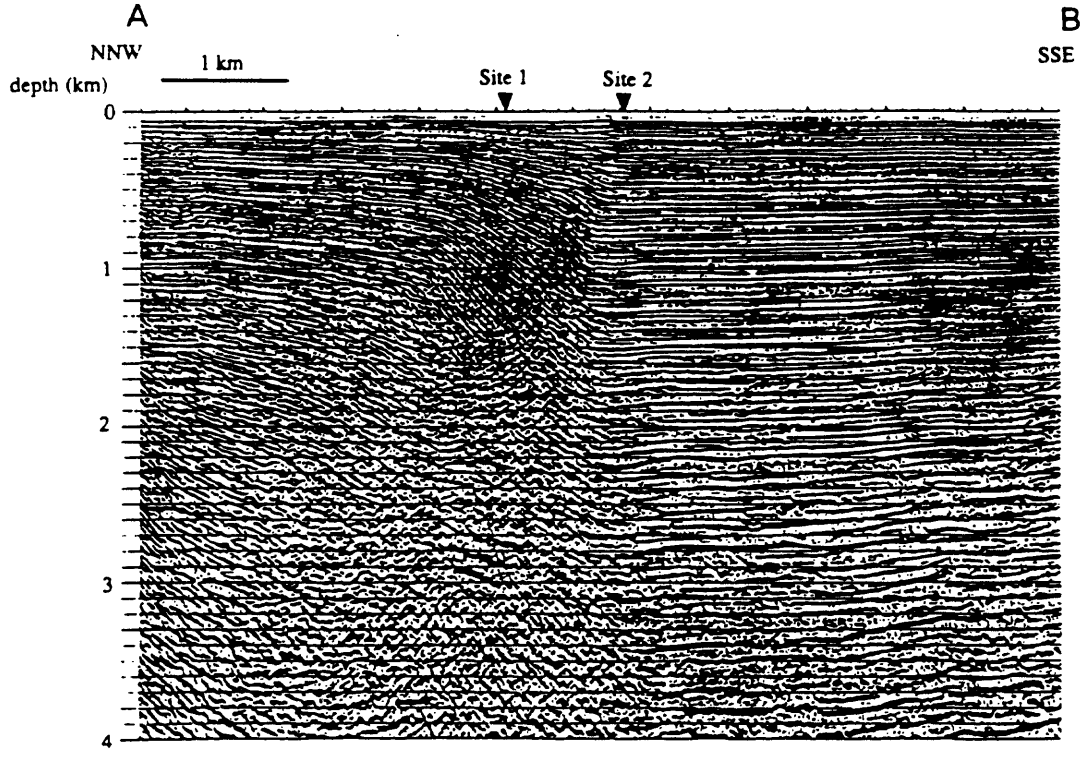

Fig. 5 Multi-channel Seismic profile across Osaka Bay Fault. Triangles show the boring sites.

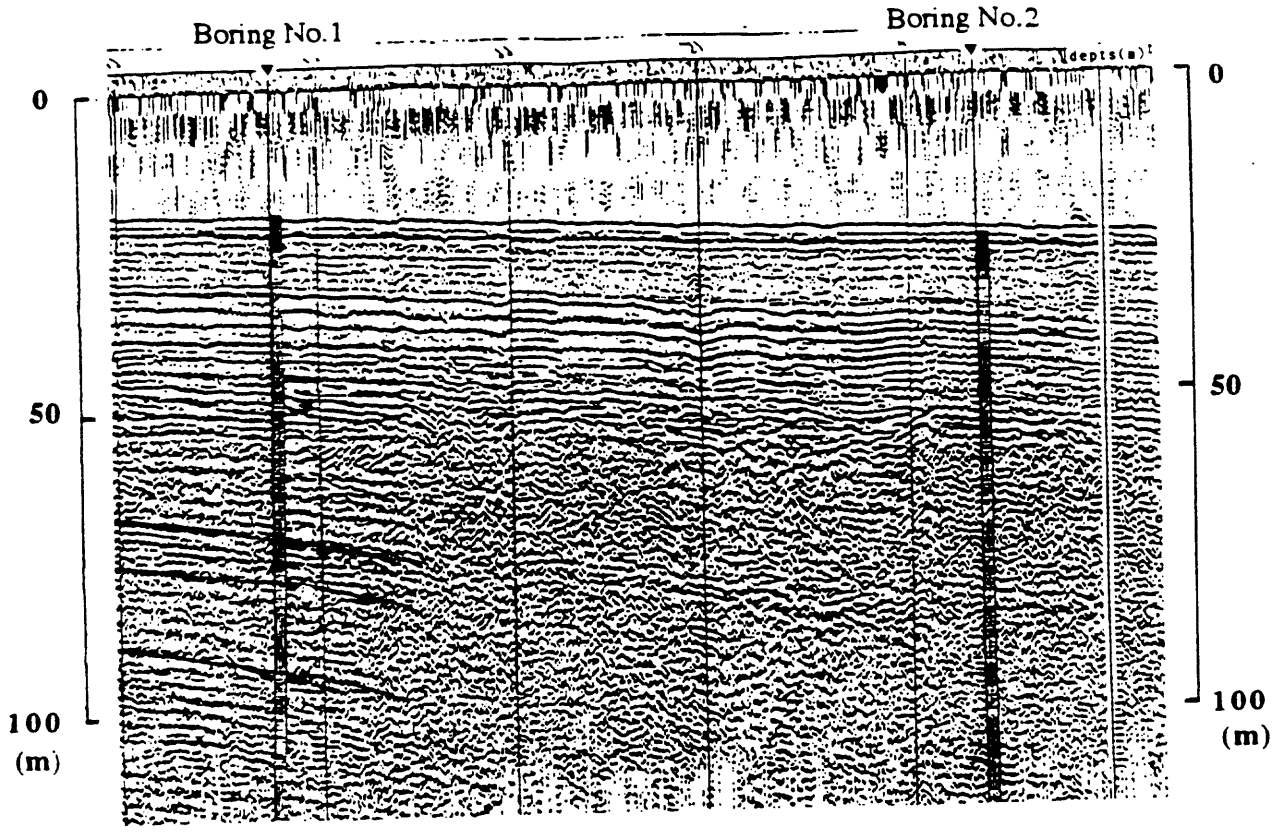

Fig. 6 Seismic profile obtained by a sparker system across Osaka Bay Fault compared with cores at the two boring sites.

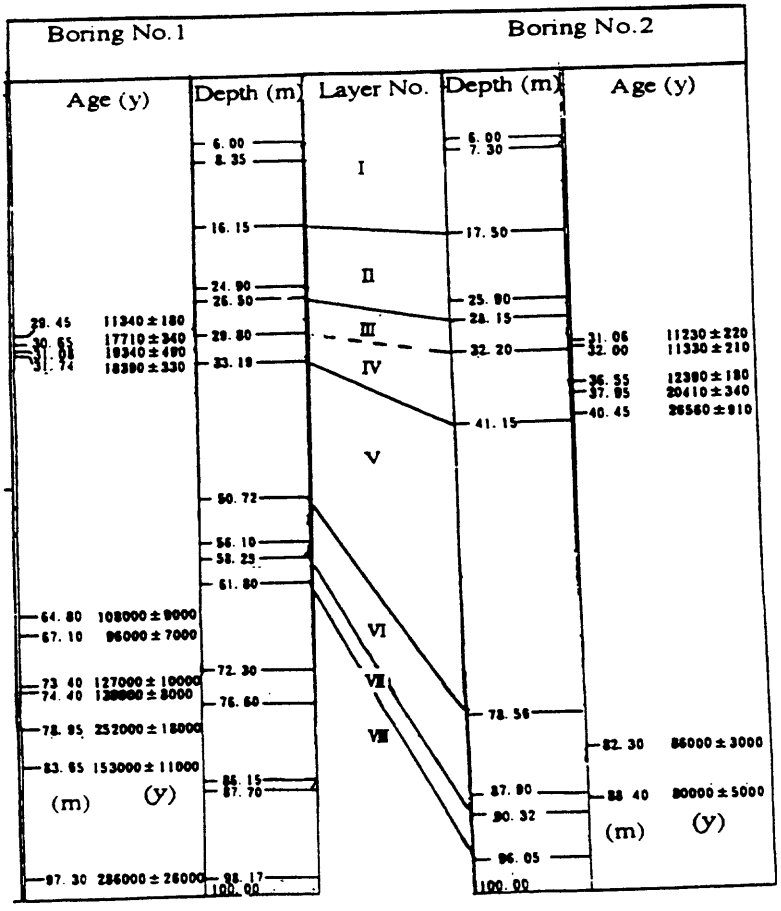

Fig. 7 Tentative results of the boring.

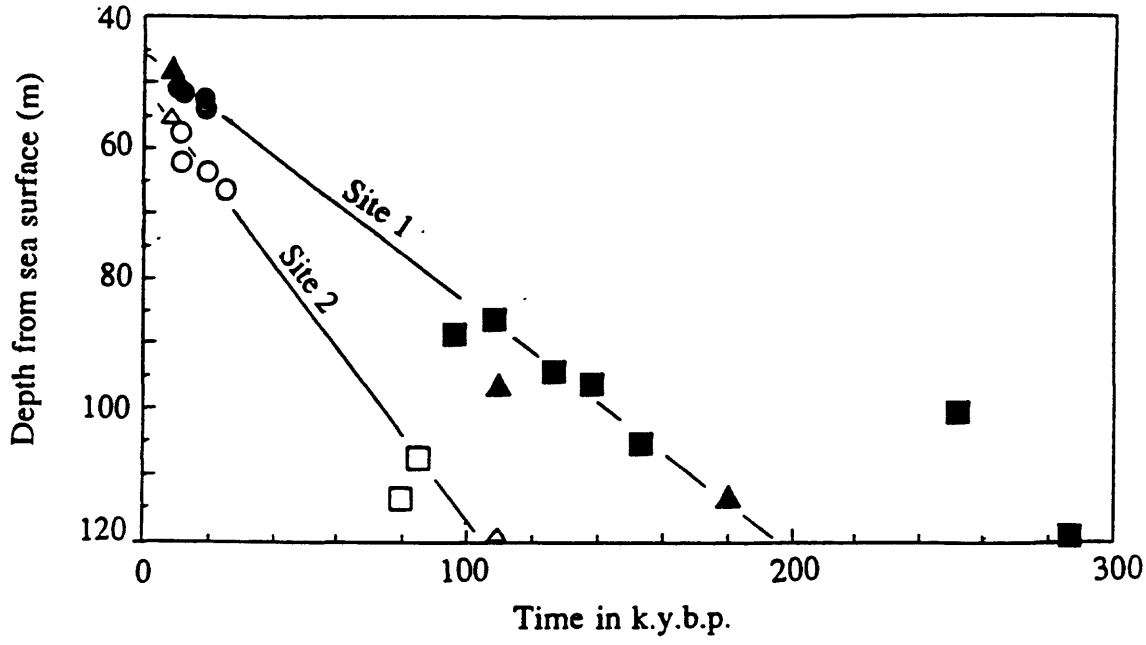

Fig. 8 Core depth and geologic time. Circle : C14 dating, Square : Thermoluminescent dating, Triangle : geomagnetic epoch or excursion, Solid symbols are at the site 1 and open symbols are at the site 2, respectively.

Investigation of earthquake potential - status quo -

Kunihiko Shimazaki
Earthquake Research Institute, University of Tokyo

After the Kobe earthquake of 1995, a shift of emphasis in earthquake prediction program from precursor-oriented research to long-term evaluation of earthquake activity has been accelerated. It is partly due to that the earthquake took place on a previously mapped active fault system. The Sub-Committee for Long Term Evaluation was set up under the Earthquake Research Committee of the Headquarters of Earthquake Research Promotion around the end of 1995. The present task of the sub-committee includes 1) examination of methods of long-term earthquake forecast, and 2) description of the characteristics of damaging earthquakes in various parts of Japan. The first probabilistic estimate of earthquake hazard in Japan is planned to be completed within a few years. The results of GPS and broad-band seismic observation will soon enable us to trace the stress accumulation and release process on quasi-real-time basis, which will be helpful to improve the accuracy of the long-term forecast.

Surface ruptures of the Kobe earthquake found soon after the earthquake, showed the event was generated by reactivation of the Nojima fault on Awaji Island. The active fault belongs to one of seven of elapsed time since the last event to the average recurrence interval. On the other hand almost all the people in the affected area had never thought of a possibility of an earthquake occurrence in their home.

The Sub-Committee for Long Term Evaluation is now preparing a booklet which describes possible damaging earthquakes in each prefecture of Japan. The major target of the writing is for those who work at disaster prevention sections of local governments to understand 'where' and 'how big' earthquake could take place. The probabilistic estimate of earthquake occurrence will partly answer the question of 'when' and needs the result of trench excavation of active faults as well as recurrence data of earthquakes along the subduction zones. The trench excavations are planned to be completed for major hundred fault systems within several years. However the Sub-Committee recognizes that an occurrence of the certain types of earthquakes cannot be evaluated at present. Intermediately deep earthquakes such as the Kushiro-Oki earthquake of 15 January 1993 and intraplate events at the subduction zones such as the Kurile earthquake of 4 Oct 1994 are the examples. Also as for a certain type of earthquakes only a magnitude-frequency distribution can be evaluated within a specified area.

In my personal view, one of major goals of the current trend would be to trace the stress change in the focal region throughout the whole duration of earthquake cycle. Once a working hypothesis of the time-invariant fault strength, which is the tenet of the time-predictable model of earthquake recurrence, is verified, the estimate of stress recovery from the release at the last event would provides us with more accurate long-term forecast of earthquakes.

Integrated Approach to Seismic Hazard Estimation

David D. Jackson
Dept. Earth and Space Sciences
UCLA, Los Angeles, CA 90095-1567
310-825-0421; e-mail: djackson@ess.ucla.edu

The Southern California Earthquake Center has recently estimated seismic hazard for the next thirty years. In this work, we integrate results from geology, geodesy, and seismology to estimate earthquake probabilities. We assume that some earthquakes will occur on known faults, and that others will occur where faults are not now mapped. We combine geology, geodesy and seismology using the principle of conservation of seismic moment. In the simplest approach, we construct three separate seismic hazard models, and then use a linear combination of them to give different weights to the different data. The geologic model assumes that all earthquakes occur on mapped faults, for which the maximum magnitude depends on the fault length, and the rate of occurrence is proportional to the slip rate on the fault. In a geodetic model, we assume that the rate of seismic moment release per unit area is proportional to the maximum shear strain rate, or some other scalar quantity derived from the strain rate tensor. In the seismic model we assume that the rate of future earthquake occurrence is proportional to historical seismicity, weighted inversely proportional to the distance between the site and past events.

Several questions, and sources of uncertainty, arose in previous studies that will require resolution if seismic hazard estimations is to be accurate. Some examples:

1. What causes the complexity of observed ground motion from a given earthquake? Source, path, and site effects each play a role. Observed accelerations or velocities from a given earthquake often differ dramatically over distances of only a few hundred meters. Can these variations be predicted for future earthquakes? Directivity of rupture is certainly important, but is there any way we can predict this effect for future earthquakes? Can strong motion be modeled using existing data from weak motions?

2. What is the magnitude distribution for earthquakes on an individual fault or fault segment? Conservation of seismic moment is a well-accepted principle for relating geologic slip rates to long term earthquake occurrence, but how is the seismic moment apportioned as a function of magnitude? The characteristic earthquake model and the Gutenberg-Richter magnitude distribution appear to be in conflict. The problem of magnitude distribution equates to the problem of what determines the eventual size of an earthquake once it starts. This problem will tax the efforts of observational seismologists, students of rupture dynamics, field geologists, geodesists, and analysts of strong-motion seismic data.

3. How do stress effects of previous earthquakes, tectonic motions, and anelastic relaxation affect future earthquake occurrence? Recent studies showing a correlation of seismicity with stress increments from recent earthquakes imply that recent stress increments are more influential than older ones. This in turn suggests a decaying memory of past stress, which must depend on the rheology of the crust and upper mantle. If older stress decays, what becomes of the time- and slip- predictable models of earthquake occurrence, which assume a linear increase of stress with time? Can observed correlations be used to estimate reliably the short term variations in earthquake probability?

4. How much do the mechanical properties vary along faults? Do major asperities control the rupture characteristics of successive earthquakes on faults, or does each earthquake essentially reset the stress and strength conditions? Do asperities imprint the

geodetic strain field? Can asperities or barriers be recognized from geomorphic, geologic, or geophysical data? Can stress concentrations at barriers explain the apparent triggering of earthquakes at long distances from major earthquakes like Landers? Why is the San Andreas so quiet on that section that broke in 1857, while other faults produce a broader mix of large and small earthquakes? How do geologic variations, curves and bends in faults, and the presence of fault gouge influence both seismicity and wave propagation during rupture?

5. What do fault maps and geodetic strain tell us about future earthquakes? Along subduction zones, faults, strain concentration, and earthquakes all seem to coincide. In more complex zones the correspondence is not so clear. Major California earthquakes of 1872, 1952, 1983, 1992, and 1994 all occurred on slow, minor or unrecognized faults. An adequate geodetic strain map is just coming into focus; does a high strain rate necessarily imply a long-term earthquake likelihood? Which components of the strain rate tensor best indicate earthquake hazard? Finite slip of faults requires finite deformation of the intervening blocks. Thus new faults must be created as a natural consequence of plate boundary deformation.

Promotion of Earthquake Research in Japan

Masanori KOIDE
Director For Earthquake Research Planning
Earthquake Research Division
Research and Development Bureau
Science and Technology Agency
Prime Minister's Office

1. Background of the Headquarters of Earthquake Research Promotion

The Hyogo-ken Nanbu Earthquake which occurred on January 17, 1995, led to the enactment of "Special Measure Law on Earthquake Disaster Prevention," which was established for the purpose of protecting lives and properties of people from disasters caused by earthquakes and was in effect on July 18, 1995.

Based on this law, "The Headquarters of Earthquake Research Promotion" was established in the Prime Minister's Office to promote surveys and researches on earthquakes.

The Headquarters of Earthquake Research Promotion is composed of State Minister for Science and Technology as director and Vice-Ministers of relevant Ministries as members. Under the Headquarters, "Policy Committee" and "Earthquake Research Committee" were organized, which are composed of experts on earthquakes and the staff of relevant Ministries.

The Headquarters of Earthquake Research Promotion and these 2 Committees have following mandates:

1) Formulating comprehensive and basic policies
2) Coordinating administrative works of relevant Ministries
3) Formulating comprehensive survey and observation plans
4) Collecting, analyzing and evaluating the results of surveys and observations
5) Public relations based on the comprehensive evaluation

2. Activities of The Headquarters of Earthquake Research Promotion

The Sub-Committee for Survey and Observation Planning under the Policy Committee formulated the Interim Report Regarding Earthquake Observations and Surveys this January. In this report, 3 items were selected as fundamental observation and surveys in land area, which serve as the basis for understanding and evaluating seismic activities by continuous nationwide observation and surveys, accumulation of basic data and extensive sharing of survey results.

One is the observation of micro earthquakes in land areas, which purpose is to improve accuracy in determining the epicenter of inland earthquakes, to elucidate mechanisms of earthquakes, and to contribute to assess the possible largest inland earthquake. The observation equipment is to be installed at intervals of between 15 to 20 km.

Next is the GPS continuous observation, which purpose is to observe distortion over broad area in order to assess the changes in stress in the earth's crust that trigger earthquakes. The GPS continuous observation stations are to be installed at intervals of between 20 to 25 km through country.

The third is the survey of active faults. In order to make long-term predictions of inland earthquakes, it is necessary to clarify the location and history of active fault, the faults' length, and the degree of displacement, in detail. Surveys should emphasize faults with a high level of activity.

Based on the interim report, The Headquarters of Earthquake Research Promotion executes development of the fundamental earthquake research system such as micro-earthquake observation, observation of crustal movements with GPS, etc., and promotion of surveys on about one hundred major active faults existing in Japan. The results of these observations and surveys are analyzed and evaluated by the Earthquake Research Committee.

The Policy Committee is also formulating comprehensive and fundamental plans for earthquake researches and observations spanning 5 to 10 years.

In addition to these activities, the Policy Committee is engaged in

discussing the public relations about seismic activities and coordinating the budget of relevant Ministries for earthquake research.

On the other hand, the Earthquake Research Committee, which is held monthly, analyzes and evaluates seismic activities throughout Japan. When an earthquake occurs, and if judged necessary, an emergency meeting of the Earthquake Research Committee will be held, and the results of the analyses and evaluation will be explained to the local government, etc.

The Sub-Committee for Long Term Evaluation was established under the Earthquake Research Committee in order to evaluate the possibility of earthquake activities in a long term. The Sub-Committee has two mandates, to extract the characteristics of seismic activities and to evaluate possibility of earthquake occurrence in a long term. Now, the Sub-Committee is investigating the quantitative evaluation method of possibility of earthquake occurrence.

The Panel on Active Faults and the Panels for Regional Seismic Activities were established under the Sub-Committee. The Panel on Active Faults is evaluating each active fault and extracting some parameters for the evaluation of possibility of shallow inland earthquake occurrence. Three Panels for Regional Seismic Activities, for Northern-Japan, Central-Japan and Western-Japan, are extracting characteristics of regional seismic activities.

3. Present topics of the Headquarters of Earthquake Research Promotion

As stated above, the Headquarters of Earthquake Research Promotion is presently formulating comprehensive and fundamental plans for earthquake researches and observations. The plans will be reported in early 1997. Based on the plans, the earthquake research activities will be further developed in Japan.

The Headquarters of Earthquake Research Promotion is also engaged in extracting the characteristics of regional seismic activities in Japan which will be reported in early 1997. The result will contribute to the evaluation of the possibility of earthquake activities in a long term.

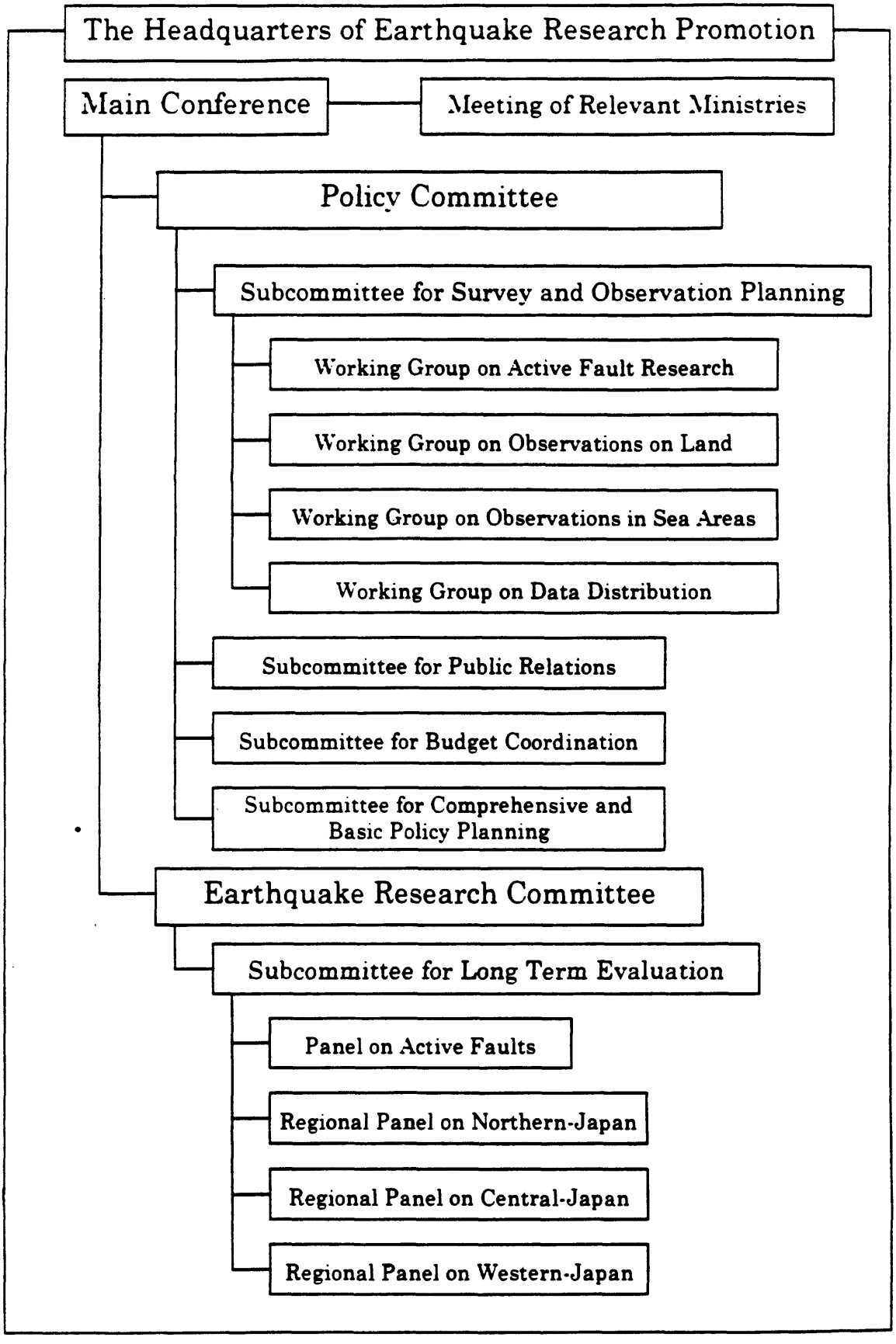
The Headquarters of Earthquake Research Promotion
Main Conference
Meeting of Relevant Ministries
Policy Committee
Subcommittee for Survey and Observation Planning
Working Group on Active Fault Research
Working Group on Observations on Land
Working Group on Observations in Sea Areas
Working Group on Data Distribution
Subcommittee for Public Relations
Subcommittee for Budget Coordination
Subcommittee for Comprehensive and Basic Policy Planning
Earthquake Research Committee
Subcommittee for Long Term Evaluation
Panel on Active Faults
Regional Panel on Northern-Japan
Regional Panel on Central-Japan
Regional Panel on Western-Japan

Promotion of Earthquake Research in Japan

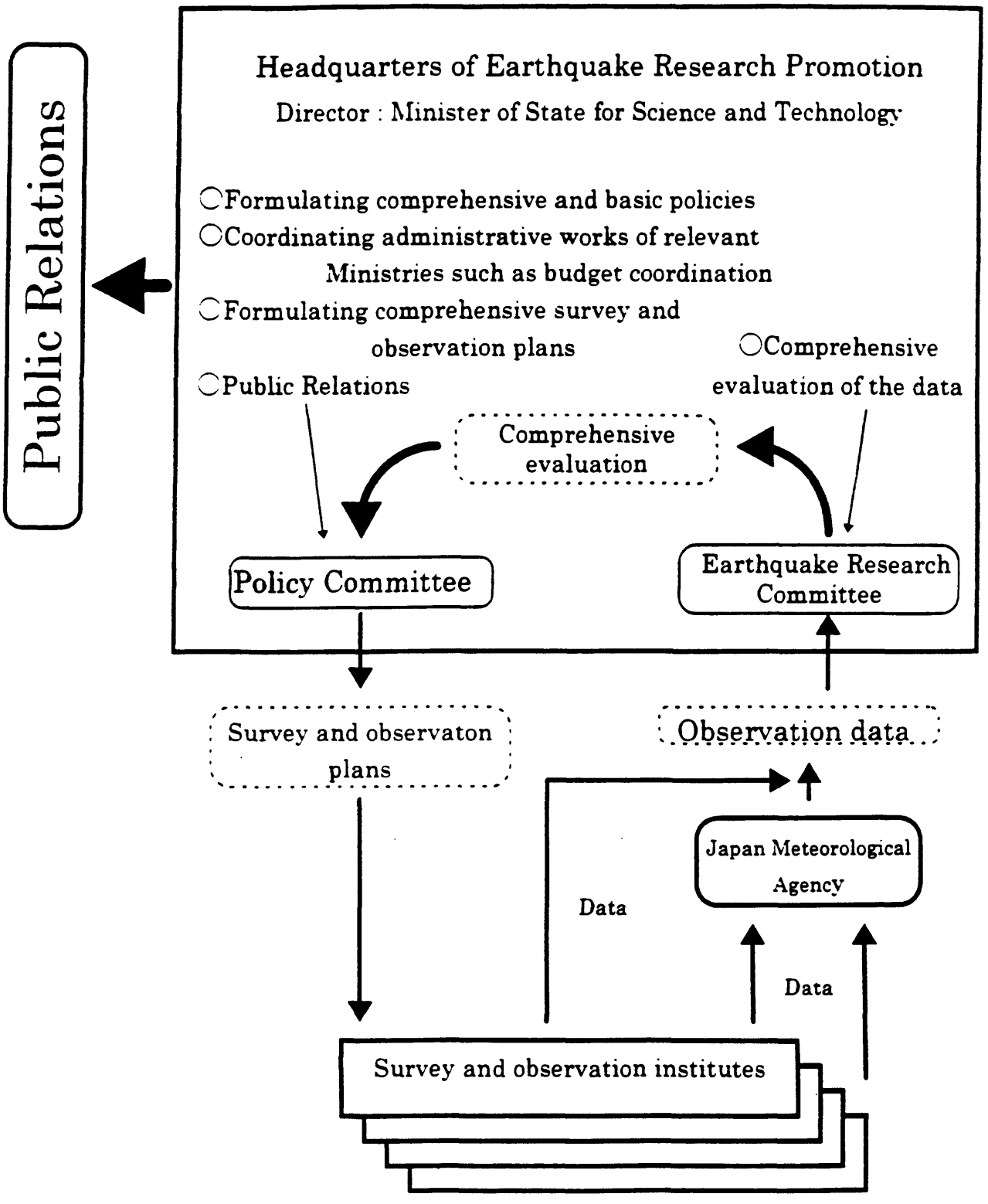

US-Japan Joint Collaborations in Natural Disaster Reduction

Noel Raufaste
NIST, Gaithersburg, MD 20899
E-mail: noel.raufaste@nist.gov
BFRL Home Page -- http://www.bfrl.nist.gov

A survey was performed of joint collaborations between the U.S. and Japan in the area of natural disaster reduction. The survey revealed there is some, but limited, documented information available on U.S.-Japan joint collaborations in natural hazard reduction. This information identified three programs: 1. U.S.-Japan Common Agenda for Cooperation in Global Perspective (CA); 2. U.S. Japan Program on Natural Resources (UJNR) with three Panels focused on natural hazard reduction, Panel on Wind and Seismic Effects, Panel on Fire Research and Safety, and Earthquake Prediction Technology; and 3. Japan-United States Science and Technology Agreement (JUST) with two activities relate to natural disaster reduction: 1. Workshops on Natural Disaster Reduction and 2. Highway Science and Technology Program (HSTP). The three UJNR Panels demonstrated the greatest benefit to development and implementation of technologies for both countries. These programs are the oldest and benefit from active support by the participating members' agencies and from their participating NGOs. The Common Agenda collaborations under its Research Cooperation in Construction Technology has shown much progress for making major contributions to advancing the state of technology. Some of their work has been advanced through joint cooperation under the auspices of the UJNR Panel on Wind and Seismic Effects. Also, the newly approved, April 1996, bilateral initiative on Natural Disaster Reduction is focused on furthering means to increase methods aimed at disaster reduction. The Japan-U.S. Science and Technology Agreement has demonstrated progress through the Highway Science and Technology Program. The JUST Workshops on Natural Disaster Reduction has revealed little documentation to effectively assess its benefits. Both the JUST and CA are young and have not had the time to demonstrate quantified impacts. Since there is much information exchanges between U.S. and Japanese universities, a new cooperative program may be considered on U.S. Japan Collection of University Research in Earthquakes (UJCURE) to capture the cooperative research underway and to stimulate joint university research. The UJCURE may need to be linked to one of the formal U.S.-Japan cooperative programs for constancy.

Testing Fundamental Theories of Earthquake Mechanics Through Fault Zone Drilling

Stephen Hickman[1], Mark Zoback[2] and William Ellsworth[1]

[1]U.S. Geological Survey, 345 Middlefield Rd., MS 977, Menlo Park, CA 94025
[2]Dept. of Geophysics, Stanford University, Stanford, CA 94305

Abstract

We propose to conduct a collaborative U.S.-Japanese scientific pilot drilling project into the San Andreas fault zone at relatively shallow (~2.5 km) depth. The scientific rationale for this project is to provide direct observational data on the composition, physical and chemical state and behavior of a major active fault zone and to test and constrain a diverse and continually expanding spectrum of hypotheses pertaining to faulting and earthquake generation. By conducting such a project we can carry out comprehensive investigations of physical and chemical processes going on within an active fault zone; we can examine, in detail, recovered fault gouge and fluids to better understand the deformational properties of major fault zones; and we can utilize the borehole for long-term in situ monitoring of an active fault zone where a moderate (M ~ 6) earthquake is expected in the next few years. We believe, as do the many scientists who have participated in planning this project, that the data we propose to collect is essential to better understand the active processes controlling faulting along major plate boundaries and that enhanced understanding of the physics of faulting will contribute appreciably to earthquake hazard reduction efforts in the U.S., Japan and around the world.

Introduction

After decades of intensive research, numerous fundamental questions about the physical and chemical processes acting within the San Andreas and other major plate-boundary faults remain unanswered. We do not know the composition or properties of fault zone materials at depth nor the constitutive laws which govern fault behavior. We have no direct knowledge of the stress and strain conditions under which earthquakes initiate or propagate. Although it is often proposed that high pore fluid pressure exists within the San Andreas fault zone at depth and that variations in pore pressure strongly affect fault behavior, these hypotheses are unproven and the origin of overpressured fluids, if they exist, is unknown. As a result, a myriad of untested and unconstrained laboratory and theoretical models related to the physics of faulting and earthquake generation fill the geophysical literature. For the past several years, we have been coordinating the efforts of several hundred scientists from the United States and abroad who propose to address these and other issues by conducting in-situ measurements, sampling and long-term monitoring directly within the San Andreas fault zone at depths up to 10 km.

As the first step toward our ultimate goal of drilling deeply within the San Andreas fault, we are proposing to continuous core an inclined "pilot" borehole through the San Andreas fault zone at a depth of about 2.5 km. As there are strong arguments in favor of locating the 10-km hole along a section of the San Andreas that is locked and likely to produce great earthquakes, we propose drilling the pilot hole where the fault is currently slipping through a combination of small-to-moderate earthquakes and fault creep. By targeting an "active" patch of the fault, the pilot experiment would allow us to address a number of important issues related both to the physics of earthquake rupture nucleation and propagation and to the transition from creeping to locked fault behavior. Also, we can use the seismicity to tell us the precise location of the active trace of the fault where it is penetrated by the borehole – an important parameter in interpreting data and samples obtained through the fault zone. This experiment would also achieve two other important objectives. First, it would enable us to obtain direct information on the structure, composition and

physical properties of the fault at intermediate depth. This information would improve current knowledge tremendously and greatly facilitate development of a comprehensive science plan for the deep hole. Second, it makes it possible to identify and begin dealing with the technical problems of drilling, coring, casing, downhole measurements and long-term monitoring that will be encountered in the deep hole.

We recently submitted a proposal for Pilot Fault Zone Drilling Project to the U.S. National Science Foundation, with additional support sought from the U.S. Geological Survey and the U.S. Department of Energy. We also submitted supplementary proposals to the International Continental Drilling Program (ICDP) and the U.S.-Japan Earthquake Disaster Mitigation Partnership. The ICDP proposal requested support in the form of project engineering and supervision; on-site analysis of core, cuttings and fluids; and data management. The U.S.-Japan Proposal sought joint funding of the Parkfield Pilot Project and arose out of an initiative by the White House Office of Science and Technology Policy and Japan's Science and Technology Agency to create a bilateral program in earthquake hazard reduction.

Site Selection for the Pilot Drilling Project

To identify potential sites for the pilot hole we conducted a systematic search of strike-slip faults in California, identifying all faults exhibiting shallow seismicity. We then convened a workshop on the scientific goals, experimental design and site selection for the pilot hole at the USGS in Menlo Park that was attended by about 45 people. Although several candidate sites along the Hayward and San Andreas faults were considered, it became clear that San Andreas fault at Middle Mountain, near the town of Parkfield, was the best place to conduct this experiment because: 1) Surface creep and abundant shallow seismicity allow us to accurately target the subsurface position of the fault. 2) There is a clear geologic contrast across the fault, with shallow granitic rocks on the west side (which provide for good drilling conditions) and Franciscan melange on the east. 3) As a consequence of the Parkfield Earthquake Prediction Experiment, the geological and geophysical framework of this segment of the fault is well-established and this site is centered within the most heavily instrumented part of a major plate-bounding fault anywhere in the world.

Beginning in the summer of 1994, members of the Site Selection Working Group for the San Andreas Pilot Project conducted a number of relatively small-scale and detailed geophysical investigations to fill critical gaps in our knowledge about subsurface structure and microearthquake locations at the Parkfield site (see Figure 1a). A temporary seismic network was installed on and around Middle Mountain to calibrate crustal structure and study fault-zone guided waves near the proposed drill site. This experiment included deployment of temporary seismic stations (to augment the permanent local networks), three chemical shot points and a 10-station REFTEK array crossing the surface trace of the San Andreas. Additionally, a small-scale seismic reflection survey was conducted along two 2-km-long orthogonal lines southwest of the San Andreas fault. The purpose of this survey, which employed a single vibroseis energy source and 128 receivers per line, was to determine the thickness of Tertiary sediments beneath the proposed drilling site. A continuous magnetotelluric profile was also conducted at Middle Mountain to determine the electrical conductivity structure of the fault zone and its surroundings. Finally, detailed geologic mapping helped to ascertain the geometry and recent faulting history near the Parkfield drill site.

Experimental Design, Scientific Goals and Timetable for the Pilot Project

Two phases of drilling are envisioned for the Pilot Project: rotary drilling and spot coring of a mostly vertical hole, followed by continuous coring through the fault zone (Figure 1b). The drill site will be located sufficiently far from San Andreas fault (as determined by surface fault creep, microearthquake locations and magnetotelluric imaging) to allow for continuous coring through the entire fault zone starting at a vertical depth of about 1.5 km and continuing until relatively undisturbed country rock is reached on the far side of the fault. In addition to exhumation of fault

zone rock and fluids for laboratory analyses and rheological studies, downhole measurements of stress, permeability and other parameters and long-term monitoring are planned within and adjacent to the active fault zone. Monitoring experiments will include near-field, wide-dynamic-range seismological observations of earthquake nucleation and rupture and continuous monitoring of variations in pore pressure, temperature and crustal deformation during the earthquake cycle.

Although the 2.5-km pilot hole is not deep enough to answer many of the scientific questions about the physics of faulting that are driving the deep drilling project, it would allow us to address a number of first-order questions related to fault mechanics:

- *What are the mineralogy, deformation mechanisms and constitutive properties of the fault gouge?* Why does the fault creep? What are the strength and frictional properties of recovered fault rocks at realistic in-situ conditions of stress, fluid pressure, temperature, deformation rate and pore fluid chemistry? What do mineralogical, geochemical and microstructural analyses reveal about the nature and extent of water-rock interaction?

- *What is the fluid pressure and permeability within and adjacent to the fault zone?* Do superhydrostatic fluid pressures exist within the fault zone and through what mechanisms are these pressures generated and/or maintained? How does fluid pressure vary during deformation and episodic fault slip (creep and earthquakes)? Do fluid pressure compartments exist at shallow depths and, if so, what is the nature of the seals between compartments?

- *What are the composition and origin of fault-zone fluids and gasses?* Are these fluids of meteoric, metamorphic or mantle origin (or combinations of the three)? Is fluid chemistry relatively homogeneous, indicating pervasive fluid flow and mixing, or heterogeneous, indicating channelized flow and/or fluid compartmentalization?

- *How do stress orientations and magnitudes vary across the fault zone?* Are the principal stress magnitudes higher within the fault zone than in the adjacent country rock, as predicted by some theoretical models? What is the strength of the shallow creeping portion of the San Andreas and how does this compare with depth-averaged strengths inferred from heat flow and far-field stress directions? What do spatial variations in stress tell us about the extent of shear localization and secondary fault slip?

- *How do earthquakes nucleate?* Does seismic slip begin suddenly or do earthquakes begin slowly with an acceleration of fault slip with time? Do the size and duration of this precursory slip episode, if it occurs, scale with the magnitude of the eventual earthquake? Are there other precursors to an impending earthquake, such as pore pressure changes, anomalous fluid flow, crustal strain changes or electromagnetic signals?

- *How do earthquake ruptures propagate?* Do earthquake ruptures propagate as a uniformly expanding crack or as a "slip pulse"? What is the effective (dynamic) stress during faulting? How important are processes such as shear heating, fault-normal opening modes and acoustic fluidization in lowering the dynamic frictional resistance to rupture propagation?

- *How do earthquake source parameters scale with magnitude and depth?* What is the minimum size earthquake that occurs on the fault? How is the long-term energy release rate at shallow depths partitioned between creep dissipation, seismic radiation, dynamic frictional resistance, chemical reactions and grain size reduction (i.e., by integrating fault zone monitoring with laboratory observations on core)?

- *What are the physical properties of fault-zone materials and country rock (seismic velocities, electrical resistivity, density, porosity, etc.)?* How do they vary with position across the fault zone and with distance away from the borehole (i.e., depth of investigation)? How do physical properties determined from core samples and wireline logs compare with properties inferred from surface geophysical observations?

- *What processes control the localization of slip and strain rate?* Are the fault surfaces defined by background microearthquakes and creep the same? Would the active slip surface be recognizable (through core analysis and downhole measurements) in the absence of seismicity and/or creep? By comparing observations on core with results from fault zone monitoring, can we identify microstructures characteristic of rapid (i.e., seismic) slip.

Our plan is for the Parkfield Pilot Project to last 5 years. Engineering, detailed planning and fabrication of a special coring string will be conducted in the first year. The rotary drilling phase of the project will be carried out in the second year, during which directional drilling techniques will be used to deviate the hole toward the fault zone at an angle of about 45°. Continuous coring through the fault zone and downhole measurements (before and after casing is cemented into the borehole) will occur in year 3. Years 4 and 5 will be used to finalize downhole measurements, analyze rock and fluid samples and install equipment for long-term fault zone monitoring. Development and testing of the fault-zone monitoring system will be spread out over the entire 5-year period.

Summary

Our ultimate goal of preventing earthquake disasters fundamentally depends on improved understanding of the earthquake source. By deep drilling and experimentation within the San Andreas fault zone, we would revolutionize our understanding of earthquake generation by obtaining direct information on the composition and mechanical properties of fault zone rocks, the nature of the forces responsible for earthquake rupture, the role of fluids in controlling earthquake recurrence, and the physics of rupture propagation. Moreover, although it has been hypothesized that a wide range of deformation processes precede failure, they have not yet been detected by surface measurements. By making continuous observations within the fault zone at seismogenic depths, we will be able to directly test and extend current theories about phenomena that might precede an impending earthquake. As the first stage in a longer-term program of deep (up to 10 km) drilling within the San Andreas fault zone, we are currently proposing to conduct a 2.5-km-deep pilot drilling experiment at Parkfield, California.

Smaller scale fault zone drilling projects are now underway along intraplate faults in Japan, most notably an ongoing multi-agency effort of scientific drilling along the Nojima fault (the fault responsible for the 1995 Kobe earthquake), as well as a shallow drift excavation through an active fault at Atotsugawa. Thus, it makes both scientific and economic sense to seek ways to combine these national efforts. An aggressive, bilateral program of fault zone drilling and experimentation would represent a major advance in pursuit of a rigorous scientific basis for earthquake hazard reduction. For example, understanding the intrinsic strength of fault zone rocks and the role of fluid pressure and chemical reactions in controlling fault strength will lead to improved intermediate-term earthquake forecasts and more realistic models of the seismic cycle. Near-field observations of the earthquake rupture process, including such effects as fault-zone dilation and short-term changes in fluid pressure, will lead to improved predictions of strong ground motions and more reliable models for rupture propagation and arrest. These latter processes are believed to control earthquake size (i.e., whether or not a small earthquake will grow into a large one) and, hence, are crucial to long-term assessments of earthquake hazard. Direct observation of the nucleation process of an earthquake will determine if earthquakes are preceded by accelerating fault slip and/or changes in fluid pressure. This will allow us to determine if short-term earthquake prediction is possible and, if so, how it might be accomplished.

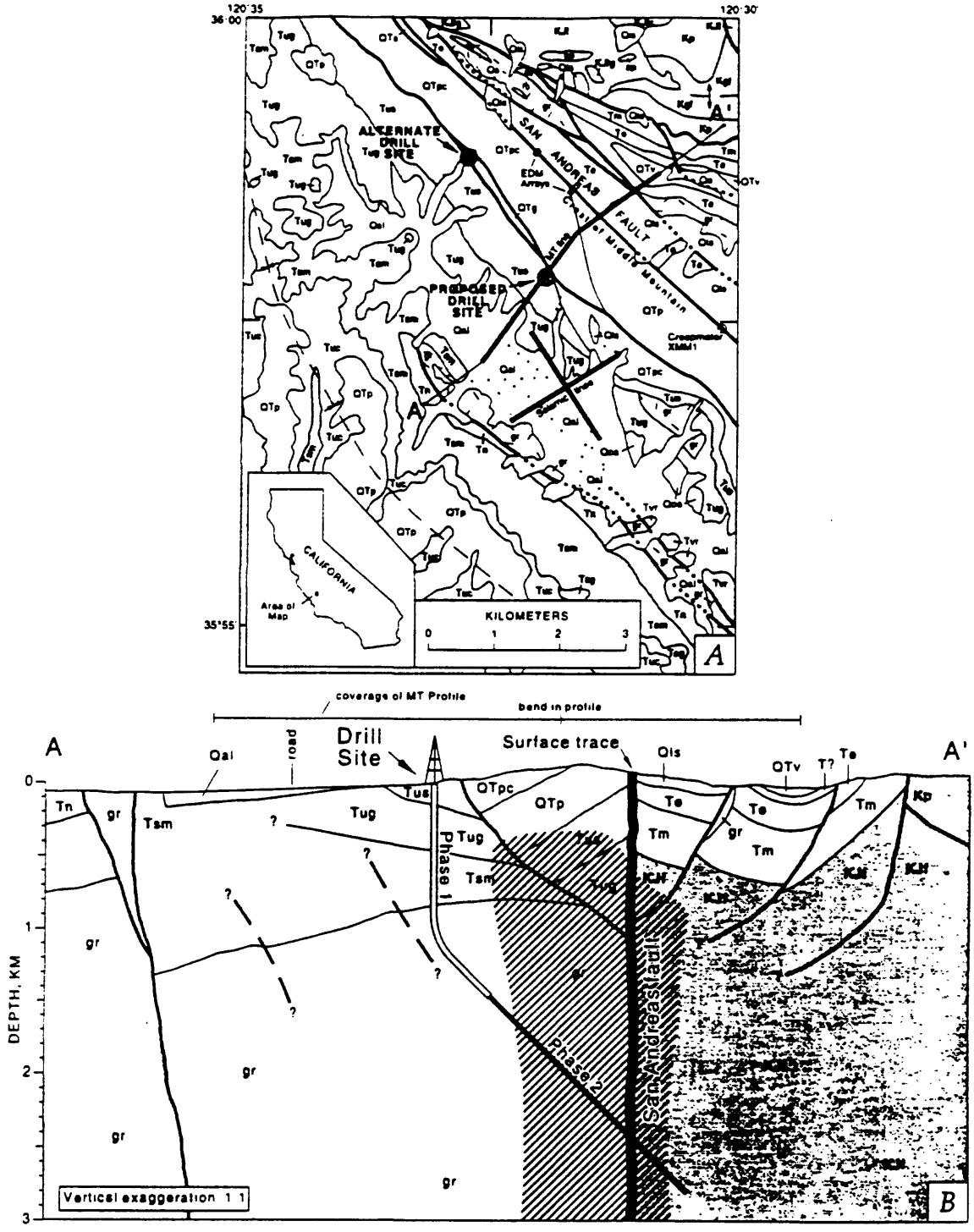

Figure 1: (A) Geologic map of the Parkfield site, showing seismic reflection lines, 1-2 km south of the proposed drill site, and a magnetotelluric (MT) profile, through the site and crossing the San Andreas fault, conducted as part of site characterization for the pilot project. Also shown are geodetic (EDM) arrays and a creepmeter defining the creeping surface trace of the San Andreas fault. (B) Cross section along A-A', schematically showing the proposed drill hole, where Phases 1 and 2 refer to the rotary drilled and continuously cored sections of the hole, respectively. The contact between Tertiary marine sediments (Tsm) and the underlying granitic basement (gr) was determined from the seismic reflection profiles shown in A (Peter Malin, written comm., 1995). The Franciscan mélange is denoted by KJf. The hypothetical location of the actively slipping fault surface, obtained through downward continuation of the creeping surface trace of the San Andreas fault, is shown as a heavy vertical line. The hachured region denotes a zone of extremely low resistivity (< 5 Ohm-m) determined from the MT profile shown in A (Martin Unsworth, written comm., 1996). This broad zone, presumably representing highly fractured and/or altered rock comprising the overall fault zone, makes continuous coring over an appreciable distance necessary.

Structure and Physical Properties of the Nojima Fault

Hisao Ito

Geological Survey of Japan, 1-1-3, Higashi, Tsukuba, Ibaraki 305 Japan

ABSTRACT

Direct observation of physical and chemical processes operating within the fault zone by active fault drilling is essential to improve our understanding of kinematics of the fault system and to advance in earthquake hazard assessment and reduction. The active fault drilling at Nojima Hirabayashi after the 1995 Hyogoken-nanbu earthquake provided us a unique opportunity to investigate subsurface fault structure and in-situ properties of the fault.

After the 1995 Hyogoken-nanbu earthquake , we installed seismometer array at Nojima Hirabayashi, where the maximum right-lateral slip was observed, and observed guided waves trapped in the Nojima fault. The results show that the width of the Nojima fault (about 30 m) is narrower than that of the Landers (180 m) estimated from the trapped wave analysis. This is consistent with relatively high peak frequency of the phase compared with that of the trapped waves observed at the Landers fault zone. The present array at Nojima Hirabayashi does not observe trapped wave for the earthquakes under the Kusumoto fault. This implies these two faults are independent. The present array observation suggests that the Nojima fault seems to continue far southward than observed at surface.

We drilled a 747 m deep borehole at Nojima Hirabayashi to penetrate the Nojima fault. The drill site is 74.6 m apart from the surface trace of the surface break. Cores were recovered for almost entire depth interval from 150 m to 746.6 m. The stratigraphy of the well is granodiorite from the surface. The fault zone is characterized by altered and deformed granodiorite from 490 m to 746.6 m (shear zone), with fault gouge at 623.3 m to 625.1 m. The shear zone has low resistivity, low density, low velocities (both P and S wave: more than 50% decrease at the fault gouge), high porosity, and high Vp/Vs. The borehole observations also revealed fine structure of the Nojima fault that corresponds to the changes in the degree of deformation within the shear zone, and the degree of deformation is very different between the footwall and hanging wall of the Nojima fault. The width of the shear zone from the drilling result (core inspection) is consistent with that estimated from the surface trapped wave observations. This shows a good correlation between *in-situ* physical properties measured in boreholes with remote geophysical observations.

Permeability distribution in the well were evaluated from the acoustic waveforms. There are

several permeable intervals in the shear zone, especially below the fault gouge. The fast shear azimuth derived from the cross dipole shear acoustic waveforms changes at the fault. The changes in fast shear azimuth are much more pronounced near the fault, which suggests a strong influenceence of the fault.

INTRODUCTION

Among the numerous key questions concerning the structure and properties of the active faults, the following information will be obtained only by direct observations with active fault drilling (Hickman et al., 1994);

- What are the principal deformation mechanisms and constitutive properties of the fault gouge?
- What is the fluid pressure and permeability within and adjacent to the fault zone?
- What is the composition and origin of the fault gouge and fluids?
- How do stress orientation and magnitudes vary across the fault zone?
- What are the physical properties (seismic velocities, density, porosity, electrical resisitivity, etc.) of the fault zone materials and country rock? What is the width of the fault zone?

It is also important to know how well and in what manner do ***in-situ*** physical properties measured in boreholes correlate with remote geophysical observations.

TRAPPED WAVE

After the 1995 Hyogoken-nanbu earthquake (Ms = 7.2) on January 17, 10.5 km long distinguished surface breaks of the Nojima fault in Awaji island appeared (Fig. 1; Awata et al., 1996). From the observation of aftershocks of the 1995 Hyogoken-nanbu earthquake with seismometer array deployed perpendicular to the Nojima fault at Nojima Hirabayashi, where maximum right-lateral slip of 1.9 m was observed, we have observed distinct low frequency phase (the peak frequency is about 5 Hz) following the S wave only for the stations close to the fault surface break (Ito and Kuwahara, 1996). The stations that are apart more than 40 m from the surface break did not show this low frequency phase. We estimated the subsurface width of the Nojima fault is several tens of meters, because the low frequency phase is observed only for the station less than 40 m apart from the fault surface break.

We have also found that this low frequency phase was observed only for the earthquakes occurred along the Nojima fault (Fig. 2). These strongly suggest that this low frequency phase after

S wave is fault related trapped waves (Li and Leary, 1990; Li et al., 1994a, 1994b) .

Then we decided to drilled a hole to penetrate into the Nojima fault at Nojima Hirabayashi, where we observed fault related trapped waves, in order to compare the fault width estimated from the trapped wave observation with the drilling results. We also obtained the logging data and conducted borehole experiments to determine *in-situ* physical properties of the fault zone.

DRILLING INTO THE NOJIMA FAULT

We drilled a 750 m deep borehole at Nojima Hirabayashi to penetrate into the Nojima fault (Fig. 3). The drill site is 74.6 m apart from the surface trace of the surface break. Cores were recovered for almost entire depth interval from 150 m to 746.6 m. The stratigraphy of the well is granodiorite from the surface. We found fault gouge from 623.3 m to 625.1 m depth. If we assume a straight plane between the surface outcrop of the fault and the fault gouge in the borehole, the dip of the fault is about 84 degrees. This is consistent with that estimated from the shallow seismic reflection survey.

LOGGING RESULTS

We conducted caliper, electrical resistivity, density, neutron, gamma ray, micro resistivity and temperature logging (Fig. 5). The main shear zone observed by core inspection is characterized by low electrical resisitivity , low density and high porosity. They gradually decrease towards the depth of fault gouge of 623.5 m to 625.4 m. The fault gouge at 623.3 m to 625.1 m has extremely low electrical resistivity of about several tens of ohm - m.

The gamma ray results show high values between 500 m and 620 m, and shows different behavior above and below the fault gouge. This is consistent with the core inspection results that the degree of alteration is high in the upper part of the main shear zone.

VELOCITY STRUCTURE

Both P and S wave velocities were determined by the Schlumberger's DSI* (Dipole Shear Sonic Imager: *Trademark of Sculumberger) tool obtained. The shear slowness was computed from upper in-line dipole data, which is one of the four component of the cross dipole data set, using the Slowness Time Coherence technique (Kimball and Marzetta, 1984).

The results show that both the P and S velocities gradually decrease towards the depth of fault gouge of 623.3 m to 625.1 m (Fig. 6), as in the case of elcctrical resistivity and density. Al-

though the velocity decrease at the boundaries of main shear zone and fresh granodiorite is not sharp, the decrease in P wave velocity at the fault gouge is very sharp; P wave velocity drops from 4 km/s (just above the fault gouge at 623.3 m to 625.1 m) to 2.6 km/s. Because the S wave signal is so weak that the S wave velocities were not determined with preliminary analysis for several depth intervals, including the fault gouge zone at 623.3 m to 625.1 m. However, there is a very sharp boundary in S wave velocity at the fault gouge.

It is very interesting that the velocity structure is very much different between the hanging wall and the foot wall of the Nojima fault; the velocity, especially S wave is much slower below the fault gouge. This is clearly shown in Vp/Vs value in Fig. 7; extremely high Vp/Vs below the fault gouge at 623.3 m to 625.1 m. This reflects the difference in the deformation degree and the deformation history.

THE MAIN SHEAR ZONE AND THE FAULT GOUGE

We observed main shear zone from about 490 m m to 713 m (Fig. 3, Fig. 4). If we consider this depth interval as the fault zone, the fault width is about 30 m thick. Core inspection show various degree of deformation in the main shear zone (Fig. 7).

BHTV (ultrasonic borehole televiewer) and FMI* (Fullbore Formation MicroImager, *Trademark of Schlumberger) logging clearly detected the fault gouge at 623.3 m to 625.1 m. The strike and dip of the fault gouge zone by FMI is about 140 degrees and 80 degrees, respectively. These are in good agreement with the surface strike of the Nojima fault and the dip estimated from the angle between the surface trace and the depth of the fault gouge.

PERMEABLE ZONE

We have tried permeability measurements with double packer system. Because of the limit of the packer sytem (the maximum depth is 500 m), we can not measure the permeability in the main shear zone. Instead of the measurements with packer system, we estimated permeable zones by tube wave generation and the Stoneley wave attenuation, reflection and slowness. The hydrophone VSP data show several tube wave generation in the Nojima Hirabayashi borehole. These suggest permeable fractures and permeable zones in the borehole. Preliminary analysis shows that the permeability of the fault gouge at 623.3 to 625.1 m is estimated as about 60 md.
The low frequency Stoneley wave, or tube wave, is sensitive to fractures and formation pore fluid mobility, and cause Stoneley wave reflections (Hornby et al., 1989), Stoneley attenuation (Brie

et al., 1988) and Stoneley slowness increase (Winkler et al., 1989). Borehole discontinuities, and formation changes also cause attenuation and reflections of the Stoneley wave. To evaluate this effect a fast modeling technique was used (Tezuka et al., 1995). This technique uses the borehole size and the formation elastic properties from the compressional and shear measurements to generate synthetic waveforms representative of the effect of borehole and formation changes without fractures. These waveforms are then evaluated with the same process as the one used for real waveforms, and the results compared.

We clearly observed a time delay in the arrivals, associated with a reduction in amplitude caused by permeable zones. We also observe chevron patterns resulting from reflections either from open fractures or from borehole irregularities. The down going feature of the chevron is caused by energy reflected from above the receivers, while the up going feature is energy reflected from below the transmitter. In a simple case these features should be symmetrical; however when the formation below or above the reflector is very attenuative one of the features is substantially reduced. Also in intervals with multiple fractures, the reflection from one fracture can be attenuated by nearby fractures.

In Fig. 8, reflection coefficients , the attenuation and slowness of the Stoneley wave are shown. We clearly observe an increase in Stoneley slowness in some sections; This could be caused either by porous, permeable formation, or by the presence of open fractures.

In a non-permeable purely elastic formation, the Stoneley slowness is a function of the formation shear slowness and its density, the mud slowness and its density, the borehole size, the Stoneley frequency. Let's call this slowness the elastic slowness or Se. Fluid movement in a permeable formation causes an increase in the Stoneley slowness S. The elastic slowness can be calculated and compared with the measured one. The difference S - Se is therefore indicative of permeability. S - Se is very large below the fault gouge and significant in the interval above the fault gouge (fault breccia zone). In the main shear zone, there are also several short intervals in which S - Se is very large: 667 m-674 m (corresponds to cataclasite zone) and 706 m-710 m (thin fault gouge zone).

FRACTURE DISTRIBUTION

With the availability of two sets of dipole transmitters and receivers in orthogonal directions, the DSI tool can measure differences in shear slowness in different directions in a plane perpendicular to the tool axis, hence acoustic anisotropy. The fast shear azimuth changes slightly by zones from the surface down to the main shear zone. It is first around NW. Above the fault gouge between 604 and 623 m it is about N, and below the fault it is about N30°W down to 675 m where it changes again to N60°E. Finally below 707 m it goes back to N70°W. The slowness

anisotropy is fairly strong above the fault gouge from 602 to 612 m, but smaller below the fault gouge.

The strike of the fractures detected by BHTV shallower than 300 m is NW, and it gradually changes to NE. In the 600 m -650 m interval, which corresponds to fault gouge zone, the strike is almost NE (Fig. 9). The strike of the surface break of the Nojima fault is NNE-NE. The fractures becomes almost parallel to the strike of the Nojima fault in the main shear zone, whereas the fractures outside the fault zone is almost perpendicular to the strike of the Nojima fault.

The changes in fast shear azimuth are much more pronounced near the fault, which suggests a strong influence of the fault.

DISCUSSION AND CONCLUSIONS

The cores from the active fault drilling at Nojima Hirabayashi revealed the subsurface structure of the Nojima fault; main shear zone at about 490 - 745 m with the fault gouge at 623.3 m to 625.1 m.

The main shear zone is characterized by low electrical resisitivity, low density, high porosity and low P and S wave velocities. These changes are not sharp at the boundaries of main shear zone and fresh granodiorite, whereas the changes at the fault gouge is very sharp.

The fine scale variations in electrical resisitivity, density, porosity, P and S wave velocities, and Vp/Vs in the main shear zone corresponds to changes in degree of deformation observed in the recovered core samples.

The width of the main shear zone from the drilling result (core inspection) is consistent with that estimated from the surface trapped wave observations at Hirabayashi. This shows a good correlation between ***in-situ*** physical properties measured in boreholes with remote geophysical observations.

In the main shear zone, there is several permeable intervals. These corresponds to the fault breccia, fault gouge and cataclasite.

The fast shear azimuth changes slightly by zones from the surface down to the main shear zone. It is first around NW. Above the fault between 604 and 623 m it is about N, and below the fault it is about N30°W down to 675 m where it changes again to N60°E. Finally below 707 m it goes back to N70°W. The slowness anisotropy is fairly strong above the fault from 602 to 612 m, but smaller below the fault.

The strike of the fractures detected by BHTV shallower than 300 m is NW, and it gradually changes to NE. In the 600 m -650 m interval, which corresponds to fault gouge zone, the strike is almost NE. The strike of the surface break of the Nojima fault is NNE-NE. The fractures becomes almost parallel to the strike of the Nojima fault in the main shear zone, whereas the fractures outside the fault zone is almost perpendicular to the strike of the Nojima fault.

The changes in fast shear azimuth are much more pronounced near the fault, which suggests a strong influence of the fault.

REFERENCES

Awata, Y., K. Mizuno, Y. Sugiyama, R. Imura, K. Shimokawa, K. Okumura, E. Tsukuda and K. Kimura, Surface fault ruptures on the northwest coast of Awaji Island associated with the Hyogo-ken Nanbu earthquake of 1995, Japan, Zisin, Suppl. 2, 49, 113-124, 1996.

Chang, S.K., H.L. Liu and D.L. Johnson, Low-frequency tube waves in permeable rocks, Geophysics 53, 519-527, 1988.

Hickman, S., M. Zoback, L. Younker and W. Ellsworth, Deep scientific drilling in the San Andreas fault zone, EOS, Trans. AGU, 75, pp. 137, 140 and 142, 1994.

Hornby B.E., D.L. Johnson, K.W. Winkler and R.A. Plumb, Fracture evaluation using reflected Stoneley-wave arrivals, Geophysics, 54, 1274-1288, 1989.

Ito, H. and Y. Kuwahara, Trapped waves along the Nojima fault from the aftershock of Kobe Earthquake, 1995, Proceedings of VIII th International Symposium on the observation of the Continental Crust Through Drilling, 399-402, 1996.

Kimball, C. V., and T. J. Marzetta, Semblance processing of borehole acoustic array data, Geophysics, 49, 274-281, 1984.

Li, Y.-G., and P.C. Leary, Fault zone trapped seismic waves, Bull. Seism. Soc. Amer., 80, 1245-1271, 1990.

Li, Y.-G., K. Aki, D. Adams, A., Hasemi and W. H. K. Lee, Seismic guided waves trapped in the fault zone of the Landers, California, earthquake of 1992, J. Geophys. Res., 99, 11705-11722, 1994a.

Li, Y.-G., J. E. Vidale, K. Aki, C. J. Marone and W. H. K. Lee, Fine structure of the Landers fault zone: segmentation and the rupture process, Science, 265, 367-370, 1994b.

Tezuka K., T. Endoand A. Brie, Fast Stoneley modeling and its application for permeable fracture evaluation, Proceedings of the First Annual Well Logging Symposium Japan, Sep. 21-22, Paper S, 1995.

Winkler, K. W., H.L. Liu and D. L. Johnson, Permeability and borehole Stoneley waves: comparison between experiments and theory, Geophysics, 54, 66-75, 1989.

Figure Captions

Fig. 1 Index map of the active faults in Awaji island (Awata et al., 1996).

Fig. 2 Hypocenters that the trapped wave was observed at Nojima Hirabayashi (shown by open circles) and that the trapped wave was not observed (shown by solid circles).

Fig. 3 The trajectory of the Nojima Hirabayashi borehole.

Fig. 4 The geological structure of the Nojima Hirabayashi borehole.

Fig. 5 The results of the conventional well logging.

Fig. 6 The velocity structure of the Nojima Hirabayashi borehole.

Fig. 7 The detailedgeological structure of the main shear zone of the Nojima Hirabayashi borehole.

Fig. 8 The stoneley wave reflections, attenuation and slowness.

Fig. 9 The lower hemisphere stereo plot of the fractures detected by BHTV for every 50 m intervals.

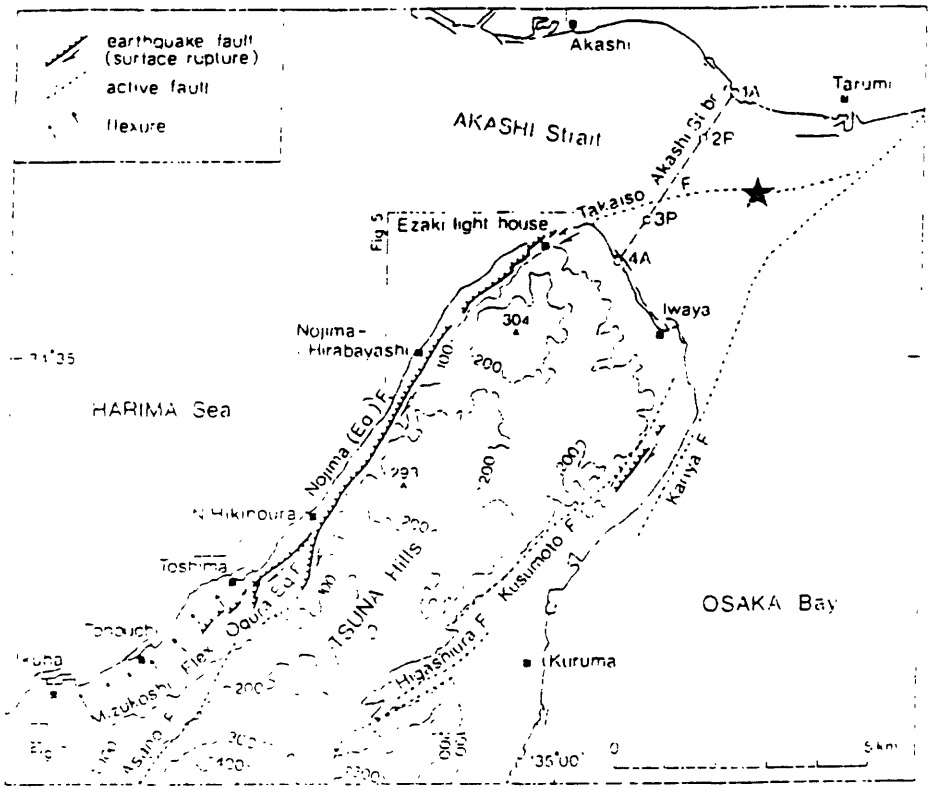
earthquake fault (surface rupture)
active fault
flexure
Akashi
Tarumi
AKASHI Strait
1A
2F
Akashi-Si br. F
Takaiso F
3P
4A
Fig 5
Ezaki light house
Iwaya
304
Nojima-Hirabayashi
HARIMA Sea
Nojima (Eo.) F
Hikiroura
Toshima
Ogura Eq.F
TSUNA Hills
Kusumoto F
Kariya F
OSAKA Bay
Kuruma
Higashinura F
Mizukoshi
Fig 3
35°00'
0
5km

Fig 1

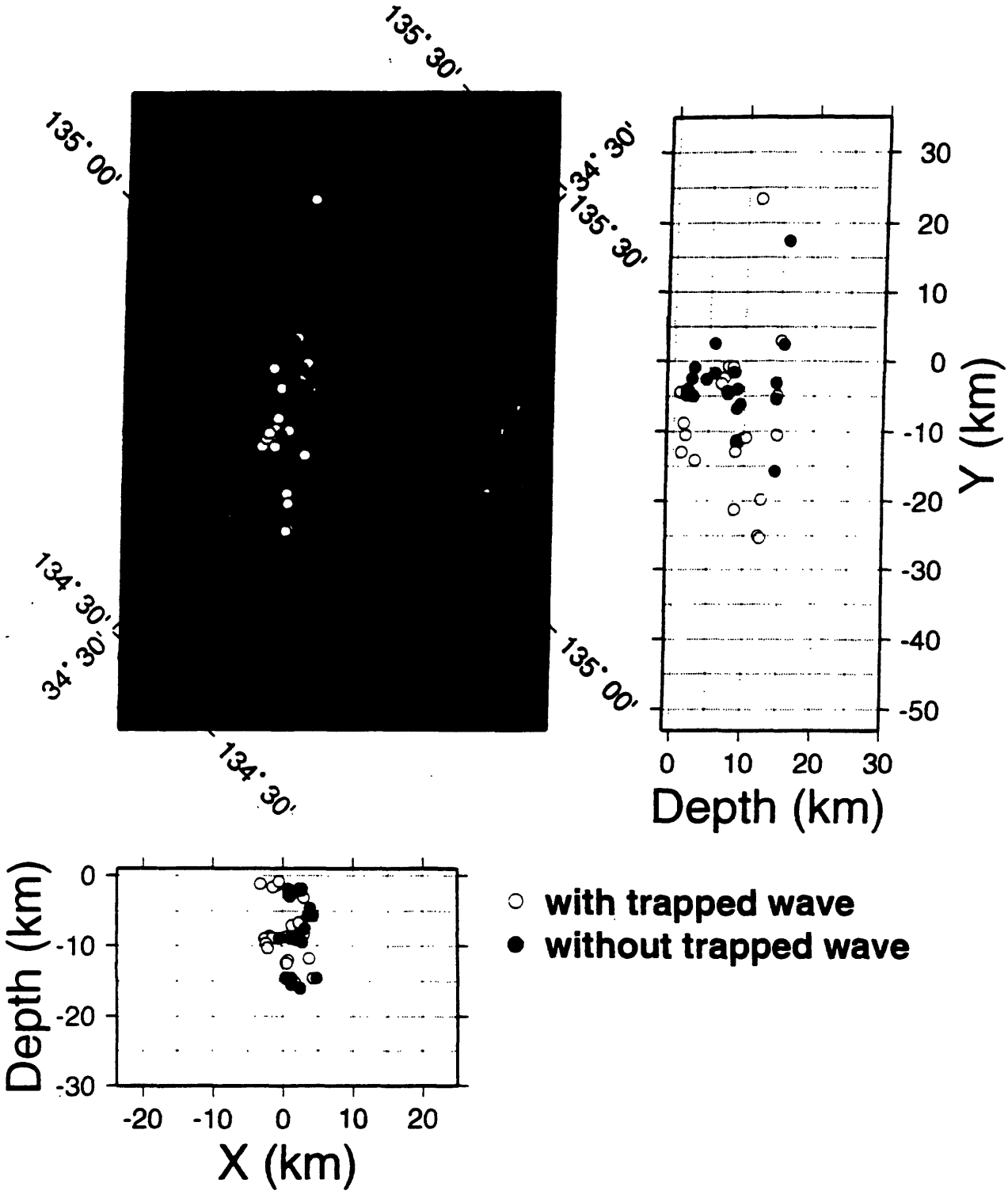
135° 30'
135° 00'
34° 30'
134° 30'
Y (km)
Depth (km)
Depth (km)
X (km)
with trapped wave
without trapped wave

Fig 2

Nojima Hirabayashi / Geological Survey of Japan

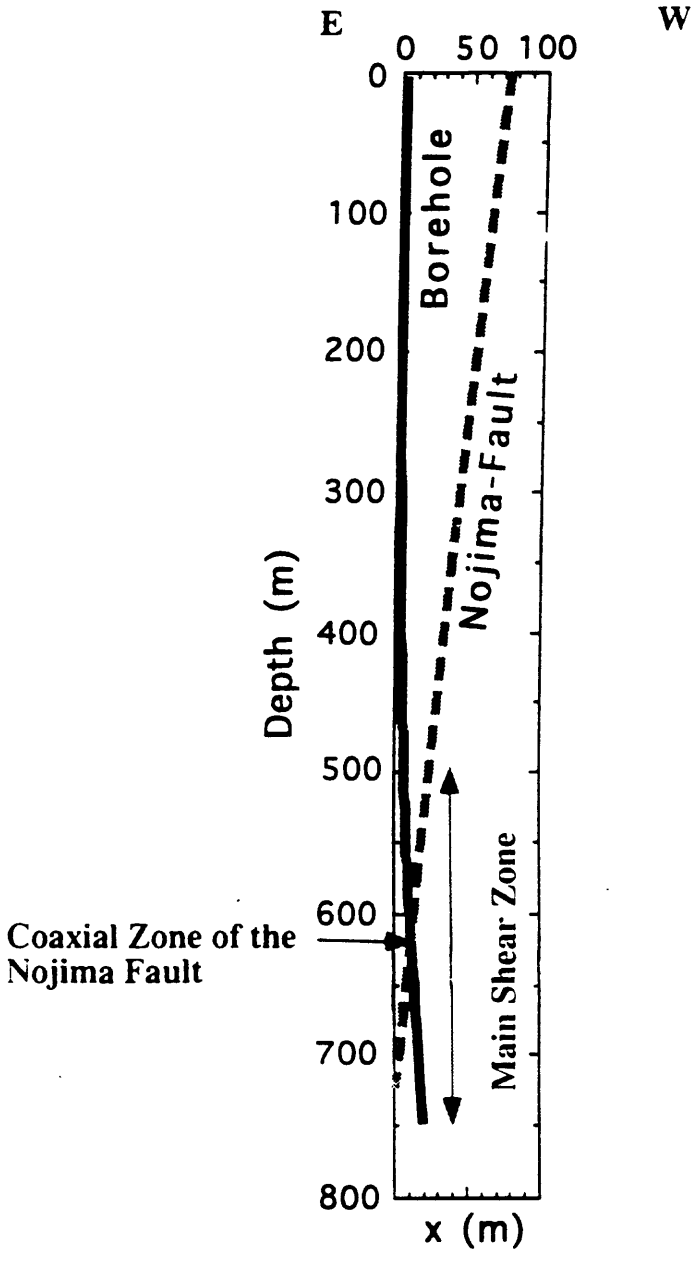

NW47 Distance

Borehole
Depth : 746.70 m
Inclination : 4°

Fault : 84°

Fig 3

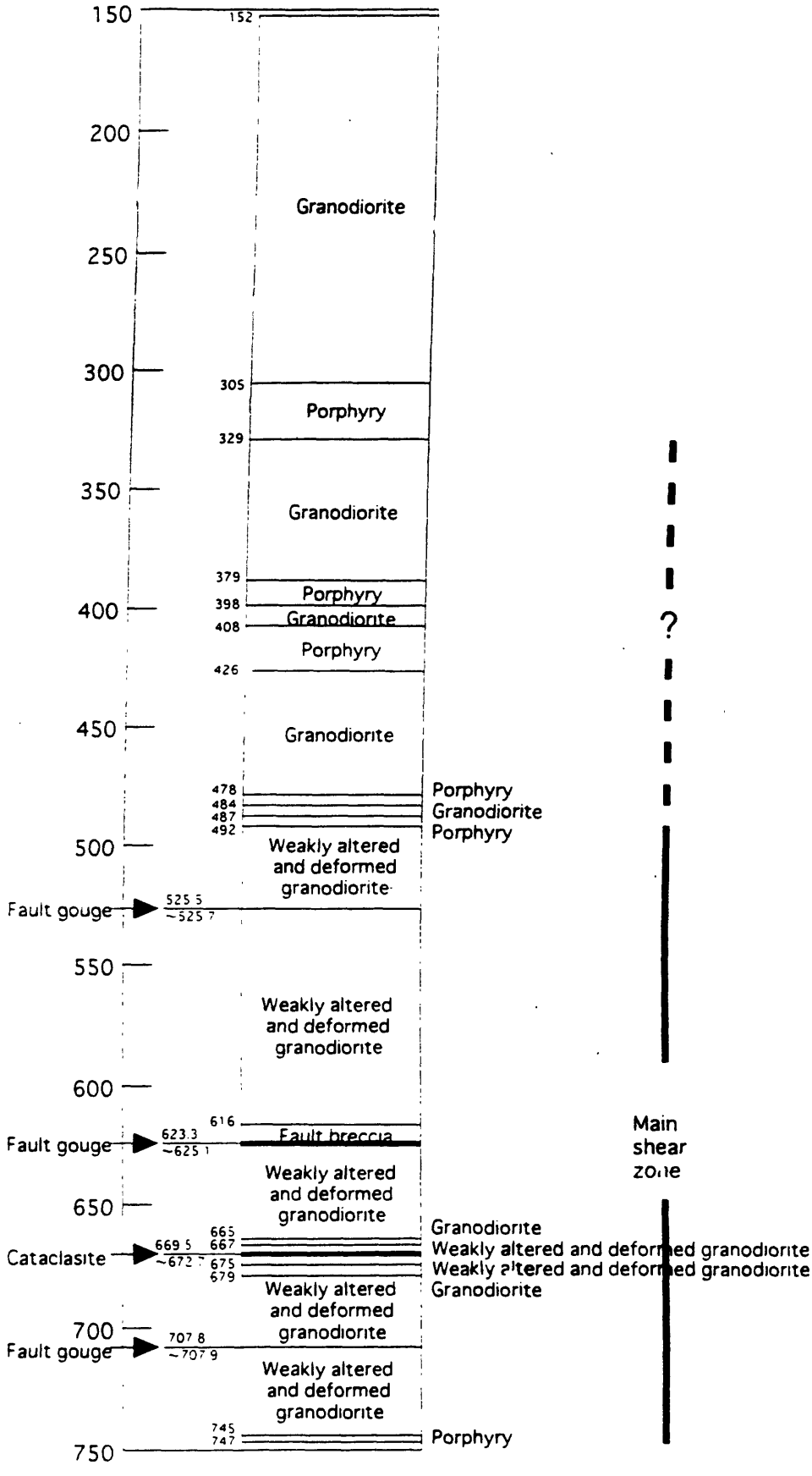
150
200
250
300
350
400
450
500
550
600
650
700
750
152
305
329
379
398
408
426
478
484
487
492
525 5
~525 7
616
623.3
~625 1
665
667
669 5
~672 ?
675
679
707 8
~707 9
745
747
Granodiorite
Porphyry
Granodiorite
Porphyry
Granodiorite
Porphyry
Granodiorite
Porphyry
Granodiorite
Porphyry
Weakly altered and deformed granodiorite
Fault gouge
Weakly altered and deformed granodiorite
Fault gouge
Fault breccia
Weakly altered and deformed granodiorite
Granodiorite
Cataclasite
Weakly altered and deformed granodiorite
Weakly altered and deformed granodiorite
Granodiorite
Weakly altered and deformed granodiorite
Fault gouge
Weakly altered and deformed granodiorite
Porphyry
?
Main shear zone

Fig 4

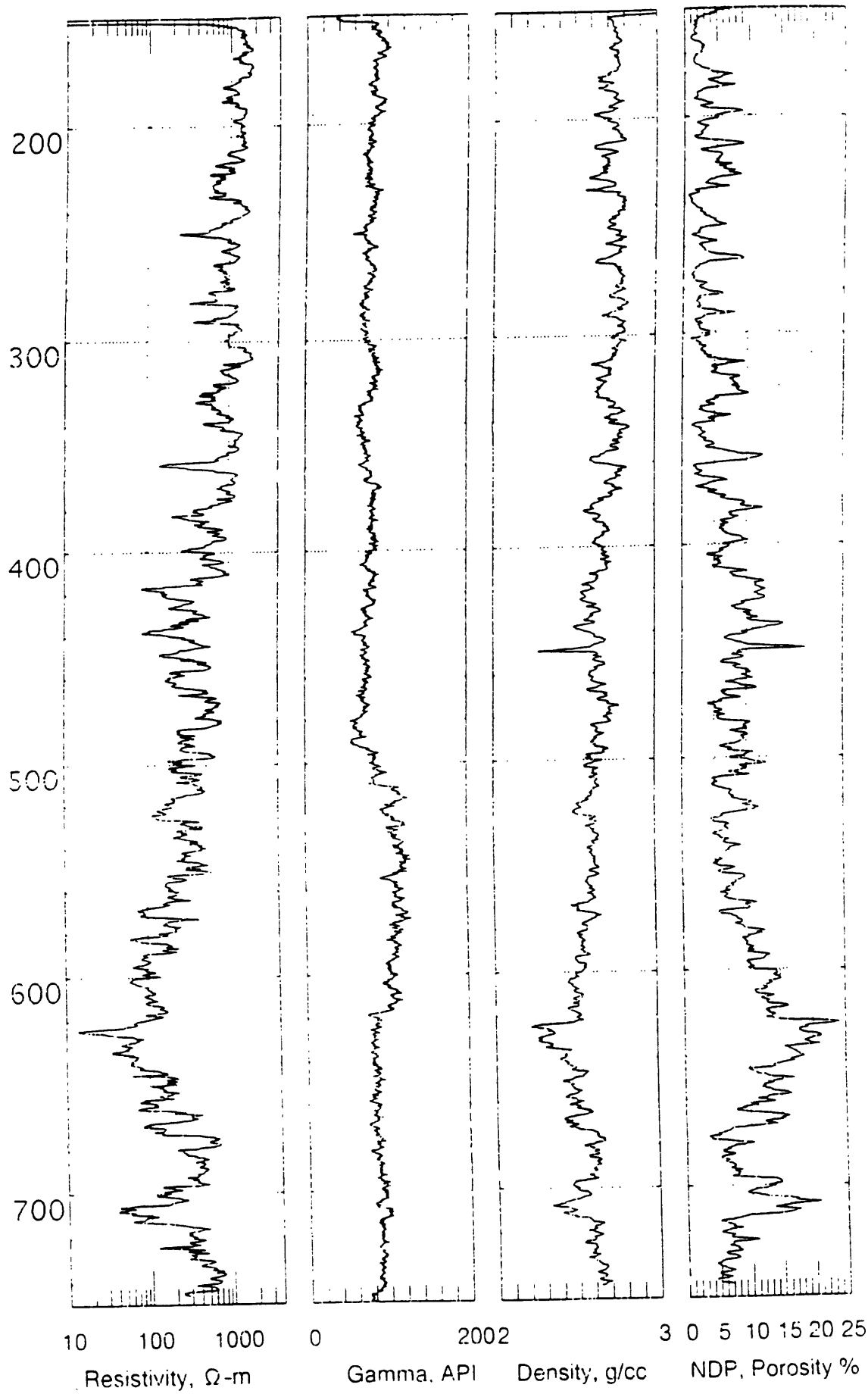
200
300
400
500
600
700
10 100 1000
Resistivity, Ω-m
0 2002
Gamma, API
3
Density, g/cc
0 5 10 15 20 25
NDP, Porosity %

Fig 5

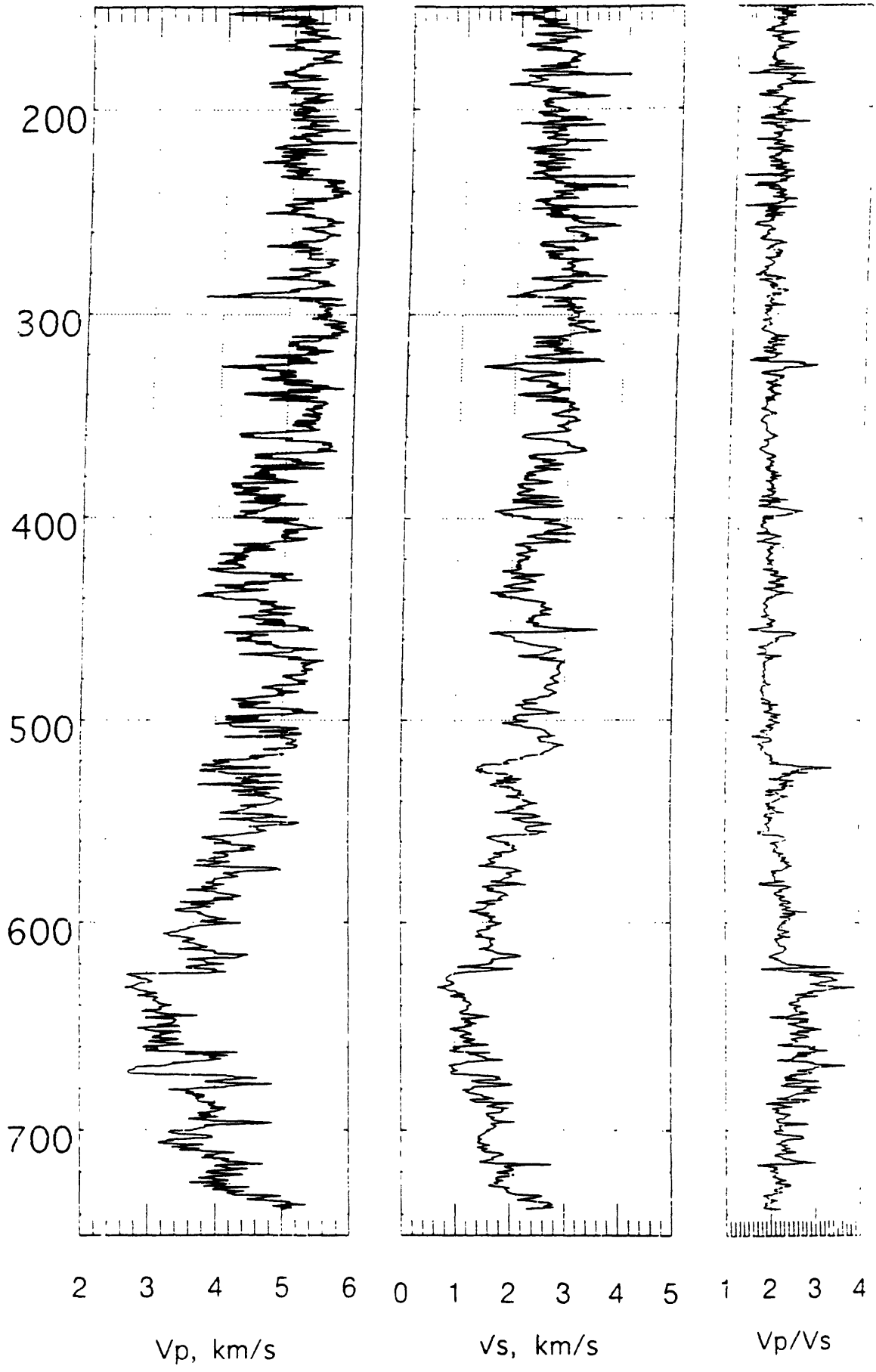

Fig. 6

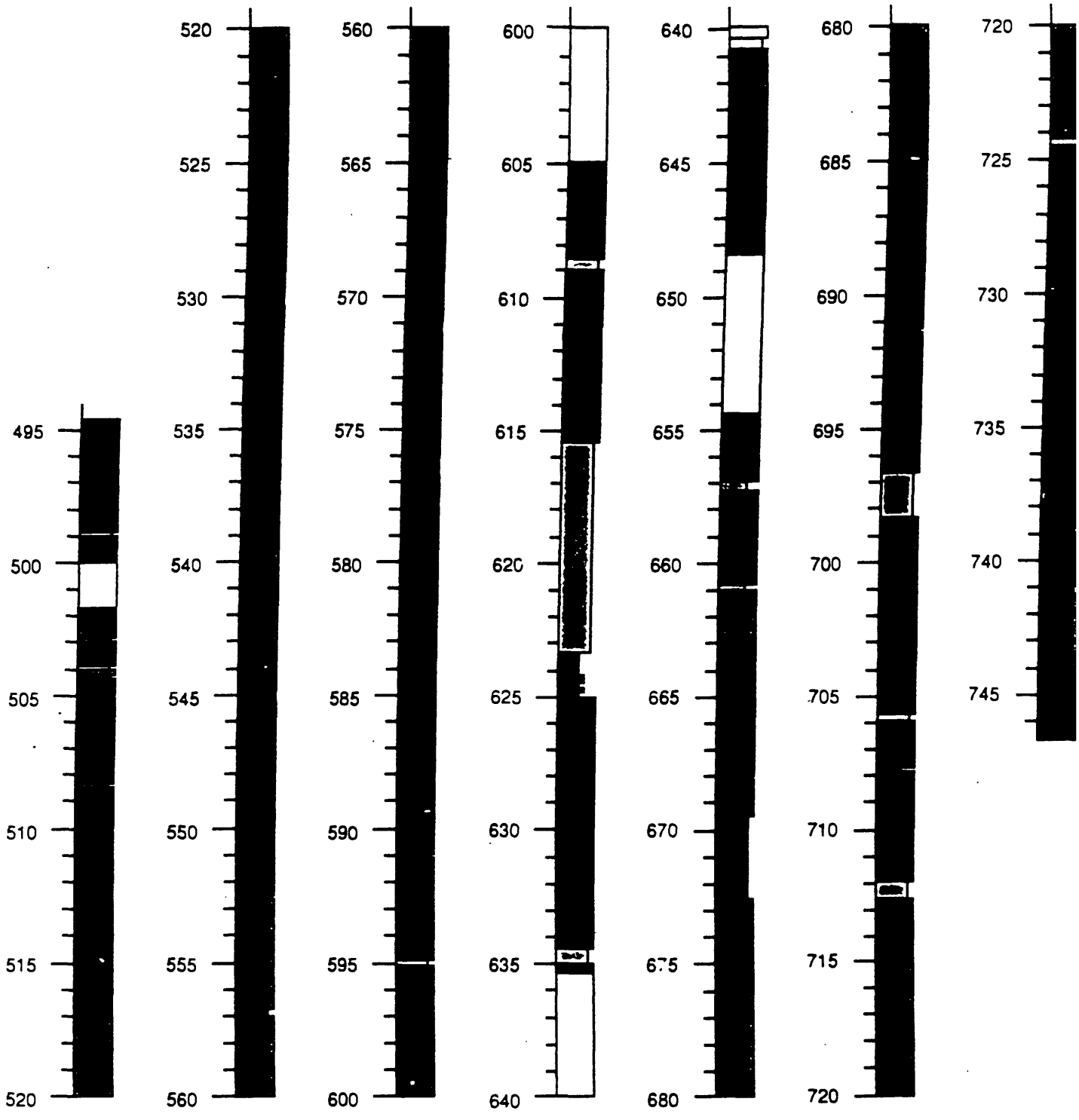

Core Description

Geological Survey of Japan Active Fault Drilling at Nojima Hirabayashi

observed by H. Tanaka, K. Fujimoto and T. Ohtani

1 : Granodiorite
2 : Weakly altered and deformed granodiorite
3 : Cataclacite
4 : Fault breccia
5 : Foliated fault gouge
6 : Light gray/light grayish green fault gouge
7 : Dark gray fault gouge
8 : Porphyry
9 : No cores (because of tri-cone bit drilling)

Fig. 7

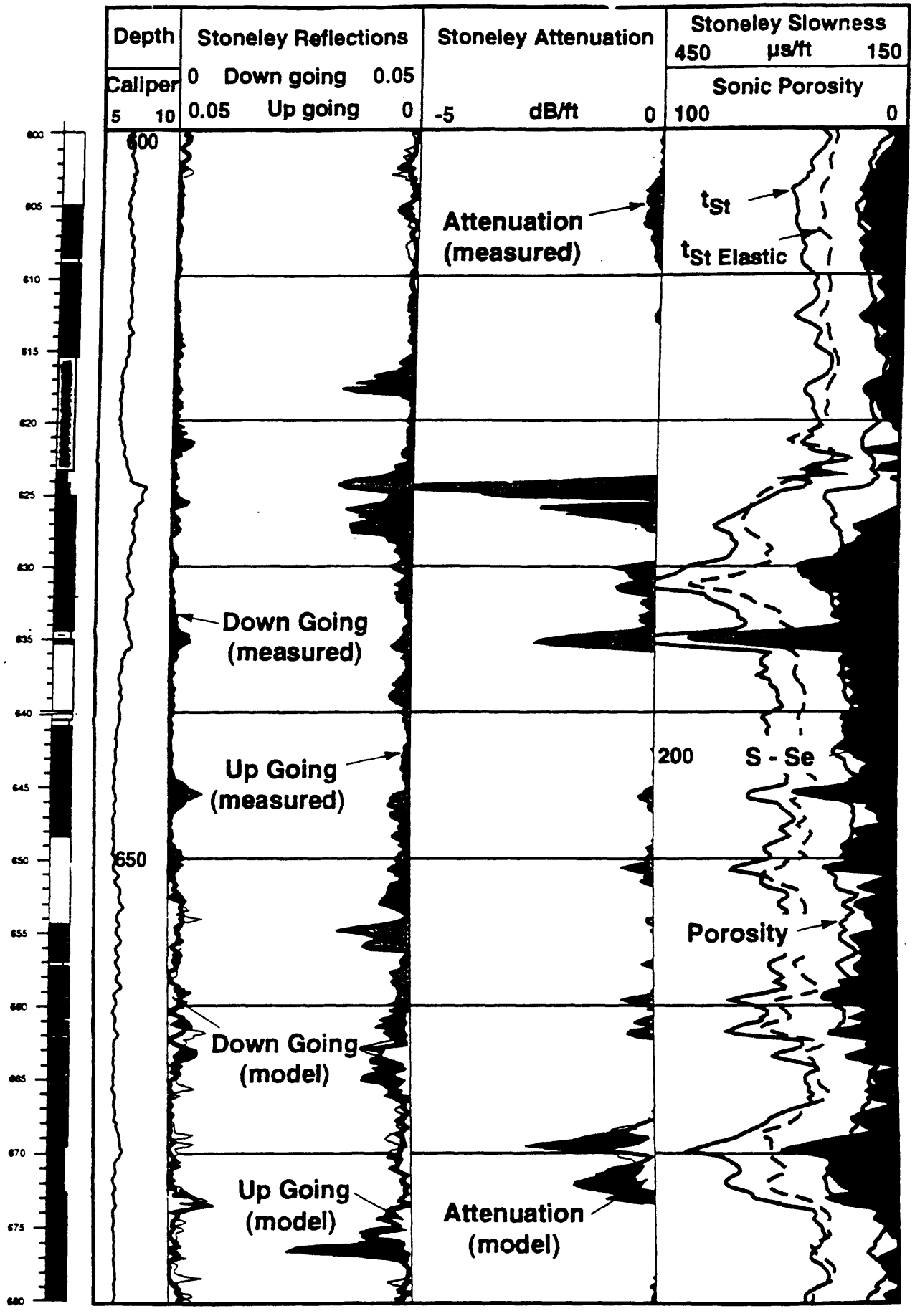
Depth
Caliper
5 10
Stoneley Reflections
0 Down going 0.05
0.05 Up going 0
Stoneley Attenuation
-5 dB/ft 0
Stoneley Slowness
450 µs/ft 150
Sonic Porosity
100 0
600
650
Attenuation (measured)
t_{St}
$t_{St\ Elastic}$
Down Going (measured)
Up Going (measured)
200
S - Se
Porosity
Down Going (model)
Up Going (model)
Attenuation (model)

Fig. 8

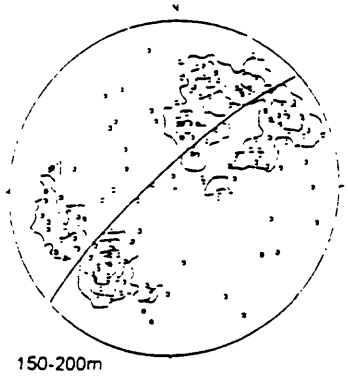
150-200m

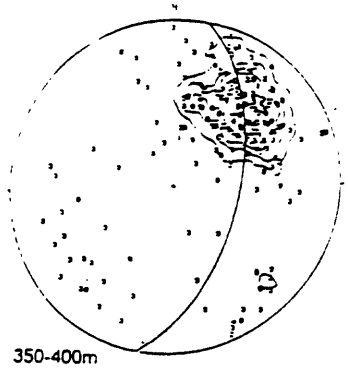
350-400m

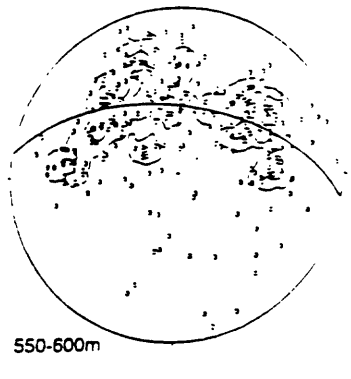
550-600m

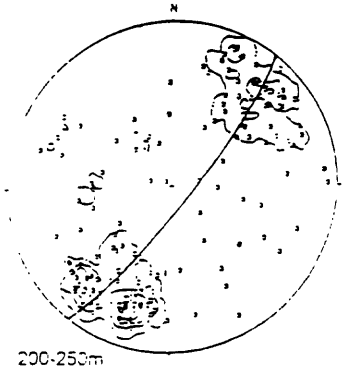
200-250m

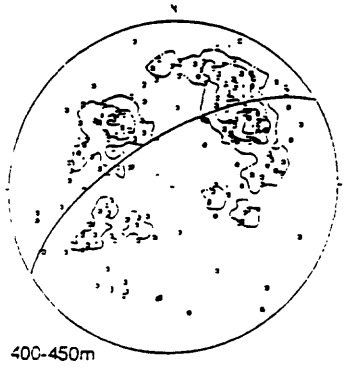
400-450m

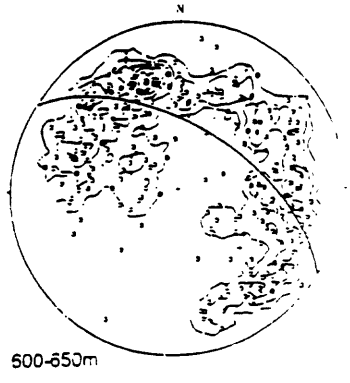
600-650m

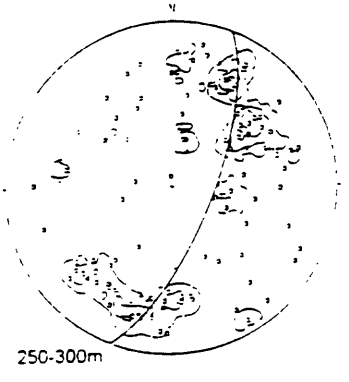
250-300m

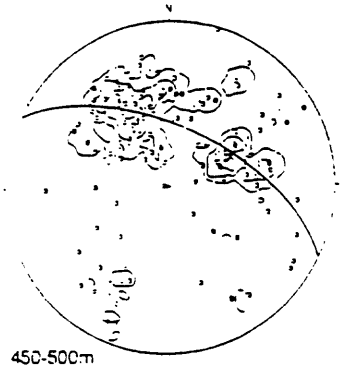
450-500m

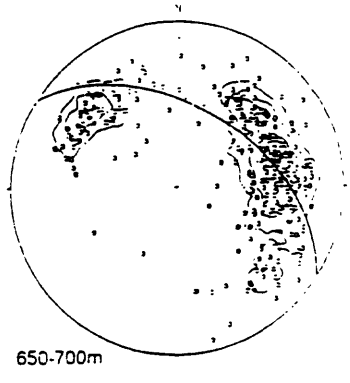
650-700m

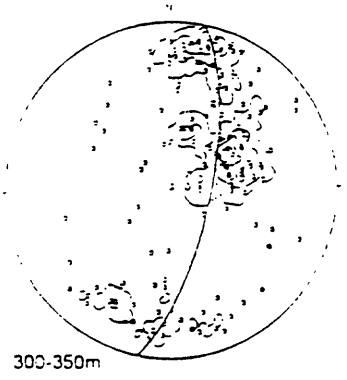
300-350m

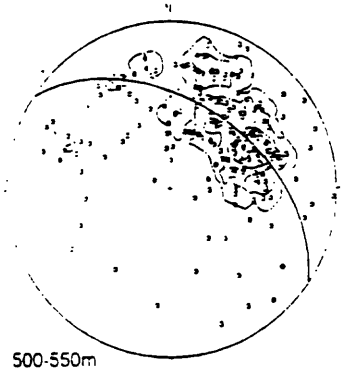
500-550m

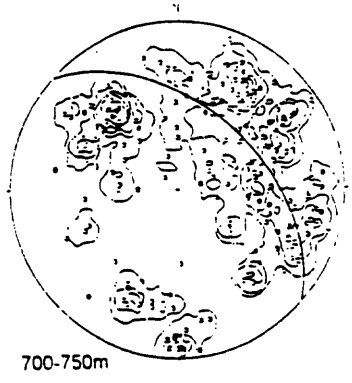
700-750m

Fig. 9

Real-Time Seismic Systems in the United States

Jim Mori
U.S. Geological Survey, Pasadena, California

What is Real-time Seismic Information?

Current technology in monitoring seismic activity can produce rapid earthquake information about location, size, and distribution of strong shaking within a few minutes (and sometimes faster) of an event. In the minutes following an earthquake, these data are of obvious importance to emergency response agencies, as well as water and power utilities, transportation companies, and the media. The main function of real-time seismic systems is to record the earthquake information and quickly distribute it to important users.

In the United States, two prototype systems that have been built to rapidly distribute real-time information following earthquakes are CUBE (Caltech-USGS Broadcast of Earthquakes) and REDI (Rapid Earthquake Data Integration), which are operating in southern and northern California, respectively. CUBE and REDI provide direct communication links through pagers to emergency response groups, utilities, transportation companies, and media. There are also World-Wide Web pages of the USGS for public access of the information. The current systems provide time, location, and magnitude in easy to understand text and graphical formats. Real-time maps showing distributions of the ground shaking and projected damage estimates are under development.

With further development, the time can be reduced to a few tens of seconds which can then be used for an Early Warning System. With very fast determinations of earthquake parameters, it is possible, in certain cases, to send a warning to populated regions before the arrival of the seismic waves that cause the damaging shaking. An example of this was used at the site of the freeway collapse in Oakland following the Loma Prieta earthquake. USGS scientists set up a system that quickly identified aftershocks and warned workers on the precarious structure 12 to 20 seconds before the shaking arrived.

The need for rapid information.

One case where there were problems with the real-time earthquake information, was following the devastating Kobe earthquake that occurred at 5:46 AM on January 17, 1995. About 15 minutes after the earthquake the Japanese Meteorological Agency (JMA) was reporting maximum JMA intensity VI. Since other locations in the heavily damaged region were not reporting, it was thought this might be an over estimate. There was some inconsistencies between what JMA was reporting and what was being broadcast on TV by NHK. As more information was gathered, the extent of the wide-spread damage became clear. In Japan one of the threshold levels that triggers governmental action is intensity VI, so this uncertainty between V and VI may have contributed to delays in emergency response. As seen in Kobe, fast mobilization is often crucial for saving lives in collapsed buildings.

For some of the local groups, it is the reliable information on smaller earthquakes that has the greater economic impact. For example, with railroad operators any report of a significant earthquakes requires them to stop their trains and inspect tracks and tunnels for possible damage. For smaller earthquakes, using rapid and reliable information, they can make the necessary inspections and if there is no damage, and quickly re-start their trains. This was the case with Santa Fe railroad during the 1991 Sierra Madre earthquake (M5.8), a moderate event that occurred in the mountains north of Los Angeles. With the information received from the CUBE system, they were able to quickly complete safety checks and minimize the time the trains were stopped. They estimated that the CUBE system saved them about $80,000 in reducing their down time.

Most current real-seismic seismic systems give post-earthquake information for emergency response, however, as the technical development improves into Early Warning, the systems will provide real life-saving capabilities.

Who should receive Real-time Seismic Information?

Information to fire, police, medical, and emergency government response groups are certainly high priorities for life-safety following a damaging earthquake. Water and power utilities, transportation companies, and communication infrastructure that serve the region also need information to enable them to reduce fires, traffic and railroad accidents, and maintain lifelines. Many of the large companies, such as some of the railroads, are controlled from national centers distant from where a large earthquake might occur. Such centers would not have immediate knowledge of an event, so it is important to disseminate information nationwide.

There are also efforts to provide quick and accurate public information to help reduce people's anxiety and panic. However, instead of trying to reach the public on an individual basis, the most efficient way is to rapidly send available information to the local TV and radio stations. Other private sector groups that may utilize fast earthquake information include the insurance companies and financial industry.

As the system develops into Early Warning capabilities, the rapid distribution of information will become an even more critical issue. It is envisioned that tens of seconds of warnings before impending shaking will be used to stop elevators, control critical highway bridges, lock up computer disks, and possibly give audible alarms to the public in schools or over the radio. One important component of such systems will need to be a public education campaign to teach people how to react to such alarms.

Assuming a high reliability in the real-time seismic information, the goal would be to disseminate information as widely as possible, limited only by the costs of building and operating the infrastructure.

Problems with reliability.

An effective information system needs the confidence of the users, which means the information must be reliable. Current systems in the US are still under development and there is an issue concerning how much of the experimental results should be broadcast to the public. In California, automated location and magnitude determinations have become fairly reliable, so these parameters are quickly released. Estimates of the ground shaking are less certain, so those results are sent only to selected groups that are directly involved in the development of the system and recognize the margins of error.

In the case of Early Warning, reliability is especially important, as well as a minimum numbers of false alarms. Such systems that require people to react, need the full confidence of the public. Early Warning alarms which are generated by real earthquakes that cause damage, but not necessarily in the region that a warning is broadcast, are not perceived as false alarms and help build public confidence. This was the case for the Mexican system which is designed to give Mexico City a 50-70 second warning from large earthquake off the west coast. There had been some problems with public confidence in the system from past performance. On September 14, 1995 a M7.3 event triggered the system causing subways to stop and setting off audible alarms for building evacuations. There were no casualties from the earthquake in Mexico City, but closer to the source in Guerrero, there was considerable building damage with several deaths and dozens of injuries. People in Mexico City evaluated the overall performance of the system as a success.

Following publicity about the success of the Mexican system in September 1995, reporters were asking why such a system was not operating in California. When told there were experimental systems being developed, they suggested that warnings from such systems should be made public, with the reasoning that even some unreliable information was better than no information. We disagree with that position and feel that the consequences of providing unreliable information that may erode public confidence outweighs the benefits of using an untested system that may get "lucky" and provide a useful warning.

Who should pay for the System?

There seems to be general agreement that real-time seismic systems are an integral part of earthquake monitoring capability in populated areas. These systems span the boundaries between the scientific research community and the governmental responsibilities for public safety, and therefore funding for these projects has been difficult in the US, especially in times of budgetary constraints. In California, pilot projects like CUBE and REDI started largely with contributions from the private sector, who recognize the value of reliable earthquake information. If real-time seismic information is to be made available in US cities, additional funds are required for the US earthquake program. Resources may continue to come from private businesses, but the infrastructure for the monitoring instrumentation is operated by the USGS and universities.

Current proposals that need support if these important public safety systems are to be fully implemented include:

- TRINET, a proposal to FEMA by Caltech, USGS, and California Division of Mines and Geology.
- Real Time Hazard Warning, an initiative by the USGS, that is currently being considered by the Dept. of Interior.

Development of realtime systems are actively being developed in both the US and Japan. This provides a good opportunity for cooperative work between the two countries as these important seismic systems are being implemented. Joint work on communication technologies, software development, and seismological applications can mutually benefit the efforts. Since damaging earthquakes are relatively rare occurrences, we can double our knowledge base by sharing experiences from the two countries. Such exchanges of information will help ensure successful operation of the realtime seismic systems during the next large earthquakes that will strike the US and Japan.

Selected References

Espinosa Aranda, J.M., A. Jimenez, G. Ibarrola, F. Alcantar, A. Aguilar, M. Inostroza, S. Maldonaldo, 1995, Mexico City alert system, *Seismol. Res. Lett. 66*, 42-53.

Flores, P.J. and J.D. Goltz, 1995, Events of the 14 September 1995, Memories of the 19 September 1985: A report on Mexico City's earthquake early warning system, EQE International Report.

Goltz, J.D., 1996, Use of real-time seismic information by government agencies, utilities and large corporations in the pre- and post-Northridge environment, EQE International Report.

Heaton, T., R. Clayton, J. Davis, E. Hauksson, L. Jones, H. Kanamori, J. Mori, R. Porcella, T. Shakal, 1996, The TriNet project, 11th World Conference on Earthquake Engineering, Acapulco Mexico.

National Research Council, 1991, *Real-Time Earthquake Monitoring*, National Academy Press, Washington D.C.

REAL-TIME PROVISION OF EARTHQUAKE INFORMATION AND TSUNAMI FORECAST

Seismological and Volcanological Department
Japan Meteorological Agency
1-3-4 Otemachi, Chiyoda-ku, Tokyo

EXECUTIVE SUMMARY

The Japan Meteorological Agency (JMA) issues information on seismic intensity, tsunami forecast, and the hypocenter and the magnitude of an earthquake immediately about two minutes after a felt earthquake occurs.

The information issued by JMA is used as key information for authorities of the national government and local governments to take measures against disaster caused by the earthquake or the tsunami. In particular, the information on seismic intensity is extremely important and effective when the authorities estimate the degree and the extent of the disaster and judge necessity or degree for emergency response to be taken. In this regard, JMA has been developing and improving its on-line systems on a real-time basis to disseminate information on earthquakes and tsunamis to the authorities by computer communications or by facsimile via dedicated lines. The information is provided to the public through radio and television of broadcasting companies under the cooperation with them. Since 1993, a communication system for disseminating earthquake information and tsunami forecast via the Geostationary Meteorological Satellite has also been operated by JMA.

In order to issue information on earthquakes and tsunamis timely and properly, JMA has developed the Seismic Intensity Meter, by which seismic intensity can be measured objectively, and has established an advanced nationwide network to observe seismic intensity and seismic wave and a system to transmit them to the data processing and analysis systems in six Regional Tsunami Warning Centers (RTWCs), and has been monitoring earthquakes and tsunamis 24 hours a day.

JMA is planning to conduct research and development to design a seismic warning system to disseminate information on estimated arrival times and amplitudes of the seismic wave before its arrival, and to enable quantitative tsunami forecasts and to subdivide coastal lines for them.

REAL-TIME PROVISION OF EARTHQUAKE INFORMATION AND TSUNAMI FORECAST

Sesimological and Volcanological Department
Japan Meteorological Agency
1-3-4 Otemachi, Chiyoda-ku, Tokyo

(1) Present situation

The Japan Meteorological Agency (JMA) is the only agency which is responsible in the government of Japan for issuing earthquake information and tsunami forecasts, and is monitoring seismic phenomena, gathering seismic data from the nationwide observation stations on a real-time basis and analyzing them using its comprehensive data processing systems 24 hours a day.

In order that authorities of the national government and local governments can take measures properly and immediately against disaster caused by earthquakes or tsunamis, JMA issues the following information successively when an earthquake which is felt by a person and/or is expected to generate tsunami occurs :

about two minutes after an earthquake : prompt report of maximum seismic intensity in each area where the seismic intensity is equal to or greater than 3;
three to five minutes : tsunami forecasts;
about five minutes : information on an hypocenter and a magnitude of the earthquake; and
five to seven minutes : information on seismic intensity at each observation station.

In particular, the information on seismic intensity is extremely important and effective to estimate the degree and the extent of the disaster when the authorities judge necessity or degree for emergency response and decide for the priority of measures to be taken immediately after an earthquake.

The information on earthquakes and tsunamis should be disseminated urgently and surely to the authorities and the public. In this regard, JMA has been developing and improving its systems used to disseminate the information to the authorities by facsimile via dedicated lines. Some of the authorities have already introduced or are planning to introduce the computer systems, directly connecting to the JMA's systems to receive and process the information from JMA through dedicated lines on a real-time basis. JMA has also been providing the urgent information to the authorities and other users through the "Satellite-based Information Dissemination System" using the Geostationary Meteorological Satellite (GMS) since 1993. In addition, the information is broadcasted to the public under the cooperation with broadcasting companies, by interrupting radio and television programs and/or superimposing on television screens to notify the occurrence of an earthquake urgently.

In order to issue the information on earthquakes and tsunamis timely and properly, there should be high-quality and high-fidelity seismic observation network and data processing and analyzing systems. Based on experiences of seismic observation for more than 100 years, JMA has operated an advanced nationwide network including about 180 stations for seismic wave observation at intervals of 60km since 1993. About 600 stations for seismic intensity observation has also been introduced by JMA every 20km since 1996. The seismic data observed at the stations are transmitted to six Regional Tsunami Warning Centers (RTWCs), and are processed and analyzed with the comprehensive systems to determine earthquake source parameters such as a hypocenter and a magnitude, and to

issue the seismic intensity information. When an earthquake occurs at the sea bottom, the generation of tsunami and its magnitude are judged using the determined parameters of the earthquake, and then tsunami forecasts are issued by JMA.

JMA receives information on earthquakes occurred in areas far from Japan such as the Pacific Coast of the American Continent from the United States Geological Survey (USGS). With a view to issuing tsunami forecasts for tsunamis generated by earthquakes in the Pacific Ocean, JMA and the Pacific Tsunami Warning Center and the Alaska Tsunami Warning Center of the National Oceanic and Atomospheric Administration (NOAA) frequently exchange the information and the data related to earthquakes and tsunamis in both countries, respectively. In order to promote the collaboration between Japan and the United States even more properly and promptly in this region, strengthening the framework for the information exchange including earthquakes and tsunamis was agreed at the United States-Japan Summit Meeting in Tokyo in April 1996 as the "Pan-Pacific Natural Disaster Watch Network" in the Natural Disaster Reduction under the "Common Agenda" .

(2) Strategic plan

a) Research and Development for real-time provision of information on earthquakes

JMA is planning to conduct researches and developments to design a seismic warning system for disseminating information on estimated arrival times and amplitudes of the seismic wave before its arrival. Such kind of information is much more effective to mitigate the earthquake disaster. If it would be disseminated to operators of their transportation system and/or to managers of their plants, they can control them appropriately. However, it should be noted that the earlier such kind of information would be issued, the less accurate it would be. JMA has been studying researches about technical feasibility concerning real-time provision system on earthquake information and the contents of available information as time goes by after occurrence of the earthquake and methodologies of their use.

b) Improvement of tsunami forecast

The tsunami forecast is represented only as a categorized grade of tsunami heights at the coast lines of Japan, which is roughly estimated from the empirical relationship between tsunami heights and earthquakes based on the past observed data, and the estimated arrival time at each tidal observation station .

In order to make a quantitative height estimations for the tsunami forecast, JMA has been developing following techniques for the forecast:

- To make numerical calculations of tsunami heights using fault models for earthquakes which are expected to occur at the sea bottom around Japan and to make a database of the result of the above calculations;
- To estimate the tsunami height of the actually occurred earthquake by the retrieval of an appropriate result of the calculations in every coastal line from the database.

c) Cooperation between JMA and local governments

All the prefectural governments are deploying around 3,000 of Seismic Intensity Meters as same as JMA's ones in their municipalities under the sponsorship of the Fire and Disaster Management Agency (FDMA), Ministry of Home Affairs. JMA is planning to collect all of the seismic intensity data and to issue more detailed seismic intensity information in cooperation with the prefectural governments and FDMA.

Key References

Seismic Intensity Measurement

Seismic intensity scale presents a degree of the ground motion by an earthquake, and it has been used as general indices of disaster caused by the earthquake In Japan, ordinary seismic intensity is used as not only the indices of quantified estimation of the past earthquake disaster, but also the preliminary information by which authorities of the national government and local governments take emergency measures immediately after an earthquake occurs. However, the seismic intensity had been subjectively determined with the observation of the motion of buildings and/or furniture and field survey There was a problem that more than 15-20 minutes are required to be disseminated to the authorities when they have to use it in an urgent situation. Therefore, JMA has developed a Seismic Intensity Meter which measures seismic intensity objectively and automatically transmits the measured seismic intensity information on a real-time basis. The first one of it has been operated since 1990, and then it is deployed to each Meteorological Observatory of JMA every year. After the "Southern Hyogo Prefecture Earthquake" in 1995, the former-type of seismic intensity meter was improved, i.e. earthquake resistant structure of a calculation unit of the instrument and the addition of an equipment for data transmission via GMS against disruption of land lines. JMA also deployed about six hundred sets of new Seismic Intensity Meters at around 60km intervals throughout Japan and has begun to operate them since April 1996.

The Explanation Table of Seismic Intensity Scale

A Seismic Intensity Meter calculates continuous values of seismic intensity after the filtering of observed seismic waves according to the former seismic intensity scale which was subjectively determined. Thus, the information of seismic intensity is issued to the public as a scale. JMA has prepared "Explanation Table of JMA Seismic Intensity Scale" for more convenient use of the seismic intensity information so that the authorities can easily estimate the phenomena caused by an earthquake. The table has been used since April 1996.

Example of use of seismic intensity value

The National Land Agency has been developing and operating "Disaster Information System" which quantitatively estimates amount of killed or injured people within 30 minutes after an earthquake. Seismic intensity data provided by JMA is used in the system as the initial values of its estimation.

EXPLANATION TABLE OF JMA SEISMIC INTENSITY SCALE

The JMA seismic intensity scale, which provides a measure of the strength of the seismic motion, is measured with a seismic intensity meter. This table describes the situations and damage which may be caused by seismic motion of each seismic intensity. When using this table, please note the following:

(1) The seismic intensity announced by JMA is a value obtained with a seismic intensity meter, and it is not determined from observed phenomena described in this table;

(2) Sites where equal seismic intensity was observed would not necessarily suffer the same degree of damage, because damage depends on the type of construction and on the nature of the seismic motion. This table describes some typical situations which may appear. More or less damage than that described in the table may occur;

(3) Amplitudes of seismic ground motion are influenced greatly by underground structure and topography. The seismic intensity is a value observed at a site where a seismic intensity meter is installed. The seismic intensity occasionally varies even within a city. The seismic intensity is usually measured on the ground, but in general, the shaking on upper stories of buildings may be amplified greatly;

(4) A large earthquake generates long-period seismic waves. Even at locations far from the epicenter, where the seismic intensity is rather small, the long-period waves may occasionally cause some peculiar damage such as the sloshing of oil in a tank and troubles with elevators;

(5) This table is prepared mainly based on the examples collected from recent damaging earthquakes. The table is subject to revision when new examples are collected or the present descriptions become inconsistent with actual situations, due to the improvement of earthquake resistant buildings and so on.

Seismic Intensity *1	JMA Scale *2	People	Indoor situations	Outdoor situations	Wooden houses	Reinforced-concrete buildings	Lifelines	Ground and slopes
-0.5	0	Imperceptible to people						
0.5-1.5	1	Felt by only some people in the building.						
1.5-2.5	2	Felt by many people in the building. Some sleeping people awake.	Hanging objects such as lamps swing slightly.					
2.5-3.5	3	Felt by most people in the building. Some people are frightened.	Dishes in a cupboard rattle occasionally	Electric wires swing slightly				
3.5-4.5	4	Many people are frightened. Some people try to escape from danger. Most sleeping people awake.	Hanging objects swing considerably and dishes in a cupboard rattle. Unstable ornaments fall occasionally.	Electric wires swing considerably. People walking on a street and some people driving automobiles notice the earthquake.				
4.5-5.0	5Lower	Most people try to escape from a danger. Some people find it difficult to move.	Hanging objects swing violently. Most unstable ornaments fall. Occasionally, dishes in a cupboard and books on a bookshelf fall and furniture moves.	People notice electric-light poles swing. Occasionally, windowpanes are broken and fall, unreinforced concrete-block walls collapse, and roads suffer damage.	Occasionally, less earthquake-resistant houses suffer damage to walls and pillars.	Occasionally, cracks are formed in walls of less earthquake-resistant buildings.	A safety device cuts off the gas service at some houses. On rare occasions water pipes are damaged and water service is interrupted [Electrical service is interrupted at some houses]	Occasionally, cracks appear in soft ground, and rockfalls and small slope failures take place in mountainous districts
5.0-5.5	5Upper	Many people are considerably frightened and find it difficult to move.	Most dishes in a cupboard and most books on a bookshelf fall. Occasionally, a TV set on a rack falls, heavy furniture such as a chest of drawers falls, sliding doors slip out of their groove and the deformation of a door frame makes it impossible to open the door.	In many cases, unreinforced concrete-block walls collapse and tombstones overturn. Many automobiles stop because it becomes difficult to drive Occasionally, poorly-installed vending machines fall.	Occasionally, less earthquake-resistant houses suffer heavy damage to walls and pillars and lean.	Occasionally, large cracks are formed in walls, crossbeams and pillars of less earthquake-resistance buildings and even highly earthquake-resistant buildings have cracks in walls	Occasionally, gas pipes and/or water mains are damaged [Occasionally, gas service and/or water service are interrupted in some regions]	

5.5-6.0	6Lower	Difficult to keep standing	A lot of heavy and unfixed furniture moves and falls. It is impossible to open the door in many cases	In some buildings, wall tiles and windowpanes are damaged and fall	Occasionally, less earthquake-resistant houses collapse and even walls and pillars of highly earthquake-resistant houses are damaged	Occasionally, walls and pillars of less earthquake-resistant buildings are destroyed and even highly earthquake-resistant buildings have large cracks in walls, crossbeams and pillars	Gas pipes and/or water mains are damaged |In some regions, gas service and water service are interrupted and electrical service is interrupted stops occasionally |	Occasionally, cracks appear in the ground, and landslides take place.
6.0-6.5	6Upper	Impossible to keep standing and to move without crawling.	Most heavy and unfixed furniture moves and falls. Occasionally, sliding doors are thrown from their groove.	In many buildings, wall tiles and windowpanes are damaged and fall. Most unreinforced concrete-block walls collapse	Many less earthquake-resistant houses collapse In some cases, even walls and pillars of highly earthquake-resistant houses are heavily damaged	Occasionally, less earthquake-resistant buildings collapse. In some cases, even highly earthquake-resistant buildings suffer damage to walls and pillars	Occasionally, gas mains and/or water mains are damaged. |Electrical service is interrupted in some regions. Occasionally, gas service and/or water service are interrupted over a large area |	
6.5-	7	Thrown by the shaking and impossible to move at will.	Most furniture moves to a large extent and some jumps up.	In most buildings, wall tiles and windowpanes are damaged and fall. In some cases, reinforced concrete-block walls collapse	Occasionally, even highly earthquake-resistant houses are severely damaged and lean	Occasionally, even highly earthquake-resistant buildings are severely damaged and lean.	|Electrical service, gas service and water service are interrupted over a large area.|	The ground is considerably distorted by large cracks and fissures, and slope failures and landslides take place, which occasionally change topographic features

*1 Value of instrumental seismic intensity

*2 The JMA seismic intensity scale

Notes

1) Instrumental seismic intensity is a numerical one indicating the strength of the seismic motion at a site and measured with a seismic intensity meter.
The JMA seismic intensity scale announced officially is obtained from the instrumental seismic intensity

2) Lifelines are utilities for power, communication, transportation and water supply.

3) The descriptions given in \| \| of the "Lifelines" describe situations concerning electrical, gas and water service in particular for information.

Seismic Data Transmission Network in Japan

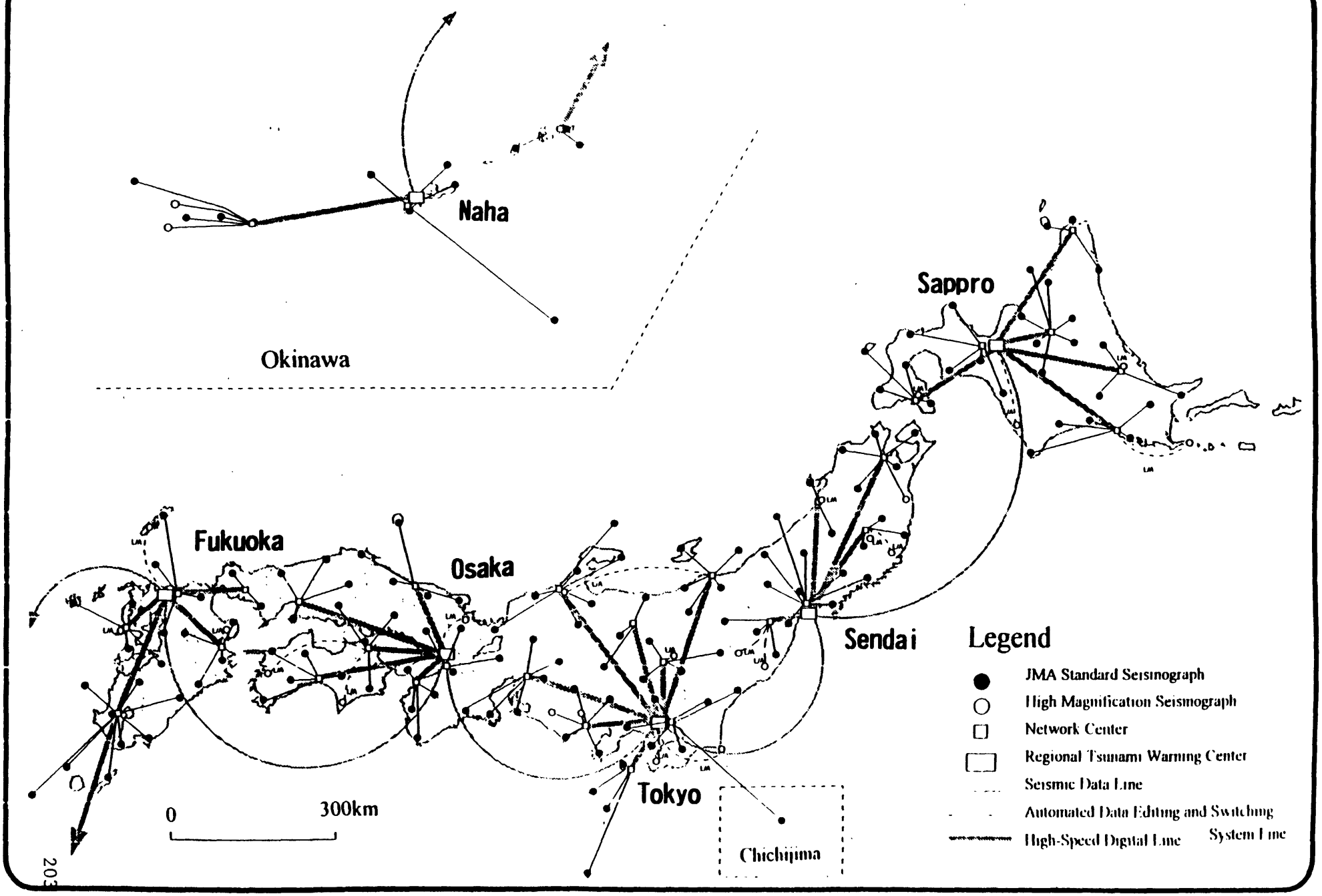

Seismic Intensity Measurement Stations

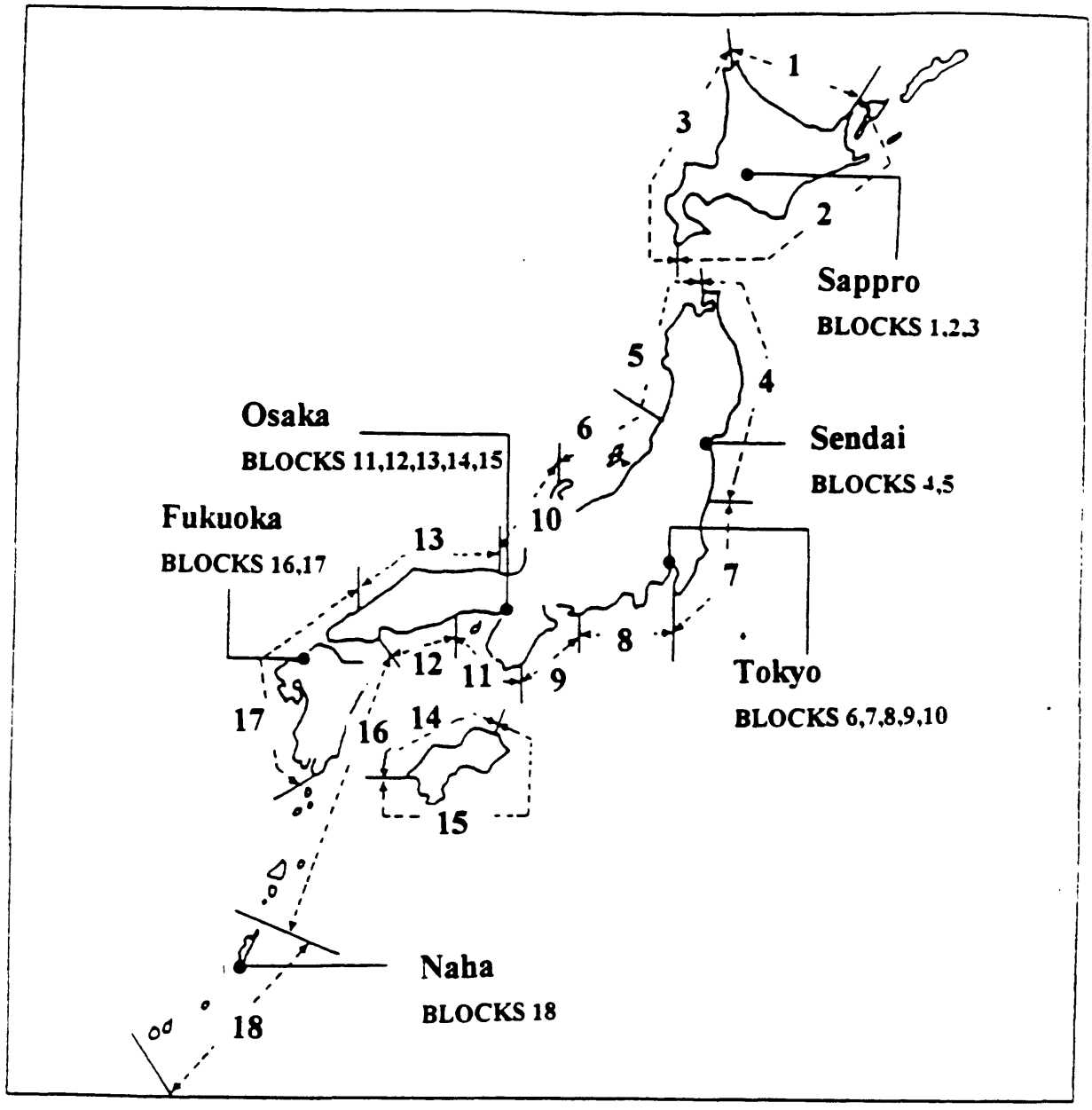

Six Regional Tsunami Warning Centers (RTWCs) and eighteen regions for tsunami forecasts. The block numbers attached to each RTWC show the responsible regions, to which the center issues tsunami forecasts

Outline of the Japan Meteorological Agency (JMA)

The meteorological services in Japan were started in 1875 at the Tokyo Meteorological Observatory, which was renamed the Central Meteorological Observatory in 1887. The weather stations had been run by the local prefectural authorities until 1939, when these stations were transferred to be controlled by the central government. In 1956, the Central Meteorological Observatory was upgraded in status to an external organ of the Ministry of Transport and was renamed the Japan Meteorological Agency (JMA)

JMA is responsible as the National Meteorological Service for contributing to the improvement of public welfare including prevention and mitigation of natural disasters, safety of transportation, prosperity of industries, and international cooperation activities (Article 1, Meteorological Service Law). The major services are to issue short-range, one-week and long-range weather forecasts; to issue the warnings/advisories against typhoon and heavy rainfall/snowfall; to issue the warnings/forecasts against tsunami, storm surge, ocean waves and flood; and to provide information on seismic and volcanic activities.

In order to ensure these services, JMA has been improving its systems of observations, national/international telecommunications and weather analysis/forecasting. Recently, more accurate and precise meteorological information has become available as a result of the following improvements: meteorological observing system including the Geostationary Meteorological Satellite, the Automated Meteorological Data Acquisition System (AMeDAS) and the associated telecommunication network have been upgraded; a high-speed super computer data processing system has been introduced; and numerical weather prediction models have been sophisticated. In March 1996, Weather Distribution Forecast and Time Sequence Forecast were put into operation.

The human being now faces global environment issues, in particular the global warming due to increasing greenhouse gases in the atmosphere. JMA operationally makes observations, and monitors atmospheric ozone and greenhouse gases both in the atmosphere and in the ocean. In 1990, JMA started the operation of the WMO World Data Centre for Greenhouse Gases (WDCGG) at its Headquarters.

Also, JMA is modernizing its seismological observation system to support the earthquake prediction system for coming Tokai Earthquake in joint cooperation with other governmental agencies, research institutes and universities. This activity is based on the Large-scale Earthquake Countermeasures Act. Since 1987, the computerized Earthquake Phenomena Observation System (EPOS) has been in operation to monitor and identify precursory anomalies of crustal movement and to support the tsunami warning service. In 1996, JMA started the operation of regional seismic information centres, which will have the responsibility for the collection of observational data and information on earthquakes from local governments and universities based on the Earthquake Disaster Prevention Special Measures Act established in 1995.

Since more diversified meteorological information is increasingly required in the development of our socio-economic system, JMA recently adopted a new framework to promote comprehensive meteorological information services through the collaboration and cooperation between JMA and the private weather industry.

Organization of the Japan Meteorological Agency (JMA)

(as of July 1996)

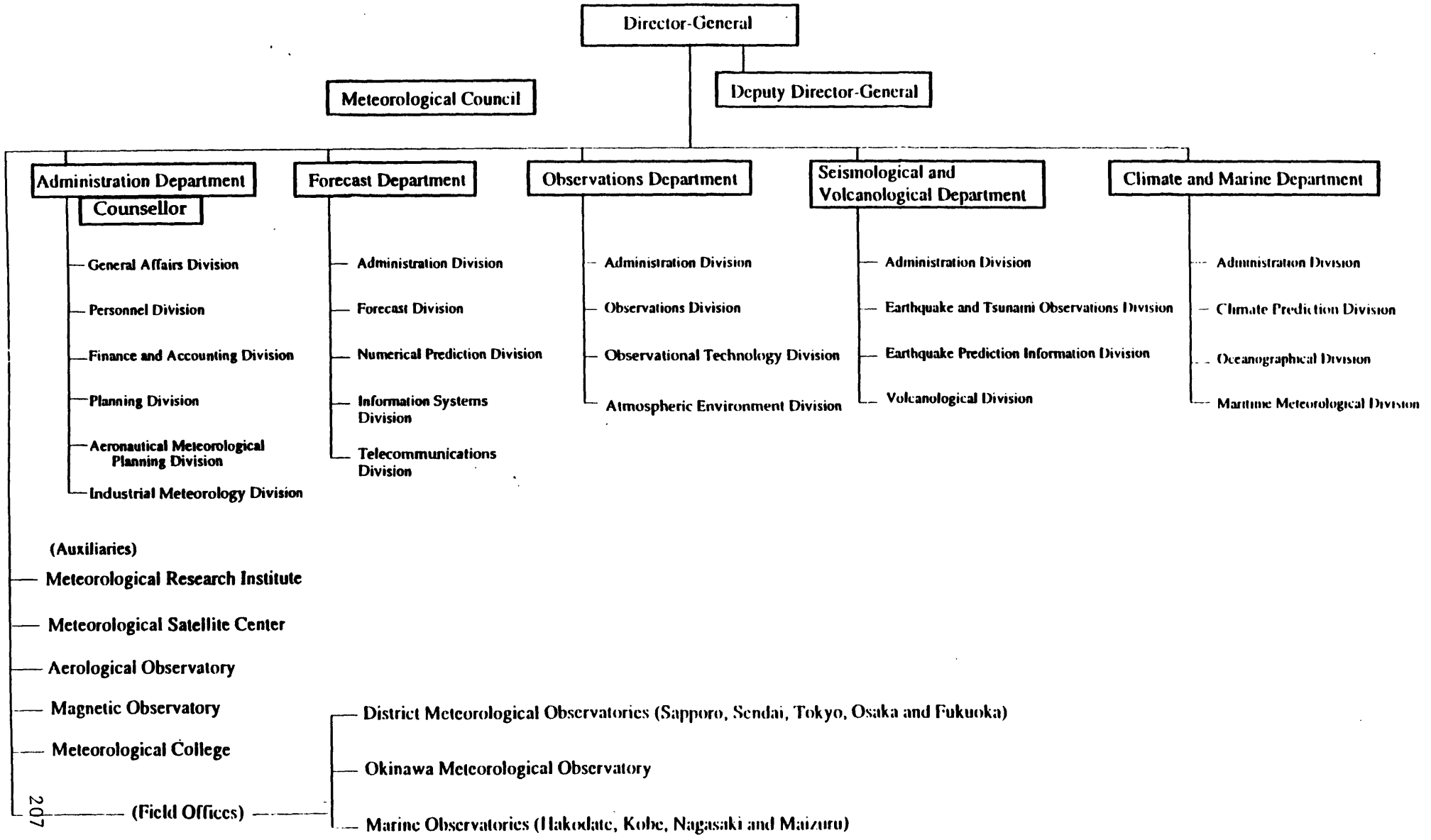

TRINET GROUND MOTION RECORDING OPPORTUNITIES: A Joint Effort of Caltech, the Division of Mines and Geology and the USGS

By
James F. Davis and Anthony F. Shakal
Department of Conservation, Division of Mines and Geology

Background: During the last decade, innovations in technology have enhanced opportunities to digitally record, transmit and analyze ground motion data in previously impractical time frames. In response to these circumstances, seismic network operators have initiated changes. The State of California Department of Conservation's Division of Mines and Geology (DMG) has been installing digital recorders at its newer stations and has recently added dial-out transmitting capability to Sacramento for near-time data processing at 60 locations in the 650 station California Strong Motion Instrumentation Program (SMIP) network. California Institute of Technology (Caltech) has added 20 TERRAscope telemetered broadband recorders as a pilot project to supplement the 250 predominantly weak motion single component stations of the Southern California Seismic Network (SCSN) that it operates jointly with the U.S. Geological Survey (USGS).

The 1994 Northridge earthquake strong motion records demonstrate again that significant regional variations exist between the projected levels of ground shaking that would be anticipated from such an event using existing models and the observed patterns. Efforts to interpret performance of damaged buildings were also limited by the sparsity of observations sufficiently close to be considered as input ground motion. Although wave form and spectral response data were provided to the Governor's Office of Emergency Services (OES) by DMG in record time after the event, it was still not rapid enough to be used in the initial deployment of disaster response personnel.

The above outcomes of the Northridge earthquake and the possibility of Federal post-disaster funding have encouraged seismic network operators in southern California to collaborate in their future development plans in order to more effectively contribute to the earthquake loss reduction needs of their constituencies. The TriNet proposal submitted to the Federal Emergency Management Agency (FEMA) through the state OES results from this cooperative effort.

TriNet Purposes: TriNet proposes to employ state-of-art technology to facilitate code improvements that better mitigate future earthquake damage to new and retrofitted construction and to better fill the immediate post-disaster information needs of emergency managers. This can be accomplished by increasing the spatial density of real-time and near-real-time recording and by enhancing analysis and data distribution. A pilot early warning system employing TriNet real-time capabilities is also proposed.

TriNet Design: TriNet proposes a strong ground motion recording, communication and data analysis system that integrates the efforts of the TriNet institutions to serve their constituencies as well as accomplishes the three TriNet purposes: improving codes; expanding real-time data available for emergency managers; and exploring the feasibility and usefulness of early warning. The discussion which follows shows the general relationship between the three principal purposes of TriNet and the components of the proposal, although this arrangement is somewhat arbitrary since the elements are mutually supporting.

- **Code improvements**--A larger number of recording stations will assure more observations of strong ground shaking in future damaging earthquakes. The rapid communication and analysis capabilities of digital technology can make data available for building performance analyses shortly after damaging events. They also expedite use of the data in emergency regulations such as those for repair of steel frame buildings after the Northridge earthquake. Data will be available earlier for investigations that can lead to code improvement in the regular 3-year revision cycle. Other benefits of digital networks include more efficient problem detection and servicing as well as greater likelihood of successfully recording damaging aftershock sequences than with analog equipment that requires film changes.

  The proposed TriNet system will consist of 600 stations and data processing centers in Pasadena and Sacramento. This is the minimum number of stations necessary for sufficient geographic coverage to achieve the basic TriNet purposes. DMG will upgrade 220 of its current analog stations and add 180 new stations. Twenty to thirty of these stations will have real-time telemetry tied in both to Pasadena and Sacramento. The remainder will have dial-out transmission to Sacramento. DMG dial-out stations will have 3-component force-balanced accelerometers (FBAs). DMG will process these data plus data from 50 of the USGS stations that will added to the U.S. National Strong Motion Project (USNSMP). These USGS data will also be shared with Pasadena. The DMG TriNet element will be able to record some ground motions from earthquakes as small as M 3, which is considerably more sensitive than its existing analog network capabilities.

  Caltech will upgrade 80 of the SCSN analog weak motion stations that are part of the existing 250 station network. These will be added to the existing 33 digital stations already operated by Caltech/USGS. The new sensors will include 3-component seismometers and FBAs that together can record both weak and strong ground shaking. Signals will also be received in Pasadena from 77 new USGS strong motion stations to be added from non-OES/FEMA funding sources to the USNSMP. Digital telemetry links will transfer data from all 220 stations in this new core network to Pasadena. All events in excess of M 2 will be recorded.

Strong motion data utilization by the engineering community is essential to building code improvement. DMG's TriNet element also includes an expansion of the existing SMIP Data Utilization Project. This project provides grants for focused structural engineering and engineering seismology investigations of observed ground motion and building performance. A number of previous investigations have influenced code changes.

DMG will digitize and process 100 analog strong motion Northridge earthquake records from code-required installations in high-rise (over 6 stories) buildings as another feature of its TriNet element. Some of these records are from damaged steel and concrete buildings and understanding the causes of damage is very important to confirm their adequate repair and to improve the code. DMG will carry out case history investigations from selected structures.

- **Post-event emergency management and informing the public**--The expansion and upgrading of monitoring stations and the development of real-time and near-real-time capabilities are as essential to enhancing emergency management and to informing the public as they are to code improvement.

  DMG will expand its data processing and distribution beyond the current 30 dial-out stations in southern California to handle a network of 400. Data distribution capabilities will be expanded in coordination with the other TriNet partners. Caltech will continue its investigations of the suitability of commercially available dedicated digital network communication technologies for seismic transmission systems. Caltech is exploring Frame Relay communication which has the advantage of multiple routings. Real-time communications by Frame Relay and Caltech's existing microwave system will be important in providing the very first ground shaking maps to emergency managers and the public only a few minutes after damaging earthquakes. Caltech plans to develop a seismic system that can handle up to 1000 stations functioning as a distributed computer system that treats the seismic recording network as an array of "computer nodes" and a parallel system that conducts central data processing.

  Caltech and the USGS will continue to distribute data on smaller and moderate sized earthquakes. A map of shaking based on preliminary real-time analysis will be available within a few minutes after large damaging earthquakes. Approximately 15-30 minutes after large earthquakes, shaking maps will display information from the entire TriNet system as TriNet products. Strong motion data from all institutions will be exchanged in this process. TriNet institutions will develop standard methods to produce ground motion maps that integrate their data and are periodically updated with continuing processing and analysis. Coordinating of deployment of hardware and software will assure adequate function and provide redundancy in data processing and analysis.